

The University of Strathclyde

Department of Electronic and Electrical Engineering

**A Reliability Method for the Analysis of Turboelectric
Distributed Propulsion Electrical Network Architectures**

By

Jennifer Catherine Shaw

A Thesis submitted in fulfilment of the requirements of the degree of Doctor of
Philosophy to

Department of Electronic and Electrical Engineering

University of Strathclyde

May 2016

This thesis is the result of the author's original research. It has been composed by the author and has not been previously submitted for examination which has led to the award of a degree.

The copyright of this thesis belongs to the author under the terms of the United Kingdom Copyright Acts as qualified by University of Strathclyde Regulation 3.50. Due acknowledgement must always be made of the use of any material contained in, or derived from, this thesis.

Abstract

A set of goals for four successive generations of cleaner, more efficient subsonic aircraft has been published and championed by NASA; the radically different Turboelectric Distributed Propulsion (TeDP) aircraft was also proposed to meet the long term goals. Such a new aircraft design places a significant additional reliance on the electrical system, requiring architectures that meet specified thrust requirements at a minimum associated weight as well as providing the greatest performance against the proposed emissions targets. This thesis presents a method for evaluating the power and reliability profiles exhibited by a number of electrical propulsion network architectures specific to TeDP aircraft. The method is used to clearly determine the probability that each variation of the network will provide a given level of thrust. Each configuration may be compared in a visual manner, using a formulation developed as part of this thesis, showing the ‘best’ candidate solutions and establishing how each performs relative to the others in terms of both reliability afforded and thrust provided. A number of case studies are presented within this thesis to demonstrate how the developed method can be applied and secondly to test the effectiveness of bringing additional redundancy to the system and the extent to which the reliability is improved. Sensitivity studies are also undertaken to quantify the extent that component substitutions and alterations impact on network reliability. The overall goal is to establish the features of a TeDP network architecture that consistently exhibits the greatest thrust reliability profile.

In conducting this research, the work of this thesis progresses the understanding of the TeDP concept with a particular focus on the NASA N3-X aircraft being used to validate the proposed method. Specifically the knowledge in the area of the concept reliability and predicted failure rates are addressed with recommendations being put forward on how each can be improved. These recommendations form a useful input to the general body of research that is working towards NASA’s future long term goals for cleaner more efficient aircraft.

Acknowledgements

Firstly I would like to thank both my supervisors Prof. Graeme Burt and Dr. Stuart Galloway for their support, time and assistance with travel which has been associated with this project over the last 4 years. I would additionally like to thank Dr. Patrick Norman for his technical guidance, his time in reviewing my work and his constant encouragement that my work was heading in the right direction.

To my colleagues in the UTC aero team, I thank you for guidance offered and time spent discussing various theories and ideas as well as practice presentations to help with my public speaking! My thanks must also be extended to the Engineering and Physical Research Council (EPSRC) for their financial backing to allow this work to have been carried out. Thanks are also extended my friends for being there for me with liberal amounts of tea, coffee and cake.

Additionally I would like to give a special mention to John Stark for all his understanding and attempts to understand what my research was about and being a shoulder to cry on in the dark moments. Thank you for your lifts in every day, being my airport shuttle and for all your distractions and for making me laugh.

My final thanks go to my family for their continued unconditional support and constant encouragement. Thanks specifically to my dad for his tireless efforts in proof reading my work as well as keeping everyone supported both psychologically and financially and to my mum for being such a strong individual.

Contents

Abstract.....	iii
Acknowledgements.....	iv
Contents	v
List of Figures.....	x
List of Tables	xiv
Glossary of Abbreviations	xvi
Definitions of Relevant Reliability terms	xviii
Chapter 1.....	1
1. Introduction.....	1
1.1 Introduction to Research.....	1
1.2 Evolution of Aircraft towards TeDP Architectures	6
1.3 Research Motivations.....	7
1.4 TeDP Network Reliability Considerations.....	9
1.5 Contribution to knowledge.....	10
1.6 Publications.....	11
1.7 Thesis overview	12
Chapter 2.....	14
2. A review of the electrical technologies contributing to the evolution of civil aircraft ..	14
2.1 Overview of Aircraft Electrical Systems: 1950 to Present Day.....	15
2.1.1 <i>What are TRL 's and why are they Relevant?</i>	16
2.1.2 <i>NASA Future Subsonic Aircraft Goals</i>	18
2.2 Overview of Current/Conventional Aircraft	21
2.2.1 <i>Conventional Aircraft Power Systems for Propulsion</i>	21
2.2.2 <i>Turbofan Engines</i>	23
2.3 The More Electric Aircraft: The future of air travel?.....	25

2.3.1	<i>Power Optimised Aircraft project</i>	26
2.4	Current State of the Art: Electrical Systems	28
2.4.1	<i>An Overview of the Electrical System of the Airbus A380</i>	28
2.4.2	<i>The B787 electrical power system</i>	30
2.5	More Electrical alternatives for Conventional Aircraft Systems	32
2.5.1	<i>The More-Electric Engine</i>	32
2.5.2	<i>Electro Hydrostatic Actuation Considerations</i>	33
2.5.3	<i>Electro-Mechanical Actuation</i>	34
2.5.4	<i>Electrical Protection Considerations for Future Aircraft</i>	35
2.6	The impact of Electrical Power Offtakes on Future Engine Configurations	36
2.7	Turboelectric Distributed Propulsion for N+3 Applications.....	38
2.8	Key Differences between MEA Aircraft and TeDP Aircraft Concepts	40
2.9	Example TeDP Network Architectures.....	42
2.9.1	<i>NASA N3-X Architecture</i>	42
2.9.2	<i>Airbus and Rolls - Royce E-Thrust Concept</i>	43
2.9.3	<i>NASA Hybrid AC-DC Configuration</i>	45
2.10	N+3 Concept Aircraft Designs Proposed for Subsonic Commercial Transport in the 2030-35 Timeframe.....	47
2.10.1	<i>Boeing, GE and Georgia Tech Concept Entry</i>	48
2.10.2	<i>SELECT Concept Aircraft Developed by Northrup Grumman,</i>	49
2.10.3	<i>Cessna Style Concept N+3 Aircraft</i>	50
2.10.4	<i>MIT, Aurora, P&W and Aerodyne Concept Aircraft</i>	51
2.10.5	<i>N+3 Concept Aircraft from NASA, Virginia Tech and Georgia Tech</i>	53
2.11	Chapter Summary	54
Chapter 3.....		56
3.	Overview of Existing TeDP Research and Applicable Reliability Methods	56
3.1	Identification of existing areas of TeDP research	56
3.1.1	<i>NASA TeDP Research</i>	57

3.1.2	<i>Existing Research in the area of TeDP Contingency Analysis</i>	60
3.2	Identification of Gaps in Existing Research in the area of TeDP Contingency Analysis	65
3.3	Identification of Research Topic.....	67
3.4	Requirement for a new Analysis Methodology	69
3.5	Reliability Methods and Requirements Considered for a TeDP Thrust Reliability Profiling Application	70
3.5.1	<i>k-out-of-n Analysis</i>	71
3.5.1.1	<i>k-out-of-n Network Architecture Example</i>	74
3.5.2	<i>Bayesian Analysis</i>	75
3.5.2.1	<i>Bayes Rule Example</i>	76
3.5.3	<i>Markov Analysis</i>	77
3.5.3.1	<i>Markov Analysis Example</i>	79
3.5.3.2	<i>Relative Merits of the Markov Analysis</i>	80
3.5.4	<i>Fault Tree Analysis</i>	80
3.5.4.1	<i>Fault Tree Analysis Example</i>	83
3.6	Down Selection and Summary of Reviewed Methods	85
3.7	Chapter Summary	86
Chapter 4	88
4.	A Method for the Analysis of TeDP Electrical Propulsion Networks	88
4.1	Introducing a Method through which to Analyse Thrust Reliability Profiles of TeDP Architectures.....	89
4.2	Defining the Case Study Network	90
4.2.1	<i>Defining Network Modular Sections to Simplify Analysis</i>	91
4.2.2	<i>System used to define Motor Feeder Positional Reference</i>	93
4.3	TeDP Design and Analysis Requirements	94
4.4	Contingency Analysis in a Land-Based Network Setting.....	95
4.5	Contingency Analysis for TeDP	96
4.5.1	<i>Network Trade-Offs</i>	96

4.6	TeDP Baseline Network Considerations.....	98
4.7	Failure Scenarios.....	100
4.7.1	<i>Implication of Failure Scenarios</i>	102
4.7.2	<i>Contingency Scenarios</i>	102
4.7.3	<i>Power- Reliability Graph</i>	105
4.8	TeDP Network Thrust-Reliability Analysis Method	109
4.9	Case Study Illustrating how the <i>k-out-of-n</i> Method in used in a TeDP Network Example	111
4.10	Chapter Summary	120
	Chapter 5.....	122
5.	Case Study Networks Identification and Development	122
5.1	Overview of Considered Network Configurations	123
5.1.1	<i>A Description of the Baseline N3-X TeDP Propulsion Network</i>	123
5.1.2	<i>A Description of the NASA Hybrid AC/DC TeDP Propulsion Network</i>	126
5.1.3	<i>A Description of the Airbus and Rolls-Royce Concept TeDP Aircraft</i>	129
5.1.4	<i>A Comparison of the Three Identified TeDP Propulsion Networks</i>	132
5.2	Case Studies: Methodology	135
	Chapter 6.....	137
6.	Case Studies	137
6.1	Case Study 1: Calculating the Reliability of the Baseline Networks using <i>k-out-of-n</i> Analysis	140
6.1.1	<i>N3-X Baseline Case Study</i>	140
6.1.2	<i>Case Study Determining the Reliability of the Baseline NASA Hybrid AC-DC Network</i> 148	
6.1.3	<i>Case Study to Determine the Reliability of the Rolls-Royce and Airbus Baseline Network</i> 157	
6.2	Summary of the Baseline Studies	166
6.3	Case Study 2: Examining the Effect of Adding Bus Ties to a TeDP Network to enhance Reliability.....	168

6.4	Case Study 3: Using Parallel Redundant Feeders to Enhance Network Reliability	174
6.4.1	<i>Using MFP to Increase the Baseline Network Reliability</i>	175
6.4.2	<i>Redundant Feeders in the GSC side of the Network</i>	180
6.4.3	<i>Parallel Feeders Case Study Using both GSCP and MFP</i>	184
6.4.4	<i>Summary of the Parallel Redundant Feeders Case Study</i>	187
6.5	Summary of Added Redundancy Case Study Findings	188
6.6	Case Study 4: Investigating the Effects to Reliability of a Common Protection System	190
6.7	Case Study 5: Network Reliability Sensitivity to changes in Component Reliability	193
6.7.1	<i>Sensitivity Study of the N3-X Architecture</i>	195
6.7.2	<i>Sensitivity Analysis of the Hybrid Network Architecture</i>	197
6.7.3	<i>Sensitivity of the Airbus and Rolls-Royce Architecture</i>	199
6.7.4	<i>Sensitivity Study Summary</i>	202
6.8	FTA of two Variations of the N3-X Network.....	203
6.8.1	<i>FTA on Baseline N3-X Network</i>	203
6.8.2	<i>FTA on N3-X Network Utilising Redundant Parallel Feeders</i>	208
6.8.3	<i>FTA Summary</i>	212
Chapter 7	213
7.	Conclusions and Further Work	213
7.1	Summary of Key Findings from <i>k-out-of-n</i> Analysis	213
7.2	Review of Chapter Summaries	216
7.3	Key Areas of Future Work.....	219
7.4	Concluding Remarks.....	222
Bibliography	223

List of Figures

Figure 2.1 Timeline of aircraft electrical systems upper voltage levels [17].....	15
Figure 2.2 Technology Readiness Levels [5].....	17
Figure 2.3 Conventional aircraft power sources [10].....	21
Figure 2.4 Layout of conventional electrical network [15].....	22
Figure 2.5 Two shaft high bypass turbofan engine [13]	23
Figure 2.6 Three shaft high bypass turbofan engine [13]	24
Figure 2.7 Side and rear view of a 16 fan HWB aircraft and a cross section of a superconducting engine [20].....	26
Figure 2.8 Power Optimised Aircraft [10, 21]	27
Figure 2.9 Airbus A380 [2].....	29
Figure 2.10 Battery Charge Rectifier Unit and Components [26]	29
Figure 2.11 Boeing B787 [1]	31
Figure 2.12 The More-Electric Engine [22].....	33
Figure 2.13 Nose Mounted Starter Generator [14]	37
Figure 2.14 N3-X TeDP Aircraft Concept [11]	38
Figure 2.15 16 MF Configuration of a TeDP Network.....	42
Figure 2.16 Rolls - Royce and Airbus TeDP Concept Aircraft [9].....	44
Figure 2.17 Electrical Propulsion Architecture of Rolls - Royce and Airbus TeDP Concept [23].....	44
Figure 2.18 NASA TeDP Network Components [16]	46
Figure 2.19 Boeing, GE and Georgia Tech Concept Aircraft [6]	48
Figure 2.20 SELECT Aircraft [4]	49
Figure 2.21 GE Aviation N+3 Subsonic Concept Aircraft [7].....	50
Figure 2.22 Self-Healing Aircraft Outer Layer Concept [8].....	51
Figure 2.23 MIT H Series N+3 Aircraft Concept [3]	52
Figure 2.24 MIT Double Bubble N+3 Aircraft [3]	52
Figure 2.25 Georgia and Virginia Tech Collaborative efficient wing design aircraft [12]....	53
Figure 3.1 N3A TeDP Concept [10]	58
Figure 3.2 NASA N3-X Concept [11]	59
Figure 3.3 Baseline TeDP Architecture [19]	61
Figure 3.4 Contingency Scenario Graph [19]	63
Figure 3.7a k-out-of-n example where $k = 1$	72
Figure 3.7b k-out-of-n general case where $k \leq n$	72

Figure 3.7c k-out-of-n example showing $k=n$ or complete redundancy	72
Figure 3.8 Example k-out-of-n network	74
Figure 3.9 Two Component Network State Diagram	79
Figure 3.10 Fault Tree Analysis Example	84
Figure 4.1 N3-X Schematic showing motor connections, not motor placement	90
Figure 4.2 TeDP Network Breakdown and associated network subsection	92
Figure 4.3 TeDP Baseline Network Schematic	93
Figure 4.4 Two Generator TeDP Network Utilising Six Motors to Provide Thrust.....	97
Figure 4.5 16 MF Configuration of a TeDP Network.....	98
Figure 4.6 Baseline TeDP Network (14 MF Configuration)	99
Figure 4.7 N3-X Network Showing Loss of Propulsive Thrust Due to the failure of a Motor Feeder.....	100
Figure 4.8 N3-X Network Exhibiting the Loss or Failure of a Bus or Generator Causing Loss of Thrust.....	101
Figure 4.9 Loss of 50 % Thrust due to Failure of an Engine.....	101
Figure 4.10 TeDP Network using Bus Ties to Mitigate the Effects of a Generator Failure	103
Figure 4.11 Parallel feeders from Generator to Bus used to Increase Redundancy in a TeDP Network	104
Figure 4.12 Loss or Failure of a Bus causing loss of 4 MF Mitigated through the use of additional MFP.....	104
Figure 4.13 A T-R Graph for an Example N3-X Network	106
Figure 4.14 T-R Graph Showing a number of Different Performance Requirements	108
Figure 4.15 TeDP Network Section Showing Component Configuration.....	113
Figure 4.16 Using Additional GSC to Increase TeDP Network Reliability	117
Figure 4.17 T-R graph for the case study network.....	119
Figure 5.1 N3-X Baseline Network	124
Figure 5.2 TeDP Network Component Configuration.....	125
Figure 5.3 N3-X baseline network configuration laid out to illustrate the network's SS....	126
Figure 5.4 NASA Hybrid Network Baseline Configuration.....	127
Figure 5.5 NASA Hybrid AC-DC network	128
Figure 5.6 NASA Hybrid network baseline configuration	129
Figure 5.7 Rolls - Royce and Airbus baseline TeDP network	130
Figure 5.8 Extrapolated Rolls-Royce and Airbus baseline TeDP network.....	130
Figure 5.9 Rolls-Royce and Airbus TeDP network architecture [23].....	131
Figure 5.10 Comparison of the three identified TeDP propulsion architectures	133

Figure 6.1 TeDP network component configuration.....	141
Figure 6.2 Baseline N3-X T-R graph for 100 % network operation.....	146
Figure 6.3 Probability of achieving at least 50% propulsive power for the N3-X network.	147
Figure 6.4 T-R Graph for the N3-X Single operational MF case	148
Figure 6.5 NASA Hybrid AC/DC network schematic.....	149
Figure 6.6 T-R Graph for probability of 100 % operation of baseline NASA Hybrid TeDP network	155
Figure 6.7 T-R graph for at least 50 % operation of the baseline NASA Hybrid TeDP network	156
Figure 6.8 T-R Graph for single operational MF case of the baseline NASA Hybrid TeDP network	157
Figure 6.9 Rolls-Royce and Airbus TeDP network architecture [23].....	158
Figure 6.10 T-R Graph showing the probability of 100 % operation of Rolls-Royce and Airbus TeDP network	163
Figure 6.11 T-R Graph Showing the Probability of at least 50 % Operation of Rolls-Royce and Airbus TeDP Network.....	164
Figure 6.12 T-R graph showing the probability of at least one operational MF on the Rolls-Royce and Airbus TeDP network	165
Figure 6.13 Comparison of Three Baseline TeDP Networks	167
Figure 6.14 N3-X architecture with added bus ties.....	169
Figure 6.15 NASA Hybrid network with bus tie redundancy.....	170
Figure 6.16 Rolls-Royce and Airbus two SS TeDP network.....	171
Figure 6.17 Rolls-Royce and Airbus TeDP network extended to 4 SS	171
Figure 6.18 T-R graph of three Analysed networks using additional Bus Ties.....	173
Figure 6.19 N3-X Using redundant parallel feeders in MF section to increase reliability ..	176
Figure 6.20 NASA Hybrid network using only parallel MF feeders to increase reliability	177
Figure 6.21 Rolls - Royce and Airbus network using additional parallel MF to increase reliability.....	178
Figure 6.22 N3-X network utilising additional parallel GSCP to enhance reliability	180
Figure 6.23 NASA Hybrid network using GSCP for enhanced reliability	181
Figure 6.24 Rolls - Royce and Airbus network utilising redundant parallel GSCP.....	182
Figure 6.25 N3-X network utilising both parallel GSCP and MFP	184
Figure 6.26 NASA Hybrid network using both MFP and GSCP redundant sections.....	185
Figure 6.27 Rolls-Royce and Airbus Network Using both MFP and GSCP	185
Figure 6.28 T-R graph for parallel feeders studies	187

Figure 6.29 Comparison of redundancy methods when supplying at least 50 % of installed power	189
Figure 6.30 N3-X (left), NASA Hybrid network (centre) and Rolls-Royce and Airbus network (right) architectures using a common protection scheme	191
Figure 6.31 Baseline N3-X TeDP propulsion network.....	195
Figure 6.32 N3-X Baseline Network Sensitivity Analysis	196
Figure 6.33 NASA Hybrid network baseline propulsion network configuration	197
Figure 6.34 Hybrid Network Sensitivity Study	199
Figure 6.35 Rolls-Royce and Airbus concept baseline architecture	200
Figure 6.36 Sensitivity analysis of the Rolls-Royce and Airbus TeDP network	201
Figure 6.37 TeDP Network schematic showing motor connections and failed MF highlighted in black.....	204
Figure 6.38 FTA of N3-X baseline propulsion network.....	206
Figure 6.39 N3-X network with parallel GSC and MF.....	208
Figure 6.40 FTA of N3-X network utilising both GSCP and MFP	211

List of Tables

Table 0.1 Definitions of reliability terms as defined by the computer dictionary	xviii
Table 1.1 Future aircraft goals as championed by NASA [24, 25].....	2
Table 2.1 NASA’s Original Future Aircraft Goals [16]	19
Table 2.2 NASA’s Updated Future Aircraft Goals [18]	20
Table 2.3 Selected Differences between TeDP and MEA Aircraft Electrical Systems	40
Table 3.1 Thrust Requirements for two TeDP Configurations [11]	60
Table 3.2 Markov Example 2 component, 4 State Network State Table	78
Table 3.3 System State Table.....	79
Table 4.1 Network Components	91
Table 4.2 Reliability of Network Components	112
Table 4.3 Enhanced Probability of Success for Additional Motors and a Single GSC	116
Table 4.4 Probability of 100 % Successful Power provision of an n MF, m GSC TeDP Network	117
Table 4.5 R_S for $k = 1$ -out-of- n Feeders Correctly Supplying Power.....	118
Table 5.1 Network Components	123
Table 5.2 Comparison of TeDP propulsion network features.....	134
Table 6.1 Network Components and Failure Rates	138
Table 6.2 Network Components and Reliability Values.....	139
Table 6.3 Probability of 100 % operation of the N3-X baseline network.....	142
Table 6.4 Probability of 50 % operation of the MF in the N3-X baseline network.....	143
Table 6.5 Probability of at least one operational MF per GSC in the N3-X baseline network	145
Table 6.6 Probability of 100 % operation for baseline NASA Hybrid network	151
Table 6.7 Probability of 50 % operation for baseline NASA Hybrid network	152
Table 6.8 Probability of at least one MF per GSC operating for the baseline Hybrid network	154
Table 6.9 Probability of 100 % operation of the Rolls Royce and Airbus concept aircraft. 160	
Table 6.10 Probability of Operation of at least 50 % of the Airbus and Rolls-Royce network	161
Table 6.11 Probability of at least one MF per GSC operating for the Airbus and Rolls-Royce network	162
Table 6.12 Network reliability when using bus tie redundancy.....	172

Table 6.13 Network reliability when using four parallel MFP per MF1 and supplying at least 50 % power	179
Table 6.14 Network reliability using 4 parallel GSCP sections.....	183
Table 6.15 Network reliability when using both 4 GSCP and 4 MFP	186
Table 6.16 Network reliability when using a common protection system configuration	192
Table 6.17 N3-X sensitivity analysis system reliability.....	196
Table 6.18 Hybrid network sensitivity analysis system reliability	198
Table 6.19 Rolls-Royce and Airbus sensitivity analysis system reliability	201

Glossary of Abbreviations

Abbreviation	Meaning
AC	Alternating Current
ADP	Aerodynamic Design Point
AEA	All Electric Aircraft
ARP	Aircraft Recommended Practice
BPR	Bypass Ratio
BWB	Blended Wing Body
CF	Common Frequency
CCF	Common Cause Failure
DC	Direct Current
DoD	Department of Defence
ECS	Environmental Control System
EEC	Electronic Engine Controller
EMC	Electromagnetic Compatibility
EPS	Electrical Power System
ESS	Environmental Stress Screening
ESVR	Electric Systems Validation Rig
ET	Exposure Time
FADEC	Full Authority Digital Engine Controller
GSC	Generator Supply Channel
GSCP	Generator Supply Channel parallel Section
HTS	High Temperature Superconducting
HWB	Hybrid Wing Body
kN	Kilo Newton's
lbf	pounds force
LDN	Day-Night Average Sound Level
LRU	Line Replaceable Unit
LTO	Landing and Take-off
MDT	Mean Down Time

MEA	More Electric Aircraft
MEE	More Electric Engine
MF	Motor Feeder
MFP	Motor Feeder Parallel Section
MTBF	Mean Time Between Failures
MTTF	Mean Time to Failure
MW	Mega Watts
NASA	National Aeronautics and Space Administration
NO _x	Nitrogen Oxides
POA	Power Optimised Aircraft
R	Reliability (of a component)
RGT's	Reliability Growth Trials
RTO	Rolling Take-off
SAE	the Society of Automotive Engineers
SCFCL	Superconducting Fault Current Limiter
SS	Subsection
TeDP	Turboelectric Distributed Propulsion
TRL	Technology Readiness Level
T-R	Thrust Reliability
VF	Variable Frequency
μ	Repair Rate
λ	Failure Rate

Definitions of Relevant Reliability terms

It is important that the terms used within this thesis are properly defined and understood. This table compiles a list of appropriate terms as used within this work and defines them based on the 1990 IEEE Standard Computer Dictionary [32] providing the appropriate context for this work. These definitions are found in Table 0.1.

Table 0.1 Definitions of reliability terms as defined by the computer dictionary

Availability	The degree to which a system or component is operational and accessible when required for use. Often expressed as a probability.
Busy Time	The period of time during which a system or component is operational, in service and in use.
Down Time	The period of time during which a system or component is not operational or has been taken out of service.
Error	(1) The difference between a computed, observed, or measured value or condition and the true, specified or theoretically correct value or condition. For example a difference of 30 metres between a computed result and a correct result.
Equivalent faults	Two or more faults that result in the same failure mode
Failure	The inability of a system or component to perform its required functions within

	<p>specified performance requirements.</p> <p><i>Note:</i> The fault tolerance discipline distinguishes between a human action (a mistake), its manifestation (a hardware or software fault), the result of a fault (a failure) and the amount by which the result is incorrect (the error).</p>
Failure Mode	The physical or functional manifestation of a failure. For example, a system in failure mode may be characterised by slow operation, incorrect outputs, or complete termination of execution.
Failure Rate	The ratio of the number of failures of a given category to a given unit of measure; for example, failures per unit of time, failures per number of transactions, failures per number of computer runs.
Fault	(1) A defect in a hardware device or component; for example, a short circuit or broken wire
Fault tolerance	<p>(1) The ability of a system or component to continue normal operation despite the presence of hardware or software faults.</p> <p>(2) The number of faults a system or component can withstand before normal operation is impaired.</p> <p>(3) Pertaining to the study of errors, faults, and failures and of methods for enabling systems to continue normal operation in the presence of faults.</p>
Idle Time	The period of time during which a system or component is operational and

	in service, but not in use.
Markov process	A stochastic process which that assumes that in a series of random events, the probability for occurrence of each event depends only on the immediately preceding outcome
MTBF (Mean time between failures)	The expected or observed time between consecutive failures in a system or component (see up time).
Redundancy	In fault tolerance, the presence of auxiliary components in a system to perform the same or similar functions as other elements for the purpose of preventing or recovering from failures.
Reliability	The ability of a system or component to perform its required functions under stated conditions for a specified period of time.
Reliability Growth	The improvement in reliability that results from correction of faults.
Reliability Model	A model used to estimate, measure, or predict the reliability of a system; for example, a model of a computer system, used to estimate the total down time that will be experienced.
Up time	The period of time during which a system or component is operational and in service; that is, the sum of busy time and idle time.

Chapter 1

Introduction

The aircraft industry is continually evolving with more novel and advanced concepts and features present on each new aircraft entering into service with the aim of improving operational efficiency. These new concepts serve a number of purposes from increasing aerodynamic performance to reducing fuel burn, acoustic noise level reduction and overall energy usage. One notable concept which has been proposed for aircraft entering into service in 2050 is that of Turboelectric Distributed Propulsion (TeDP) which utilises a number of electrical propulsors connected through an electrical distribution network to wing mounted generators. This chapter will introduce the concept of highly efficient future aircraft, identify some of the research challenges as well as introduce the research topic, objectives and contributions made within this thesis.

1.1 Introduction to Research

Conventional aircraft were designed in an era when oil prices were consistently low and when inefficient, heavy aircraft networks reliant on large volumes of fuel oil could be utilised with minimal perceived cost both in monetary terms and in terms of environmental pollution. In recent years however, social conscience is at an all-time high with environmental lobby against hydrocarbons resulting from greenhouse gases identified as a key contributor towards temperature rises of the climate and stricter political pressure surrounding fuel emissions, it has become necessary to design more efficient aircraft – both in terms of fuel burn and noise emissions. To quantify the necessary efficiency measures, a set of goals for the next three

generations of aircraft, as championed by NASA has been compiled detailing ever-greener standards of aircraft. These are outlined in Table 1.1 below. This move towards more environmentally efficient aircraft has seen advances in airframes to both shield noise through selective engine placement and provide a more aerodynamic shape as well as using advanced aerodynamic concepts to reduce the perceived noise, such as through the use of chevrons on the engine nacelle to smooth the combination of ‘messy’ air at the engine exit [33].

Table 1.1 Future aircraft goals as championed by NASA [24, 25]

Corner of the Trade Space	Technology Generations (Technology Readiness Level 4-6)		
	N+1 (2015)	N+2 (2020)	N+3 (2025)
Shape	Conventional Tube and Wing	Unconventional Hybrid Wing Body	Advanced Aircraft Concepts
Noise Emissions	-32 dB	-42 dB	-71 dB
LTO NO_x Emissions	-60 %	-75 %	-80 %
Cruise Emissions	-55 %	-70 %	-80 %
Aircraft Fuel/ Energy Consumption	-33 %	-50 %	-60 %

The reference vehicle for the N+2 aircraft, is the B777-200 running with GE90 engines, a much larger aircraft than the reference vehicle for the N+1 and N+3 aircrafts, a single aisle B737-800 aircraft running with CFM56-7B engines [24, 25].

While shorter term solutions are most likely to centre on improving the design and utilisation of gas turbines for both propulsion and electrical energy generation and distribution, more advanced approaches may incorporate novel technologies such as

superconducting electrical motors and generators [34] in order to further reduce noise levels and improve efficiency [11, 34].

For more rigorous aircraft goals to be realised, a radical departure from familiar aircraft systems must be made to keep power loading to a minimum, emission levels low and system availability up to 100 times greater than the traditional hydraulic counterpart [26]. One method of achieving optimal energy efficiency, is to consider the move towards a More Electric Aircraft (MEA) and the power saving benefits that follow with an optimally configured Electrical Power System (EPS) [15]. Conventional aircraft consist of four secondary power systems: mechanical, electrical, pneumatic and hydraulic where each system has a similar level of importance; in more modern designs such as MEA these secondary, non propulsive power systems are gradually evolving with more emphasis placed on electrical alternatives [10, 15, 22, 35]. All things being equal, it is self-evident that lighter aircraft have a lesser fuel burn over equal flight durations than heavier aircraft. With this in mind there has been a continued and sustained effort in the industry to reduce weight of aircraft of all types through the use of new designs, materials, technologies and fuels.

With respect to the secondary power systems, through moving to a more electrical equivalent there has been a great degree of interest brought about by the potential savings in weight and efficiency that are (potentially) offered. Replacing the traditional heavy, 'power hungry' pneumatic power (obtained through taking bleed air from the intermediate pressure (IP) or high pressure (HP) compressors [36]) through a series of ducts and valves, gives scope for easily controlled [15], lighter [37] and greener electrical systems. Similarly, hydraulic systems inclusive of large pumps presenting a continuous load upon the system [38] and can cause problems for the network in the case of a failure. Should a conventional hydraulic system leak, this would cause the isolation of the entire circuit and require urgent maintenance [26]. Conversely, Electro-Hydrostatic actuators (EHA) providing localised hydraulic actuation to a number of smaller pumps, require power only when there is a significant demand from a controlled load (such as a change in direction). Additionally, should a fault or leakage event occur on an Electro-Hydrostatic

actuator (EHA), these could be easily isolated and only the specific affected subsystem would require to be removed from operation [38].

Traditionally, pneumatic systems have provided energy for subsystems such as the environmental control, cabin pressurisation and wing anti icing [36] and the hydraulic system powered systems such as the brakes and pumps [26]. While the pneumatic and hydraulic systems may not be completely removed in the first instance [26], by replacing these systems with a more electric alternative, condition monitoring allows faults to be located and isolated, allowing the system to remain operational until maintenance facilities are available.

Two recent examples of greener aircraft moving forward and exploiting these more electrical techniques are the Boeing B787 'Dreamliner' and the Airbus A380 'Superjumbo'. Both aircraft utilise more electrical techniques such as Electro-Hydrostatic Actuation (EHA) [39], however it is the unique no-bleed system [15] concept of the B787 as described below which may potentially offer the first true step towards the future aircraft goals.

The new Boeing B787 combines many advanced techniques such as fabrication from composite materials [40], an electrically controlled Environmental Control System (ECS) [41] and an electric architecture based round the elimination of the pneumatic bleed [15, 41]. The electrical systems on Boeing's B787 replace most of the pneumatic counterparts found in traditional commercial Aircraft [14, 15]. The replacement of these systems is the result of the aircraft's unique 'no bleed' engine, with no heavy bleed air ducting, allowing all the air entering into the core of the engine to be turned into thrust. Producing thrust in this more efficient manner results in up to 35 % less power being extracted from the engines for non-thrust producing purposes [15, 41]. This alternative more-electric architecture, similar to that of the A380 has variable frequency power generation. The power is then conditioned in an electronics bay before being distributed around the aircraft. By drawing less power, less fuel is burned, and as a result, in the cruise section of the flight envelope alone, this useful fuel saving can amount to 1-2 % on conventional aircraft [15].

The no bleed system has many advantages, including a predicted 3 % fuel saving over other aircraft due to efficient secondary power extraction and transfers [15] which helps to reduce fuel burn in keeping with achieving future aircraft targets. These savings are predicted based on simulations carried out prior to the introduction of the aircraft so may be optimistic to increase the appeal of the new aircraft to operators. The use of modern power electronics and reduced number of components in the engine of the state of the art electrical system helps to increase aircraft reliability levels, coupled with reduced maintenance costs from a simplified construction by using a small number of electrical components allows for shorter aircraft out of service times [15]. There are significant weight benefits for the system resulting from the removal of the heavy and expensive titanium ducting for the distribution of the bleed air around the aircraft, which more than offsets the weight penalties associated with the additional electrical components as part of the more-electric architecture [10, 15].

Both the EHA system of the A380 and the no bleed system of the B787 show extremely positive steps towards achieving the required performance levels of the N+1 aircraft. Work to further remove the bleed system and hydraulic systems should contribute towards the more challenging N+2 goals [15, 26]. The B787 alone has made a notable step towards the realisation of NASA's goals with a 20 % reduction in fuelburn, CO₂ emissions and a noise footprint 60 % smaller than that of the B767, plus a reduction of NOX emissions by 28 % on 2008 industry standards.

Another key area where improvements can be made to the efficiency of an aircraft electrical system, is in the engine, where a number of More Electric Engine (MEE) concepts are under consideration [22]. Concepts such as electric fuel pumps, electric actuation systems as well as active magnetic bearings all contribute to the operation of an electrical engine with all of the conventional gearbox-driven systems replaced with new state of the art electrical alternatives [22]. These more electric engine concepts have been successfully demonstrated on the electrical systems validation rig (ESVR) as part of the power optimised aircraft project [22]. Through the ESVR tests it was shown that large engines with more-electric counterparts to their traditional alternatives, suitable for use on a commercial aircraft were viable and that

technologies for supporting the MEE were also viable. It was realised that these MEE techniques, utilised as part of the POA programme, could reduce non-propulsive power consumption by approximately 35 % on a conventional aircraft [10, 22, 35]. These technologies however remain at a low TRL and as such may not be instantly integrated into modern day aircraft designs.

It has also become apparent, through studies undertaken by organisations such as NASA [16] the traditional tube and wing shape of the aircraft does not offer the optimal airframe shape. In addressing this matter, further aircraft efficiency improvements can be realised. Instead swept wing designs, specifically the Blended wing body (BWB) style aircraft has particular advantages with regards to noise experienced on the ground as noise emissions experienced are far lower [42].

1.2 Evolution of Aircraft towards TeDP Architectures

Through utilising a combination of these energy efficient techniques, the Turboelectric distributed propulsion (TeDP) concept was created. This concept combines a blended wing body airframe with a number of embedded electrically driven propulsors located along and spanning the aft of the airframe [16]. These motors and propulsors are configured in such a manner that symmetrical thrust may still be maintained even in the event of a single engine failure [16]. Using a superconducting DC distribution system the propulsion motors can be electrically connected to a number of wingtip generators, allowing the generator and motor shaft speeds to be decoupled, hence minimising electrical losses [43]. Providing the connections in this manner, combined with the use of power electronics allows the electrical system to act as a variable ratio gearbox [16]. DC transmission is further used to address the synchronisation challenges which arise when connecting multiple generators to a single bus [44].

In order for the TeDP concept to be competitive against more conventional propulsion system configurations, it is necessary to use superconducting machines with high power densities, significantly exceeding the 3-4 kW/kg typically associated

with conventional technologies [44]. To ensure that the system temperature remains within operating limits, cryogenic coolers will also be required [20]. These however add further weight to the system, detracting from the total available mass for the propulsion system. Research work looking to increase the efficiency and reduce the weight penalty attributed to cryogenic systems has been carried out through a partnership between Rolls-Royce and Cranfield University and has been published in [45, 46].

With the identified changes from conventional aircraft advancing architectures towards more efficient TeDP designs, a new generation of aircraft is slowly emerging. The specific architectural details of this new generation of aircraft are steadily being developed and early stage architectures being proposed as detailed within Chapter 2 sections 2.9 and 2.10. As with any aircraft concept and especially in the early stages of development, the need to study the reliability of the architecture is of utmost importance to ensure that the safest designs are carried forward. The work of this thesis will investigate the reliability of three predefined TeDP networks to determine which concept proves the most reliable and which redundancy methods can help to most effectively enhance network reliability.

1.3 Research Motivations

Existing research work in the TeDP field has mainly been conducted by NASA with a number of papers published by NASA Glenn Research Centre [11, 16, 34, 42, 47]. These publications covered a number of aspects of the TeDP concept such as the specific weight and efficiency trades offered by network component selections in [42] and how different conductors and superconducting components affect the aircraft efficiency, concluding that advances in the materials (such as composites and superconducting cables) used would further the concept to becoming a reality within [34]. The work within [47] reviews the turbogenerators and embedded engine performance while [11] and [16] focus on the aerodynamic aspects of the Hybrid Wing Body airframe and how they compare to the future aircraft goals.

Another body of work was led by Rolls – Royce North American Technologies [19, 43, 48, 49]. [43] and [49] reviewed the N3-X architecture, reviewing architecture trade-offs and component considerations: these papers described both the baseline network and how the network could be altered to introduce redundancy as well as how voltage levels and protection systems would have to adapt to enable the propulsion system to operate as desired. The work of these papers was expanded upon in [19] where further analysis was run on thrust requirements and yaw moments achievable from the effects of thrust vectoring. This work made a number of assumptions based upon the predicted failures and the effect on the network without a full analysis of the effects to both network reliability and unit capacity, importantly omitting the effects of common cause failures. While the electrical system, in particular the efficiency, operating voltage and temperature of electrical components, forms a part of the more recent considerations, the majority of the existing research material concerns aerodynamic and mechanical considerations [48].

As this field continues to mature it has become a timely consideration for the reliability of such concept aircraft to be studied so that the feasibility of the aircraft may be more fully explored. After safety, a high reliability of any electrical network is of utmost importance. This minimises the effects of network outages and avoidance of critical failure events. It is necessary that the most appropriate means of analysing the TeDP network for reliability are identified and hence implemented. Furthermore, a complete analysis would be one way of determining the technical competitiveness of the concept; a reliability of thrust analysis (explored in this thesis) helps to determine any relevant oversizing of heavy electrical machines and other associated network components which contribute to the weight penalties exhibited by the network. A complete and thorough reliability analysis at this stage is a key part of understanding how the network operates and how fault events are linked and how they impact upon the operation of the network as a whole. An effective reliability analysis is also important at a low pre-prototype TRL level so that costs may be kept to a minimum and any identified short fallings in the network may be identified at an early a stage as possible. Research identifying highly reliable network designs allows poor performing networks to be discounted and research efforts focussed on

enhancing the operation of the network constituent parts or components that with additional effort could further improve the reliability of the network.

As noted previously, the available research on TeDP has focussed upon the aerodynamic and mechanical aspects of the concept [11, 16, 34, 47] with comparatively less research being undertaken on the electrical system. More recent studies however have focussed on the voltage levels [50, 51] and upon expected fault behaviours of superconducting networks [52] as well as upon proposed parallel generation architectures for civilian aircraft in [53]. The work of this thesis has addressed this by analysing the electrical system of a TeDP concept aircraft and provides a reliability analysis on a number of suggested variations of the concept. This includes a method which allows a novel analysis of aircraft reliability for both full and partial operation of a TeDP network and has identified a unique means by which to compare networks based on a number of parameters namely, reliability and thrust available to the network.

1.4 TeDP Network Reliability Considerations

Commercial aircraft must adhere to strict safety legislation stipulating that any critical failure must occur with a rate not greater than once in every 1×10^9 hours [17]. This figure has currently not been updated in line with the development of future concepts however it has been used in existing studies for TeDP as the comparison metric [19]. It has been recognised that not every failure occurring on an aircraft electrical system will lead to a critical failure. Through using methods such as the k -out-of- n analysis presented within Chapter 4 of this thesis, the probability of a critical failure can be determined as well as the likely combination of faults which would lead to such a failure in the context of TeDP electrical network.

Through careful evaluation of failure modes within the TeDP network and the determination of the probability of each failure event occurring, the required overrating and hence weight of selected network components can be determined. For any TeDP network configuration, a number of failure modes may exist including:

failure of a motor, motor feeder, generator or bus; or even in a worst case scenario for propulsion, failure of an engine. However to what extent any component failure affects the overall thrust will depend on the redundancy of the network. In order to better understand the level of overrating required and the impact to available thrust resulting from each individual failure mode, Thrust – Reliability (T-R) trade-offs are considered and an aircraft specific contingency analysis must be undertaken. This is developed within Chapter 4.

This thesis considers the timely requirement for a full and thorough T-R analysis and proposes a number of case studies in Chapter 5 to address this gap in knowledge and its application to the TeDP networks under consideration. The optimisation studies conducted to achieve required reliability targets with minimal weight penalties provide a measure of the effectiveness of system redundancy in maximising available thrust whilst keeping the effects of faults and system weight to a minimum. This will be achieved by evaluating the total available thrust from any fully or partially operational architecture and calculating the probability that this thrust will be supplied. This combined with an assessment of the system's overall mass and volume penalties provides a thorough prototyping method. With the future for the full specification of TeDP and other future concepts still at a very early stage, the results of this thesis provide an early basis for understanding the relative merits of the trade-offs offered in the inclusion of redundancy and component selection within the electrical network. In doing so the thesis contributes new work to the body of knowledge relating to the TeDP network component configuration and further opens up the discussion in this area of aircraft research.

1.5 Contribution to knowledge

In conducting the research work reported in this thesis a number of contributions to knowledge have been realised. These are summarised as follows:

- A methodology has been established that enables Turboelectric Distributed Propulsion aircraft electrical networks to be analysed and assessed in terms of reliability and their ability to provide thrust to a prescribed minimum level.
- The methodology has been applied to future aircraft electrical networks to assess their suitability to achieve at least a minimum level of thrust to a specified level of reliability without compromising system loading integrity.
- The research work on the thrust reliability methodology was published in "A Method for the Evaluation of the Effectiveness of Turboelectric Distributed Propulsion Power System Architectures", see publication list below.
- The first comparison of three published TeDP network concepts in terms of their overall reliability. It has also been analysed how each network compares with the others with reference to a baseline network and as a result of additional included redundancy features.
- The first comparison of how additional redundancy features affect the reliability performance of each of TeDP networks.
- The first fault tree analysis applied to a TeDP network. This work was published in "Failure Analysis of a Turboelectric Distributed Propulsion Aircraft Electrical Network: A Case Study" [130]
- The first academic review and collation of the academic literature on contribution technologies for the evolution of aircraft from the present day to TeDP concepts. An early version of this was published in "Aircraft Power and Propulsion Systems-Research Challenges and Opportunities for Electrical Systems," and "More electric power system concepts for an environmentally responsible aircraft (N+2)"

1.6 Publications

Publications that have arisen as a direct result of the research are listed below:

- Shaw, J. C., Fletcher, S., Norman, P., Galloway, S., Burt, G. "Failure Analysis of a Turboelectric Distributed Propulsion Aircraft Electrical Network: A Case Study", SAE Technical Paper 2015-01-0299, 2015

- Shaw, J., Norman, P., Galloway, S., and Burt, G., "A Method for the Evaluation of the Effectiveness of Turboelectric Distributed Propulsion Power System Architectures," *SAE Int. J. Aerosp.* 7(1):35-43, 2014, doi:10.4271/2014-01-2120.
- Shaw, J., Galloway, S., Norman, P., and Burt, G., "Aircraft Power and Propulsion Systems-Research Challenges and Opportunities for Electrical Systems," SAE Technical Paper 2012-01-2212, 2012, doi:10.4271/2012-01-2212.
- Shaw, Jennifer Catherine, Fletcher, Steven, Norman, Patrick, Galloway, Stuart (2012) *More electric power system concepts for an environmentally responsible aircraft (N+2)*. In: UPEC 2012, 2012-09-04 - 2012-09-07, London.
- Support for *White Paper for High-Power Electric Grid for a TeDP Aircraft NASA RTAPS Follow-On Research*, Michael Armstrong, 05/04/2013
 - Contributions include work on the "Evaluate Impact of Voltage at the System Level" section describing work which would have to be undertaken to upgrade existing capabilities.

1.7 Thesis overview

This thesis will focus on a reliability analysis of the propulsion system of three variants of the TeDP concept aircraft: the NASA and Rolls-Royce N3-X, the NASA Hybrid network and the Rolls-Royce and Airbus AC network. The work will provide a thorough analysis of the three separate TeDP networks comparing the relative merits of each and will present the findings on the TeDP architectures in terms of Thrust- Reliability profiles of each.

Chapter 2 of this thesis will present a thorough review of the aerospace field and the TeDP concept – this will include reasons for the adoption of the concept, the benefits that TeDP has over existing aircraft and the timeframe (in terms of the future aircraft goals) for the adoption of new and novel technologies which will enable distributed propulsion architectures. Chapter 3 will provide an overview of the identified gap in the existing research within the field of TeDP for this work. The chapter will then proceed to identify and provide examples of reliability and failure rate analysis methods through which the TeDP network may be analysed. This chapter will also provide the background for the reliability method requirements presented in Chapter 4. Chapter 4 will continue by introducing the specific reliability problem upon which this work is based and provides a detailed analysis methodology illustrating the method by which the reliability of a TeDP network may be determined and through which the reliability of each network configuration may be compared. This chapter introduces the probable fault modes which the networks may experience as well as illustrating how the Thrust - Reliability (T-R) graph is constructed. Chapter 5 will then provide a number of Case Studies to which the developed methodology will be applied. In this way the effectiveness of a number of redundancy methods used to enhance the baseline reliability may be determined. The Case Studies chapter also presents a sensitivity analysis to act as a discussion point where areas of required additional component research are defined as well as highlighting trends in network construction. To conclude the chapter, an FTA is undertaken on the N3-X network, identifying the most common failure modes and any reliability choke points. The observations from this analysis are used to assess the effectiveness of the previously analysed redundancy methods such as in failure space. Chapter 6 concludes this thesis by summarising the contributions of this thesis and suggesting work which could be undertaken in order to further the research.

Chapter 2

A review of the electrical technologies contributing to the evolution of civil aircraft

Tube and wing style aircraft designs have been in operation since the early days of flying and were made more common due to their extensive use during WWII. While the size and power requirements of aircraft have increased greatly over this time, from the 12 hp 4 cylinder engine on the original Wright brothers aircraft [54] to the 54,400 hp [47, 55] Trent XWB turbofan on the modern A350 XWB, the airframe itself has remained largely the same. This chapter will present an overview of conventional aircraft with regard to their power and propulsion systems as well as an overview of the shift towards the More Electric Aircraft (MEA). The overview of the MEA will then lead naturally into the reasons for adopting new concepts and provide some of the background for studying the Turboelectric Distributed Propulsion (TeDP) aircraft, and in particular the reliability considerations of such a dramatically different aircraft. The chapter will then conclude with contributions and areas identified for further study within this thesis: A selection of reliability methods used to analyse network architectures are described separately in Chapter 3.

2.1 Overview of Aircraft Electrical Systems: 1950 to Present Day

The Vickers Valiant, introduced in the 1950's exhibited electrically actuated landing gear which signalled the change of the power requirements for modern aircraft [56]. The landing gear required four 115 V AC generators each powered from a separate engine. To allow for no break power, these generators were paralleled thus increasing the level of both control and protection circuitry [17]. Since the introduction of this aircraft the power requirements have continued to increase, with the most recent passenger aircraft, the Airbus A350 XWB exhibiting an upper AC voltage of 230 VAC [57]. These increasing voltage requirements are highlighted in Figure 2.1.

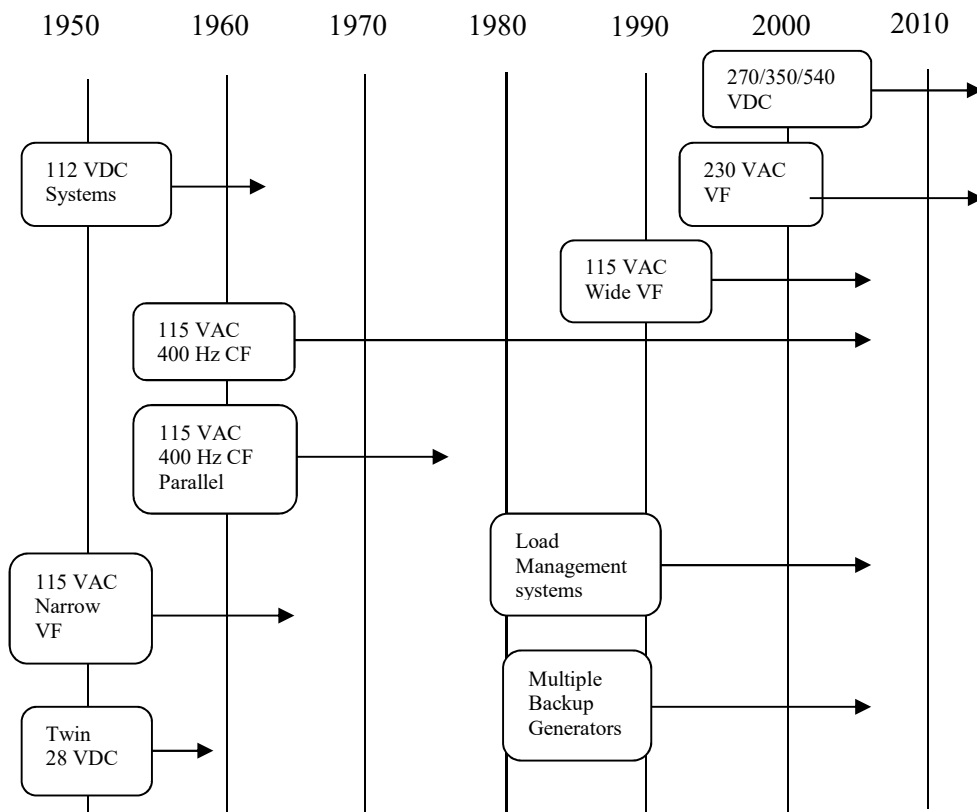


Figure 2.1 Timeline of aircraft electrical systems upper voltage levels [17]

Figure 2.1 shows that since the 1950's aircraft voltages have not only increased but the preferred operating frequency has also changed. Higher voltages have been

adopted in line with greater aircraft power requirements for both critical flight instruments as well as passenger entertainment systems [58] while the adoption of 400 Hz systems allow for smaller, lighter transformers [58]. Operation at this frequency however means that the system can be susceptible to voltage drops resulting from the inductive properties of the current carrying conductors [131]. The evolution of aircraft systems from this point in the 1950's until the present day also includes use of not only AC voltages but additionally DC voltages in both single and parallel channel configurations [17] as well as either one or two electrical generators per engine. Present day aircraft may exhibit, in the case of the A380, up to four 150 kVA VF generators and two 120 kVA CF generators, many times that of aircraft from relatively recent years [36].

The ever evolving nature of aircraft as defined above requires the continual introduction of new and novel technologies to drive improvements and enhance efficiency within the networks' operation. The evolution of these technologies can be measured against a standardised system of requirements which requires each technology to demonstrate and adhere to in order to achieve each grading within the system. Two separate sets of linked requirements exist developed by both the US [59] and NASA [5]. The system of metrics used within this thesis is the TRL system developed by NASA.

2.1.1 What are TRL's and why are they Relevant?

Technology Readiness Levels (TRL's) are a measurement system by which to measure the maturity of an individual technology or group of technologies in a larger system [5]. This method of classification is used within the aircraft industry to provide a set of metrics by which to compare technologies coming into service. For example in Table 1.1 it states that the technologies considered for each new generation of aircraft must be at a suitable and comparable stage of development as defined by this ranking of technology readiness. This particular classification system has 9 individual milestones as shown in Figure 2.2, ranging from the most basic principles exhibited at level 1 through to the most stringent and thoroughly tested at

level 9. Each readiness level consists of a number of parameters and developmental milestones through which a particular technology is assessed before a TRL level is assigned [5].

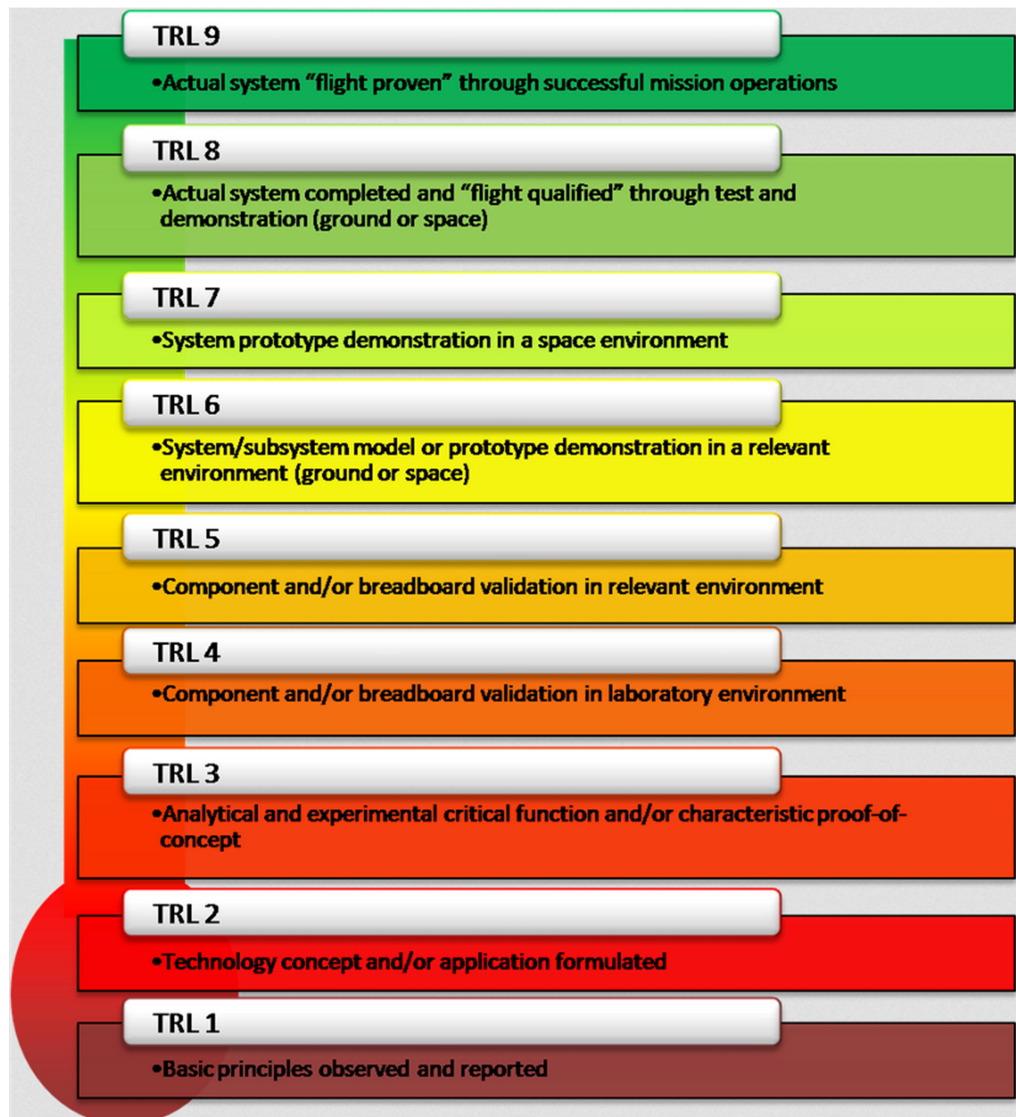


Figure 2.2 Technology Readiness Levels [5]

Figure 2.2 shows all 9 TRL's. It also shows that advancing from TRL 1-3 requires the active study of a concept, where TRL 2 is completed once all the basic principles have been studied and developed and the findings have been applied to a practical application. TRL 3 is then gained when active research has begun. It is in this stage that a proof-of-concept model is constructed and viability studies are undertaken to ensure that the concept may proceed through the technology levels. TRL 4 and 5 can

then be achieved once the studies of TRL 3 have been completed: here a number of components are tested together and once more rigorous breadboard testing is undertaken the technology can achieve a TRL 5 rating. TRL 5 tests include those in environmental conditions as close to that of the intended operating environment as possible. Once this has successfully been demonstrated, the technology moves on to TRL 6 where a fully functional prototype of the technology is expected in order to progress to TRL 7. At this technology level the working prototype must be demonstrated in a space environment in order to gain TRL 8 where the technology may be flight qualified and ready to use in an existing system. During operating in a pre-existing system, if the technology in conjunction with the pre-existing system successfully completes the mission then the technology is advanced to TRL 9.

Through the provision of a clear set of milestones for technologies to be scored against as work progresses a clearer understanding of what remains bring these new technologies in line with the industry standard hence becomes clearer. This scoring system can allow developers to more accurately provide timescales for introduction to service and further enhance the move towards MEA and eventually concepts such as TeDP. Understanding technology development and readiness is an essential factor when planning the future of aircraft concepts such as the Future Subsonic aircraft goals as described within section 2.1.2.

2.1.2 NASA Future Subsonic Aircraft Goals

With the “boom and bust” volatility of global oil prices and the consequences of tighter legislation governing greenhouse gas emissions becoming ever stricter [60], it has become increasingly necessary to design aircraft with optimal levels of efficiency both in terms of their environmental impact and fuel burn. In December 2006 NASA embarked on a Future Subsonic Fixed Wing Project [61]: to quantify the necessary efficiency measures and emissions cuts, they compiled a set of goals, detailing ever greener standards of aircraft as outlined in Table 2.1.

Table 2.1 NASA’s Original Future Aircraft Goals [16]

Corners of the Trade Space	Technology Generations (Technology Readiness Level 4-6)		
	N ^a +1 (2015)	N ^a +2 (2020)	N ^a +3 (2030)
	Relative to B737/CFM56	Relative to B777/GE90	
Shape	Conventional Tube and Wing	Unconventional Hybrid Wing Body	Advanced Aircraft Concepts
Noise Emissions	- 32 dB	- 42 dB	55 LDN at average airport boundary ^d
LTO NO _x Emissions	- 60 %	- 75 %	Better than - 75 %
Performance: Fuel Burn	- 33 % ^b	- 40 % ^b	Better than - 70 %
Performance: Field Length	- 33 %	- 50 %	Exploit metroplex ^c concepts

a “N” represents current state of the art aircraft

b An additional reduction of 10 % may be possible through improved operational capacity

c Concepts that enable optimal use of the airports within metropolitan areas with shorter runways

d The average day-night noise levels over a 24 hour period, where the noise levels between 10 pm and 7 am are artificially increased by 10 dB to account for increased public annoyance

Table 2.1 shows that with each successive generation of aircraft there is a step change in the requirements for efficiency improvements. It can be seen that the greatest performance improvement comes in the form of reduced fuel burn – where there is a requirements to reduce this by over 75 % on 2006 levels [11, 16]. Another goal of note is the performance field length (runway lengths): it is intended that more aircraft make use of Cruise Efficient Short Take-off and Landing (CESTOL) principles [11, 16, 47, 62] to utilise more of the smaller, regional airports allowing

more point to point flights in place of using airport hubs. In 2012 these goals were updated to become more stringent and are shown in Table 2.2 [24, 25, 63].

Table 2.2 NASA’s Updated Future Aircraft Goals [18]

Corners of the Trade Space	Technology Generations (Technology Readiness Level 4-6)		
	N+1 (2015)	N+2 (2020)	N+3 (2025)
	Relative to B737-800 using CFM56-B engines	Relative to B777-200 using GE90 Engines	Relative to B737-800 using CFM56-B engines
Shape	Conventional Tube and Wing	Unconventional Hybrid Wing Body	Advanced Aircraft Concepts
Noise Emissions	- 32 dB	- 42 dB	- 71 dB
LTO NO_x Emissions	-60 %	- 75 %	- 80 %
Cruise Emissions	-55 %	- 70 %	- 80 %
Aircraft fuel/ Energy Consumption	-33 %	-50 %	- 60 %

The most noticeable change in the performance goals of Table 2.2 over Table 2.1 is the move away from the metric of fuel burn and instead naming this parameter, Aircraft Fuel/Energy consumption. Through including this change to the metric the desired move towards MEA and the All Electric Aircraft (AEA) can be incorporated and represents power savings throughout the aircraft: as different technologies move forward, improvement in areas such as thermodynamic efficiency, electric actuation and airframe technology may contribute towards this goal [64]. Additionally Table 2.2 shows a significant increase from Table 2.1 in the level of desired cruising, landing and take-off NO_x emissions exhibited as well as defining a definite noise goal for the N+3 generation.

Both Table 2.1 and Table 2.2 show how stringent targets have been compiled for future aircraft generations. As noted in both versions of the table, savings of a large magnitude must be made against conventional aircraft to reach the N+1 generation of

goals necessitating major improvements in aircraft design. It is also apparent that in order to achieve the N+2 and N+3 targets, advanced concepts such as TeDP must be considered. This chapter will now describe both the MEA/AEA and TeDP concepts in detail to demonstrate how both aircraft types may provide viable solutions for these goals.

2.2 Overview of Current/Conventional Aircraft

In order to provide a baseline to compare the benefits afforded by the MEA, first it is important that conventional aircraft have been described and their merits understood. This section will review modern day aircraft electrical networks for propulsion before moving on to describe the MEA.

2.2.1 Conventional Aircraft Power Systems for Propulsion

Conventionally, aircraft make use of two to four turbofan engines, each with an associated generator on each to transform the kinetic energy of the jet flow into electrical energy [65]. Conventional aircraft make use of 4 secondary non propulsive power systems: pneumatic, hydraulic, mechanical and electrical, each with a similar level of importance in the operation of an aircraft. This is illustrated in Figure 2.3.

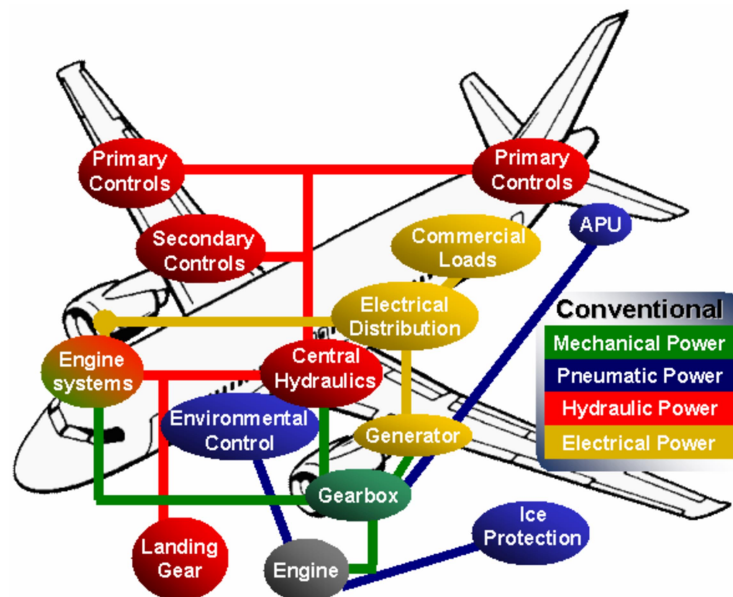


Figure 2.3 Conventional aircraft power sources [10]

Figure 2.3 shows how each of the four different power sources are used within the aircraft as well as showing how they are interlinked. Pneumatic power for the aircraft is drawn from the bleed air of the high pressure compressor. Traditionally this is used to power the environmental control system and supply hot air for the wing anti icing system [10]. Mechanical power can also be extracted from the aircraft engines through the use of an accessories gearbox which provides power to the central and local hydraulic pumps and other mechanical subsystems [10] such as electro-mechanical and electro-hydraulic actuation [66]. The hydraulic system of the aircraft provides an effective yet heavy power system for both primary and secondary flight controls [67]. This power system provides power to both the primary and secondary flight control surfaces actuator systems [10] as well as aircraft landing gear and retractable undercarriage and braking systems [67].

The accessories gearbox also provides mechanical power to the generators located at the engine [10]. These generators provide the avionics, galleys and cabin with the required electrical power [10]. Figure 2.4 illustrates an example of how the electrical system is configured in greater detail.

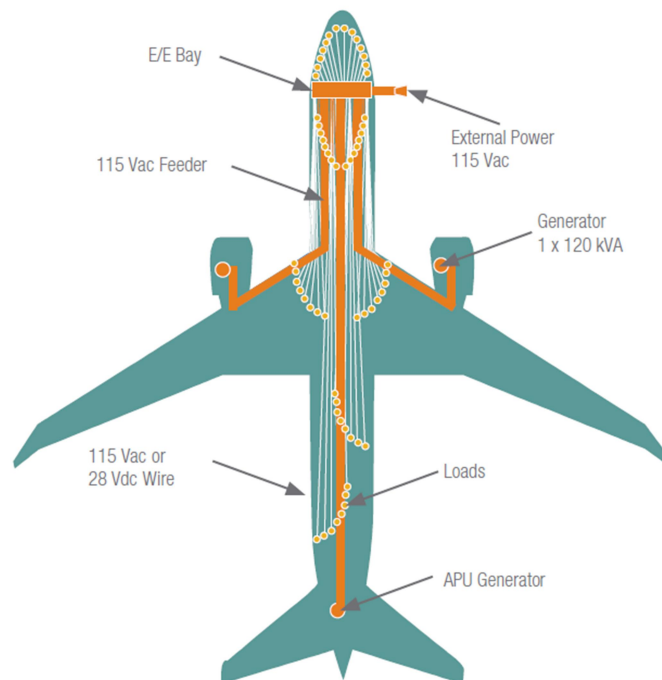


Figure 2.4 Layout of conventional electrical network [15]

Figure 2.4 shows a traditional aircraft electrical network. It can be seen that in this configuration that power is routed from the engines to a centralised electronic and electrical bay. From the centralised bus, long heavy cables connect and supply loads with the required electrical power [15]. It can also be seen that from this point both AC and DC wires extend around the network to locations to supply the required power.

2.2.2 *Turbofan Engines*

Conventionally the power for both thrust and for the secondary power plants of an aircraft is derived from a number of turbofan engines located on the wings and tail plane of the aircraft [68].

In a turbofan engine [13], air is compressed in a compressor which is then sent into a high pressure combustion chamber or combustor where fuel is subsequently added and burned. Upon exiting the combustor stage, the hot, high pressure air enters a multi stage turbine before the hot exhaust gasses leave through the rear of the engine providing the required propulsion. This can be seen in both Figure 2.5 and Figure 2.6 illustrating simplified diagrams of air flow and central components of both a two shaft Figure 2.5 and a three shaft Figure 2.6 engine.

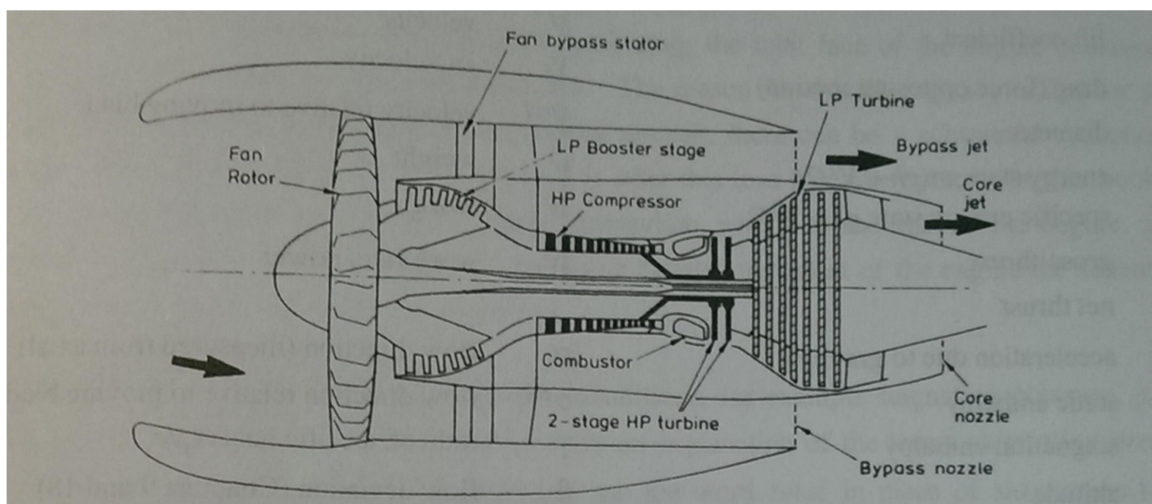


Figure 2.5 Two shaft high bypass turbofan engine [13]

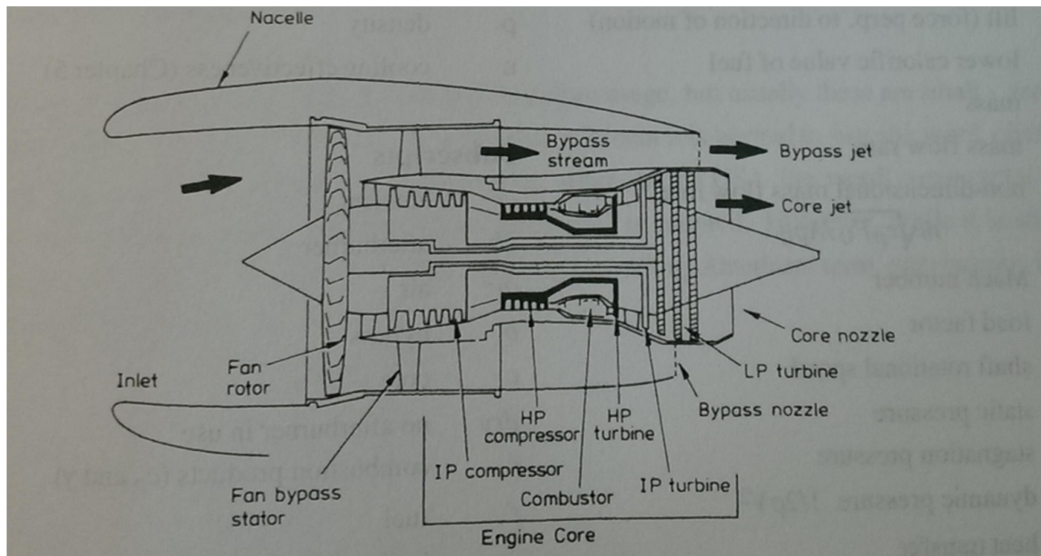


Figure 2.6 Three shaft high bypass turbofan engine [13]

The figures schematically illustrate that upon entering the turbine fast flowing air either enters the central core of the engine or may pass through the bypass stream: it is the ratio of the air through the core of the engine to that through the bypass stream which gives the engine's bypass ratio [13, 69]. The bypass of the engine allows the engine to operate quieter and helps to provide more thrust at lower rotational speeds [69]. The air flow which passes through the core of the engine (the compressor, combustor and the turbine) is conditioned to produce hot, fast flowing exhaust gas at the exit at the core nozzle as shown in both Figure 2.5 and Figure 2.6 [70]. The air which is diverted into the core of the engine is accelerated rearwards to be ejected at the nozzle at a slightly elevated pressure of 1.6 times that of normal atmospheric pressure at take-off [70] and at jet speed [70]. The air is first passed through the engine's compressor: a series of bladed disks ("blisks" [71]). These blisks force the air passing through into a continually smaller area and hence the air is squeezed and compressed while undergoing only a relatively small increase in temperature. The turbines at the rear are connected via a shaft to the compressor as well as the intake fan at the front of the engine: alternate blisks are either fixed or rotate with the shaft. This compressed air then enters into the combustor where the fuel is injected, mixed and then burned, increasing the temperature significantly while maintaining approximately the same pressure (Boyle's Law). Upon exiting the combustor the hot,

fast flowing and expanding air passes through the low (LP) (intermediate (IP)) and high pressure (HP) turbines where work may be extracted from the rotating blades. Most of the pressure created in the core of the engine is used in the low pressure turbine: the pressure is spent through repeatedly accelerating the flow of air through a set of rotors which extract shaft work [70]. The air which has passed through the core of the engine leaves through the nozzle at a different speed to that which has passed through the bypass and mixes causing the exhaust which results in a forwards thrust [72].

The principles of operation of a turbofan engine are important, not only for conventional aircraft but for future aircraft too. Near future concepts such as More Electric Aircraft (MEA) as well as far-future concepts such as Turboelectric Distributed Propulsion (TeDP) both make use of a form of turbofan engines for either thrust [35], subsystem generation of electrical and mechanical energy [11] or both [10]. Other proposed future subsonic aircraft, such as those presented within section 2.10 would also make use of a form of turbofan engines.

2.3 The More Electric Aircraft: The future of air travel?

For the N+1 aircraft concepts to be eventually surpassed, not only is a significant departure from traditional tube-and-wing airframe shape likely required [18, 73], a radical departure from familiar aircraft systems must be made to keep power off-takes to a minimum, emission levels low and system availability up to 100 times greater than the traditional hydraulic counterpart [26]. One method of achieving optimal energy efficiency is to adopt an MEA and enable the power saving benefits that follow with a suitably (optimally) configured Electrical Power System (EPS) [15]. The removal of power hungry hydraulic and pneumatic systems gives scope for easily controlled [15], lighter [37], greener electrical systems which, given the correct redundancy can provide the same if not better levels of reliability and reduce hours lost to maintenance [26]. While the pneumatic and hydraulic systems may not be completely removed in the first instance [26], by replacing the systems with a more electric alternative, condition monitoring could allow faults to be located and

isolated and for the system to remain in operation until maintenance facilities are available [39].

Looking further to the future, there is potentially much greater diversity in radical more-electrical system architecture design [16], an example of which can be seen in the Hybrid Wing Body (HWB) aircraft concept shown in Figure 2.7 [20].

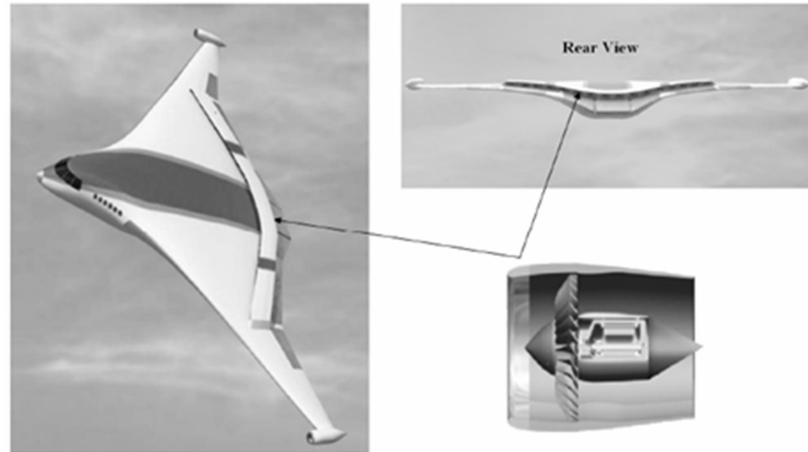


Figure 2.7 Side and rear view of a 16 fan HWB aircraft and a cross section of a superconducting engine [20]

This HWB concept makes use of an electrical propulsion system utilising a number of electrical motors which are powered via a superconducting gas turbine at each wingtip. A more detailed review of the TeDP concept will be provided in section 2.7 of this chapter.

2.3.1 Power Optimised Aircraft project

The reasons for the shift towards a MEA was summed up in the Power Optimised Aircraft (POA) project [10, 21], which aimed to create an aircraft which could run more efficiently than current day aircraft and was based on the MEA concept [10]. The POA project had several outcomes, which was hoped would be achieved over the course of the 6 year study and are noted below:

- Reduction of peak non-propulsive power usage of 25 %
- Usage of non-propulsive power to be reduced

- Fuel consumption to be reduced by 5 %
- Reduction of overall equipment weight

The objectives of the project were achieved whilst simultaneously not having any adverse impact upon reliability, production or maintenance costs [10, 21]. To achieve the proposed goals, the architecture in Figure 2.8 [10, 21] was proposed, shifting the supplied power away from traditional hydraulic and pneumatic systems and concentrating more on electric power and on local hydraulic loads.

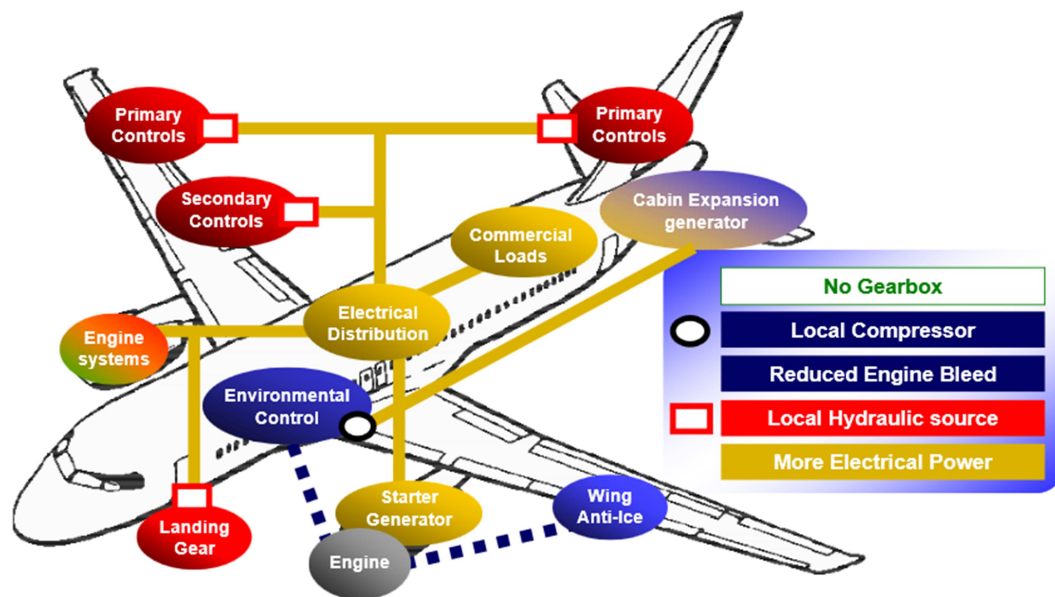


Figure 2.8 Power Optimised Aircraft [10, 21]

Aircraft have traditionally had a large peak power rating in order that the large, heavy, generation equipment can sufficiently supply the peak system loads, which usually occurs during take-off and the initial climb and during the final approach and landing [10]. The main peaks during these flight phases are caused by the operation of the landing gear and secondary flight controls supplied from the power intensive central hydraulic and mechanical systems. When powered by a local hydraulic source and the electrical system on the POA, the peak power drawn was reduced by over 25 % on a traditional aircraft [10], the maximum required load of the generation was smaller and could be sized smaller, thus incurring a lower weight penalty [10]. Due to the increased weight attributed to the on-board electronics [10] of the MEA electric systems over traditional aircraft systems, it should hold that the heavier,

MEA would result in a higher fuel burn; however, the fuel consumption on the POA MEA is far smaller in comparison, than the conventional aircraft. The POA project demonstrated a 2 % reduction [10, 21] in fuel burn from current aircraft which can be attributed to the more energy efficient electrical systems [21]. Operations using the electrical systems result in fewer losses than the hydraulic or pneumatic counterparts [21]. This is exemplified in the Environmental Control System (ECS), where bleed pressure and temperature are no longer required resulting in 14 % less power being drawn to run this essential operation [10]. This coupled with the independence of electrical system operation in regards to the speed or thrust of the aircraft engine [10] can be directly associated with the reduced fuel burn [10] which in turn corresponds with less overall power consumed in hydraulic and pneumatic sub-systems.

2.4 Current State of the Art: Electrical Systems

The shift towards the MEA has seen an important step forward in recent years with the introduction of both EADS Airbus A380 in 2007 [74] and Boeing's B787 in 2011 [75]. These aircraft demonstrate that the shift towards aircraft with more-electric capabilities in the commercial sector is being embraced by utilising designs and architectures which are pushing towards the N+1 goals. Although both of these aircraft incorporate more-electric sub-systems, the systems in use by each are very different; the A380 architecture contains a series of Electro-Hydrostatic Actuators (EHA) and the B787 has been designed with a unique 'no bleed' system [26, 40, 41], both of which are detailed in the following sections.

2.4.1 An Overview of the Electrical System of the Airbus A380

The A380 as shown in Figure 2.9 is currently the largest passenger plane in service, accommodating up to 853 passengers [76]. It is the first modern passenger aircraft to utilise a variable frequency alternating current (VFAC) electrical system [26], allowing simplification of the drivetrain and gearbox. This change of frequency generation resulted in fixed frequency loads like induction motor pumps being

replaced with loads supplied by power electronic convertors capable of accommodating supply frequencies of between 360 Hz and 800 Hz [14, 26, 77].



Figure 2.9 Airbus A380 [2]

This concept can be extended further to facilitate network functionality. For example, whilst low voltage DC (LVDC) systems such as those currently employed by the A380 [78] are traditionally supplied by passive transformer rectifier units (TRU's), replacing these with a Battery Charger Rectifier Unit (BCRU) comprising an Auto Transformer Rectifier Unit (ATRU) with a controlled DC to DC chopper [26], as shown below in Figure 2.10, provides improved control of the LVDC voltage level. It is also worth noting that the bidirectional DC-DC convertor unit would also be readily applicable to HVDC schemes.

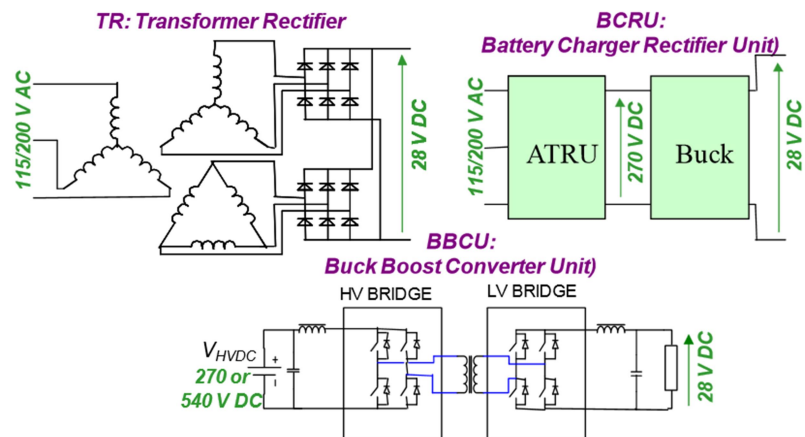


Figure 2.10 Battery Charge Rectifier Unit and Components [26]

The A380 and B787, both share a similar EHA system [39], in which a distributed hydraulic system is utilised. This is an electric system which provides localised

hydraulic actuation to a number of smaller pumps, which is beneficial as localised pumps can easily be isolated in the event of failure and unlike a conventional hydraulic actuator, the EHA only draws power when there is a significant demand from a controlled load (when the aircraft is making a change in direction) [38].

2.4.2 The B787 electrical power system

The Boeing B787 shown in Figure 2.11 combines many advanced techniques such as fabrication from composite materials [40], an electrically controlled Environmental Control System (ECS) [41] and an electric architecture based round the elimination of the pneumatic bleed [15, 41]. The electrical systems on Boeing's B787 replace most of the pneumatic counterparts found in traditional commercial aircraft [15, 41]. The replacement of these systems is the result of the aircraft's unique 'no bleed engine, with no heavy bleed air ducting, allowing all the air entering into the core of the engine to be turned into thrust. Producing thrust in this more efficient manner results in up to 35 % less power being extracted from the engines [15, 41]. Similarly to the electrical architecture of the A380, this alternative more electric architecture also uses variable frequency power generation. The power is then conditioned in an electronics bay before being distributed around the aircraft. By drawing less horsepower, less fuel is burned, and as a result, in the cruise section of the flight envelope alone, this fuel saving can amount to 1-2 % on conventional aircraft [15].



Figure 2.11 Boeing B787 [1]

The no-bleed system has many advantages, including, but not limited to, a 3 % fuel saving over other aircraft due to efficient secondary power extraction and transfers [15] which helps to reduce fuel burn and can help towards achieving the next generation aircraft performance metrics. The use of power electronics in the state of the art electrical system helps to increase aircraft reliability levels which coupled with reduced maintenance costs from a simplified construction using a small number of electrical components, allows for shorter aircraft out of service times [15]. There are significant weight benefits for the system resulting from the removal of the heavy titanium ducting for the distribution of the bleed air around the aircraft which more than offsets the weight penalties associated with the additional electrical components as part of the more-electric architecture [15].

Both the EHA system of the A380 and the no bleed system of the B787 show extremely positive steps towards achieving the required performance levels of the N+1 aircraft. Work to further remove the bleed system and hydraulic systems should contribute towards the more challenging N+2 goals [15, 26]. The B787 alone has made a notable step towards the realisation of NASA's goals with a 20 % reduction in fuel burn, CO₂ emissions and a noise footprint 60 % smaller than that of the B767, [https://www.gov.uk/government/uploads/system/uploads/attachment_data/file/4515/future-aircraft-fuel-efficiency.pdf] a reduction of NO_x emissions by 28 % on 2008

industry standards. The following sections will review the candidate technologies for these goals to be achieved.

2.5 More Electrical alternatives for Conventional Aircraft Systems

While section 2.4 identified how entire aircraft have been redesigned to allow greater overall energy efficiency and to reduce emissions such as NO_x and noise, individual aspects of the architecture may also be adapted to provide more electrical alternatives. This section will provide an overview of a number of such enabling technologies as well as outlining the benefits that they could bring to an aircraft.

2.5.1 The More-Electric Engine

In order for the MEA to advance into an All Electric Aircraft (AEA) the aircraft's engine as well as its subsystems need to be electrically powered [35]. The image of Figure 2.12 below outlines the key technologies separating the MEE from a conventional engine. The MEE used for the POA project¹ composed many benefits, inclusive of improved efficiency, flexibility and the ability to carry a higher level of power [35]. The engine system validation rig (ESVR) for this project further demonstrated that each of the systems conventionally driven by a gearbox could be replaced with a corresponding electrical system [22]. The power generation for the engine came from two parallel connected fault tolerant generators and the distribution of the power within the MEE took place at 350 VDC with the loads connected through power electronic interfaces [35]. The connected loads as shown in Figure 2.12, included electric fuel metering and electrically actuated engine guide vanes [21, 35].

¹ Although the POA project took place in the mid 2000's it remains one of the only MEE public domain projects to date.

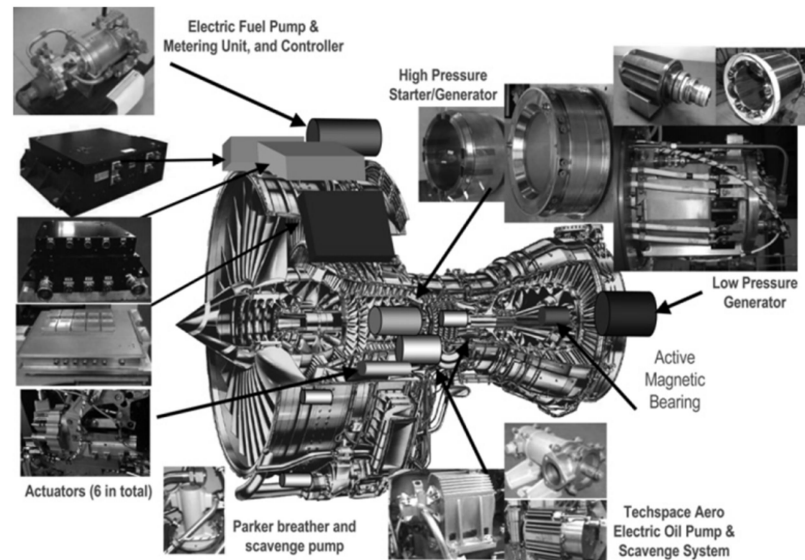


Figure 2.12 The More-Electric Engine [22]

Through the ESVR tests it was shown that large more electric engines exhibiting a number of new technologies which allowed more electric operation than the traditional alternatives were suitable for use on a commercial aircraft and with the correct development path would be viable [10]. The study also found that a number of technologies proposed for supporting the development of the MEE were also viable [22]. The study went on to achieve engine start up using an embedded electrical machine and control fuel and oil flows without pumping excess levels of the liquids [22]. The ESVR managed to prove by using more electric technologies in an engine structure for both propulsion and engine control that the concept is feasible [22], although future work is still required to ensure that the technologies can be successfully integrated to achieve a true POA without encountering any ill-effects.

2.5.2 Electro Hydrostatic Actuation Considerations

The EHA as seen in the Airbus A380 [26] and as proposed in the POA studies [10, 21] utilises a brushless DC or switched reluctance motor driven by a DC voltage source through a power electronic inverter circuit allowing accurate control of the speed of the motor and as such the position of the flight control surface [79]. The flight control surfaces only utilise their full range a small number of times during a

flight envelope and the majority of this movement occurs at take-off and landing [79]. The power delivered to the actuator is proportional to the delivered torque from the motor and to its speed, so high levels of power are only required when the flight control surfaces are moving. When the actuator is not moving the background power requirement only accounts for around 10 % of the peak power required [79]. This is compared to the conventional hydraulic system which requires to be fully powered at all times so that the reserves of hydraulic fluid may be accessed and pumped through the system at any time throughout the duration of the flight [67]. One noteworthy characteristic of an electrical actuator is the ability to regenerate electrical energy during some operating modes [79]. This regenerated power is dissipated as heat in a resistive dump circuit. With an advanced rectifier circuit however, two-way power flows are possible and the regenerated power could be absorbed by other loads within the aircraft electrical network [79, 80]. If usage of the power regenerated by the actuator was not prohibited under current regulations [66] the heavy ‘dump’ circuits could hence be removed allowing for both weight benefits and efficiency increases for the electrical system [80].

2.5.3 Electro-Mechanical Actuation

The addition of a reliable, jam free Electro-Mechanical Actuator (EMA) [39] could see the further operational improvement for future generations of the MEA. The EMA is currently only available for secondary flight control functions as it is susceptible to single point failures which could lead to a mechanical jam [39]. The EMA could potentially provide a number of operational improvements over the EHA if utilised for the same applications, these consist of: elimination of heavy, flammable hydraulic fluid, a reduced requirement for maintenance and a greatly reduced power drain from the engines [39]. A considerable amount of research is being undertaken to address the jamming problems of an EMA [81-83] which can achieve the lesser power drain because, unlike the EHA system, it can be switched to an idle mode when not required and therefore draws a far reduced level of power from the engine [39]. The move away from offline condition monitoring to online methods of predictive and preventative condition monitoring, the advances of fault

tolerant systems and a high level of reliability of the available power electronics and motors should allow the EMA to be a feasible alternative to current primary flight control actuators [39]. The utilisation of online condition monitoring should further enhance the reliability of aircraft electric drives [39] and if implemented successfully the EMA could further benefit the move towards N+2 and MEA goals by taking a step towards eliminating the maintenance intensive hydraulic system [39, 81] and enabling optimal use with other electrical subsystems to reduce engine power offtake [39]. The reduced weight and power offtake and from the engine can help to reduce both the level of fuel burn and in turn emissions levels, both important for achieving the future aircraft goals.

2.5.4 Electrical Protection Considerations for Future Aircraft

Within all power systems however especially in the aerospace sector, the safety of the system is a critical design consideration. As the use of electrical systems within the MEA becomes increasingly widespread, the reliability of these electrical systems and their protection is fast becoming an increasingly critical part of an aircraft's architecture design. Electrical system supply performance requirements are inclusive of [31]:

- That no single point failure should lead to the loss of any channel
- That all mechanisms are fail safe and the occurrence of cascading failures is prohibited
- That no common mode faults should occur that is no single fault should cause disruption to multiple areas of the system
- On-board equipment has to be designed for at least 24 years in service and withstand environmental factors such as: electromagnetic compatibility (EMC), vibrations and acoustic noise.

The increased level of criticality placed on the electrical system is coupled with shifts in the means of power distribution and associated voltage levels. Traditional aircraft electrical power systems (EPS) have consisted of relatively low system voltages of 28 VDC and 115 VAC [78], however with the move to keep the losses associated

with the EPS on the MEA as low as possible, these levels have been increased to 230 VAC and 540 VDC (± 270 VDC) for commercial aircraft [41] and 270 VDC in military aircraft [78]. The changes made in the distribution voltages create a number of challenges for protecting MEA power systems, notably there are a number of unresolved issues in the protection of higher voltage DC networks, particularly those utilising converter interfaces [31].

Solid State Power Controller (SSPC) technologies have shown potential for network protection applications [78]. SSPCs are used as alternatives to traditional contactors or circuit breakers that connect loads to the main distribution bus, providing the functionality to protect loads and components from system overloading and from damaging short circuit currents [78]. The SSPCs provide some major benefits over electromagnetic breakers for this purpose, including a faster switching response time, a greater level of reliability, lower power dissipation and functionality to allow remote monitoring of a load's health and condition [78]. One of the main drawbacks experienced by the use of current SSPC designs is that the current carrying capability is limited and particularly at 270 VDC, their application is restricted to load protection [78]. This particular aspect of SSPC design must undergo major development in order for these devices to be utilised more widely and effectively within the MEA electrical power networks. Technical protection challenges aside, it is of vital importance from a design perspective that the benefits of any new or alternative means of power distribution are not outweighed by any additional protection system requirements. This is an important factor of consideration which will influence the adoption of the MEA concepts for N+1 aircraft designs and beyond.

2.6 The impact of Electrical Power Offtakes on Future Engine Configurations

Future aircraft require a reduction on the current levels of noise emissions by at least 42 dB to meet the N+2 targets and by 71 dB for the N+3 targets [18] and as such new

methods must be sought to reduce the noise level of modern aircraft. Open rotor engines have been identified as one area for increased research, as they have the potential to contribute towards achieving noise reduction and efficiency goals [84]. Using advanced modelling techniques to aid the understanding of an engines noise output, it has been shown that open rotor engines can be designed to emit less noise and therefore help towards the N+2 noise reduction target [14]. If a quiet open rotor engine is to be implemented, efficient means of electrical power off-takes from these engines are required [14]. The nacelle of the open rotor has limited empty space and as such the placing of an electrical generator is a vital consideration in its effective use [14, 84]. Reference [14] carried out a number of trials, varying the placement of the starter/generator and found, that due to a number of reasons associated with weight, efficient power off-takes and ease of access for maintenance, the preferred placement of the starter/generator is within the nose cone. Unfortunately as can be seen from Figure 2.13, when drawn to scale the machine is not entirely enclosed in the nose and as such impedes the airflow path. Until this can be remedied, this option is not viable.

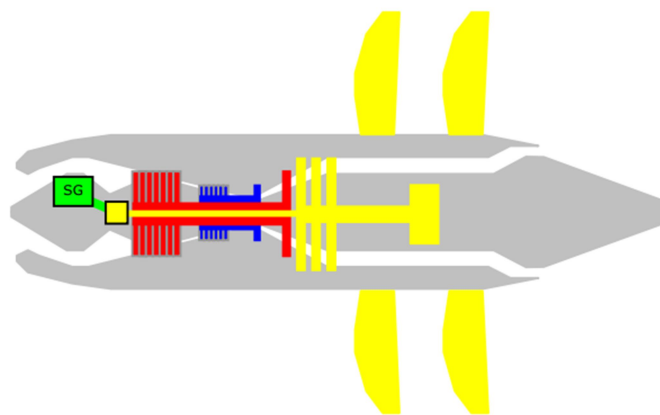


Figure 2.13 Nose Mounted Starter Generator [14]

The offtake options from the free power turbine could be viable with modification to optimise any configuration. A possible increase of the length of the engine by ≈ 25 mm is estimated but related negative effects such as increased weight penalties would need to be further researched [14]. The open rotor option appears promising provided that issues with the clutching mechanism and the size of the nose cone can be addressed.

2.7 Turboelectric Distributed Propulsion for N+3 Applications

Building on the MEA concept and all the enabling technologies presented in sections 2.5 and 2.6, Turboelectric Distributed Propulsion (TeDP) is an intriguing design approach which promises a highly reliable aircraft allowing evenly distributed thrust even in the event of a single engine failure [37]. The current TeDP concept aircraft is based upon a 300 passenger aircraft with both a maximum speed of M 0.84 and a range of 7500 nm [63]. Previous TeDP studies have proposed architectures exhibiting 12-16 high bypass turbofan propulsors embedded on the upper trailing edge of an HWB aircraft airframe, the preferred airframe for N+2 concepts and beyond, with each propulsor providing roughly 31,000 N of thrust [16]. The embedded turbofans are interconnected electrically allowing the required level of redundancy for a single engine failure scenario. The turbofans are further connected to two superconducting wingtip mounted turbo-electric generators to allow the efficiency benefits associated with the MEA or even the AEA [16]. An example of the N3 - X TeDP concept aircraft can be seen in Figure 2.14.



Figure 2.14 N3-X TeDP Aircraft Concept [11]

These TeDP systems in turn may benefit from the introduction of superconducting machines and cryocoolers [20]. The output power density of conventional non superconducting machines is approximately 1 kW/kg [44], limited by the generation of heat in the copper windings [20]. This prevents the weights of these machines

reducing to a level where they could replace traditional gas turbines without significant weight penalty, regardless of any reliability benefits through utilising a known and mature technology, rendering them infeasible [20]. In order for the TeDP concept to be competitive with more conventional propulsion system designs, the use of superconducting machines with power densities significantly in excess of the 3-4 kW/kg typically associated with current technologies will be required [44]. While offering a significant improvement in power density, the reliability of such a fully-superconducting machine remains unproven under normal, ground-based operations and as such proves to be a major risk for this air-based TeDP concept. Cryogenic coolers are also required in order to keep the temperature of the superconducting system within the required operating range [20], adding further weight and complexity to the system and detracting from the available mass intended for other more commercial purposes. As with the fully superconducting machines, however, this technology is in its infancy and hence will also be detrimental to network reliability. Arrangements such as this TeDP system could provide great efficiency from large core engines while maintaining cruise efficiency benefits [37], provided that the emerging technologies are subjected to stringent reliability growth tests to ensure that the reliability of the concept is not compromised.

The use of superconducting machines and their associated electric components such as an electric gearbox can provide an acceptable density and allows for the turbines to rotate independently of the fan shaft, and in turn for the turbine to rotate independently of the generator's speed and therefore more efficiently [16]. Separation of the turbine from the fan shaft means that as the altitude and airspeed change, the speed of the turbines could remain at the most efficient level to provide a reduced fuel burn and allow an increased load efficiency to be achieved [16].

The weight benefit of the superconducting machine over conventional machines at current technology levels is minimal as the operating temperature of superconducting machines lies in the cryogenic region [16] and so some form of cooling mechanism must be associated with the machine. Much work must still be completed so that a feasible, efficient machine with minimal AC losses may be utilised by the aircraft electric propulsion system [20] and as yet, cryocoolers are very inefficient with only

10-15 % Carnot efficiency [20] meaning large heavy coolers must be utilised to maintain the system in the correct temperature range. With technology developments expected over the next 20 years, a lighter more efficient cooling system is expected [16], so the superconducting machines and cryocoolers can be enhanced such that they will become feasible for use within future, reliable aircraft propulsion systems [20].

2.8 Key Differences between MEA Aircraft and TeDP Aircraft Concepts

A key distinguishing factor between current MEA and TeDP network architecture designs is the power level at which critical loads must be supplied [16]. Specifically, the power supply to the high power propulsion motors in TeDP systems must be of similar reliability to the traditional low power critical loads, such as the avionics in present day aircraft. In line with the increased power levels of the aircraft, the voltage levels are expected to rise accordingly. Specifically, the highest voltages utilised in the MEA generation of aircraft are ± 270 VDC and 230 VAC with current levels in line with these. Although there are no firm voltage levels for the TeDP concept aircraft yet, these will reflect the anticipated superconducting system current carrying capabilities [85]. These differences as well as a number of others are summarised within Table 2.3.

Table 2.3 Selected Differences between TeDP and MEA Aircraft Electrical Systems

Comparison Metric	Conventional/MEA	TeDP
Propulsion System	2 – 4 Turbofans with two or three shaft configurations on each	Multiple connected Propulsors and 4 wingtip generators

Power System	<p>4 secondary power systems:</p> <ul style="list-style-type: none"> • Mechanical • Electrical • Pneumatic • Hydraulic 	Increased focus on the electrical system and increased importance on the distribution of electrical power
Electrical Distribution System	Uses both AC and DC distribution	Enhanced use of the DC distribution network making use of the reduced losses over the AC system and the ability to decouple electrical machines rotational speeds
Voltage Levels Used	<p>230 VAC</p> <p>± 270 VDC</p>	Non-standard voltage and current levels to be used in line with the superconducting network capabilities

Table 2.3 shows comparisons over 4 different metrics but this is not an exhaustive list. It highlights that possibly one of the most radical changes to the network aside from the use of superconducting networks is the potential enhanced use of the DC distribution network over the conventional AC network. As noted previously, one of the benefits of this is to allow generators to be used in parallel with no synchronisation problems [86] while another reason for this switch is to increase system reliability [19].

2.9 Example TeDP Network Architectures

The network architecture of a conventional aircraft differs greatly from the expected TeDP network architectures for propulsion with one of the notable features of the TeDP concept being the decoupling of generation and propulsion aspects of an aircraft's thrust production. This section explores three potential TeDP electrical propulsion architectures as developed by NASA [16], Airbus [87] and Rolls-Royce [23] highlighting both the similarities and differences between the three. This section will also provide an assessment of how it is expected each of the three will perform with respect to the other two in terms of overall network reliability.

2.9.1 NASA N3-X Architecture

The TeDP network that has been the subject of most of the available literature has been the NASA and Boeing collaboration's N3-X aircraft [19]. The N3-X features 16 superconducting thrust producing motors connected so that symmetrical thrust (when the same force is exerted in the direction of movement from each side of the aircraft) may be maintained throughout the flight envelope. A DC distribution network connects these rear located motors, each with an associated propulsor to one of two wingtip located turbofan engines, each housing two superconducting generator. A potential architecture for this configuration is shown in Figure 2.15.

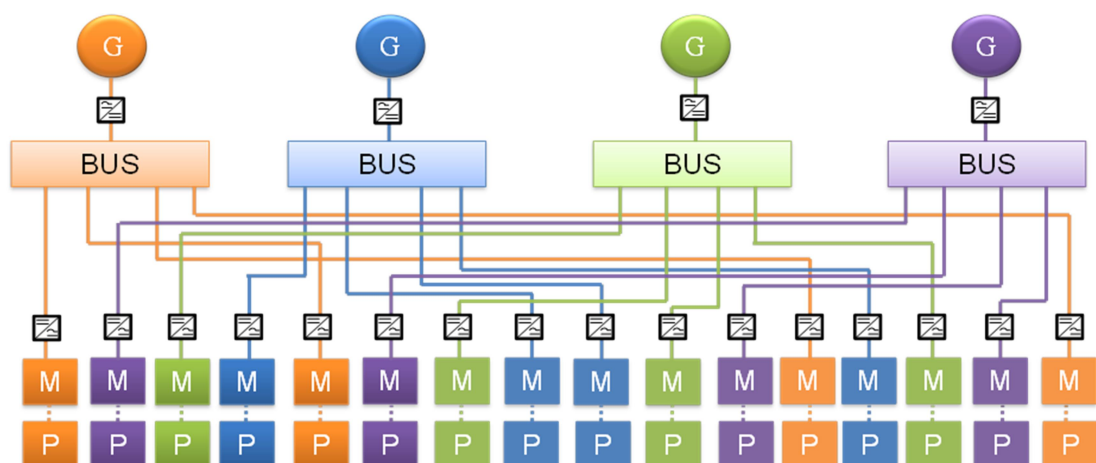


Figure 2.15 16 MF Configuration of a TeDP Network

Figure 2.15 shows how the motors (M blocks) and propulsors (P blocks) of the network may be connected via busbars to the aircraft's generation (G blocks). This architecture uses a predominantly DC electrical distribution network, allowing a number of generators to be connected to the same bus without having to be synchronised. This distribution method also allows the generators and motors to rotate at their own optimal speed and perform at their optimal design point. One additional benefit of the propulsion motors connected in this symmetrical manner is through the use of thrust vectoring to control the roll and yaw moments, the tailplane of the aircraft and associated redundant flight surfaces may be removed allowing additional weight savings [11, 16, 19]. This network architecture is intended to supply at least 22.4 MW of electrical power (30,000 hp in electrical thrust) in order to achieve safe rolling take-off [19, 43, 49] and is the N+3 equivalent of the B737-800, capable of carrying 189 passengers. Protection for this architecture is provided through a number of Superconducting Fault Current Limiters (SCFCL) as well as both DC and three phase breakers [43, 49].

This network architecture consists of a large number of components to protect against dangerous fault currents, potentially overcompensating to the detriment of the overall reliability score. This design does however provide a useful first pass design allowing analysis to be undertaken and new reliability methods for the analysis of the propulsion system to be considered; such as the T-R method described by this work.

2.9.2 Airbus and Rolls - Royce E-Thrust Concept

Another TeDP aircraft concept which utilises only a single engine [9] to power six smaller rated electrical machines to provide the aircraft thrust was conceived by Airbus and Rolls-Royce. This concept is shown in Figure 2.16.



Figure 2.16 Rolls - Royce and Airbus TeDP Concept Aircraft [9]

Unlike the network of the N3-X, this concept does not utilise a DC distribution network, relying fully on an AC architecture to link the engine and the motors and remove heavy power electronic components. This also introduces a reliability benefit through the decision to not use additional features within the power network and hence minimise complexity. This network architecture is shown in Figure 2.17.

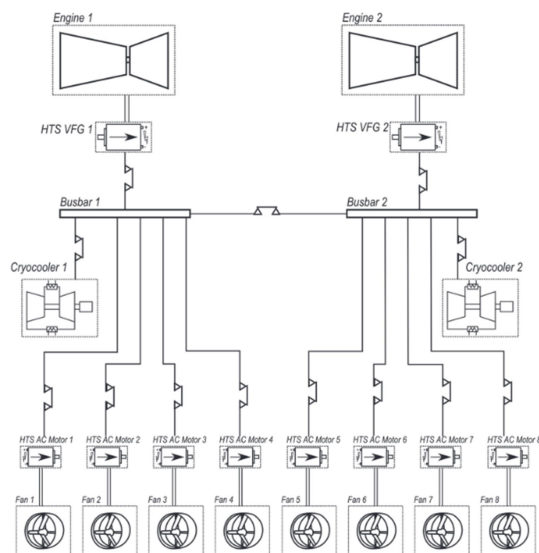


Figure 2.17 Electrical Propulsion Architecture of Rolls - Royce and Airbus TeDP Concept [23]

The concept architecture of Figure 2.17 is designed to supply a total of 9 MW of electrical power, where safe rolling take off may occur only if at least one of the two generators is operating fully. Both the voltage and current that this network will operate will be determined through future network optimisation studies. This results in a much smaller aircraft than the N3-X concept identified in section 2.9.1. A novel feature to this configuration, as mentioned above is the lack of power electronic devices within the network. Through the removal of power electronics and running both the generators and motors in synch allows weight savings to be made within the network however restricts control of motor speeds which run in line with the speed of the generation. Protection for this network is provided through the use of breakers or isolators which can be shown to operate to the same standards [23].

Unlike the N3-X configuration this TeDP architecture only has a single protection network, using only breakers and not superconducting fault current limiters and therefore does not use as many components to form the network architecture. This, as well as the fewer number of motors and propulsors plays an important role in maintaining a reliability level that is as high as possible. Another notable feature of the network is that even though the fewer components may result in a more preferable reliability score, the losses incurred through running all machines at the same frequency may incur greater electrical losses than the TeDP network.

2.9.3 NASA Hybrid AC-DC Configuration

The final considered network and an early concept which was devised for the purpose of TeDP was a hybrid AC-DC network as proposed by NASA. This network was further developed and was renamed becoming the N3-X, however the differences which form this initial concept provides an interesting comparison network. This network has a similar power requirement to the N3-X network where each generator is rated to provide 30,000 hp of thrust [16]. The overview of this network is shown in Figure 2.18.

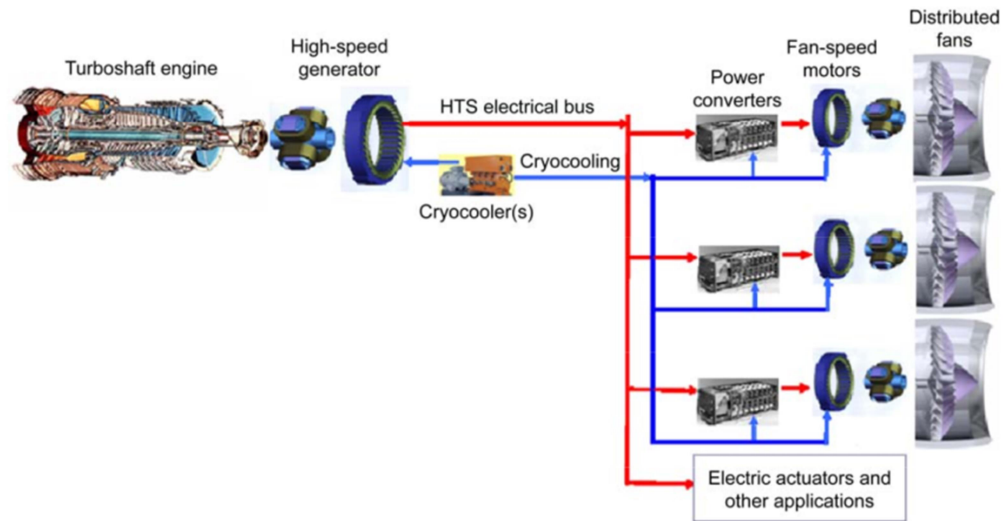


Figure 2.18 NASA TeDP Network Components [16]

Figure 2.18 shows the key components of the 2008 concept network. This network architecture was designed to operate using 16 independent turboelectric motors and distributed fans along the upper aft of the aircraft and would require 63 MW (84000 hp) of available electrical power at sea-level and 19 MW (25000 hp) at cruise: this corresponds to roughly 1.1 MW (1500 hp) per fan at cruise [16]. Similarly to the N3-X, both the power and thrust-producing machines are decoupled allowing each to rotate to their own optimal speed as well as using the fan thrust for yaw control. This configuration has no identifiable protection system and likely relies on the quenching (localised increased current and magnetic field over a set threshold of a local component returning it to a normal resistance with an increased heat) of superconducting cables to prevent the flow of fault current [88].

Unlike the other two concepts this network does not feature a dedicated protection network, meaning only the network quenching properties protect against high levels of fault current. This would appear to be a somewhat risky option and perhaps would not be viable from a power system protection perspective, as there are no components to physically isolate faulted areas of the network and protect the healthy areas of the network from high levels of fault current. Furthermore, the heat generated by fault currents in affected areas of the network may cause damage to otherwise unaffected components. This design does however result in fewer

components than the other two networks and hence will provide a greater level of reliability in comparison. This network was however a predecessor to the N3-X network and should be taken into consideration when considering the network composition.

The further development of a TeDP system considering all existing conceptual ideas may further help the evolution of future aircraft meet the more rigorous N+3 targets through allowing significantly reduced field lengths (the required distance for aircraft take-off and landing), much quieter operation and dramatically reduced fuel burn [37].

2.10 N+3 Concept Aircraft Designs Proposed for Subsonic Commercial Transport in the 2030-35 Timeframe

In response to a 2007 research call from NASA [89], a number of concepts were proposed to meet the N+3 future subsonic aircraft targets. As well as the N3-X TeDP concept, there were a number of alternative designs proposed, all with varying passenger capacities and maximum flying range. Some of the concepts focussed more heavily on certain targets, for example the GE, Cessna and Georgia Tech offering, which exploited metroplex (smaller regional airports) aspects, however the N3-X concept offered progress against all of the targets. All of the proposed concepts within this section responded to the research call [89] for the N+3 subsonic set of targets however did not perform as favourably in all four parameters. While the TeDP concept was chosen through a process of down selection (reducing the number of considered options for the project) over a number of phases of the project for further research effort, the remaining options, while promising, were not provided with additional NASA funding. These will be reviewed in this section to provide a complete view of all concepts considered by NASA against which the N3-X proved the strongest as well as providing an overview of some of the technologies which will help shape the future of the aircraft industry.

2.10.1 Boeing, GE and Georgia Tech Concept Entry

This concept, the result of a project undertaken by Boeing, GE (General Electric) and Georgia Tech saw the design of a 154 passenger aircraft with a range of 3500 nm and maximum speed of Mach 0.7. This concept is shown in Figure 2.19.



Figure 2.19 Boeing, GE and Georgia Tech Concept Aircraft [6]

It utilises an electric battery gas turbine electric propulsion system and was found to exhibit a fuel burn reduction of 70 % on the reference vehicle and a reduced energy usage of 55 % when utilising the battery. The concept exhibited long wings for greater lift and reduced drag which could be folded when being serviced at a conventional airport gate [90]. While the use of battery technology could potentially see an aircraft concept perform well against the fuel burn, emissions and field length goals, ultimately it is the same extensive use of battery technology which prevented NASA continuing with the idea. Unfortunately for the further advancement of the concept, the projection of how battery technology may advance from the conventional technology is unclear and could potentially, in a worst case scenario, prevent the aircraft from being competitive [6].

2.10.2 SELECT Concept Aircraft Developed by Northrup Grumman,

The Silent Efficient Low Emissions Commercial Transport, or SELECT, future aircraft design was conceived by a group led by Northrup Grumman Systems Corporation [91] with collaboration from Rolls-Royce, Tufts, Sensis and Spirit. The SELECT concept had a 120 passenger capacity with a maximum range of 1600 nm and a top speed of Mach 0.75 [63] and a concept design is shown in Figure 2.20.



Figure 2.20 SELECT Aircraft [4]

This aircraft concept is relatively similar to conventional aircraft however novel features include shape memory alloys, nanotechnology, the use of lightweight ceramic composites as well as exhibiting Short Take Off and Landing (STOL) capabilities [4]. The STOL capabilities of the aircraft mean that this aircraft would be able to utilise smaller airfields as dictated by Table 2.1 and therefore help increase the capacity of future air transportation networks.

2.10.3 Cessna Style Concept N+3 Aircraft

The design submitted by the GE, Cessna and Georgia Tech collaboration was the smallest of the concepts with a private jet style aircraft with a maximum passenger capacity of only 20. The range of this aircraft was predicted to be approximately 800 nm and with a maximum speed of Mach 0.55 [63]. A conceptualisation of this aircraft is shown in Figure 2.21.



Figure 2.21 GE Aviation N+3 Subsonic Concept Aircraft [7]

Figure 2.21 shows the small Cessna style aircraft which was developed with the unique feature of having a ‘self healing’ outer airframe [92]. This airframe exterior would allow the surface of the aircraft to self repair in the event of exterior impact, lightning strikes, extreme temperature or electromagnetic interference through the use of a conducting film used in conjunction with an energy absorbing foam covering the whole aircraft. An additional benefit to the self healing outer aircraft layer is that of noise shielding from exterior noise [8, 92]. Figure 2.22 shows a comparison between conventional aircraft outer layers and the new self healing concept.

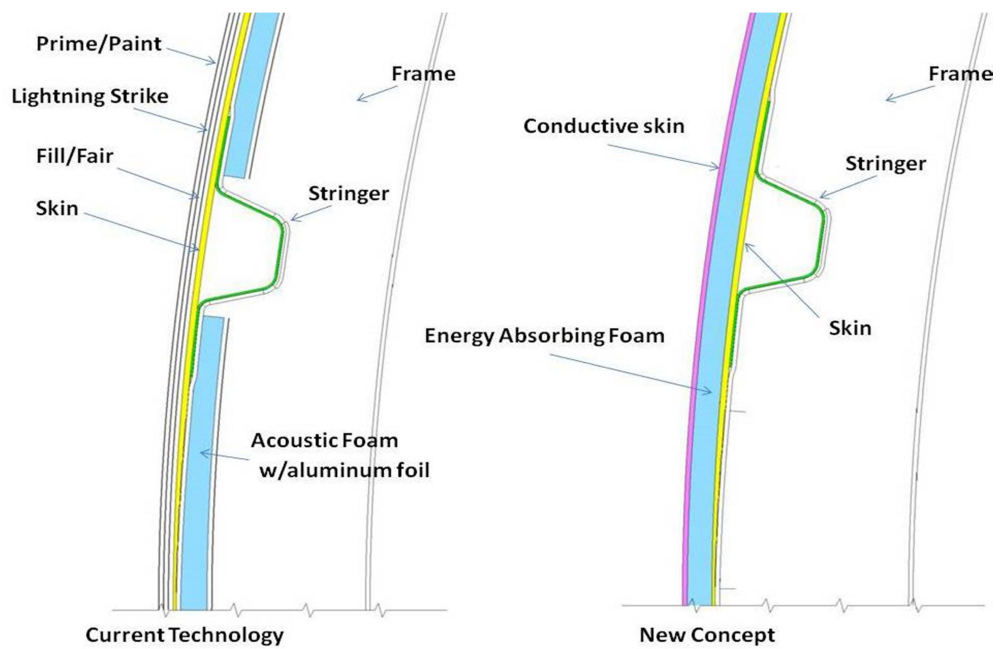


Figure 2.22 Self-Healing Aircraft Outer Layer Concept [8]

From this figure some idea of how the energy absorbing foam may replace the several, heavier conventional layers on the aircrafts surface allowing a potential weight saving [8, 92]. While this aircraft was developed to be lightweight and to reduce fuel burn the propulsion concepts remained largely the same as for modern day aircraft and is likely the reason this concept was not chosen for further funding.

2.10.4 MIT, Aurora, P&W and Aerodyne Concept Aircraft

This consortium came up with two similar designs under the N+3 concept study. The first had a 354 passenger limit with maximum speed of Mach 0.83 and range of 7600 nm [63], and the second, a smaller 180 passenger aircraft with a top speed of Mach 0.74 and a range of 3000 nm [63].

The first of the two concepts put forward by the MIT consortium was the 354 passenger H series blended wing body (BWB) aircraft as shown in Figure 2.23 [93].



Figure 2.23 MIT H Series N+3 Aircraft Concept [3]

Figure 2.23 shows the ‘H’ series concept. This HWB style aircraft was designed for international travel and as a direct replacement for the current Boeing 777 [93]. The second of the concepts, the D series ‘double bubble’ 180 passenger aircraft as shown in Figure 2.24 is another concept based upon the tube and wing design, however utilising a wide fuselage provides greater lift for the aircraft [94].



Figure 2.24 MIT Double Bubble N+3 Aircraft [3]

The D series aircraft of Figure 2.24 also makes use of BLI with its' aft located engines ingesting the slower moving boundary air to increase the available thrust for no additional fuel burn [94]. Both of the concepts put forward by this consortium seem promising, using BLI techniques to make a more efficient use of thrust – in fact the double bubble concept seems to share many similarities with the Rolls-Royce and airbus concept mentioned within section 2.9.2. The H series shares many similarities with the N3A NASA concept which will be described in further detail in section 3.1.1. All of these concepts utilise raised nacelles and a small number of distributed fans raised above the upper aircraft surface to allow an efficient ingest of boundary layer air as well as wide bodies to create more efficient lift.

2.10.5 N+3 Concept Aircraft from NASA, Virginia Tech and Georgia Tech

The final concept aircraft considered was the 305 passenger Mach 0.85 aircraft with the longest range: 7730 nm [63]. This aircraft is shown in Figure 2.25.



Figure 2.25 Georgia and Virginia Tech Collaborative efficient wing design aircraft [12]

This efficient wing aircraft uses a truss based wing design. The merits associated with this design mean that the aircraft is not affected by aircraft weight penalties like in a conventional aircraft which allows the aircraft to exhibit a reduced fuel burn [12] and hence move towards the future targets of Table 2.2.

2.10.6 Summary of the Presented N+3 Aircraft Concepts

This section has reviewed the range of alternative future aircraft proposed in response to a NASA research call that were intended to solve the same problems as the N3-X TeDP aircraft, which has been promoted as the foremost of the available options which will be capable of addressing N+3 aircraft efficiency metrics. While not directly chosen for further research, a number of the principles featured in these aircraft have featured in other concepts which are still being developed. All of the noted designs utilise their own novel features allowing the future aircraft goals to become ever closer to reality. The inclusion of techniques such as novel wing designs to more effectively manage the airflow both through and over airframes and battery technology which allows a quieter flight experience for both passengers and those living in the flight path have shown how both air framers and engineers alike envisage the future of air travel. Although these concepts vary greatly and in each case have a different approach to the NASA targets, there have been a number of trends which have been consistently highlighted between the designs [63]. Most notably is the frequent use of composite materials from which the airframe is constructed and wide body or lengthened wing designs. Another feature which features heavily in a number of designs from the N3-X to the Double Bubble and H-Series is the increased use of BLI techniques to increase the aerodynamic efficiency of future aircraft.

2.11 Chapter Summary

The evolution of aircraft towards a MEA or even an AEA and eventually to the TeDP concept presents a number of challenges, some of which have been presented in this chapter; this review however is not exhaustive. Despite the challenges which exist in meeting emissions and efficiency targets for the aircraft electrical systems of the future, this chapter has highlighted the on-going efforts both in the research community and in the aerospace industry to address the challenges that these goals present.

With a number of architecture designs under consideration and future concepts still in low TRL's, this chapter has presented a review of a number of advanced concepts with potential to help contribute to the aircraft of the future and has highlighted areas where improvements are essential to ensure that safety and efficiency targets are met. Some of the research areas featured in this chapter are still in the early concept stages and the means of optimally integrating these advanced concepts, considering both entire electrical architectures and individual component performance requirements are still required.

Through the undertaking of this literature review, a thorough understanding has been gained of the concepts which underpin the current trend in the aircraft industry of moving towards more environmentally responsible air travel. These concepts will be used to form the basis of future technologically advanced aircraft architectures and with increasing research will in turn form viable more reliable solutions.

Chapter 3

Overview of Existing TeDP Research and Applicable Reliability Methods

The Turboelectric Distributed Propulsion (TeDP) concept was developed as an entry for a future subsonic aircraft of a project proposal announcement by NASA in 2007 [89] for entrants to share their vision of the future of civil aircraft. To fulfil the needs of the research call, concepts were required to exhibit a number of technologies that could be entered into passenger service in the 2030-2035 timeframe [89] to realise a more environmentally responsible aircraft. The TeDP concept was selected as one of the three concepts as well as a concept from Lockheed Martin and Northrup Grumman from those described within section 2.10 for a further 24 months of funding to further develop the concepts [18, 89]. This chapter reviews the additional work undertaken on the TeDP concept, specifically the N3-X during this time and identifies an undeveloped area of work which can be exploited and developed within this thesis.

3.1 Identification of existing areas of TeDP research

As part of the further studies which were undertaken on the TeDP concept a number of aspects were investigated such as the aerodynamic properties, laminar flow and the efficiency of the electrical machines operation within the system. Furthermore, as

mentioned in Chapter 1 NASA commissioned a number of studies through their NASA Glenn Research centre relating to network weight and efficiency as well as general mechanical and electrical network considerations with results published in [11, 16, 42, 47]. Further extensive studies have been carried out by Rolls-Royce Liberty Works and the University of Strathclyde on network power and mass trades as mentioned in Chapter 1 as well as more recent studies on mass and voltage levels. These more recent studies examined the potential N3-X architecture and varied the operating voltage to determine the results on system weight and protection capabilities with findings published in [48, 51, 95]. Other supplementary research undertaken by the University of Strathclyde has been completed on both superconducting network behaviours and voltage sensitivities and can be found in [50, 52]. This work considers the component variations and parameters of potential future DC networks and how their variation in fault response may impact of future network protection solutions.

3.1.1 NASA TeDP Research

Most of the initial research into the TeDP concept undertaken by NASA focussed on the aerodynamic aspects and concepts which aid the efficient and quiet design of the airframe [11, 16, 47]. A number of variations of the airframe were considered by NASA before finally proceeding with the N3-X aircraft, including airframes with large geared turbofans located on the upper aircraft surface as shown in Figure 3.1 as well as concepts using liquid Hydrogen (LH2) cooling [11].

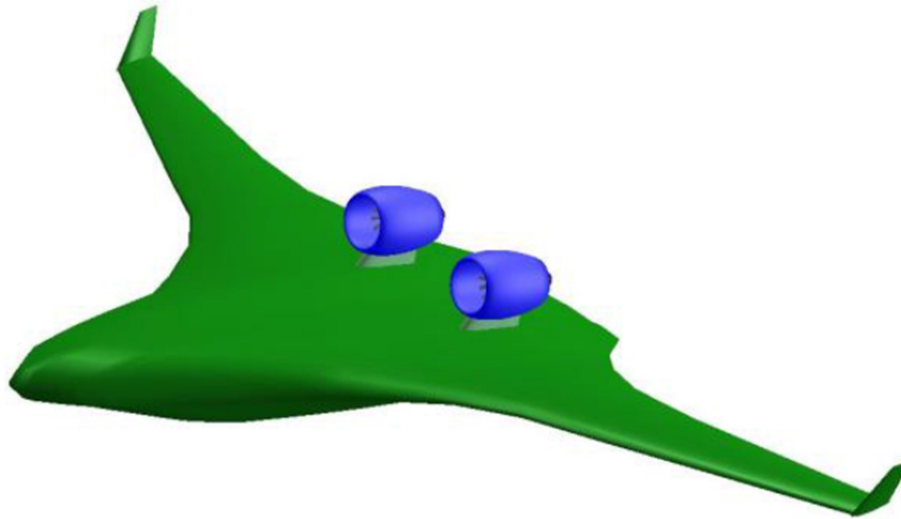


Figure 3.1 N3A TeDP Concept [10]

In [11], the N3A shown in Figure 3.1 and the N3-X as shown in Figure 3.2 were compared to determine which of the aircraft performed best when simulated against a number of metrics. This study is outlined within this section as it provides a useful background to the existing TeDP research in areas such as the cooling and airframe choices. Two versions of the N3-X concept were considered each utilising a different cooling system: cryo cooled and liquid hydrogen (LH2) cooled [11] as both methods allow the network components to be cooled such that the critical current densities required of the superconducting network may be achieved [11].



Figure 3.2 NASA N3-X Concept [11]

The N3-X concept, as shown in Figure 3.2 makes use of two wingtip located turbogenerators which although not used as the prime thrust generators do produce a small net thrust when at cruise speed to avoid any resultant drag [11, 16]. The turbogenerators are located on the wingtips as opposed to the more familiar under wing location to simultaneously minimise noise in the cabin, to reduce the bending moment in the wing and to reduce aircraft drag [11]. The N3A concept of Figure 3.1 however makes use of two geared turbofans mounted on pylons on the upper surface of the hybrid wing body (HWB) airframe and are used to create the same thrust [11]. The geared turbofan concept and the turbogenerators concepts are both assumed to have the same efficiencies [11].

The studies conducted within this paper investigated boundary layer ingestion: determining the optimal boundary layer conditions such as shape and height of the airframe [11] as well as understanding the thrust requirements for such an aircraft for the condition of both rolling take-off (RTO) as well as at the aerodynamic design point (ADP) of 30,000 ft [11]. The thrust requirements at both RTO and ADP can be seen in Table 3.1.

Table 3.1 Thrust Requirements for two TeDP Configurations [11]

Configuration	Flight Condition	Uninstalled Thrust lbf (kN)
N3A	RTO	78766 (350.37)
	ADP	25378 (112.89)
N3-X	RTO	54888 (244.15)
	ADP	19293 (85.82)

Table 3.1 shows the thrust requirements in both lbf and kN for the two configurations of the TeDP aircraft before installation of their retrospective engines; the TeDP concept required a significantly less thrust due to the drag penalties encountered by the installation of the geared turbofans of the N3A [11].

Comparisons between the two concept aircrafts' weight were also conducted within this study, concluding that the N3-X attributed a lesser weight penalty to the propulsion system than the N3A [11]. One of the factors contributing to this lower weight penalty is the specific fuel consumption as exhibited by the N3-X is lesser than that of the N3A: this leads to a reduced fuel burn over the N3A allowing less fuel to be carried and the N3-X to be lighter and smaller. This in turn reduced the thrust requirements of the N3-X engines enabling a smaller overall engine size [11].

Due to a combination of these factors, the N3-X concept could perform far more favourably than the N3A and hence further studies into TeDP would be conducted upon the N3-X concept.

3.1.2 Existing Research in the area of TeDP Contingency Analysis

Extending the work which NASA has completed in the field of TeDP, a research contract was awarded to Rolls-Royce North American Technologies in Indianapolis to undertake trade studies on the performance of the N3-X TeDP architecture [19]. During these studies a number of configurations of the propulsion system were

considered and a high level contingency analysis was performed to determine the level of reliability with which the network could supply power [19, 49]. The baseline network used for this study is shown in Figure 3.3.

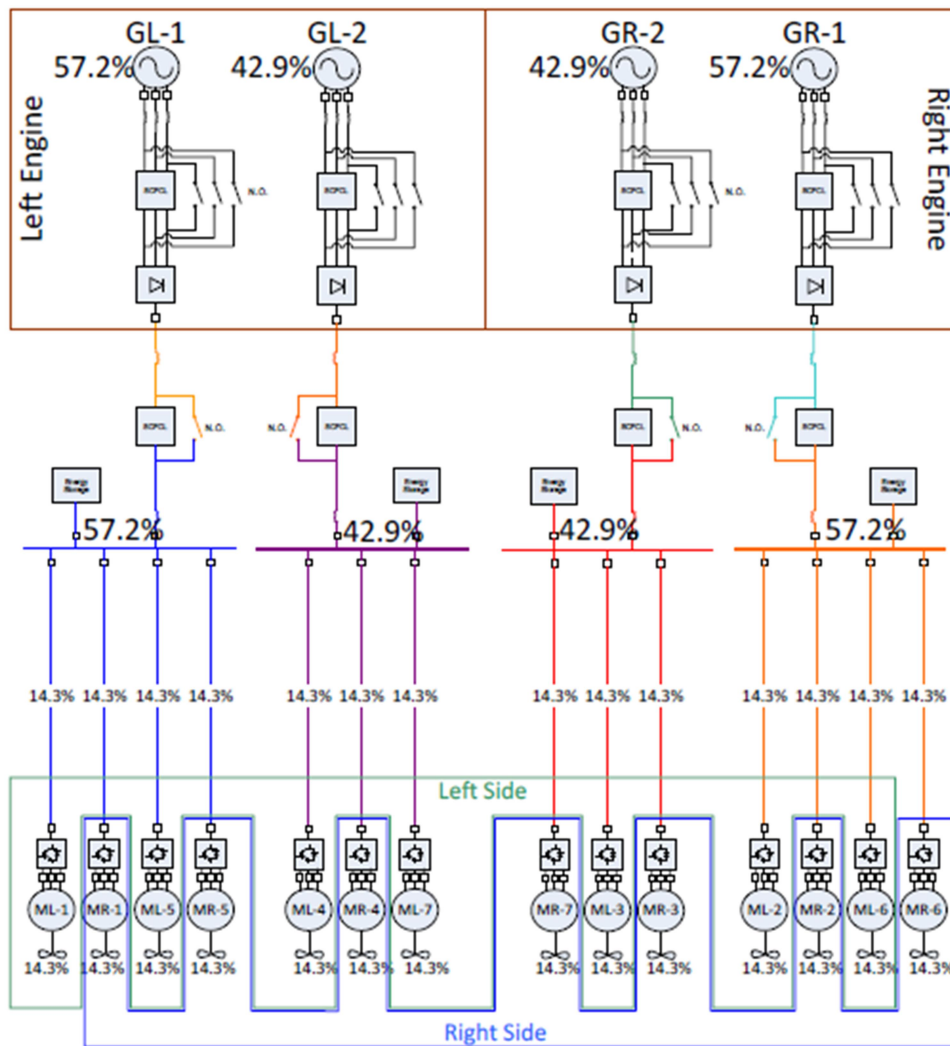


Figure 3.3 Baseline TeDP Architecture [19]

Figure 3.3 shows the baseline network architecture for the N3-X which was developed from the requirements provided for this body of studies. This architecture employs two sets of two generators (two per engine) rated so that each pair may supply 30,000 hp or approximately 23 MVA at a voltage yet to be determined. The motors are connected to the distribution network in groups of 3 or 4 and the solid line groups them into two sets showing the relative location on the aircraft (also identified by the L and R positional reference on each). The percentage values located next to each generator and bus indicates the power distribution of the network and that the

generator and bus loaded with a larger number of motors and propulsors supplies 57.1 % of the power from each engine while the other generator and bus combination supplies 42.9 %. The percentage value next to each motor shows which proportion of the overall aircraft thrust that motor contributes. The network diagram is shown with energy storage on each bus which could be added to the network architecture however hasn't been considered within the case studies of chapter 6.

A contingency analysis was conducted within this body of work to achieve a balance between redundancy, reliability and unit capacity of power generating units within the final baseline network. This analysis within [19, 49] made a number of assumptions to be included:

- The assumption that the failure probability of the TeDP system should be no greater than 1 failure in 10^9 hours based upon [96, 97].
- 30,000 hp should be available at sea level for safe execution of a rolling take off.
- No single point failures should result in any catastrophic consequences.
- The electrical architecture must be able to supply the required thrust to maintain operation in the event of a unit failure that is suitably isolated from the unaffected network.
- Individual components exhibit failure probabilities of less than 10^{-4} .
- Common cause failures (CCF) were neglected.

The requirement for 30,000 hp of installed thrust resulted in the total available generation on the aircraft to be rated at 45 MVA. This power is distributed dependant on the network interconnections, ensuring that even under a single bus failure the required thrust may be maintained [49]. These assumptions and hence the contingency analysis can be formally quantified using simple equations for the probability of the failure of the network to supply some level of thrust and of the probability of the network being able to supply thrust, these are:

$$F_j = \bigcap_{\forall i \in S_j} F_{unit_i} \quad (3.1)$$

where

$$F_T(T_{Avail}) = \bigcup_{\forall j: T_j \leq T_{Avail}} F_j \quad (3.2)$$

where F_j is the probability of scenario S_j occurring and set S_j indicates a group of simultaneously occurring failures independent of failure F_{uniti} , the failure probability of unit i . Additionally, equation 3.2 provides the probability of having a certain level of thrust (T_{Avail}) available $F_T(T_{Avail})$ and is the combination of all the probabilities of the failure scenarios occurring.

The authors of [19, 49] then used these equations to calculate the probability of loss of thrust using 28 single point failures and 378 two unit failures (where two units fail independently of each other either sequentially, simultaneously or as a cascade), analysing results to consider only the statistically significant failure scenarios. Figure 3.4 shows a graph of this contingency analysis produced by the study and was populated using Equation 3.1 and Equation 3.2 and the assumption that each of the considered failures had a probability of failure of less than 10^{-4} .

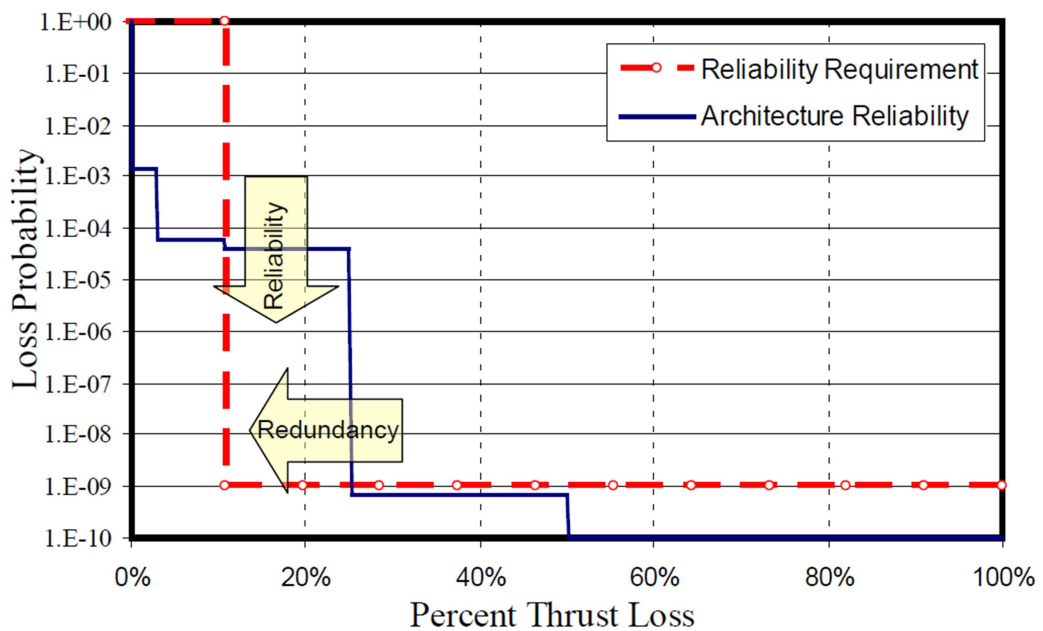


Figure 3.4 Contingency Scenario Graph [19]

Figure 3.4 shows the outcome of the contingency analysis undertaken on an N3-X network architecture for a design point of 30,000 hp being provided at a reliability of

at least 10^{-9} . The red dashed line shows the requirement specification for reliability while the blue solid line shows the results of the performed contingency analysis on the architecture. While the solid architecture reliability line is below the dashed reliability requirement line this architecture is meeting the requirements; while it is above the line it is failing to do so. The two arrows of the graph show the trends which are desired for the network; as the redundancy is increased, each failure reduces the total loss of thrust, while increased reliability of the network reduces the loss probability. These arrows reiterate that while it is desirable to keep any loss of thrust to a minimum, it is equally desirable to keep the failure probability as low as possible. Within the study, failures which did not result in a catastrophic loss of thrust i.e. those which left at least 30,000 hp were permissible within the network at a loss probability of 1, as these failures would not affect the design point.

Conclusions of the study performed within [19, 49] determined that configurations of the TeDP architecture which exhibited two generators per engine to provide the same capacity as a single generator per engine were preferable as the reliability of the system was enhanced for a similar weight penalty [19]. Additionally it was concluded that not all potential network connections between power transmission lines and distribution busses were made in undertaking contingency analysis and that the resultant network may not represent an ideal solution in terms of both network complexity and overall weight penalties attributed to the propulsion network.

This thesis will explore the gaps left in the existing contingency analysis, determining an appropriate method which should be used to determine the reliability of TeDP style networks. This thesis will then demonstrate this method, performing reliability and failure rate studies to determine which TeDP architectures provide the greatest reliability and hence lowest failure rates. The scope of this work and the identified gaps in existing research will be described in section 3.2.

3.2 Identification of Gaps in Existing Research in the area of TeDP Contingency Analysis

Reliability of an aircraft is a key requirement in both military and civil aircraft and current research in this area with respect to TeDP as mentioned above in section 3.1.2 is limited to mainly aerodynamic aspects, as it is in this area where the biggest gains can be made over existing aircraft designs. Other limitations exist in terms of electrical network specifics, such as an optimal nominal operating voltage and current level as well as a limited body of work relating to safety and reliability aspects. Most of the available research with regards to the contingency analysis of the TeDP concept, is based upon assumptions of the network architecture and was conducted to provide initial generation sizing [19, 49]. There is no evidence to suggest that a further analysis into the network weak points and optimal network connectivity with regard to an optimised Thrust-Reliability (T-R) profile was ever carried out beyond the work reviewed in section 3.1.2. This T-R analysis is an essential aspect to the development of the TeDP concept as a rapid profiling tool allows for a number of concept architectures to be compared with minimal cost to development teams.

The contingency analysis of [19] and subsequently [43, 49] neglected the effects of common cause failures. As described by [98], ‘Common cause failures often dominate the unreliability of redundant systems by virtue of defeating the random coincident failure feature of redundant protection.’. As such to neglect such a failure could result in significant failure events not being accounted for. An example case where a common cause failure resulted in the loss of power to a flight control surface is the case of United Flight 232 where a DC-10 suffered an engine failure which resulted in shrapnel being thrust through the tail of the aircraft. This debris simultaneously cut all the hydraulic supplies to the actuator of the tail control surface resulting in a complete loss of control of that surface. This case also serves as an example of using differential thrust to control the movement of the aircraft as the remaining two engines were used to primitively control the movement of the aircraft and return it to the ground [99].

The conclusions provided by the studies of [19, 49] on the contingency analysis conducted used the graph of Figure 3.4 to provide a single outcome profile for loss probability and percentage loss of thrust. This work showed the profile that arises from analysing one specific architecture and component sizing combination. While this is a useful study, there is scope to expand this and to conducting further studies which produce a number of similar profiles on the same graph to allow variations on a specific TeDP architecture to be compared. This graph could be used to better compare a number of failure events and sizing combinations for a set of architectures or could be used to compare the reliability scores achievable by a network using different levels of redundancy. Extending this graph not only allows a number of operating conditions to be examined, however adds the opportunity for a number of different architectures to be compared. In this manner engineers could determine which changes could be made to make network architectures more competitive with alternative designs and airlines could make informed decisions on which aircraft perform better at different stages of a flight envelope and hence choose the aircraft most suited to their needs.

Section 3.1.3 of [19] stated that for a system with 14 propulsors, 12 must be able to support the minimum thrust load. There is potential in a network with a large level of interconnectivity to provide the required thrust with a lesser number of propulsors operational, provided that at least the minimal required level of thrust remains. Of course the impact of CCF would also have to be taken into account with any sizing exercise to ensure that any events such as shrapnel or bird strike would not result in a catastrophic loss of thrust.

The previous analysis in [49] only assumed that each unit within the architecture exhibited a single failure probability. Through conducting a sensitivity analysis where the failure probability of key components within the network are varied, more robust findings can be obtained to determine which aspects of the network require a greater research focus to enhance network reliability. Through the variation of network failure probabilities the robustness of the network to faults in a given area of the network could be more thoroughly understood and hence reduced.

Research undertaken at this stage can aid knowledge about the network and reduce future costs as modelling can be undertaken at a low TRL level before costly prototypes are created. Research effort can be focussed on areas and components of the network which yield the greatest positive change to overall reliability with a reduction in failure probability. A sensitivity analysis of three identified TeDP networks is conducted within Chapter 5 to address this requirement.

3.3 Identification of Research Topic

Providing a thorough contingency analysis which simultaneously addresses failure rates, failure probability and sensitivity of a TeDP network to failures yields a tool which is of great importance at this relatively early design stage of the TeDP concept. Addressing the findings of section 3.2, it is apparent that it is a timely requirement to address this matter and undertake a full contingency analysis of the TeDP concept. This analysis will determine both weak points within the electrical network, where failures of certain components may result in a significant loss of thrust, as well as determining the effects of changing the percentage of operational propulsion motors on network thrust and reliability.

The work of this thesis considers a number of pre-existing TeDP architectures for comparison; each architecture will be defined in terms of the propulsion system components and then analysed in terms of both the reliability and predicted failure rate. The performance of each network will be measured against the T-R profile as outlined in section 3.1.2 and detailed further in chapter 4. As well as assessing the predefined networks, this work will also present a number of redundancy options added to the network and repeat the analysis to determine the overall effect to the T-R profile. A number of these options or redundant parallel paths have been presented in [19, 49]; however a repeat of the contingency analysis of section 3.1 of [19] was never conducted on the new configurations in subsequent studies. The analysis of additional redundancy measures will determine how effective the redundant parallel paths in the network are in terms of reducing failure rates of the network at critical points. Through considering the impact of CCF's on the network, more informed

architecture decisions may be made. This allows effective decisions to be made relating to the inclusion and specific levels of electrical redundancy required. To enhance the presented reliability analysis, due consideration of the network's sensitivity to changes in reliability will be made: determining how the network responds to step improvements in reliability informs network architects on where to optimally focus engineering effort.

Determining a failure rate profile for any TeDP network is important to both enhance network understanding and to further the TeDP concept. One method of providing this profile is through conducting a fault tree (failure) analysis as featured in the SAE ARP 4761 [100] for all civil aircraft architectures. Through undertaking a thorough FTA to compliment any reliability analysis additional network intricacies may be revealed which are more easily identified through observation of the flow diagram than through the simple use of equations. This thesis provides an analysis of a TeDP network using the FTA method to highlight how this analysis can be undertaken and the value to the TeDP concept. This is presented within Chapter 6.

To study the effects of varying both operating voltage and current levels within the large complex TeDP network would have been impractical before an initial study to determine if the reliability levels of the concept networks allowed for a feasible civil aircraft. Additionally intense work on the intricate superconductivity requirements of such a network when it was initially unclear how the concept would perform in terms of reliability would be counter intuitive. Since the work of this thesis has been undertaken, subsequent studies have been undertaken in both voltage considerations [48, 50, 51, 95] and in terms of superconducting performance [52, 101-103].

Having now determined an area that can be exploited to expand upon the existing knowledge, and having provided reasoning for the requirements for the study it is appropriate to determine the means by which analysis must take place. The application of appropriate models can account for both the reliability of individual components, sections of network or even the full network, as well as accounting for both common cause and isolated failures. As well as considering the reliability of network architectures, models can be used to determine to what magnitude the failure rate of the system may be and be used to complement reliability studies. Undertaking

sensitivity studies in conjunction with both failure and reliability models can further enhance and compliment the knowledge obtained on the TeDP network and how variations of the network perform in a number of scenarios. These studies can help identify areas where additional redundancy may be required in future TeDP systems.

3.4 Requirement for a new Analysis Methodology

A key distinguishing factor between current more-electric aircraft (MEA) and TeDP network architecture designs is the power level at which critical loads must be supplied [16]. Specifically, the power supply to the high power propulsion motors in TeDP systems must be of similar reliability to the traditional low power critical loads, such as the avionics in present day aircraft. In line with the increased power levels of the aircraft, the voltage levels are expected to rise accordingly. Specifically, the highest voltages utilised in the present MEA generation of aircraft are ± 270 VDC and 230 VAC with current levels in line with these. Although there are no firm voltage levels for the TeDP concept aircraft yet, these will reflect the anticipated superconducting system current carrying capabilities [50, 51] and may indeed be lower than the modern day aircraft due to the high current carrying capabilities of superconducting cables. Such TeDP concepts place a new and significant reliance on an aircraft's electrical system for safe and efficient flight. Accordingly, in addition to providing certainty that supply reliability targets are being met, performing a contingency analysis to evaluate the probability of component failure within the electrical network and the impact of that failure upon the available thrust must also be undertaken for architecture designs. Given that individual electrical components are unlikely to meet the stringent provision of 30,000 hp [43] at a failure probability of less than 10^{-9} per flight hour [10], this target is expected to be achieved through an optimised combination of the overrating of system generation components and lightweight system redundancy measures. Solutions that meet specified thrust requirements at a minimum associated weight are desirable as these will likely achieve the greatest performance against the proposed emissions targets.

SAE standard, SAE 4761 [100], provides guidelines and methods for performing safety assessments for the certification of civil aircraft. One such tool as described by this standard and mentioned in section 3.3 is Fault Tree Analysis (FTA) which uses probability and logical operators to determine whether candidate network architectures meet specified parametric requirements [104]. One particular example of the use of FTA in the aerospace sector is determining the ability of a set network to meet the Civil Airworthiness Authority (CAA) requirements that catastrophic failures or those failures leading to the complete loss of an aircraft should occur less than once in 10^9 flight hours [105]. Hence the failure rate of components or combinations of components which would result in this occurrence must be less than 10^{-9} per flight hour. While FTA provides a well-known and reliable analysis tool – the nature of the TeDP network presents a highly complex analysis which expands rapidly with each additional network path or redundancy feature. Other methods which could be used to analyse a TeDP network to obtain a Thrust Reliability profile are detailed within section 3.5, next.

The work of this thesis asserts that both an FTA and a *k-out-of-n* method [106] should be used to undertake both a failure rate analysis for the electrical system and thrust reliability analysis of TeDP aircraft propulsion system architectures. This approach extends beyond the single failure rate provided by traditional FTA methods by profiling the reliability and thrust provision of each possible system configuration as mentioned in section 3.2 (i.e. following the failure of one or more components), which when combined provides an effective design capability. In addition this approach provides a rapid profiling tool, removing the requirement to build an extensive fault tree for each new network and enables quick analysis to be undertaken when comparing network configurations.

3.5 Reliability Methods and Requirements Considered for a TeDP Thrust Reliability Profiling Application

Before proceeding with the reliability method which was chosen for the T-R profiling work of chapter 5, a number of reliability methods were studied during the

research reported in this thesis. A number of methods were found to be relevant to this application and a number were found to have merit, yet not be suitable in their current form to be meaningfully applied to a TeDP network. This section considers a number of these methods and discusses the reasoning for and against adoption of each for the purpose of analysing the chosen TeDP network.

In order to determine which reliability methods may be suitable to provide a thorough analysis and provide new information of the TeDP network, a number of metrics must be employed to provide a suitable basis for analysis. These main metrics considered when selecting appropriate analysis methods included: determining whether the method allowed for complex network analysis – if not, it was ascertained whether the network could be reconfigured to allow analysis to be undertaken or indeed for more succinct analysis to be performed. Considerations also questioned whether the analysis allowed by each method provided new information on a TeDP architecture and whether the results from the analysis were usable and could they be presented in an informative manner. The two final metrics which reliability methods were assessed against were ascertaining if the required data for the method equations was available (and if not, whether representative figured could be used) and whether the method was part of a current certification process (such as ARP 4761 [100]) and could therefore be easily incorporated into current reliability engineering processes.

Once all the of identified criteria had been assessed, the most appropriate methods outlined for the purpose of Thrust Reliability (T-R) profiling of a TeDP network were chosen. The chosen reliability analysis methods provide a robust analysis tool to enable a thorough reliability and failure rate study for any TeDP network.

3.5.1 k-out-of-n Analysis

K-out-of-n analysis is a reliability technique which uses the binomial probability distribution [106]. The *k-out-of-n* analysis method can be used in instances where there is a requirement within a system for a subset of k out of a total of n identical and parallel components to be operational at any point in time and with $k \leq n$. An

example of this is in a conventional two engine civil aircraft where both engines must be operational to allow for take-off. This can be summarised using the simplified TeDP network diagrams of Figure 3.7 below where a generator and section of the distribution network is connected to a bank of 4 parallel MF sections. In each case the number, k , which are to be operational are rendered blue. Those which are not required to be operational ($n-k$) are highlighted in red. In every case the unparallelled GSC section is required to operate and is not connected in parallel. For instances where $k = 1$ (Figure 3.7 a), the system is in a state of complete redundancy; for instances where $k = n$ (Figure 3.7 c) the system components may be considered to be connected in series [106]. Figure 3.7 b shows the general case where $k \leq n$. In the case of a large, complex network such as that proposed for TeDP aircraft, the k -out-of- n approach [106] can be applied in several ways but for the purposes of this thesis it allows the probability of the successful supply of power from a number of parallel feeders to be determined. This method will subsequently be used to determine the T-R profiles of a number of TeDP architecture variations.

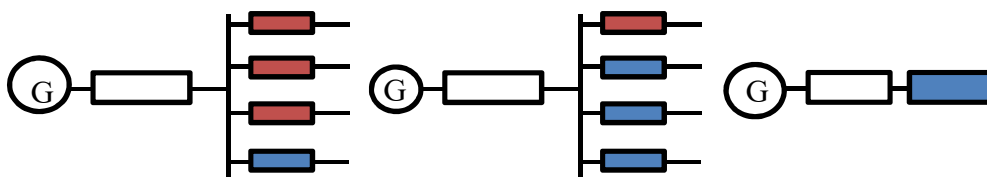


Figure 3.7a k -out-of- n example where $k = 1$

Figure 3.7b k -out-of- n general case where $k \leq n$

Figure 3.7c k -out-of- n example showing $k=n$ or complete redundancy

Key assumptions made in the application of this technique within this thesis are:

- Motor feeders are identical and independent, thereby exhibiting an identical reliability of supply value which remains constant.
- The failure of one feeder does not increase the probability of another feeder failing.
- Components in each feeder are identical – exhibiting same specification and sourced from the same manufacturer.
- Each separate section of the network used for the studies are islanded (isolated), with no connections to other generators, bus ties or feeders.

- A failure of a motor feeder is any component failure which prevents the successful supply of power to the motor

To obtain the probability of successful power provision as exhibited by the network, a binomial probability distribution [106] is assumed, using the assumption that each feeder exhibits a reliability R as a constant probability of success. The total number of propulsors connected in parallel is denoted by n and of these n propulsors, those that are required to be operational for the successful supply of power are denoted by k .

Employing these definitions, the binomial probability distribution is given as

$$P(k) = \binom{n}{k} R^k (1 - R)^{n-k} \quad (3.3)$$

where $P(k)$ is the probability that exactly k out of the total n components will operate – or in this case that k feeders out-of- n total feeders will successfully supply power to the loads and that $n-k$ feeders will fail to supply power successfully for a set architecture. The binomial coefficient is defined as

$$\binom{n}{k} = \frac{n!}{k!(n-k)!} \quad (3.4)$$

and determines the number of ways that k feeders can be successfully transmitting power from n total feeders. The following relationship can be derived from these equations

$$R_S = \sum_{x=k}^n P(x) \quad (3.5)$$

to provide the probability of k or more feeders successfully supplying power. Here, R_S is the probability of x or more feeders successfully supplying power. These equations can then be combined to show the effect of altering parameters on the overall probability of successful operation. This is illustrated in the following section where a simple example is presented showing the effects on overall probability of successful operation of a simple network by altering the number of available components as well as the reliability value of a dedicated component.

3.5.1.1 *k-out-of-n Network Architecture Example*

A simple network, constructed using illustrative figures is presented, where a single generator is connected to a bank of six independent motors is constructed as shown in Figure 3.8. For successful operation of this network, both the green generator component with reliability $R= 0.98$ and at least 4 of the 6 purple motor components with reliability 0.8 must operate as desired for the network to be considered to operate correctly. The challenge is to determine the reliability with which the network will successfully operate.

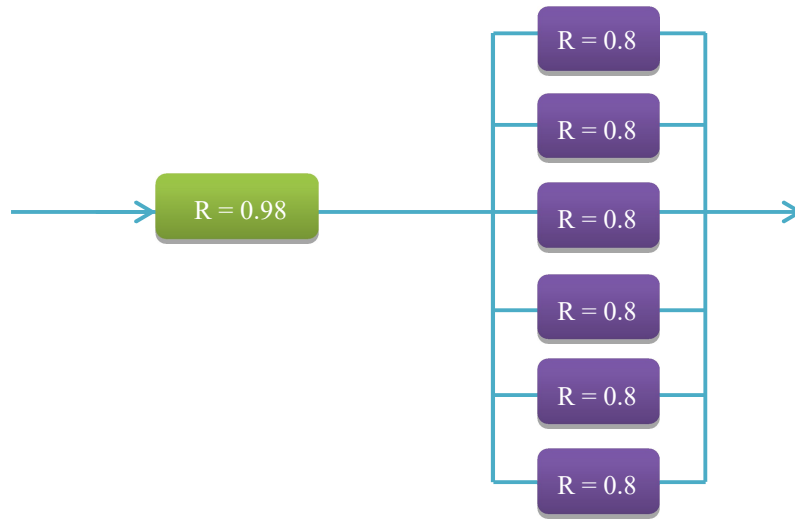


Figure 3.8 Example k-out-of-n network

The overall system reliability will require a two stage analysis. Firstly, a calculation to determine the reliability of the parallel connected purple motor components and then a calculation with the green generator in series with the resultant of the first calculation.

Considering the parallel motor section first and substituting into Equation 3.5 yields;

$$R_S = \sum_{x=4}^6 \binom{6}{x} 0.8^x (1 - 0.8)^{6-x} + \binom{6}{6} 0.8^6 (1 - 0.8)^{6-6}$$

$$= 0.90112$$

This relation shows the probability of either 4 or 5 or 6 of the motor components operating as desired. The reliability, R_s of this section of network operating successfully is 0.90112. To complete the example and determine the reliability with which the whole network will operate successfully, the generator component must now be analysed; the reliability of the generator is considered in series with the result of the parallel motors which is solved using the rules of series reliability:

$$R_s = 0.98 \times 0.90112 = 0.88310$$

Therefore the network operates with reliability 0.88310.

This example calculation is used to illustrate the process adopted later in the thesis to assess TeDP reliability against a thrust constant.

3.5.1.2 Benefits of applying a k-out-of-n Analysis

The use of k-out-of-n analysis in this application delivers a number of benefits. The most notable benefit of using this method is the simple nature of the resultant network analysis, where the level of complex equations is kept to a minimum rather than forming a rapidly expanding calculation with each additional parallel connection as in the fault tree analysis (3.5.4). Another benefit of the network analysis method is that it is maintained as a combination of a number of simplified lumped components allowing the network structure to be easily altered without major changes to the resulting analysis. This enables calculations to be undertaken quickly and in a manner which allows transparency of each network configuration.

3.5.2 Bayesian Analysis

The Bayesian Analysis method allows analysis to be undertaken to estimate the probability of an event occurring where there exists prior knowledge on that event happening based on another related event [107]. Bayes theorem can also be used to determine how the probability of operation of a system may be affected due to a new piece of evidence [108]. Bayes Analysis assumes that events within the sample space considered are linked and that all events are dependant and are defined using

conditional probability [109]. The probability of a new event A occurring ($P(A)$) when it is known that another linked event B ($P(B)$ where $P(B) \neq 0$) has occurred is given by:

$$P(A|B) = \frac{P(B|A)P(A)}{P(B)} \quad (3.6)$$

This equation allows the probability of event A occurring given that event B has already occurred to be determined. When there exists a number of events which could occur within the same subset, that is $B_i, i = 1, 2, \dots, n$, the probability of event A occurring can be shown to be

$$P(A) = \sum_{i=1}^n P(A|B_i)P(B_i) \quad (3.7)$$

When event B_i is mutually exclusive and combinations of event A and B_i consist the entire sample space then both Equation 3.6 and Equation 3.7 can be combined to give

$$P(A_k|B) = \frac{P(B|A_k)P(A_k)}{\sum_{i=1}^n P(B|A_i)P(A_i)} \quad (3.8)$$

which defines Bayes rule for the probability of two mutually exclusive and collectively exhaustive events within their system [109]. An example using this type of analysis method is given in the following section.

3.5.2.1 Bayes Rule Example

For this example, a hypothetical TeDP aircraft is considered, which may only take off if all of its components are operating as desired. This example uses figures set up for illustrative purposes only and they are not proposed as having any particular bearing upon reality. An attempt is made to determine the probability that the available thrust condition is not satisfied and the aircraft cannot take off given that there is a 5 % probability that there has been a failure in one of the motors and that there is a 12 % chance that the aircraft may not take off. It has also been previously determined that 80 % of the events leading to failure of take-off are caused due to a fault with a propulsion motor.

Let A be the event that one of the propulsion motors has failed.

Let B be the event that the aircraft cannot take off.

Given the provided information, it can be determined that:

$$P(A) = 0.05, P(B) = 0.12, P(B|A) = 0.8$$

This can then be substituted into Equation 3.6 yielding:

$$P(A|B) = \frac{P(B|A)P(A)}{P(B)} = \frac{0.8 \times 0.05}{0.12} = 0.3$$

Therefore the probability that the aircraft cannot take off due to the failure of a propulsor is 0.3.

This example is based upon an example found in [110].

3.5.2.2 Relative Merits of Bayesian Analysis

The most significant benefit that Bayesian Analysis provides on the TeDP network is the determination of the probability of failure of one section of network based upon the failure of another identical section of that same network. Early data to populate these tests could come from Environmental Stress Screening (ESS) of a prototype to determine where likely weak points exist. This analysis can be used to predict failures within the network and prevent serious failure within the network. Conversely, this analysis could prove costly if a number of apparently healthy units are replaced based on the assumption that if one unit is faulty after x hours then so must other identical units. Another drawback of this method is the processing power associated with the calculations required to provide this analysis.

3.5.3 Markov Analysis

Markov analysis is a powerful modelling and analysis tool with time based and load sharing reliability applications [106]. The analysis assumes that any considered

network exists in a number of ‘states’ for example all components operating as desired would be state 1 or one component failure within the network being state 2. The reliability characteristics of a network can be represented in a state transition diagram which shows the states in which the network may exist and the failure transition rates, λ , between each state the rate at which the network transitions into the new state. Markov Analysis also uses repair rates, μ , however similarly to conventional aircraft the failed components of the TeDP electrical network may not be repaired during flight and as such this analysis has no repair rates [111]. Once the system has transitioned into a new state with a rate of λ it may not then transition back to the previous state until it has been repaired with rate μ or until there has been an external input into the system to return it to the original state.

To highlight the rate in which the network transitions into each new state a two component network is considered as detailed in Table 3.2. Component 1 fails with the rate λ_1 while component 2 fails with the rate λ_2 .

Table 3.2 Markov Example 2 component, 4 State Network State Table

Network State	State Description	Transition from Previous State	
1	No Failures	-	
2	Failure of component 1 only	λ_1	
3	Failure of component 2 only	λ_2	
4	Failure of both component 1 and 2	From State 2	From State 3
		λ_2	λ_1

Table 3.2 shows how the network starts off in state 1 with all components unfaulted and can then transition directly into either state 2 or 3 with a transition rate of λ_1 should component 1 fail or with a transition rate of λ_2 with a failure of component 2. When the network transitions from state 3, the only permissible state into which the network may transition is into state 4. As previously there was a failure of component two, the transition into state 4 is with a failure of component 1 and hence rate of λ_1 .

The analysis concepts as discussed within this section may be illustrated expanding on the two component network from this section and is presented in the following section.

3.5.3.1 Markov Analysis Example

Figure 3.9 shows the state diagram for a simple 2 component network where both components are identical and can have one of two states – operating as desired or failed. Therefore for a network with n components there exist 2^n network states; in this case 4 states. This analysis assumes both components operate independently and only one out of the two needs to operate as desired for the network to remain operational.

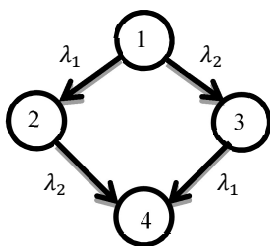


Figure 3.9 Two Component Network State Diagram

Table 3.3 System State Table

State	Component A	Component B	System operational?
1	Operating	Operating	Yes
2	Failed	Operating	Yes
3	Operating	Failed	Yes
4	Failed	Failed	No

Figure 3.9 shows how the network transitions into the different identified states. With the aid of Table 3.3 and from the principles of the transition rate table of Section 3.5.3, it can be seen that component A fails with rate λ_1 and that component B fails with the rate λ_2 . Table 3.3 shows each state for the network of Figure 3.9 and whether each transition results in a failure of the network to operate as desired. Figure 3.9 further shows that from state 1 the system may transition into either state 2 with failure rate λ_1 or into state 3 with a failure rate of λ_2 . From state 2 the system may further transfer into state 4 with a rate of λ_2 or starting from state 3, the system may transition to state 4 with a rate of λ_1 .

Due to the specific requirements of the network, three different states allow the network to remain operational. States 1, 2 and 3 have one component operational and therefore satisfy the requirement. If however the network transitions into state 4 the network will transition into a failed state and will no longer remain operational.

This example is based on an example in [112].

3.5.3.2 *Relative Merits of the Markov Analysis*

Markov analysis provides a powerful tool to provide analysis of a system or system of systems, showing how the network may transition between states and how frequently transitions may occur. This information is invaluable to designers of the network who wish to create the most reliable network whose transitions into a failed state are minimised. Not only does a thorough Markov analysis provide information on transitions in an analytical manner, providing state tables and state diagrams helps to visualise these transitions and quickly identify where design effort may be further required. More, Markov analysis can be used within standby systems where the failure rate of the standby system is greatly reduced until that system is required by the network. A Markov analysis is appropriate in this setting due to the state of the initial system when the standby system is activated [112]. The drawback of the Markov analysis however is the manner in which the number of calculations required in the analysis quickly builds with the number of components constituting the network. As noted within Section 3.5.3.1, the number of components, n , within the network dictates the number of states in the relation 2^n . Therefore for a network with over 100 individual components the analysis would have to undertake over 2^{100} calculations resulting in a slow analysis far more complex than the *k-out-of-n* counterpart.

3.5.4 *Fault Tree Analysis*

Fault Tree Analysis (FTA) is a systematic method through which information on a system may be obtained [113, 114]. This method makes up one aspect of system

analysis, which, by definition “is the directed process for the orderly and timely acquisition and investigation of specific information pertinent to a given decision” [113]. From this definition it can be determined that the prime motive for carrying out such analysis is for the acquisition of information on the network and not for designing a new system architecture [113]. FTA however can additionally be used within the design process of a network [104] and is hence useful in the application of determining optimal TeDP architectures. Specifically, when used to analyse an existing system, FTA can identify points in the network which may cause a bottleneck (large, dominating failure rate within the overall failure rate of the network) and can then help to determine means to mitigate such occurrences. Used in this way FTA can also be used to diagnose likely causes of specific failures and, further, determine the potential corrective measures for any specific failure [104]. Unlike other methods which have been described within this section, such as Bayesian analysis and *k-out-of-n* reliability, FTA works in failure space [104] and considers failure rates and not reliability scores.

FTA is ‘an analytical technique, whereby an undesired state of the system is specified (usually a state that is critical from a safety or reliability standpoint), and the system is then analysed in the context of its environment and operation to find all realistic ways in which the undesired event (top event) can occur’ [104]. FTA is a top down (or bottom up) technique where analysis starts with a ‘top event’, this analysis shows the faults or reasons which are likely to cause the fault (or other event) of interest and each subsequent cause of failure, working systematically through the network. The analysis provides a methodical evaluation of an aircraft electrical network and shows how each individual fault in the network impacts upon the failure rate of the network as a whole.

FTA is mentioned in a number of standards and ARP’s (Aircraft Recommended Practice), specifically CS-25 [115] and ARP 4761 [100] and therefore this analysis must be undertaken in order for a network to become certifiable at an acceptable rate of failure. Specific features of fault tree analysis include [116]:

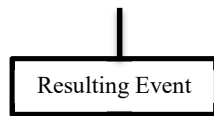
- Provides an exhaustive analysis of failure causes

- Provides an extensive risk analysis: this analysis uses scenarios to determine all possible failure paths and consequences
- Lists of consequences can be easily identified
- Probabilities of consequences can be determined
- Helps the generation of ideas for mitigating consequences of failures

This list of features is by no means exhaustive and further benefits of the FTA may be found within the works [104, 113, 116]. Through the identified features it is clear to see why FTA provides such a useful tool for identifying fault causes throughout a specified network. There are a number of symbols which are used within FTA to represent a number of different logical operators and mathematical operations. The symbols which will appear within the case studies section are described below:



Top Event: the event which provides the focus of the analysis.



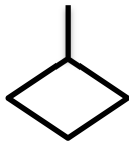
Resultant Event: An event which is the result of a combination of faults and is usually displayed as the output of a logic gate.



The AND gate: This gate is used when all inputs must hold true for an event to occur – that is when all input events have occurred. The failure rate that results from this gate is the equivalent of the multiplication mathematical operator.



The OR gate: This gate is used when either of the inputs to the gate must hold true for an event to happen; that is if either event occurs the output event will occur. The failure rate resulting from this gate is the equivalent to the ‘addition’ mathematical operator.



An Incomplete Event: An event which cannot be further developed due to lack of knowledge or information on what the causes of the fault are. Alternatively the event may not have been developed due to a lack of importance to the overall top event.



Basic Event: An independent basic failure which concludes the analysis. There are no further events after this event.

The operation of these symbols and their associated functions can be seen in Section 3.5.4.1 where a simple example is presented highlighting how the analysis is performed.

3.5.4.1 Fault Tree Analysis Example

The fault tree of Figure 3.10 shows the causes of faults for an example network and which combination of faults provides the cause for the top event. It can be seen that the top event occurs if both feeder A fails AND feeder B fails. It can also be seen that for feeder A to fail, either the battery supplying the power to the feeder fails OR the battery has been previously turned off. The failure of the battery is a basic failure event while the event of the battery having been turned off is considered incomplete until it is determined for what reason it has been turned off. In the case of the failure of feeder B however the two causes of its failure could be either the basic failure event of the battery failing OR there was a loss of power from the second linked part of the system OR the connection between the battery and the feeder failed.

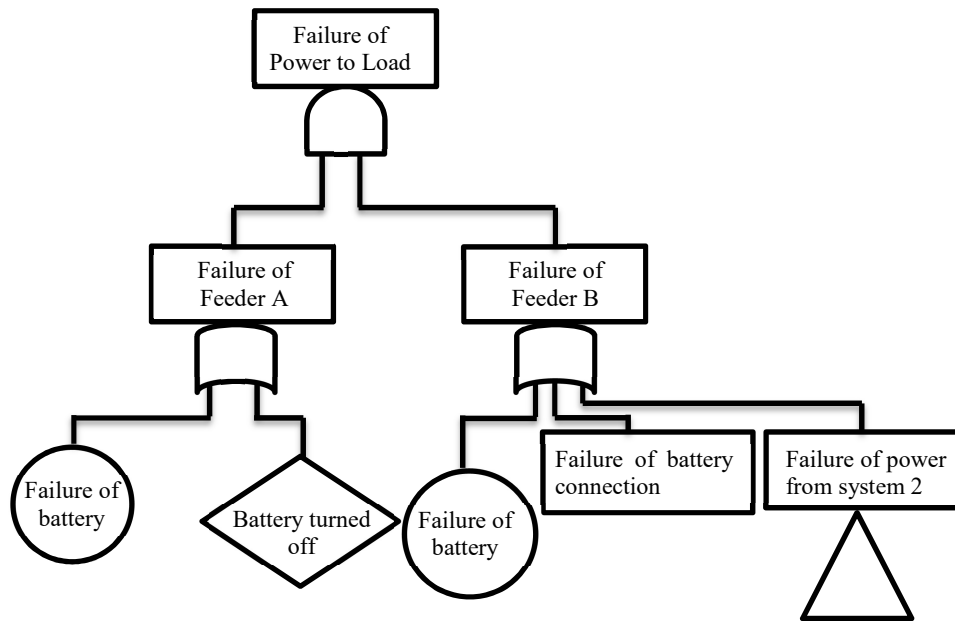


Figure 3.10 Fault Tree Analysis Example

FTA has many applications within aircraft design, a number of which are safety related to enable the designers to avoid architectures which would likely result in injury or loss of life [117]. One such application of FTA is in the determination of the cause of engine failure. An engine failure analysis can determine the events which are likely to cause such a failure, their relative probability and how each event is linked [118]. Such an analysis is useful as the most likely causes of failure can be easily identified, effort in improving this reliability profile can be undertaken and the time and cost involved in diagnosing engine failure events reduced.

3.5.4.2 *Benefits and Drawbacks of FTA*

Similarly to the Markov analysis, the FTA provides a clearly laid out visual analysis which allows network choke points and peaks in failure rate to be easily identified. Further this analysis allows common cause failures (CCF) to be identified and mitigating action to be designed into subsequent network build standards. Like the Markov analysis this analysis also falls down in that analysis complexity builds rapidly for each additional component added to the network: while complexity is only minimally affected by the addition of series components each parallel path

significantly adds to the number of options at any logical operator. This causes large fault trees to be constructed and can lead to confusing pathways within diagrams.

3.6 Down Selection and Summary of Reviewed Methods

After careful review of all the benefits and drawbacks of the methods considered within this chapter, it was decided that the methods most suited to analysis of a TeDP network at this stage were both *k-out-of-n* analysis and FTA. The lack of field data for the failure rate methodologies makes a reliability method preferable, as it can be run with representative figures to reveal informative trends. Additionally, using a reliability method such as *k-out-of-n* uses a far lower level of processing power over other methods such as Bayesian analysis and Markov analysis. The format of the *k-out-of-n* method means that reliability trade studies on TeDP networks are relatively simple to perform and results are quick and easy to interpret, the way in which analysis is carried out means this method is naturally suited carry out evaluations. The *k-out-of-n* method allows for rapid prototyping of networks and changes to be made to reliability values and component selection with minimal costs to the time or complexity in outputting results. The *k-out-of-n* analysis is a valuable method which allows the T-R profile of a network (mentioned in Section 3.2 and again in Chapter 4) to be determined for both full and partial networks, where the results can be quickly mapped into graphical form for quick visual analysis. This method will be used to determine the minimum number of thrust-producing propulsors required to be operational at the RTO stage of the flight cycle as well as determining the effect to the reliability of the network of using *k-out-of-n* redundant feeders at varying locations throughout the network. This is a useful method for providing information on the effectiveness of added redundancy and possible provision of additional propulsors in quantifying the change of overall reliability of the network. The natural benefits of utilising this method mean that it provides a far superior analysis at an early prototype stage for this network concept and the benefits of which will be illustrated within the case studies chapter.

FTA is another valuable tool which will be used to provide information using failure rates for the network. This method graphically allows places where the failure rate within the network may be significant, and hence dominate over other failures to be quickly identified as well as enabling the user to quickly identify failures which may have a greater effect on the system as a whole. This method can also allow the user to determine the effect to failure rate of additional redundant paths through the network and the net benefit for any additional redundant pathways.

Using these two methods as well as performing a sensitivity study, the TeDP network may be comprehensively analysed to obtain information relating to the reliability of the network and tolerance of the network to failure. The studies conducted using these methods may be found in chapter 5.

While this review of reliability methods is not exhaustive, it was considered that the methods detailed within this chapter were the most relevant to the analysis of the TeDP style network architecture. All considered methods are useful for analysing the network as a whole or in part, although some perform better when analysing larger sections of the networks defined within Chapter 5 of this thesis. Other more complex methods include analysis of a time varying system however at this early stage of network development the available data is not yet available to conduct a meaningful analysis.

3.7 Chapter Summary

This chapter has reviewed a number of topics within the subject of TeDP reliability and has provided information in a number of areas summarised within this section. The chapter reviewed the research which was pre-existing on the concept, providing an overview of a number of shape and engine configurations before refining the research topic to reliability of TeDP. The main contribution of this chapter was to summarise the research which currently exists in the area of TeDP reliability and through careful consideration of the available information detecting a niche area to be exploited and enhance the knowledge which is available. As well as identifying an

area of TeDP reliability analysis to expand upon, a number of suitable reliability methods which could be used to analyse this network were also suggested. These methods were discussed, considering both pros and cons to determine which methods could provide the most thorough yet concise analysis of a complex TeDP propulsion network. The final methods chosen for analysis were the *k-out-of-n* reliability method and the FTA method.

Chapter 4

A Method for the Analysis of TeDP Electrical Propulsion Networks

Such radical new aircraft concepts as TeDP place a new and significant reliance on an aircraft's electrical system for safe and efficient flight. Accordingly, in addition to providing certainty that supply reliability targets are being met, a contingency analysis evaluating the probability of component failure within the electrical network and the impact of that failure upon the available thrust must also be undertaken for each architecture design. Solutions that meet specified thrust and reliability requirements at a minimum associated weight are desired as these will likely achieve the greatest performance against the proposed emissions and noise targets [119]. This chapter presents a contingency analysis based design and analysis approach for thrust reliability analysis of the electrical propulsion system of TeDP aircraft architectures.

This Thrust-Reliability (T-R) analysis approach extends beyond the single failure rate provided through traditional FTA methods and, with a more powerful methodology that is more sympathetic to understanding the complex reliability practicalities, provides a significant contribution of this work. Through fully considering the reliability and thrust provision of each possible system configuration i.e. following the failure of one or more components, as well as the most common considered faults to the network a number of contingency scenarios can be produced to allow a greater understanding of the network to be gained. This contingency analysis method combined with an additional measure of total system weight and volume provides an effective design capability.

This chapter presents a case study for an N3-X TeDP design configuration showing how the Thrust – Reliability (TR) profile of the network may be evaluated and manipulated using the contingency analysis method and utilising k -out-of- n reliability analysis as described within Section 3.5.1.

4.1 Introducing a Method through which to Analyse Thrust Reliability Profiles of TeDP Architectures

Due to the timescale for the long term subsonic future generation of aircraft goals (new technologies are required to be at TRL 4-6 by 2030), to meet these goals the potential exists for a wide range of unconventional and novel aircraft concepts to be considered. In order to meet the N+3 goals as identified in [18], a Blended Wing Body (BWB) aircraft, powered by Turboelectric Distributed Propulsion (TeDP) is subject to a detailed study. TeDP is an encouraging design approach which offers a potentially highly reliable supply of propulsive power, even in the event of a single engine failure [37].

Power supplied to the high power propulsion motors utilised in TeDP systems must be of similar reliability to that provided for the traditional low power critical loads (such as avionics) in present day aircraft [43]. Necessary to achieving supply targets for current systems is the use of battery backup; however, the provision of reliability through additional supply for high power loads, either through dedicated generators or bulk energy storage, is inefficient in terms of weight. A more effective solution appears to be in the provision of interconnectivity within the electrical system architecture and to utilise available capacity in the generation mix. The drawbacks of this approach however include greater system complexity and dependency [16]. Achieving the required reliability targets with minimal ensuing weight penalties and system complexity in TeDP systems therefore is a significant design challenge, placing new requirements on previously adequate design approaches (such as FTA described within Section 3.5.4). The associated optimisation problem should ideally provide a measure of the effectiveness of system redundancy in maximising available thrust whilst minimising contributions to overall system weight. More specifically, it is desirable to evaluate the available thrust provided by an architecture and its

associated reliability for a broad range of system configurations, (i.e. following single and combination failures), which combined with a measure of total system mass and volume provides an effective design and rapid prototyping capability.

4.2 Defining the Case Study Network

Before any analysis may be undertaken, it is important that the network under consideration is properly defined and there exists a mechanism for identifying specific components within the network. For this purpose, the baseline TeDP network utilised in this thesis may be redrawn as shown in Figure 4.1; this clearly shows the network consisting of 4 identical and parallel subsections where G = generator, M = motor and P = propulsor (the fan connected to the motor), the next symbol from the generator represents the AC/DC convertor and the similar symbol adjacent to the Motor block represents the AC motor drive as defined within Table 4.1.

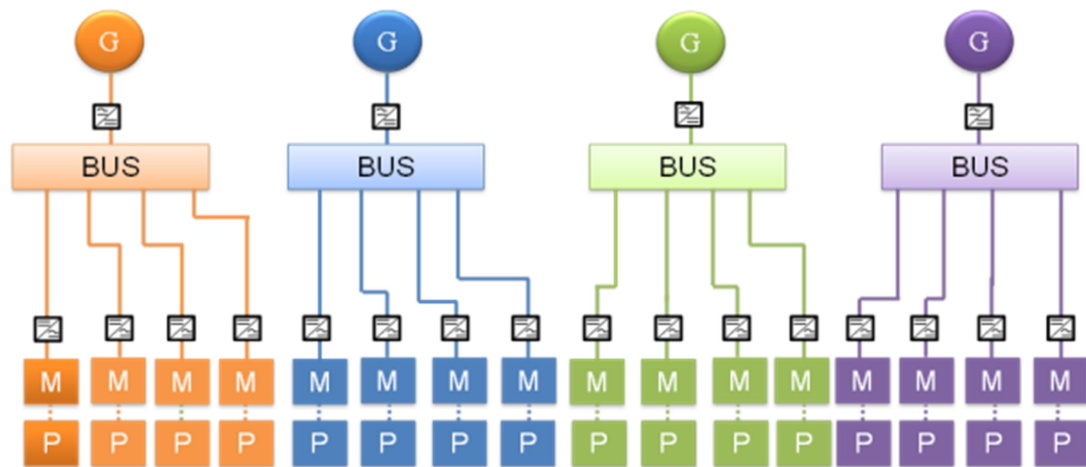


Figure 4.1 N3-X Schematic showing motor connections, not motor placement

Figure 4.1 shows a simplified lumped model showing the physical connections of the N3-X network, clarifying the schematic view presented elsewhere throughout this thesis. Presenting the network in this way provides a means to quickly establish all connections within the network as well as to further define modular sections and to reference individual aspects of the network as described in the following Subsection 4.2.1.

4.2.1 Defining Network Modular Sections to Simplify Analysis

To aid in analysis, it is important that the full network is broken down into smaller modular sections allowing existing probabilistic methods to be used in analysis. All components as will be used in the network are shown in Table 4.1.

Table 4.1 Network Components









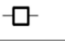


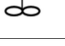
<i>Symbol</i>	<i>Component</i>
	Generator
	EEC
	Bus
	Three Phase Breaker
	DC Cable
	3 Phase Cable
	SCFCL
	AC-DC Convertor
	DC Breaker
	DC-AC Motor Drive
	Motor
	Propulsor

Table 4.1 shows each component as used in the network in the ‘symbol’ column (where EEC is the Electronic Engine Controller) with a corresponding component name in the ‘component’ column. Through careful observation of the network as presented in the right hand side of Figure 4.2, it can be seen that each identical subsection can be described by the constituent components as shown in the left hand image. For the purposes of this analysis, only the propulsion network and not the cryogenic system which is required to cool the superconducting network is considered. This is in part due to the undefined nature of such a cooling system and part due to the low level of understanding of the technology as a whole.

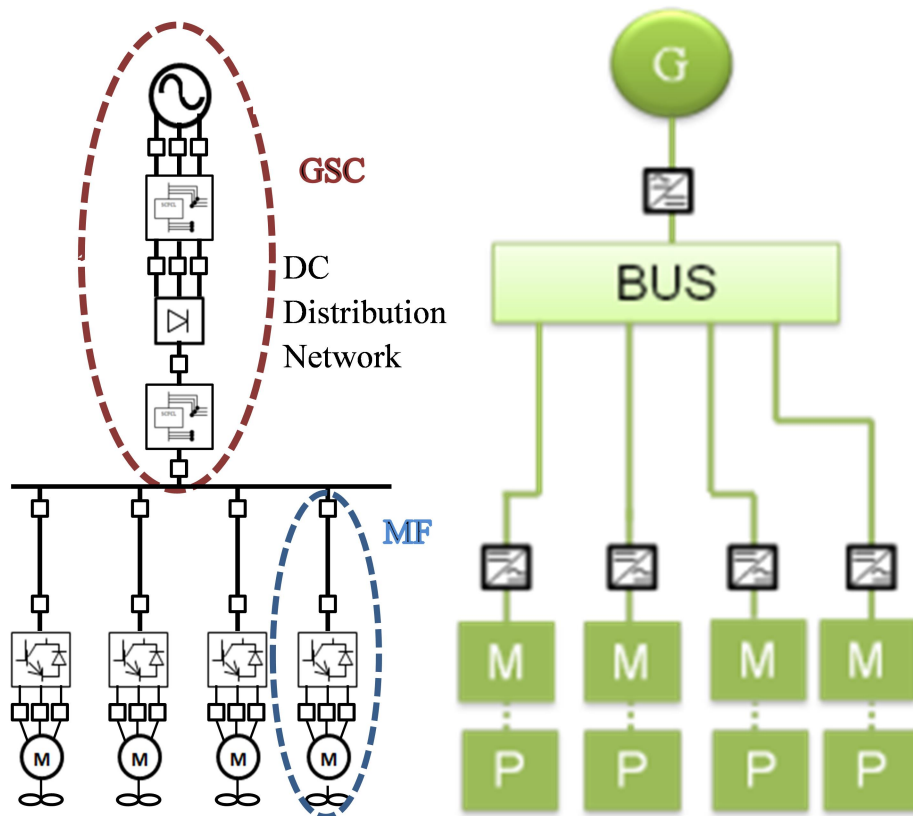


Figure 4.2 TeDP Network Breakdown and associated network subsection

Figure 4.2 shows how each of the subsections of Figure 4.1 maps to the specific component layout. Figure 4.2 (above) also shows that the modular subsections can be further broken down into two further modular sections: the Generator Supply Channel (GSC) and the Motor Feeder (MF) which have been highlighted in the left hand schematic of Figure 4.2.

The schematic shows that the GSC extends from the (superconducting) generator through to the propulsion bus, the bus that both the GSC and MF are connected. The schematic also shows that each of the MF are identical and thus probabilistic calculations can be conducted on a number of parallel sections. As such the MF extends in a series manner from the first component after the bus (in this case a DC breaker) through to and including the propulsor. A number of MF's are connected in parallel to each GSC and a number of these identical network subsections combine to create the TeDP network. This example shows 4 parallel MF sections and 4 parallel network sections. The busses of the network are not included within either the MF or

the GSC and are considered separately, and in series with the other sections for reasons that will be described in the following section.

4.2.2 System used to define Motor Feeder Positional Reference

To further simplify analysis and network understanding, MF and GSC of the connection diagram of the reference baseline TeDP network (Figure 4.1) has been given a positional reference dependent on where it has been connected in to the network and not where it is positioned on the aft of the aircraft. This referencing is most useful when undertaking Fault Tree Analysis (FTA) in the chapter 6 where the failure of specific components are referenced and the consequences are flowed through the fault tree.

The numbering system works from the left to the right of the network where each motor feeder MF has a positional term MF_{ij} where i indicates a connection to the i^{th} bus from the left of the schematic and j represents the j^{th} motor from the left of the propulsion bus. This numbering system may be clarified in the following example shown by the network of Figure 4.3, with 5 generators connected to 4 propulsion busses and each propulsion bus with 4 parallel connected MF.

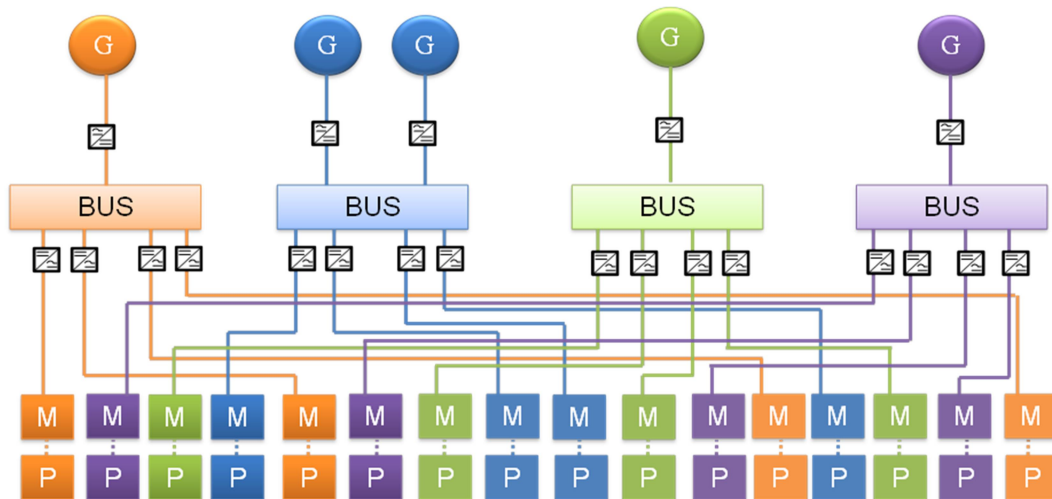


Figure 4.3 TeDP Baseline Network Schematic

Figure 4.3 shows 4 parallel and differently coloured network sections. Should reference to the first (orange) MF on the very left of the network be made, this would have the positional term $MF_{1,1}$ as this is the leftmost MF connected to the leftmost propulsion bus of the network. However, the (purple) MF located to the immediate right of $MF_{1,1}$ in Figure 4.3, has the positional term $MF_{4,1}$ as, through observation it can be determined that this is the leftmost MF of the 4th propulsion bus to the left of the schematic. Similarly for the GSC, for a case where there are no parallel connections to the propulsion bus (orange, green and purple), the positional reference remains as $GSC_{1,1}$ in keeping with the terminology. If however there is a parallel connection as in the blue generator case of Figure 4.3, the right hand blue generator would be assigned the notation $GSC_{2,2}$ as it is the 2nd generator from the left of the 2nd propulsion bus from the left of the network.

Thus by introducing the positional notation in this section through the case study used in Figure 4.3, it is now possible to make reference to any required modular section of network in a TeDP architecture. Although the notation has been illustrated with a 4-section example, it can be readily generalised for use within variations of any TeDP architecture.

4.3 TeDP Design and Analysis Requirements

SAE standard, SAE 4761, provides guidelines and methods for performing safety assessments for the certifications of civil aircraft [100]. One such tool as described by this standard is Fault Tree Analysis (FTA) [100] which uses failure rates and logical operators to determine whether candidate network architectures meet industry specified parametric requirements [104] such as the critical reliability level of no faults in 10^{-9} hours [105].

One particular example of the use of FTA in the aerospace sector is determining the ability of a set network to meet the Civil Airworthiness Authority (CAA) requirement that catastrophic failures (e.g. leading to the complete loss of an aircraft) should occur less than once in 10^9 flight hours [105]. Hence the failure rate of components or

combinations of components which would result in this occurrence must be less than 10^{-9} per flight hour.

For TeDP systems, a key reliability requirement is that any failure or series of failures which leaves the aircraft with less than 30,000 hp of rated thrust (the minimum required for safe rolling take off for the aircraft size in consideration) [43] should occur with a rate of less than 10^{-9} per flight hour [49]. Given that individual electrical components are unlikely to meet this specific rate on their own, this target is expected to be achieved through the overrating of system generation components and provision of system redundancy. The process of assessing of the effectiveness of these measures to deliver the required thrust reliability is referred to as contingency analysis in this thesis. This is explored in further detail in the next section.

4.4 Contingency Analysis in a Land-Based Network Setting

In a conventional utility grid setting, contingency analysis is used to determine the potential overloading in a network branch following the outage of a network line, usually focusing on the power flow before and after a contingency plan has been implemented [120].

Large scale network models as used in contingency analysis for AC distribution networks are not exact models and only consider whether overloading currents or voltages actually occur when sections of the network are lost to a fault [121]. In most cases linear models are employed and super position used where resistances are often considered negligible to create a purely reactive network [121]. Undertaking analysis in this manner allows quick determination of new line currents and voltages when lines are switched on or off or even if a circuit breaker has been put into action and currents have been redistributed throughout the network [121].

4.5 Contingency Analysis for TeDP

Similarly when applied to TeDP, the flow of power before and after the contingency plan has been introduced is considered in addition to weight penalties due to the weight sensitive nature of aircraft [42] and forms a key part of the Thrust-Reliability method described within this thesis. Each contingency scenario for the network architecture should ideally exhibit the minimum possible take-off weight for the highest possible provision of power under any network outage scenario [44]. The effectiveness of contingency measures such as the oversizing of components or the addition of redundant feeders in enabling that particular design to meet the thrust probability specification are determined. The evaluation of the impact of such contingency measures on system mass and volume enables the most weight effective contingency measures or combination of measures to be determined, ultimately facilitating the optimisation of architecture designs. The following subsections illustrate an example TeDP contingency analysis.

4.5.1 Network Trade-Offs

One of the key design considerations for TeDP applications is the determination of the optimum number of generators and propulsors to produce the required propulsive power and deliver this as thrust [11]. For example, it may be possible to employ two generators and just six motors in an architecture design (as illustrated in Figure 4.4).

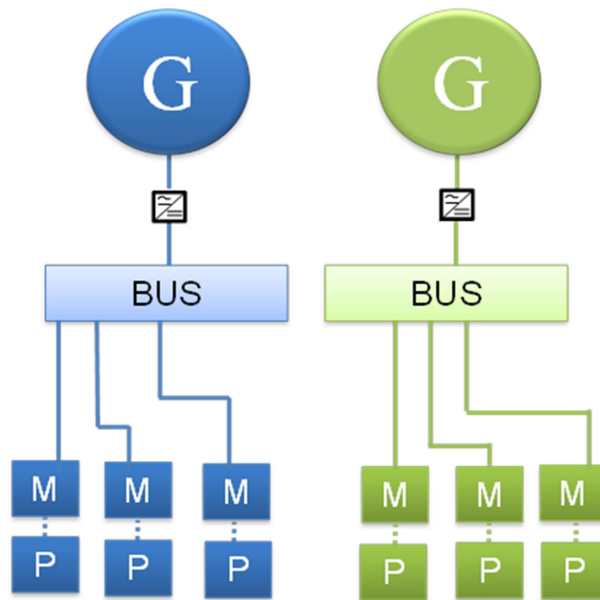


Figure 4.4 Two Generator TeDP Network Utilising Six Motors to Provide Thrust

However, unless the reliability of the network components is sufficiently high, it will be necessary to overrate the generation and thrust providing components such that the required level of thrust is still delivered even following the failure of a number of key components.

Owing to the small number of generators and propulsors of the design shown in Figure 4.4, considerable oversizing may be required to meet this requirement. In any network blindly oversizing the generators and propulsors to meet the reliability specifications may achieve a solution but at the expense of significant weight penalties. Optimal solutions maintain the efficiency provided through using a small number of generators each exhibiting a large core while including redundancy to protect against a single engine failure hence the inclusion of a total of four generators, two per engine [16]. The architecture design sees the number of propulsors and motors dictated by the requirement for the provision of symmetrical thrust, one of the major benefits of the TeDP concept. The careful placement of the large number of motors and propulsors is used to provide symmetrical thrust, even under fault conditions and enables weight savings to be made through the removal of the tail plane section [19, 43]. Using a greater number of motors and propulsors would result in only a minimal impact to thrust in the event of a failure within the network, and a function of the total width of the aft of the aircraft [16].

While the configuration shown in Figure 4.4 may be capable of supplying the required thrust in a scenario with no failures, if the reliability of the components within this configuration were not significantly high or a failure were to occur within one of the critical paths, the rating of the generation components would need to be set so that the network would still be able to provide the required level of thrust. In this simplified network example, a failure within the GSC section could lead to a 50 % loss of thrust therefore each generator would have to be rated to supply twice the required power for that section of network to overcome such an event. The significant over rating of the small number of motors and generators within this network would lead to significant weight penalty on the network.

4.6 TeDP Baseline Network Considerations

Employing a network architecture which splits the total required power over a greater number of units to potentially reduce the weight dedicated to each generator for oversizing could provide a lower probability of failure or failure rate for the minimum required thrust and a lesser weight penalty for the network [47]. Two variations of the N3-X baseline network of Figure 4.4 are shown in Figure 4.5 and Figure 4.6.

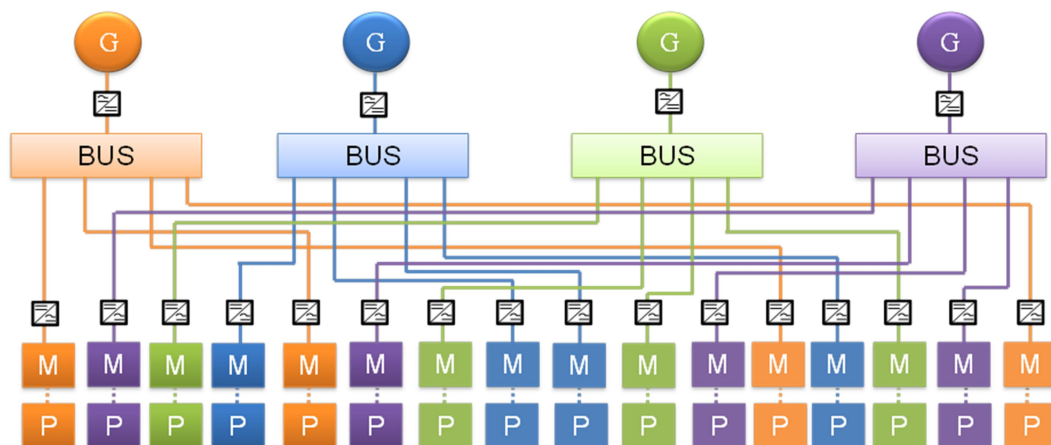


Figure 4.5 16 MF Configuration of a TeDP Network

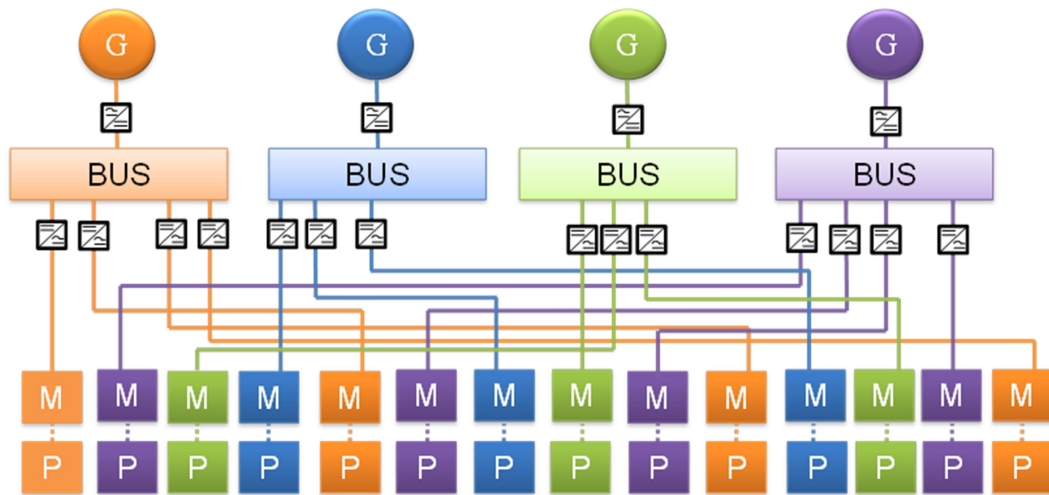


Figure 4.6 Baseline TeDP Network (14 MF Configuration)

Both Figure 4.5 and Figure 4.6 show a baseline configuration for the TeDP network. Both configurations have been used by NASA and Rolls-Royce; the 14 MF configuration was used from the early concept until late 2013 [Armstrong papers] when the 16 MF configuration superseded it in order that purely symmetrical thrust may be, maintained under all motor failure scenarios [51]. Both of these baseline network configurations have no contingency for failure other than oversizing of the generators and motors dependant on the probability of failure of the supply of power. It can be seen from both of these configurations that the motors associated with each generator have been selectively placed on the network to enable symmetrical thrust in the event of an engine out scenario. This motor placement allows thrust vectoring to take place and for the removal of the aircraft control surfaces such as the tailplane which houses the rudder in a conventional tube and wing aircraft, enabling weight savings [11, 16]. The pitch, roll and yaw functionality traditionally undertaken by this section of the plane can then be undertaken through thrust vectoring using the large number of electric fans [11, 16].

This section has considered options for a baseline TeDP network based upon the principles of contingency analysis. Through understanding how events such as a generator failure affects the required overrating of the remaining un-failed generators, trade-offs can be made in the number included within a network architecture. Similarly through careful placement and sizing of motors, oversizing of individual motors may be minimised and symmetrical thrust provision may be

maintained in the event of a number of failures. These failure scenarios are explored within section 4.7.

4.7 Failure Scenarios

A key requirement in determining the extent of generation component overrating within the TeDP network is the evaluation of failure modes within that network, whether a fault mode may lead to a Common Cause Failure (CCF) and the probability of each failure event occurrence. First, it is important to understand the most common causes of failure to provide power within the network; these can be determined by the relative failure rate of each supply path within the network. These can be shown in the following series of figures; this will start from the failures causing the least impact on thrust, running to that which would cause the greatest perceived loss of thrust. Each failure is represented through that section of the network being rendered in black.

The first case considered is a loss of thrust resulting from the failure of either a single propulsor, a single motor or an entire MF path. This case is illustrated in Figure 4.7, with the equipment section in a failure state identified with black components.

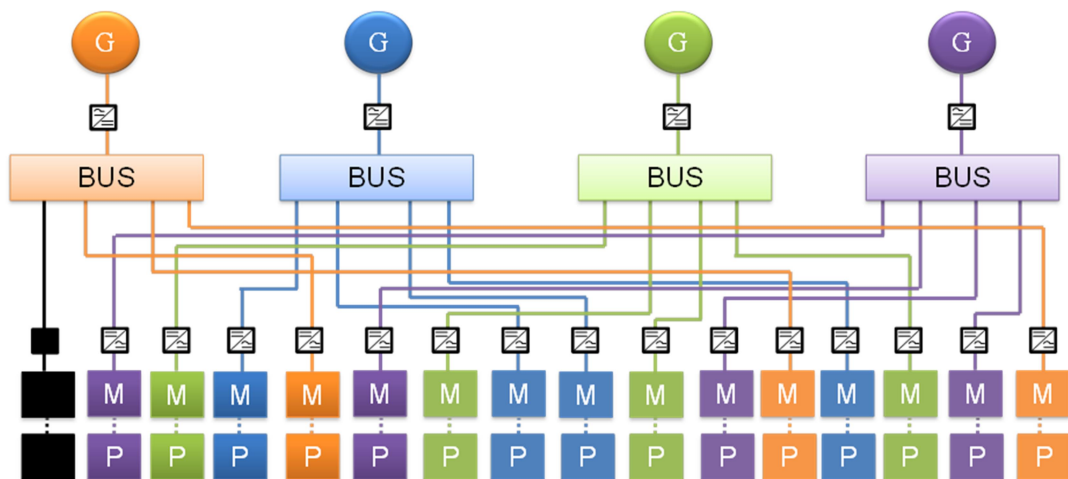


Figure 4.7 N3-X Network Showing Loss of Propulsive Thrust Due to the failure of a

Figure 4.7 shows that should only a single instance of this failure occur, there would be a loss of thrust proportional to the number of individual MFs that had failed, in

this specific case 1/16 or 6.25 % of the total available thrust. Another, slightly more costly failure event for thrust would be the failure of a propulsion bus or a single generator as illustrated in Figure 4.8. Again with compents in a failed state are shown in black.

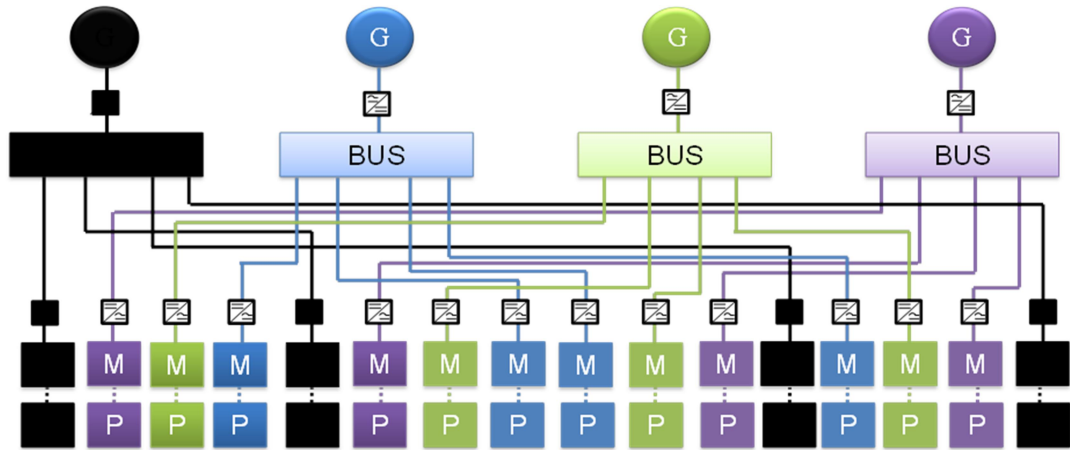


Figure 4.8 N3-X Network Exhibiting the Loss or Failure of a Bus or Generator Causing Loss of Thrust

It can be seen from Figure 4.8 that a loss of this nature is considerably more costly for the network. In this specific case, the total thrust lost is equal to one quarter or 25 % of the connected thrust and a failure resulting in this level of lost thrust may have wider implications on take-off or other flight functions. The final major event for loss of thrust considered would be the failure of an engine as shown in Figure 4.9. Again with compents in a failed state shown in black.

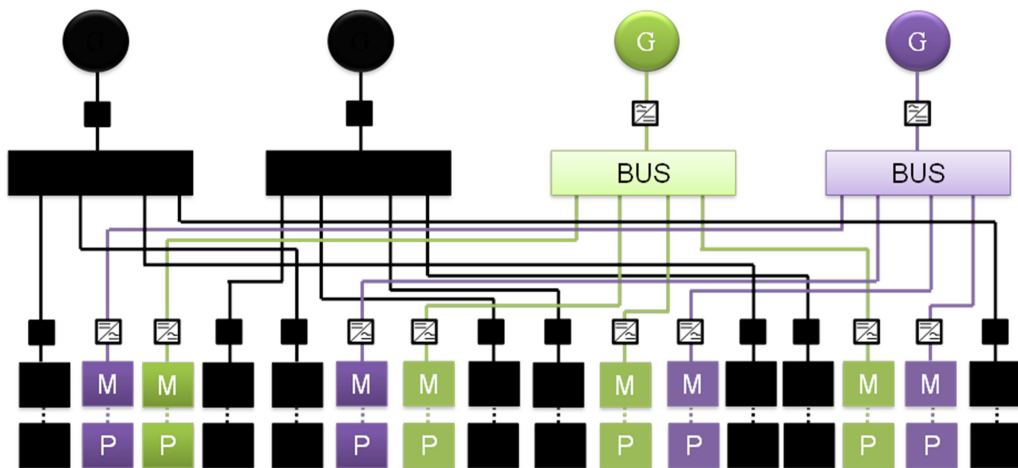


Figure 4.9 Loss of 50 % Thrust due to Failure of an Engine

Figure 4.9 illustrates that should an engine on the aircraft fail, that is two generators and their associated connected components, the failure would reduce the available thrust by at least 50 % and substantially affect the ability to use thrust vectoring for roll, pitch and yaw manoeuvres. Such a significant loss of thrust would prevent any take-off event and restrict continued flight based upon the individual aircraft's ETOPS certification [122, 123].

This section has shown how different failure scenarios could potentially lead to large losses in aircraft thrust if suitable preventative measures have not been put in place. Understanding where the losses may occur and what levels of thrust loss can be attributed to each failures allows informed decisions to be made in network design.

4.7.1 Implication of Failure Scenarios

The level of component overrating required in each of the highlighted cases is dependent on the failure mode occurring more frequently than is specified in the minimum thrust requirements. Currently aircraft are rated to supply twice the minimum required thrust for take-off at sea level [43]. For example, if it is likely that an engine will fail more than once in every 10^9 flight hours, then the architecture components for a two-engine N3-X TeDP aircraft will need to be rated to supply the minimum required 30,000 hp for take-off at sea level with only half the propulsion system available. In order to fully understand the required overrating of components and the impact of each failure mode, Thrust-Reliability (T-R) trade-offs are considered in this Chapter and an aircraft specific contingency analysis conducted.

4.7.2 Contingency Scenarios

Contingency measures exhibiting low weight penalties can be readily implemented to mitigate the effects of component failures with the aim of reducing the level of overrating required. This section will introduce a number of measures which could be introduced in order to mitigate the effects of a failure with associated diagrams.

The first failure effect considered will be the mitigation of a single generator failure. Previously in the scenario of Figure 4.14 above in Section 0, it was identified that should this failure occur, then it would result in the loss of thrust from all downstream motors and propulsors with a direct connection to this generator. However, a bus tie could be introduced as shown in Figure 4.10 that would provide an alternative current path. Bus ties create a link between two busses within a network, linking them with a protection device such as a circuit breaker and provide a method of isolating a faulty generator from its load bus and re-supplying the bus by connecting power from another compliant bus.

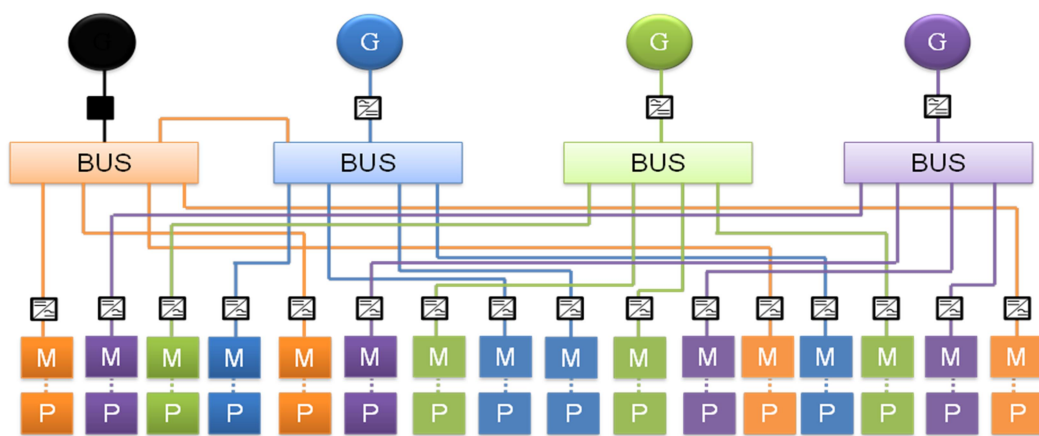


Figure 4.10 TeDP Network using Bus Ties to Mitigate the Effects of a Generator Failure

This method is only appropriate in cases where the bus and loading remains unfaulted and supplementary power can be routed from a fully compliant and unfaulted adjacent generator to recover power to the MF affected by the failed generator. Bus ties can be added in this manner between adjacent propulsion busses provided that the generators were rated to accommodate these at the design stage; however the ties still add a significant level of complexity to the network. Whereas each motor may not be able or constantly required to operate at rated levels when being powered via an alternative generator in this manner, using bus ties would allow all MF to continue operation and provide thrust for the aircraft at the appropriate point in time. The results of generator failures can also be eased through the introduction of parallel feeders. This type of parallel connection is illustrated in Figure 4.11.

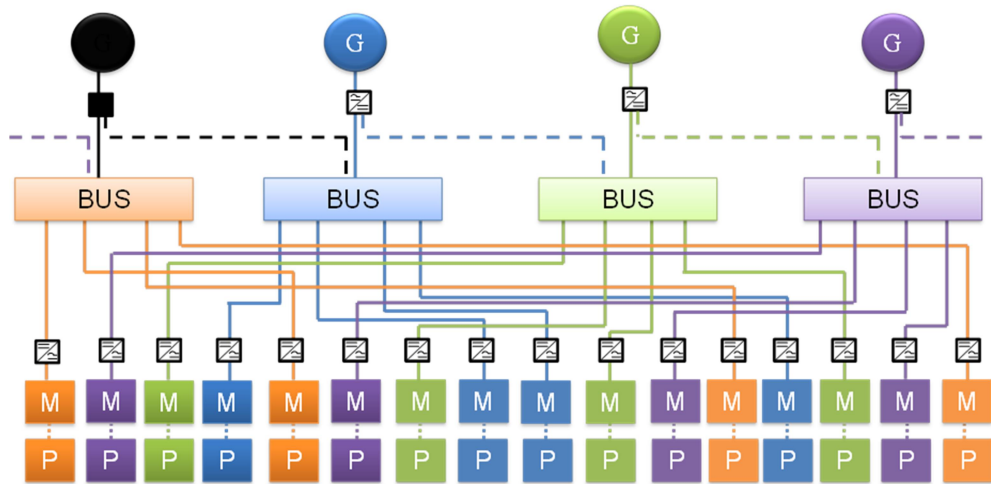


Figure 4.11 Parallel feeders from Generator to Bus used to Increase Redundancy in a TeDP Network

Figure 4.11 shows that parallel feeders may be added between the AC/DC converter and the propulsion bus where there may be n parallel feeders to each bus, where n is the number of busses within the network. This method has an advantage over bus ties, as the power supplying an adjacent bus is not reliant on another bus being able to supply the power however adds significantly more weight and complexity to the network. Similarly to the use of parallel feeders from the generator side of the network (GSCP), parallel feeders can be added on the motor and propulsor side of the network (MFP) as illustrated in Figure 4.12.

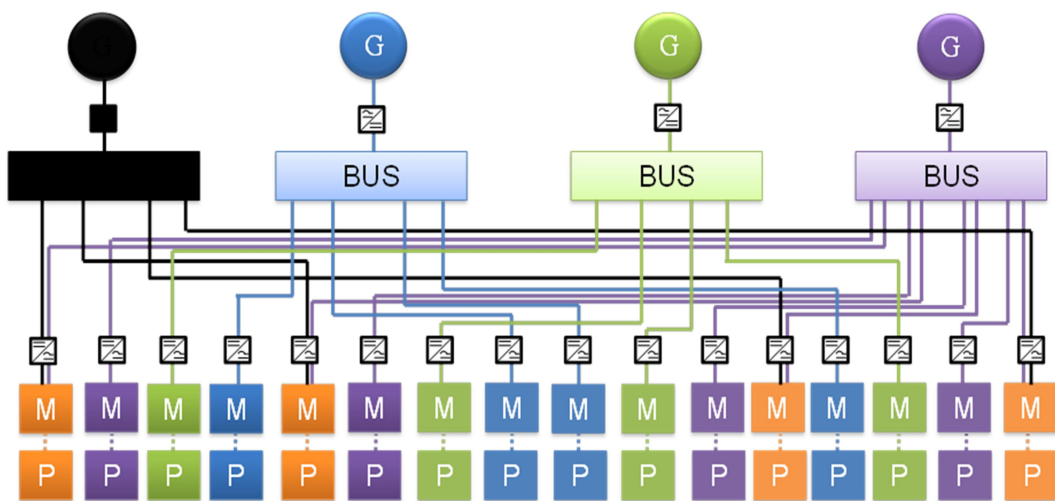


Figure 4.12 Loss or Failure of a Bus causing loss of 4 MF Mitigated through the use of additional

Figure 4.12 shows that MFP may be added to the network between the propulsion bus and the AC motor drive. As with the GSCP n feeders may be paralleled to each AC motor drive where n , again is the number of busses. This method is beneficial as it can mitigate the effects of a failure of both a bus and generator (as power may be routed through to the opposite end of a network) where other methods may only ease the effects of one or the other.

4.7.3 Power- Reliability Graph

It is possible to display the results of a contingency analysis for a given architecture graphically using a propulsive T-R plot similar to that shown in [49]. This work extends the work of [19] through displaying discrete reliability values for each architecture against the associated provided level of thrust, being able to accommodate a number of architectures on any one graph. In this manner, the propulsive thrust provided by every possible configuration design corner of a given architecture is mapped against the system reliability while in that state or configuration.

Through mapping the thrust reliability and superimposing an additional trace of that networks T-R requirements onto the T-R plot produced for the considered architecture, it is possible to gain a visual assessment of a particular architecture's compliance; given the superposition process of mapping thrust and reliability can be usefully automated a powerful benefit of the plot is seeing at a glance where the architecture reliability falls short of minimum threshold template levels.

A T-R graph for an example N3-X TeDP network is illustrated in Figure 4.13.

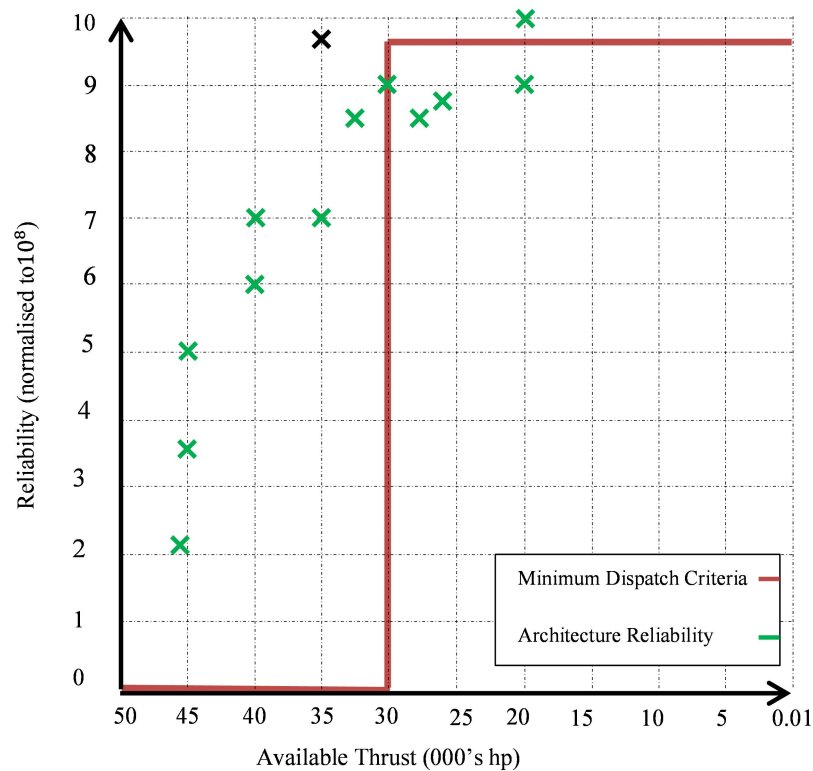


Figure 4.13 A T-R Graph for an Example N3-X Network

In this figure, the red trace shows the required T-R specification for the minimum reliability of take-off thrust for an example N3-X network, while the green points show the T-R profile for that N3-X network architecture under all identified failure scenarios. Each point represents an individual configuration of the architecture under consideration, with or without redundancy and potentially under faulted conditions, where the most probable methods of achieving the desired level of thrust have been adopted. While this graph has been designed to show potential points of a singular network the graph is also of great value when comparing the T-R profiles of a number of networks. The figure shows the thrust levels at which the architecture exceeds the required reliability levels in its provision of thrust (above or left of the solid red line), where it is failing to meet the required reliability (located under the red line). Additionally those points which lie exactly on the vertical red line represent an architecture which exactly meets only the available thrust requirement and those on the horizontal red line represent configurations which meet only the reliability requirement however under achieving the thrust requirement. The ideal location for the architecture capability on the T-R graph is in the region represented by the black

cross (top left) of the graph. Here both criteria are being met and thus the aircraft architecture is meeting the required targets. While some points may not quite meet either T-R target, through plotting them on the graph, the network architect is able to readily view the severity of non-conformance with network design requirements. Furthermore, the plotting of all evaluated network configurations allows the designer to determine which network configurations would be feasible under alternative operating requirements or under an alternative design. Extending this graph to include a weight parameter would additionally allow a number of concept networks to be compared to determine an optimal design to fulfil contractual or desired requirements. Where a number of points exist on a single chord of the x-axis, this could represent a number of architectural solutions all with varying configurations providing the same level of thrust. Alternatively this scenario may represent a single network where a number of alternative redundancy measures are being considered, in this case the additional weight parameter could act as the discriminating factor between two or more similarly reliable networks. The work to be presented in this thesis will make use of this graphical T-R representation within the case study presented within this chapter, as well as the case studies of Chapter 5 to show how configurations of an architecture perform relative to other configurations of the same network. Chapter 5 also used this network to providing comparison of how different redundancy methods enhance different network reliability. It should be noted that Figure 4.13 shows no minimum reliability requirement for thrust power levels above 30,000 hp of rated thrust; this comes about due to the minimum take-off thrust requirement as specified by the authors of [19]. As such, the sole design focus in the presented case study in Section 4.9 would be attaining the required propulsive thrust reliability for at least 30,000 hp of thrust whilst minimising weight and complexity.

Other performance requirements could also be included with this process, for example those relating to Time Limited Dispatch (TLD), where an aircraft architecture may be allowed to operate for a specified duration with a fault or faults present within a redundant section of the network as dictated by SAE ARP 5107B [124]. This is shown in Figure 4.14, where the compliance of an example architecture's Thrust-Reliability capability is assessed against three typical performance requirements for a

TeDP aircraft network such as those set out by SAE ARP's for TLD [124] and airworthiness of engine components [125].

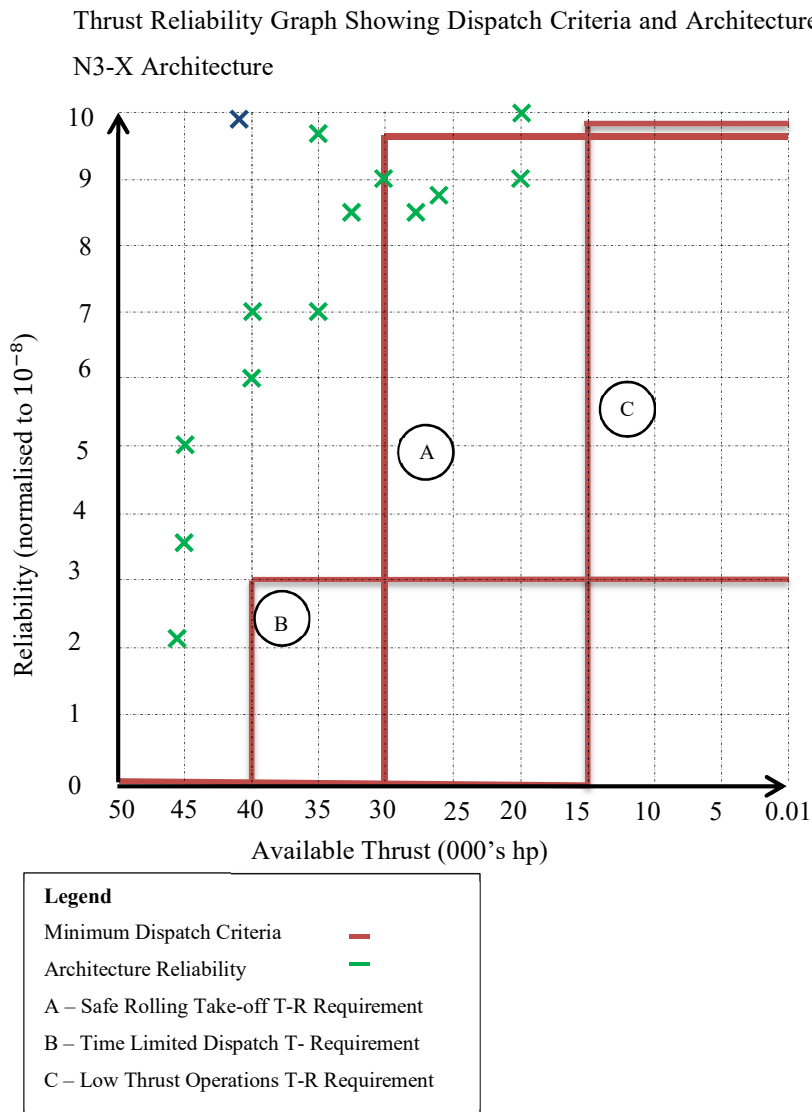


Figure 4.14 T-R Graph Showing a number of Different Performance Requirements

Figure 4.14 shows a number of arbitrary performance requirements for the network. More, it shows that whereas some configurations may meet a number of the requirements, only a small number meet all the criteria. This allows a useful tool to determine the most effective use of redundancy for the network or when there are a number of separate requirements that an architecture is required to meet. While multiple requirements are not directly compared within a single T-R graph in this

thesis, these principles are used when comparing the most effective redundancy method used within the considered network architectures in Chapter 5.

4.8 TeDP Network Thrust-Reliability Analysis Method

Key to the implementation of a contingency analysis based reliability of thrust study for any network is the utilisation of appropriate probabilistic methods. In the case of a large, complex network such as that proposed for TeDP aircraft, a *k-out-of-n* approach [106] as discussed in Chapter 3, allows the probability of the successful supply of power from a number of parallel sections of network to be determined. Key assumptions made in the application of this technique in this method are:

- Parallel MFs are identical in construction
- Parallel MFs are sufficiently independent of each other that common cause failures are negligible
- The components within each feeder are identical – using the same specification and manufacturer
- Should one feeder fail, the probability of another feeder failing remains unchanged
- The failure of a motor feeder is any event preventing the successful supply of 100 % of available power to the motor
- Analysis is undertaken at a fixed point in time
- A constant rate of failure is applied for each component

These assumptions are required in order that the *k-out-of-n* results hold true. The method considers identical parallel paths in the production of results at a set point in time and these assumptions ensure that the correct criteria are utilised for accurate analysis. To obtain the probability of successful power provision as exhibited by the network, a binomial probability distribution [106] is assumed, using the assumption that each feeder may be in either one of two mutually exclusive states, that is operational or failed [126], and exhibits a reliability R as a constant probability of successful supply of power. The binomial probability distribution is further used due to the probability of either event being independent of any other failure (as mentioned within the assumptions above) and uses a bell curve distribution which is

appropriate in the case of fixed probability outcomes [127]. In this example, the total number of MF sections connected in parallel is denoted by n and of these n MF sections, those that are required to be operational for the successful supply of power are denoted by x .

Employing these definitions, the binomial probability distribution is given as:

$$P(x) = \binom{n}{x} R^x (1 - R)^{n-x} \quad (4.1)$$

where $P(x)$ is the probability that exactly x out of the total n components will operate – or in this case that x feeders out-of- n total feeders will successfully supply power to the motors and that $n-x$ feeders will not supply power successfully for a set architecture. The binomial coefficient is defined:

$$\binom{n}{x} = \frac{n!}{x!(n-x)!} \quad (4.2)$$

calculating all permutations of x feeders successfully transmitting power from n total feeders. Based upon equations (4.1) and (4.2), the following relationship can be derived:

$$R_S = \sum_{x=k}^n P(x) \quad (4.3)$$



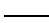









to provide the probability of k or more feeders successfully supplying power. Here, R_S is the probability of x or more feeders successfully supplying power. These equations can then be combined to show the effect of altering parameters on the overall probability of successful operation.

This methodology is illustrated within the next section, 4.9 where a case study is presented showing the effects on overall probability of successful operation by altering the number of available GSC and MF as well as altering the reliability R_S of the network. This case study is used to highlight how the k-out-of-n method can be easily used within the TeDP network setting supporting the contingency analysis to obtain meaningful T-R information on TeDP network architectures. This study additionally shows how the network is broken down into modular sections to aid the speed and ease of the analysis.

4.9 Case Study Illustrating how the *k-out-of-n* Method is used in a TeDP Network Example

To clearly demonstrate the methods used within the T-R profiling and contingency analysis, a case study is presented in this section. This case study uses a basic architecture and component configuration as shown in Figure 4.15 based upon the components described by the ‘Symbol’ and ‘Component’ columns of Table 4.2 and the reliability values presented within the ‘Normalised Reliability’ column of in Table 4.2. The values in this column have been normalised with respect to the figures presented within Table 6.1 of chapter 6 and are presented in a probabilistic form. While some of the reliability values may appear somewhat counter-intuitive and unrepresentative, they have been chosen only to populate the example and it is the resultant trends which are important.

Table 4.2 Reliability of Network Components

Symbol	Variable	Network Components	
		Component	Normalised Reliability
	R_G	Generator	0.94
	R_E	EEC	0.91
	R_B	Bus	0.99
	R_{3PHB}	Three Phase Breaker	0.75
	R_{CDC}	DC Cable	0.71
	R_{CAC}	3 Phase Cable	0.83
	R_{SFCL}	SCFCL	0.88
	R_{CON}	AC-DC Convertor	0.79
	R_{DCB}	DC Breaker	0.8
	R_{ACD}	DC-AC Motor Drive	0.81
	R_M	Motor	0.92
	R_P	Propulsor	0.98

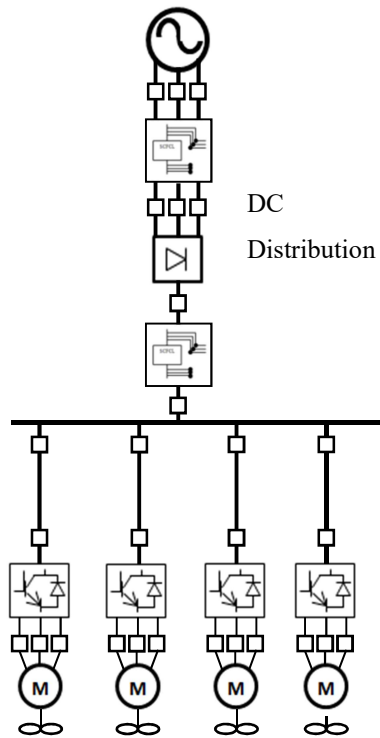


Figure 4.15 TeDP Network Section
Showing Component Configuration

Figure 4.15 shows the components which combine to create the network schematic as defined in [43, 49] and is configured as any of the individual parallel network subsections (Figure 4.5) or either of the outer network subsections of Figure 4.6. Importantly, the reliability values supplied in Table 4.2 for this example network are arbitrarily specified as to highlight the value of this study lying in the understanding of the method and how the results are calculated. Further benefit is also derived from the ratio of the reliability scores from both before and after adding additional network redundancy. Additionally, the engine controller is not explicitly included as an icon in Figure 4.15, but is rather incorporated into the reliability icon for the generator. The reliability of the engine itself is not considered in this case.

The first part of this case study will examine how the probability of successful provision of propulsive thrust power from 50 % of available MF varies with the total number of installed MF. Next, a refinement of the case study will show how the benefits gained from increasing the number of MF are limited by the reliability of supply of the GSC before relating these results to the total weight penalties these configurations impose on the network. A thorough understanding of how the

likelihood of power being available can be managed is crucial to the contingency analysis so network architectures capable of meeting criteria such as the minimum take-off T-R profile (no failures resulting in available thrust of less than 30,000 hp in 10^9 hours) may be designed. Different combinations of Motor Feeders (MF) and Generator Supply Channels (GSC) will combine to provide similar yet equally valid provision for failure so it is crucial that not only their T-R profile is understood but the relative effect each component has upon the network as a whole. This study will enable designers and other interested parties to understand the level of redundancy required within the network to attain the T-R criteria such as the minimum required take-off thrust as described above.

To simplify the evaluation, the TeDP network is considered as a combination of modular parts formed using the common components as detailed in Figure 4.15. The specific connection of these parts is determined by the particular architecture configuration such as that shown in Figure 4.5 and relates directly to the contingency scenarios under evaluation. When evaluating a network such as that of Figure 4.15, the GSC extends from the generator to the 15 MVA bus and each MF incorporates the series connection of components between this bus and the propulsor.

Analysis of the network can be carried out by constructing separate equations for the GSC and MF sections of the network and combining these with equations (4.1) to (4.3) according to the network architecture as described by Figure 4.15. Contingency plans can then be created to determine whether the reliability of supply meets the required dispatch criteria and it is at this point a T-R graph may be plotted to help visualise the results of each contingency scenario.

From inspection of the network schematic shown in Figure 4.15, it can be seen that the reliability of the GSC (from the generator to the component preceding the propulsion bus) can be expressed as a series reliability calculation:

$$R_{GSC} = R_G R_E R_{3PHB}^2 R_{CAC} R_{SFCL}^2 R_{CON} R_{DCB}^2 R_{CDC}. \quad (4.4)$$

Similarly, the reliability of the MF (the component immediately succeeding the propulsion bus to the propulsor) can be expressed as

$$R_{MF} = R_{DCB}^2 R_{CDC} R_{ACD} R_{3PHB} R_M R_P. \quad (4.5)$$

Using the supplied component values from Table 4.2, the MF and GSC reliability are:

$$R_{GSC} = 0.11102 \quad \text{and} \quad R_{MF} = 0.24888.$$

The values of R_{GSC} and R_{MF} can then be substituted into equation (4.3) to determine R_S , the reliability that the system is successfully operating as per the required criteria in each case within the study. Alternatively, to find the reliability of a single subsection of network, R_{SS} , they may be combined to form:

$$R_{SS} = R_{GSC}^m \times R_{MF}^n \quad (4.6)$$

Where m is the number of parallel GSC within each subsection and n , the number of parallel MF within each subsection as defined within section 4.2.1. Substituting the values from above and assuming all components are operating as desired yields:

$$R_{SS} = 0.0004$$

While this reliability value appears low, it is important to remember that the figures used were for illustration only. By repeating the calculation process for a single GSC connected to parallel MFs through a single bus, it is possible to evaluate the reliability of power provision for this network in any desired combination of operational GSC and MF. The output of this exercise is detailed in Table 4.3 where the probability of achieving a minimum of 50 % propulsive power for a single GSC and a number of MF (based on the normalised values presented in Table 4.2) is given along with two other cases, the probability that at least 1 MF being operational and the probability that 100 % of the MF are operational. This assumes that the GSC is directly connected to a maximum of 16 MF and the GSC must be operating in its normal un-faulted mode to supply power. At first, the probability of success figures presented within this table would appear to be probability of failure figures: this is not the case. In order to produce meaningful trends, the reliability figures were chosen so that they were significantly different between components and such that large volumes of results would not be tending towards 1; this required a large range of values to be used to ensure the trends were visible. As a direct result of the range of reliability figures used, much lower than expected probabilities of success were recorded.

Table 4.3 Enhanced Probability of Success for Additional Motors and a Single GSC

Total no. of MFs	Prob. of at least 1 MF Operational	Prob. of at least 50 % of MF Operational	Prob. of 100 % of MF Operational
4	0.0749	5.51×10^{-3}	4.22×10^{-4}
8	0.0988	2.94×10^{-3}	1.62×10^{-6}
12	0.1064	1.53×10^{-3}	6.21×10^{-9}
14	0.1079	1.1×10^{-3}	3.85×10^{-10}
16	0.1088	8×10^{-4}	2.38×10^{-11}

Table 4.3 shows that the probability of at least one MF operating increases with each additional MF added to the bus however the incremental benefits diminish with each addition. Table 4.3 further shows that the probability of at least 50 % and 100 % of the MF operating at any one time decreases with the number of propulsors connected to the bus. This reduction in system reliability suggests that rather than for reliability gains, the key driver behind utilising a larger number of connected MF is to provide aerodynamic benefits, through the incorporation of smaller physical motors spread over a large area to maximise boundary layer ingestion (BLI) benefits [16]. BLI is a method of improving propulsive efficiency through ingesting and re-energising the wake air which flows over the airframe and directly to the propulsor [47]

Additional MF modules added to the network in this manner will continue to improve the reliability of supply of power for the system, however the overall increase will be determined by the reliability of supply from the GSC. As the GSC and MF are connected in a series manner to the propulsion bus, a low probability of successful supply from any of the modular sections could pose a significant reduction in the overall probability of successful supply through the network. In this particular study, where $R_{GSC} = 0.11102$ any benefit resulting from increasing the number of MF is capped to 0.11102 of the initial increase exhibited by the MF. In order to achieve the additional reliability benefits gained from the connection of further MF additional parallel GSC must also be added (as shown in Figure 4.16) to enhance the attainable benefits to reliability.

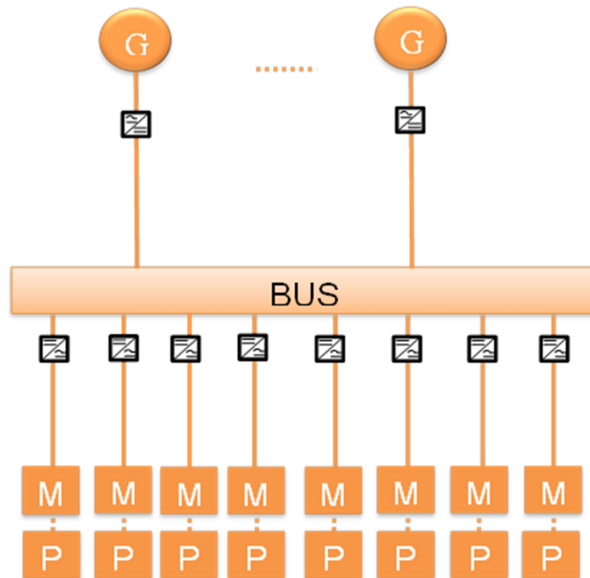


Figure 4.16 Using Additional GSC to Increase TeDP Network Reliability

By resolving expressions for the probability of operation of parallel connected GSC and MF in the same manner as shown earlier, rapid assessment of the reliability benefit afforded by increasing the number of these components can be performed. Accordingly, Table 4.4 shows the probability of successful power delivery from each of the m GSC to each of the individual n MF connected to the propulsion bus (i.e. providing 100 % thrust).

Table 4.4 Probability of 100 % Successful Power provision of an n MF, m GSC TeDP Network

No. of MF	Number of Generators (GSC)			
	1	2	3	4
4	4.2×10^{-4}	4.68×10^{-5}	5.2×10^{-6}	5.77×10^{-7}
8	1.6×10^{-6}	1.80×10^{-7}	2×10^{-8}	2.21×10^{-9}
12	6.2×10^{-9}	6.89×10^{-10}	7.65×10^{-11}	8.49×10^{-12}
14	3.85×10^{-10}	4.27×10^{-11}	4.74×10^{-12}	5.26×10^{-13}
16	2.38×10^{-11}	2.64×10^{-12}	2.94×10^{-13}	3.26×10^{-14}

It is clear from Table 4.4 that as the number of MF and GSC in the network increases, the probability of the combination of each section all working correctly decreases. As before, the probability of successful power provision may seem low,

however the values used in calculation are not representative of true components in order to amplify and highlight the trends of the analysis. The probability of successful supply from 16 MF is 17.65×10^6 times less than when operating with only 1 GSC however is due to the significantly larger number of components required within the 4 GSC network and the fact that the reliability values have been deliberately skewed to illustrate the method and key point in reliability following a rule of diminishing returns. For fixed values of R_{GSC} and R_{MF} , increasing the number of generators connected to the bus should increase the overall reliability of supply. As this is not clearly demonstrated in Table 4.4, the k -out-of- n method was utilised to show how the probability of supply of only $k=1$ for both the GSC and MF was affected by the increase to the overall respective totals. This can be highlighted in Table 4.5 where the probability of achieving $k = 1$ -out-of- n is shown.

Table 4.5 R_S for $k = 1$ -out-of- n Feeders Correctly Supplying Power

Probability of Successful Network Operation				
No. of MF	Number of Connected GSC			
	1	2	3	4
4	0.075	0.142	0.201	0.253
8	0.099	0.187	0.265	0.334
12	0.106	0.201	0.285	0.360
14	0.108	0.204	0.289	0.365
16	0.109	0.205	0.291	0.368

Table 4.5 provides a greater insight into the additional reliability of the system gained from increasing the number of GSC and MF. The table shows that as the number of GSC and MF are increased the probability of only one MF operating as desired also increases. It can be seen that the largest gains in reliability occur when there is a lower number of MF connected to the propulsion bus. There is an increase in R_S of 0.0239 or 32 % when the number of MF is increased from 4 to 8 with only 1 associated GSC, however when the number of MF is increased from 8 to 16 this increase is reduced to only 0.01 or 10 % of the initial R_S . The gains in reliability diminish in a similar manner for each additional MF for each number of incorporated GSC. Interestingly, the benefits gained from an additional GSC are far greater than

for an additional MF. Increasing the number of GSC from 1 to 2 yields an increase in each of the connected MF cases of around 88 % - 89 % on the R_S exhibited by the network. Similarly to the MF cases the benefit diminishes with each additional GSC, with the benefit gained from adding a 4th GSC yielding an increase of only 26 %.

The values from Table 4.5 can then be displayed in a T-R graph so that the profile of each configuration of this example may be observed. This is shown in Figure 4.17.

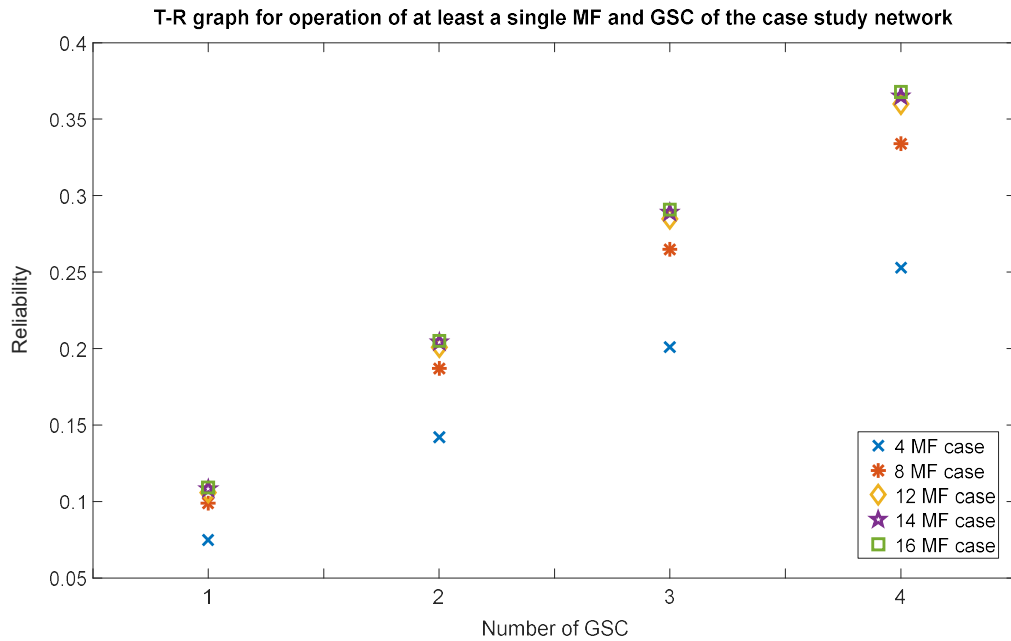


Figure 4.17 T-R graph for the case study network

Figure 4.17 shows the results of Table 4.5. For each additional generator added to the network (on the x axis) the equivalent probability of success is displayed against the reliability of the y axis. In this case, no minimum power requirement has been indicated as for this data as the requirement only stipulated 1 out of a possible 4 GSC had to be operational; the red indicator would not be representative in this case. Table 4.5 not only has a significant bearing on the reliability of the aircraft network, but also the weight too. Each additional generator added to the network adds a significant amount of undesired weight to the system and whereas it may be desirable to increase the number of GSC's until there is no observable increase to reliability, the weight penalties of each generator added must be carefully considered. Through the use of a small number of electrical machines, overrated to provide excess power to the

network, a better power density could be attainable than through using a larger number of lower-rated generators [128]. Using a smaller number of machines also introduce efficiency benefits from using larger bypass ratios and reduced weight from the minimised duplication of machinery. It is also important to note that the largest benefits to reliability come through adding additional GSC, as the GSC has the lowest reliability and dealing with this as a key element brings the biggest gain in reliability. Significant benefits may also be observed through increasing the initial values of R_{GSC} and R_{MF} – all as expected. This particular sensitivity study of increasing values of R_{GSC} and R_{MF} is shown in chapter 6.

4.10 Chapter Summary

The presented *k-out-of-n* method with T-R graph and Case Study shows how a contingency analysis may be carried out for a TeDP network architecture using a *k-out-of-n* reliability technique in conjunction with a failure analysis. The results of this Case Study have shown the importance of using such a technique due to the non-finalised nature of TeDP network architectures and the large number of variables therein. This investigative contingency analysis and reliability approach also shows that the addition of feeders will increase the probability of a percentage of power supplied successfully; however the inclusion of additional parallel generation enhances reliability to a much greater degree allowing the required probability of successful supply to be achieved. This chapter has shown how the T-R profile of a network may be derived and hence displayed on a graph. The graph can then be used to simultaneously display information on a number of architectures.

The method presented allows a number of further studies to be made and provides a good start point for any design exercise of a TeDP network. The method provides a logical and methodical approach as well as a visual aide for assessing how varying architecture configurations perform against one another as well as against performance criteria. Further applications of this method can be found within sensitivity analysis studies, allowing investigations to be made into alterations of specific component reliability and how this affects the network reliability as a whole.

This method will hence be used throughout chapter 6 to undertake both reliability studies and sensitivity studies to allow conclusions to be drawn on the performance of such network architectures.

Chapter 5

Case Study Networks Identification and Development

There have been a number of TeDP networks proposed by NASA [11, 16, 47], Rolls – Royce [23, 129] and Airbus [87]; each architecture with its own merits and distinct electrical network design. This Chapter considers the three TeDP network configurations as identified within Chapter 2, namely

1. The N3-X concept with 4 generators and 16 motors and propulsors
2. The 16 motor electrically interconnected Hybrid AC – AC configuration as designed by NASA.
3. The Rolls-Royce and Airbus concept consisting two bus – tied generators with 8 motors and propulsors









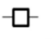



A Thrust-Reliability (T-R) analysis is conducted to determine how each network performs in terms of the thrust available at each achievable reliability level. To achieve this a *k-out-of-n* analysis is presented for all three networks to provide T-R profiles comparing the two metrics and assessing the relative performance of the network at a number of operating/failed scenarios. The analysis however does not consider the required cryocooler as part of the electrical propulsion network and assumes that there is no electrical storage connected as featured in some of the designs. These features are important but they are not well enough understood across even basic parameters (e.g. size, weight, technology) to be well enough captured in the analysis work of this chapter. Including these two aspects within the modelling will be reconsidered in Chapter 7 as areas of future work. Each of the identified

networks will be profiled within section 5.1, next before an analysis of each baseline in Chapter 6.

5.1 Overview of Considered Network Configurations

As a precursor to any analysis within this chapter, the three networks under investigation will first be described, highlighting both their similarities and differences and showing a network schematic for each. The components for each schematic are described by the symbols shown in the Symbol column of Table 5.1.

Table 5.1 Network Components

<i>Symbol</i>	<i>Component</i>
	Generator
	EEC
	Bus
	Three Phase Breaker
	DC Cable
	3 Phase Cable
	SCFCL
	AC-DC Convertor
	DC Breaker
	DC-AC Motor Drive
	Motor
	Propulsor

5.1.1 A Description of the Baseline N3-X TeDP Propulsion Network

The first of the three considered networks and the most recent of the NASA baseline architectures is the N3-X TeDP aircraft which is defined and described within [48, 50, 51] (The power ratings for the generators and motors for the network can be obtained from [19, 49]). A plan view of how the network is configured is shown in

Figure 5.1 and a clearer view of the motors associated with each generator in Figure 5.3.

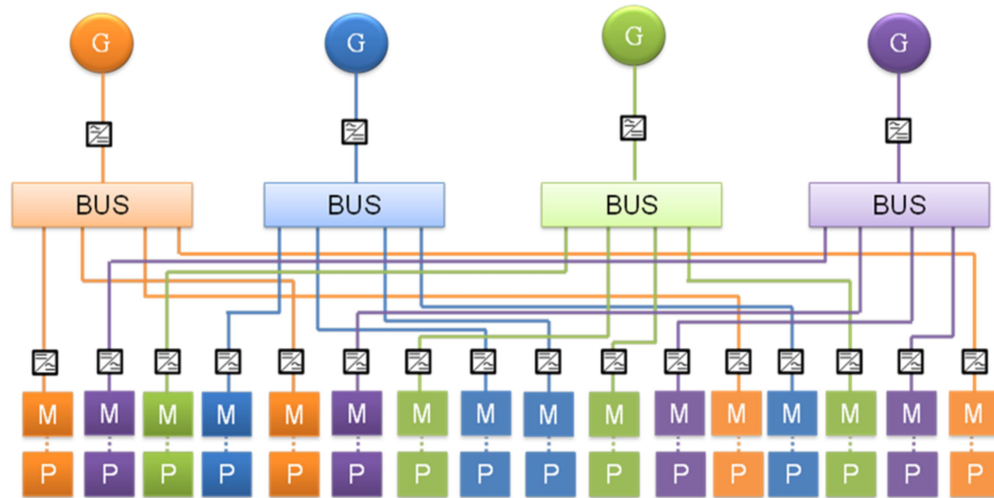


Figure 5.1 N3-X Baseline Network

Figure 5.1 shows there are 4 electrical generators in this network, [19] shows that the two generators on the left are associated with the left wingtip engine and the two generators on the right, with the engine on the right aircraft wingtip. Figure 5.1 provides a representation of how the converters motors and propulsors of the network are placed along the aft of the aircraft.

As described in Chapter 4, in order to determine the reliability of the network, a more modular approach is adopted that allows it to be analysed more simply through breaking it down into smaller sections: the sections for the N3-X are shown in Figure 5.2.

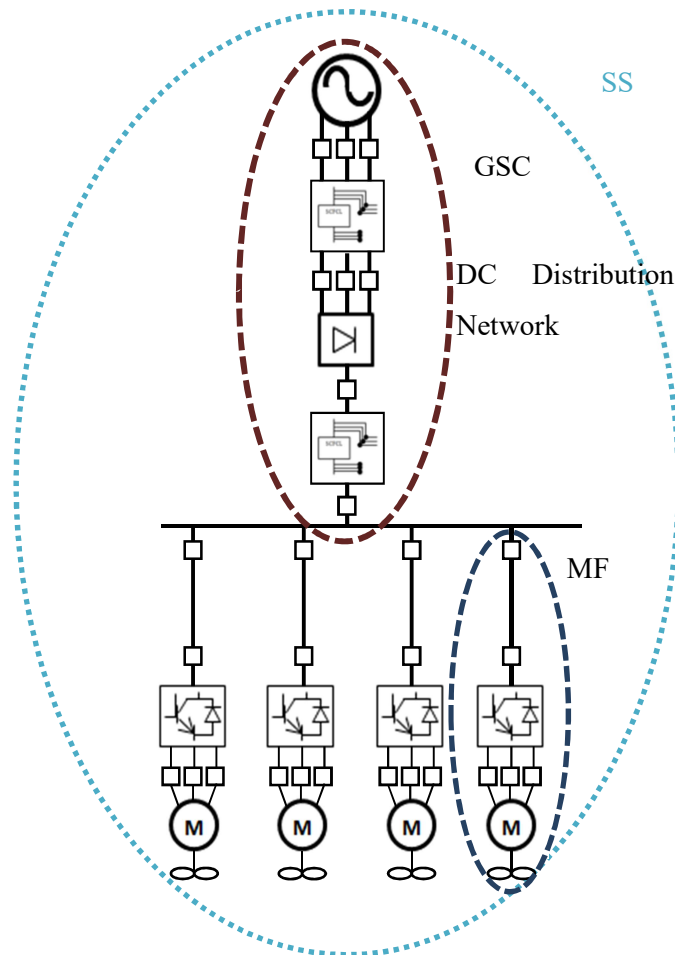


Figure 5.2 TeDP Network Component Configuration

Figure 5.2 shows the N3-X network configuration described with all the relevant constituent components as presented in Table 5.1, it should be noted however that the engine controller (EEC block) is not explicitly included as an icon in Figure 5.2, but is rather incorporated into the icon for the generator. The reliability of the engine itself is not considered in this thesis. Figure 5.2 shows the network's two modular sections; the GSC which extends from the generator up to and including the bus and the MF which extends from the first component after the bus through to the motor and propulsor. A number of MF sections may be connected in parallel. Finally Figure 5.2 shows that the modular GSC and associated MF sections can be combined to create a network subsection (SS). The N3-X consists of 4 SS which can be viewed clearly in Figure 5.3, which can be resolved in conjunction with the network plan of Figure 5.1 using the rules of series and parallel reliability and the components

reliability values listed in Table 6.2 to determine the overall reliability of this network.

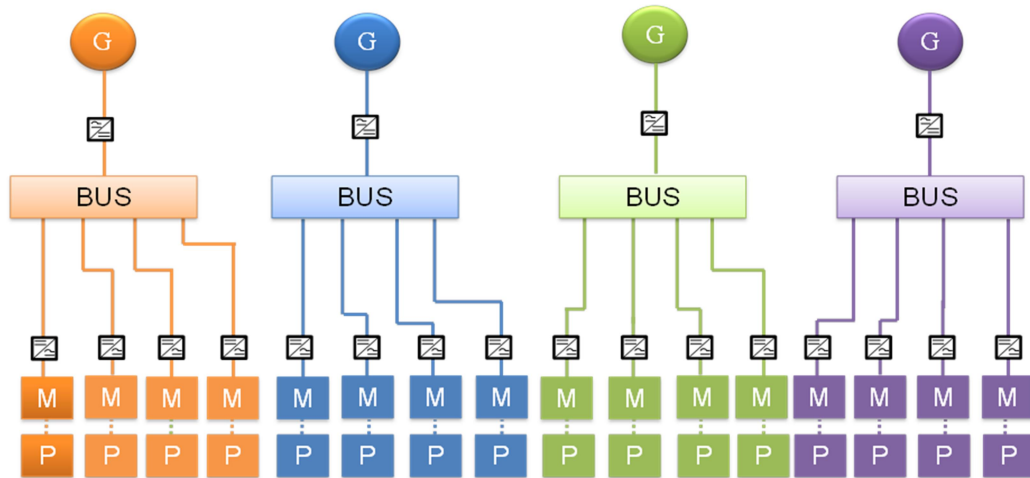


Figure 5.3 N3-X baseline network configuration laid out to illustrate the network's SS

Figure 5.3 shows the network redrawn to show that the architecture is comprised of 4 identical and parallel SS. In each SS, one generator is connected in series to a bank of 4 parallel connected MF. In this view it can be easier visualised than in Figure 5.1 how the rules of series and parallel reliability, and in turn how the *k-out-of-n* method may be applied.

5.1.2 A Description of the NASA Hybrid AC/DC TeDP Propulsion Network

Another early design that NASA proposed for a TeDP aircraft was described in [16] and was the predecessor to the N3-X network. Like the N3-X this concept makes use of 16 aft located fans on the top of an HWB airframe. This network is shown in Figure 5.4.

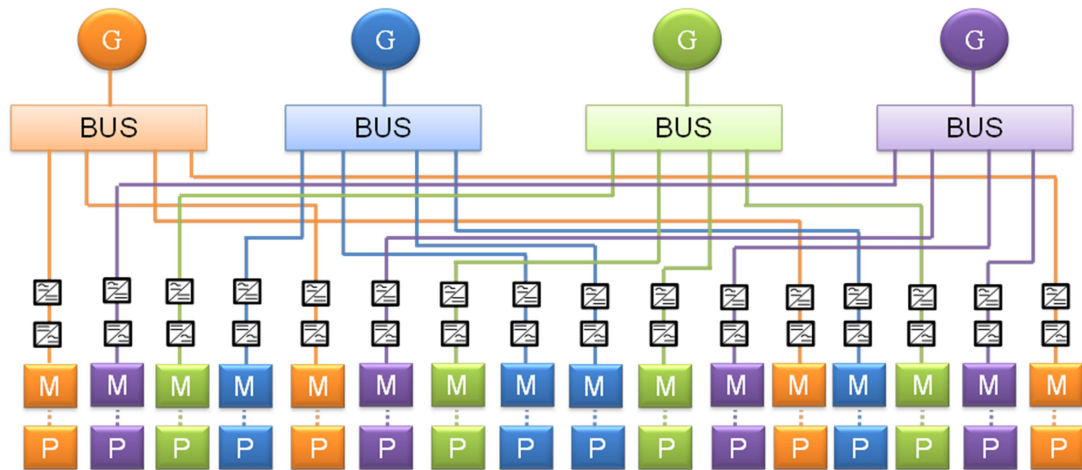


Figure 5.4 NASA Hybrid Network Baseline Configuration

Figure 5.4 shows the network architecture layout as alluded to within [16]. The paper, [16] describes a network which uses a common bus network and like the N3-X can provide symmetrical thrust in the event of a turbine engine or generator failure. This aircraft was rated to supply 63 MW of power at sea level and 19 MW at cruise. There is no mention of a dedicated electrical protection network and as such protection from the effects of large fault currents is likely to be provided through the quenching of the superconducting cabling. While the quenching of cabling could theoretically protect components from the effects of superconducting network faults, in practicality this may not be effective, the superconductor could be damaged through sustained operation in “quenched” mode, there could be further widespread network damage and thus long term solutions should consider some form of measurement and isolation system to underpin the protection of such networks. The network described in [16] utilises back to back AC/DC and DC/AC converters which allows the frequency of the generators and the motors to be decoupled and for each machine type to rotate at their own optimal speed and hence to enhance network efficiency. As before the network may be redrawn showing the constituent components so the modular sections may be determined, this network is shown in Figure 5.5 and uses the components described within Table 5.1.

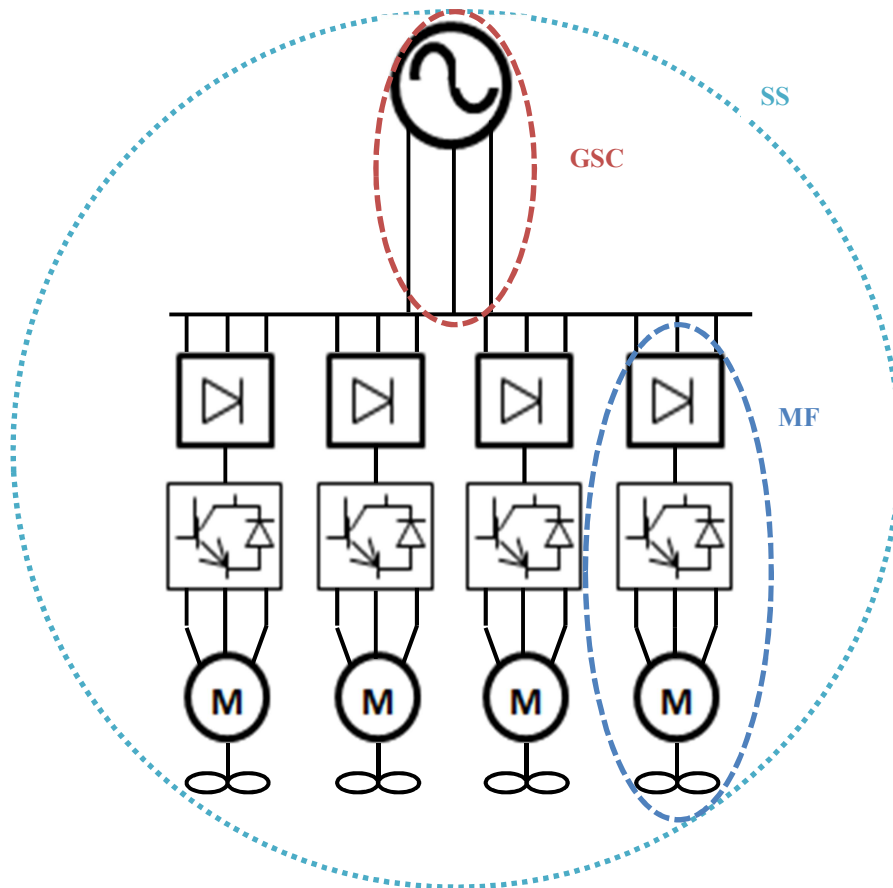


Figure 5.5 NASA Hybrid AC-DC network

Figure 5.5 shows the schematic for this network configuration described with all the relevant constituent components except for the EEC which similarly to the N3-X case is included within the generator block. Again, the reliability of the engine itself is not considered in this case study. As with Figure 5.2, Figure 5.5 also shows the SS broken down further into the two apparent modular sections: the GSC which incorporates the generator cabling and bus: and the MF which extends from the first component after the bus through to the motor and propulsor. As with the N3-X configuration a number of MF sections may be connected in parallel, in this case four. Figure 5.6 shows how the network SS may be combined with a further 3 identical SS to create the network of Figure 5.4.

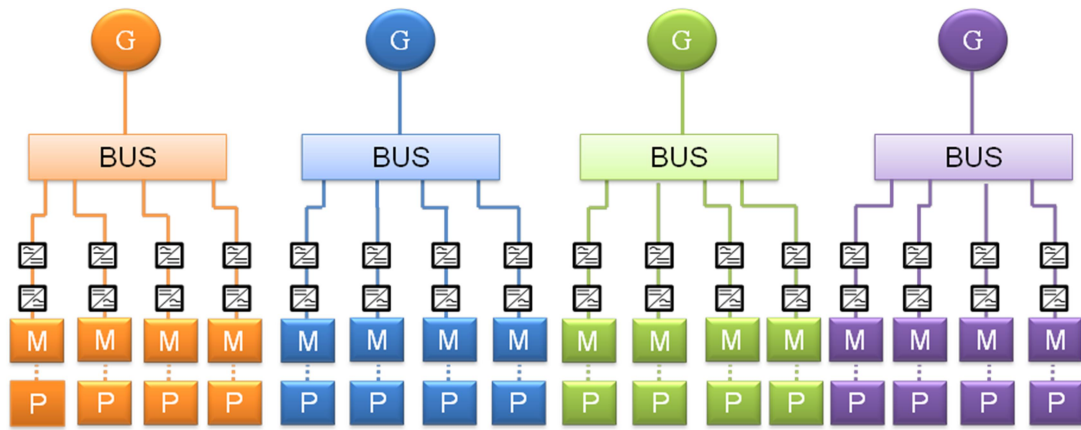


Figure 5.6 NASA Hybrid network baseline configuration

Figure 5.6 shows that like the N3-X network architecture, the hybrid network can be redrawn to show that the architecture is comprised of 4 identical and parallel SS. These modular network subsections can be resolved in conjunction with the network plan as in Case Study 6.1.1, using the components' reliability values as listed in Table 6.2 to determine the overall reliability of this configuration of the TeDP network.

5.1.3 A Description of the Airbus and Rolls-Royce Concept TeDP Aircraft

The third and final of the three considered designs and the smallest of the three networks with a combined output power from two generators of only 9 MW [23] is the result of a collaborative effort between Airbus and Rolls-Royce. Unlike the previous two designs, this concept makes use of only 8 aft located fans on the top of the airframe and instead of lying flush with the upper airframe the fans are housed in a raised nacelle [9]. In keeping with the other network concepts, at least half of the installed number of generators must be operational to provide the required thrust for take-off. The network architecture for this concept is shown in Figure 5.7.

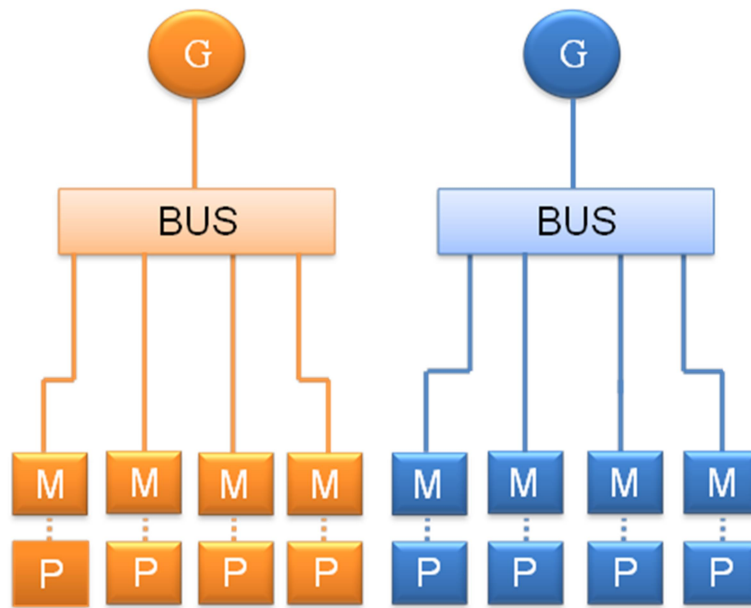


Figure 5.7 Rolls - Royce and Airbus baseline TeDP network

Figure 5.7 shows the network architecture layout as described within [23]. This network is significantly smaller than the other two configurations, and in order to provide a fair reliability comparison with the others, this network architecture may be extrapolated as shown in Figure 5.8 to incorporate an additional two generators and 8 motors.

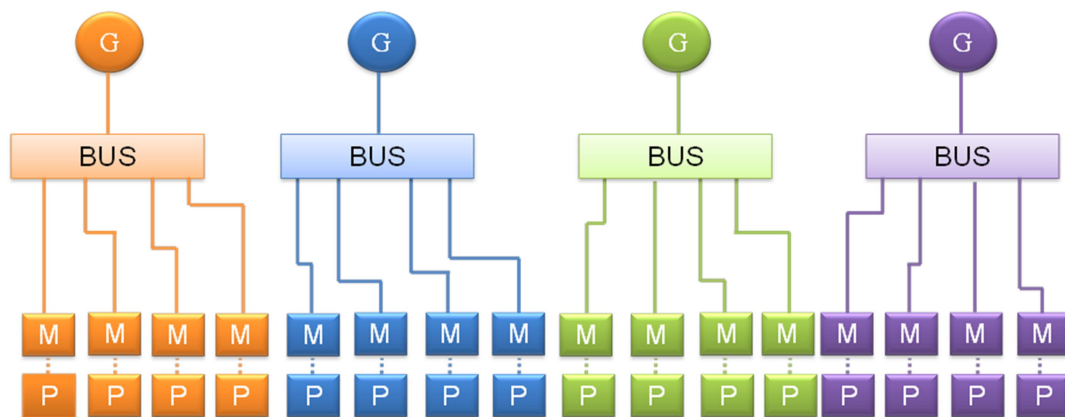


Figure 5.8 Extrapolated Rolls-Royce and Airbus baseline TeDP network

In an additional deviation from the configurations of the previous NASA networks, this configuration also requires a tailplane as the motors and propulsors are not configured in a way to provide symmetrical thrust in the event of motor or propulsor failures [23]. The most radical difference from the other two networks, however, is

the lack of power electronics within the network, resulting in a purely AC architecture. The lack of power electronic converters and drives means that the network would have to operate at a relatively low AC frequency to reduce losses and utilise gearboxes to reduce shaft speeds between the generation and the thrust producing motors [23]. This architecture also has a specific protection network inclusive of isolators and breakers to protect from the effects of fault currents. Similarly to the N3-X and Hybrid networks, the extrapolated Rolls-Royce and Airbus configuration has four identical SS each consisting of a single GSC and four parallel MF: the schematic highlighting each section and showing all network components is shown in Figure 5.9.

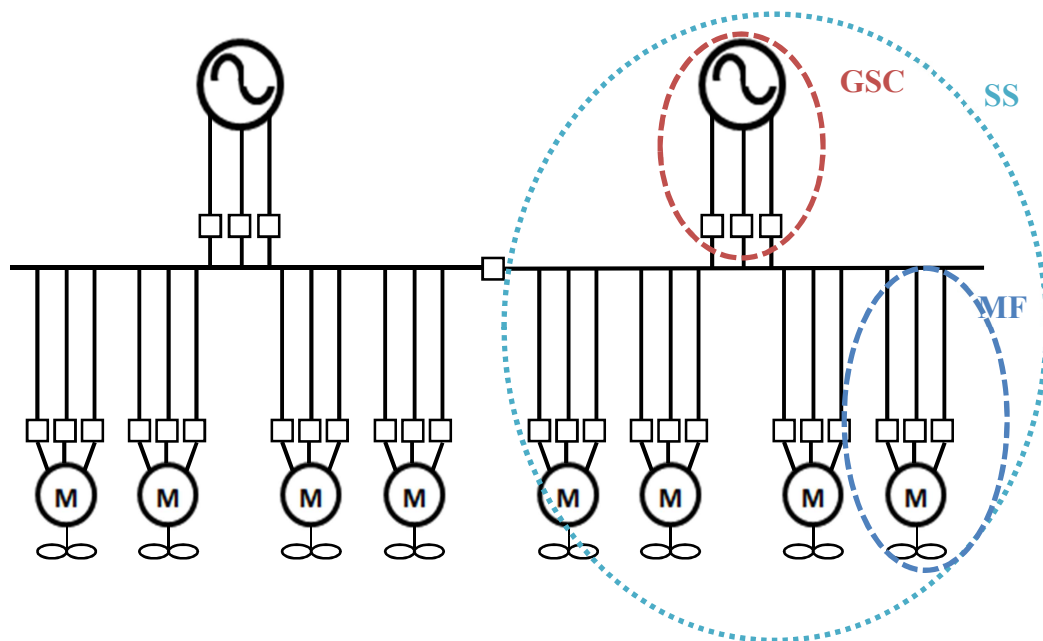


Figure 5.9 Rolls-Royce and Airbus TeDP network architecture [23]

Figure 5.9 shows the schematic for the collaborative Rolls-Royce and Airbus network described with all the relevant constituent components as described in Table 5.1 and that two identical network subsections are connected through a bus tie (which is normally open) to create the full network architecture. Again, similar to the N3-X and the Hybrid network architectures, the reliability of the engine itself is not considered in this case study. One unique feature to this network is that the initial design has allowed for only one generator per engine, however this is an assumption based on the reliability of the individual components [23]. The addition of another

generator per engine would likely result in a network similar to that of the extrapolated network of Figure 5.8. Figure 5.9 shows the two network SS broken down into the two modular sections; the GSC which incorporates the generator through to the bus and the MF which extends from the first component after the bus through to the propulsor. As with the other two configurations a number of MF sections may be connected in parallel. These sections can then be resolved as before using the rules of series and parallel reliability and the components' reliability values as listed in Table 6.2.

5.1.4 A Comparison of the Three Identified TeDP Propulsion Networks

There are a number of similarities within the three presented networks, most notably between the N3-X network and the NASA Hybrid AC/DC network. Both operate using both AC and DC currents and voltages to decouple the rotational speeds of the motors and generators and in their significantly higher power ratings than the Rolls-Royce and Airbus equivalent. This is potentially the most notable differences between the networks as there are no power electronics and hence no decoupling of generator and motor speeds. There are also similarities in the N3-X and the Rolls – Royce and Airbus network in that both use dedicated power systems protection devices to protect against fault voltages and currents and to isolate affected areas of the network without relying on the superconducting network quenching as in the NASA Hybrid network. The Rolls-Royce and Airbus network takes the protection system a step further in the baseline network by including a breaker to link both halves of the propulsion network. In order to provide fair comparison with the other networks, this breaker is considered normally open in the baseline study. Other similarities are also notable within the NASA Hybrid network and the Rolls-Royce and Airbus network in their significantly reduced number of network components in comparison with the N3-X, suggesting that these will perform better in terms of achievable network reliability. The NASA Hybrid network utilises the fewest number of components within the GSC section and the Rolls-Royce and Airbus

architecture uses fewest components within the MF suggesting that their reliability gains and sensitivities will be greatest within these areas. In order to provide a clear comparison of all three networks, schematics of all three are shown in Figure 5.10.

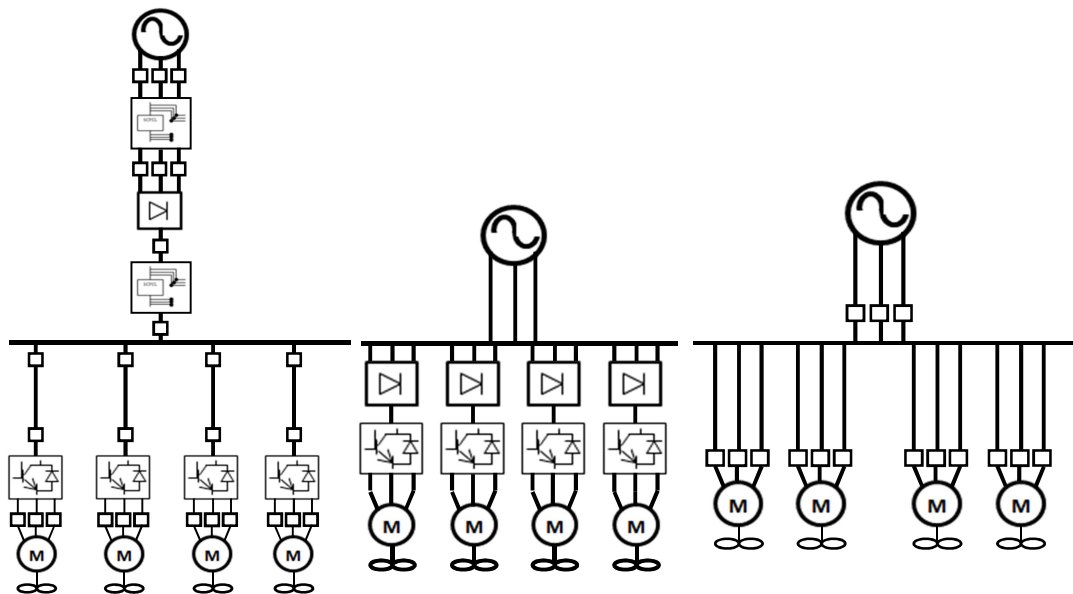


Figure 5.10 Comparison of the three identified TeDP propulsion architectures

Figure 5.10 shows the schematics of the N3-X network (image left), NASA Hybrid AC/DC Network (image centre) and the Rolls-Royce and Airbus network (image right) to aid the comparison of the three networks. While for the N3-X and NASA networks these schematics represent only a quarter of the total network composition, for the Rolls –Royce and Airbus network this is one half of the full propulsion network. The main differences between these networks architectures are clearly visible: the Rolls-Royce and Airbus network is relatively simple, only exhibiting breakers in addition to generation and propulsion components. In contrast the N3-X is a highly complex architecture exhibiting a number of power electronic components as well as a number of fault current limiters and breakers. The NASA AC/DC network however has no dedicated protection system yet has a back to back convertor/inverter architecture. As well as these differences there are a number of similarities within the three networks, for example all networks utilise banks of 4 parallel connected MF as well as only a single GSC in each case. A summary of the main features of each architecture is shown in Table 5.2.

Table 5.2 Comparison of TeDP propulsion network features

Network Feature	N3-X	NASA Hybrid	Rolls-Royce and Airbus
Total Available Power	44.8 MVA	63 MW	9 MW
Protection System	Both fault current limiters and breakers	Quenching of superconducting feeders and cables	Breakers
Distribution Network Power Type	DC	AC	AC
Baseline Network Redundancy	Provided through a large number of motors and propulsors to over-rate the network	Provided through a large number of motors and propulsors to over-rate the network	Provided through a normally open busbar and large number of motors and propulsors to over-rate the network
Total Number of Propulsion Motors	16	16	8

Table 5.2 shows that each network has its own unique features within the scope of a TeDP network. The most notable of these differences is potentially the much reduced power rating and lack of power electronic components exhibited by the Rolls-Royce and Airbus network. Through the combination of all noted differences each network will perform differently when analysed using the k -out-of- n method as described within Chapter 4. The analysis which will be undertaken is described within section 5.2, next.

5.2 Case Studies: Methodology

There are a number of case studies presented within the case studies chapter which combine to provide the basis for an in depth assessment of both the reliability and failure rate of the three variations of the TeDP concept architectures as detailed within section 5.1.

The methodology applied when analysing the baseline network of each proposed configuration will utilise the k -out-of- n method to explore the T-R properties when operating under the following three variations:

- When 100 % of the network components are operating as desired.
- When at least 50 % of the connected MF are operating as desired.
- At least 1 of the MF sections are operating as desired.

Reviewing these T-R profiles for each of the three variations of the TeDP architecture will allow solid conclusions regarding the most reliable architecture to be made as well as identifying areas of each network prone to failure and which should be considered for additional redundancy measures.

Subsequently, each of these architecture variations will be analysed after parallel connected redundant backup feeders have been added to either then both of the generation side and the propulsion side of the network. These redundant parallel feeders will be used to enhance the reliability of the network at the identified reliability weak spots from the first studies; conclusions have been drawn as to the effectiveness of the redundant feeders with respect to the improvement in reliability and the weight penalties they add to the network.

Further to adding redundancy to the network, additional sensitivity studies will be executed allowing conclusions to be drawn on how sensitive the network is in regard to specific components. The first of the sensitivity studies will compare the reliability of the three networks when operating using a common fault current protection system. This will enable a clear representation of how the concept architectures perform when all operating using breakers and isolators as suggested by the Rolls-Royce and Airbus architecture to protect against the effects of fault currents. The

second of the two sensitivity case studies will use components which exhibit both greater and lesser initial reliability scores to determine how the reliability of the network as a whole is affected by these changes and hence how tolerant the network is to these changes. This study shows how minimal changes to the reliability of even a single component can have significant benefits to the reliability of both the modular sections of the network and the network as a whole. Again, this study will be implemented on all three of the candidate networks to assess how each performs in comparison.

Finally, an FTA will be undertaken on each of the three TeDP networks. This will provide an analysis in failure space and will help to aide understanding as to the faults and failures which lead to the loss of thrust which result in a remaining thrust level of less than 30,000 hp. The FTA studies will also help to confirm the network weak spots as identified in the initial k-out-of-n analysis both visually (through the use of an interconnected fault tree) and numerically through the failure rates obtained. These case studies will be developed in chapter 6.

Chapter 6

Case Studies

In order to allow for a true comparison of the network alterations and redundancy features investigated within this chapter, it is first necessary to undertake the same k -out-of- n analysis on the baseline networks presented in Section 5.1. The results obtained from the reliability analysis in this Baseline Study will provide a benchmark to which comparison within subsequent studies will be drawn. The results obtained from these k -out-of- n studies will be both tabulated as well as presented on a T-R graph.

All of the case studies within this chapter refer to either Table 6.1 or Table 6.2 for components used and both reliability values and failure rates.

Table 6.1 Network Components and Failure Rates



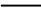





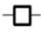




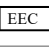
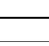



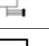
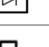
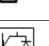



Network Components			
<i>Symbol</i>	<i>Variable</i>	<i>Component</i>	<i>Failure Rate (per hour)</i>
	λ_G	Generator	5×10^{-4} [17]
	λ_F	EEC	2×10^{-4} [17]
	λ_B	Bus	1.01×10^{-7} [27]
	λ_{3PHB}	Three Phase Breaker	2.3×10^{-5} [28]
	λ_{CDC}	DC Cable	1.01×10^{-6} [28]
	λ_{CAC}	3 Phase Cable	1.01×10^{-6} [28]
	λ_{SFCL}	SCFCL	5.82×10^{-7} [29]
	λ_{CON}	AC-DC Convertor	2×10^{-5} [28]
	λ_{DCB}	DC Breaker	1.53×10^{-5} [28]
	λ_{ACD}	DC-AC Motor Drive	2×10^{-5} [28]
	λ_M	Motor	1×10^{-5} [30]
	λ_P	Propulsor	4.75×10^{-6} [16, 31]

Table 6.1 provides both a component key and failure rates (λ) for all possible components used within the case studies. The table also includes the failure rate variable names as used within the equations of the FTA case studies. The table also provides a reference location for the source of all failure rates. Some of the failure rates stated within this table are surprising: the extremely low failure rate of the SCFCL for example was based on an extremely low rate of field returns. It would also be expected that components with the most number of moving parts would exhibit the highest failure rates and those network elements with the least switches or moving parts, the lowest. Sourcing failure rates within the public domain remains difficult and as such the rates referenced here may not accurately reflect the aircraft equivalent componentry. The accuracy of these rates does not affect the outcome of these studies however, the key findings within the case studies of this thesis lies within the observed trends and network sensitivity to changes which are revealed.

Table 6.2 Network Components and Reliability Values

Network Components			
<i>Symbol</i>	<i>Variable</i>	<i>Component</i>	<i>Reliability</i>
	R_G	Generator	0.75
	R_F	EEC	0.78
	R_B	Bus	0.98
	R_{3PHB}	Three Phase Breaker	0.8
	R_{CDC}	DC Cable	0.92
	R_{CAC}	3 Phase Cable	0.92
	R_{SFCL}	SCFCL	0.96
	R_{CON}	AC-DC Convertor	0.83
	R_{DCB}	DC Breaker	0.84
	R_{ACD}	DC-AC Motor Drive	0.83
	R_M	Motor	0.86
	R_P	Propulsor	0.9

Similarly, Table 6.2 provides a key for components used within the case studies as well as the reliability variable symbols and constants as used within the equations of the presented case studies. The reliability values as presented within the *Reliability* column are directly related to the failure rates of Table 6.1, in that components with the most frequently occurring failure rates have a correspondingly lower reliability value from those with a lesser rate of failure. The values of Table 6.1 were normalised to a probability based upon the sourced rates over a true representative figure revealing figures which appear low for a reliability value. As stressed above, it is not the figures which form the integral part of the analysis, it is the trends and ratios which are formed from the analysis on which emphasis must be placed.

The first part of this case study will examine the probability of successful provision of thrust from 100 % of available MF and how it varies with the total number of installed MFs. Additionally the probability of successful provision of thrust from 50 % of the installed MF will be investigated: this analysis is included as it is assumed that the aircraft should be able to perform safe rolling take-off with only 50 % of the total installed power available [16, 19, 23]. A thorough understanding of reliability of

power is crucial to the contingency analysis, so network architectures capable of meeting the minimum dispatch criteria (in this case the provision of 30000 hp) may be designed. Different combinations of MFs and GSC will combine to provide similar yet equally valid provision for mitigation of failure so it is crucial that not only their T-R profile is understood but the relative effect each component has upon the network as a whole.

6.1 Case Study 1: Calculating the Reliability of the Baseline Networks using *k-out-of-n* Analysis

6.1.1 N3-X Baseline Case Study

As shown in Chapter 4, analysis of the network is carried out through constructing separate equations for the GSC, MF and SS sections of the network and combining these with equations (4.1) to (4.3) according to the network architecture. In this case described in Figure 5.2 and repeated for clarity in Figure 6.1 below. The results of this study can then be used to determine the relative benefits gained through adding redundancy methods as in case studies 6.3 and 6.4 and used to create a T-R graph to help visualise the results of each contingency scenario.

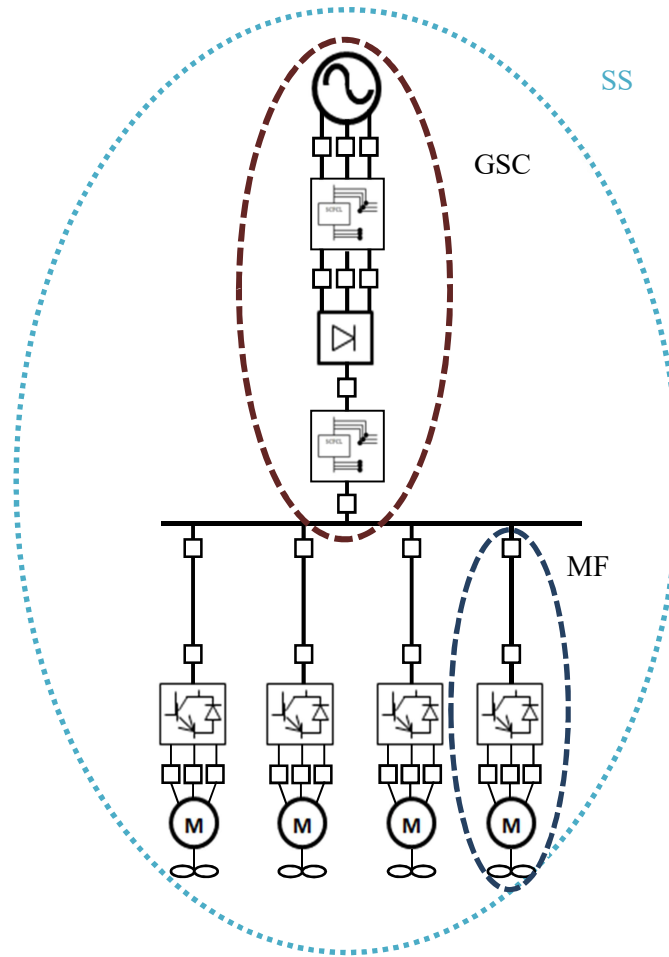


Figure 6.1 TeDP network component configuration

From inspection of the network schematic shown in Figure 6.1, it can be seen that the reliability of the GSC section can be expressed as a series reliability calculation of all the constituent components from the generator to the bus:

$$R_{GSC} = R_G R_F R_{3PHB}^2 R_{CAC} R_{SFCL}^2 R_{CON} R_{DCB}^2 R_{CDC} R_B. \quad (6.1)$$

Similarly, the reliability of the MF section of network can be expressed as the series combination of all those components within a single modular MF section from the first component after the bus to the propulsor:

$$R_{MF} = R_{DCB}^2 R_{CDC} R_{ACD} R_{3PHB} R_M R_P. \quad (6.2)$$

Finally through observation it can be determined that the reliability of each of the 4 network subsections can be described as:

$$R_{SS} = R_{GSC} R_{MF}^4 \quad (6.3)$$

Using the component values from Table 6.2, the specific SS, MF and GSC reliability values (assuming all components are operating as desired) can be shown to be:

$$R_{GSC} = 0.167616 \quad R_{MF} = 0.333623 \quad R_{SS} = 0.002077$$

The values of R_{GSC} and R_{MF} can then be used in equation (4.3) to determine R_S , the reliability of the entire network. It is obvious that in this case the reliability of the SS is significantly adversely affected by the poor reliability score of the GSC. In addition these values will be used as reference to compare new values after the introduction of redundancy measures and within sensitivity studies.

By repeating the calculation process for a single GSC connected through a bus to an increasing number of parallel MF, it is possible to evaluate the reliability of power provision for a network SS and hence the full N3-X network. The results of this exercise are detailed in Table 6.3 for the case where 100 % successful operation is required and in Table 6.4 for the case where at least 50 % propulsive power is required. A further study is presented and detailed in Table 6.5 to show how the reliability changes as more components are added to the network.

The following results show how the reliability of the network changes as extra GSC with associated MF are added to a network. The network is built up from a single GSC and associated MF to 4 GSC all with 4 associated and parallel connected MF as in the baseline design. In this example, for 100 % operation, $k=n$ and n is increased incrementally from 1 to 4 as indicated in the table.

Table 6.3 Probability of 100 % operation of the N3-X baseline network

Number of MF per GSC	Number of GSC			
	1	2	3	4
1	0.055921	0.0031271	0.0001749	9.7789×10^{-6}
2	0.018656	0.0003481	6.4936×10^{-6}	1.2115×10^{-7}
3	0.006224	3.87406×10^{-5}	2.4113×10^{-7}	1.5008×10^{-9}
4	0.002077	4.31198×10^{-6}	8.954×10^{-9}	1.859×10^{-11}

Table 6.3 shows the probability of achieving 100 % successful supply of power from the network. Due to the low reliability figures used the numbers within the table are

small, however the statistics used make the identified trends clearer than when using larger component reliability figures, where the differences between options may appear marginal. It is clear from Table 6.3 that, as expected, as the number of MF and GSC in the network increases, the probability of the combination of each working correctly decreases, given the larger number of components which could fail. The probability of successful supply from one MF and one GSC is 3×10^9 times greater than the case where the network is operating with four GSCs and a combined total of 16 MFs. Additionally it is clear that with each additional MF per GSC the reliability of the system drops significantly: around one or two orders of magnitude for the addition of the 2nd feeder and around six orders of magnitude smaller for the addition of the 4th parallel feeder. The overall reliability value of the network, while very small is not the prime concern within this evaluation the most important factor to consider is the ratios and overall effect to reliability of adding the parallel sections. As noted within section 6, these reliability scores are related to the failure rates of the components and do not reflect those of specific ‘in service’ components.

The follow-on evaluation examines network probability of successfully supplying at least 50 % of the installed power, the level required for safe rolling take-off. The first part of the evaluation shown in Table 6.4 assumes that all GSC must be operational and studies the effect of failed MF in the successful supply of power. For the case where there are 3 MF connected to a single GSC the required number of MF has been rounded up to supply at least 66.6 % power, that is $k = 2$ -out-of- n , as in the case that part of the MF fails no power will be available in that feeder. This analysis assumes that each GSC is directly connected to a maximum of 4 MF and that there are up to 4 parallel SS as in the considered baseline network.

Table 6.4 Probability of 50 % operation of the MF in the N3-X baseline network

Number of MF per GSC	Number of GSC			
	1	2	3	4
2	0.093185	0.008683	0.000809	7.54109×10^{-5}
3	0.043521	0.001894	8.2431×10^{-5}	3.5875×10^{-6}
4	0.068374	0.004675	0.0003197	2.1856×10^{-5}

Table 6.4 shows the probability of successful operation of all GSC and at least 50 % of the installed MFs. It shows, as expected, that in all cases the network can supply a minimum of 50 % of the available power with a higher reliability than it can supply 100 % power. In the case of 1 GSC and 2 associated MF the power can be supplied 4.99 times more reliably than in the 100 % successful supply case, however more importantly in the case of 4 GSC each with 4 associated MF the network can provide the minimum level of power with a reliability which is greater by 1.1757×10^6 when only 50 % of the MF are required to supply power than 100 % of the MF. This 6 orders of magnitude increase in reliability demonstrates that the enhanced number of propulsion motors and fans provides a significant level of inherent back-up against a partial loss of power.

In addition to considering the effect of only failed MF on the ability of the network to supply at least 50 % power, the network can be analysed in a different manner to incorporate the potential failure of GSC. In this alternative analysis, at least $k=2$ out-of-4 SS have to be successfully operational in order for the network to successfully supply the required power. In this evaluation, using the reliability for R_{SS} (0.002077) from above, the probability that the network can successfully supply at least the 50 % required power is 2.5812×10^{-5} and 1.18 times the reliability of the network operating with four GSCs and four MFs and only considering failed MF. The probability of successfully supplying at least 50 % propulsive power in this case is 1.18 times greater than that when only considering MF failures, showing that allowing for a different failure type allows the probability of network failure to be reduced.

For the final analysis of this case study, the reliability of the system is determined when only a single MF is required to be successfully supplying power. Table 6.3 and Table 6.4 show that the probability of at least 50 % and 100 % of the MFs operating at any one time decreases with the number of propulsors connected to the bus. This reduction in system reliability suggests that rather than for reliability gains, the key driver behind utilising larger numbers of connected MF is to provide aerodynamic benefits, through the incorporation of smaller physical motors spread over a large area to maximise boundary layer ingestion (BLI) benefits [16]. In this last section of the N3-X baseline study, the reliability of the network when $k \geq 1$ -out-of- n is

investigated. For fixed values of R_{GSC} and R_{MF} , increasing the number of MFs connected to the bus should increase the overall reliability of supply. As this is not clearly demonstrated in either Table 6.3 or Table 6.4, the *k-out-of-n* method was utilised to show how the probability of supply for the scenario where $1 \leq k \leq n$ for the MF section can be affected by the increase to the overall total number of MF connected. This study is highlighted within Table 6.5 where the probability of achieving at least $k = 1$ -out-of- n for the MF section is shown.

Table 6.5 Probability of at least one operational MF per GSC in the N3-X baseline network

Number of MF per GSC	Number of GSC			
	1	2	3	4
2	0.093185	0.008683	0.0008092	7.5402×10^{-5}
3	0.118017	0.013928	0.0016437	0.00019399
4	0.134564	0.018108	0.0024366	0.0003279

Table 6.5 shows that the probability of at least one MF operating increases with each additional MF added to each of the buses within the network, however the incremental benefits diminish with each addition. Additional MF added to the network in this manner will continue to improve the reliability of a supply of power for the system; however the overall increase will be limited by the reliability of supply from the GSC. As the GSC and MF are connected in a series manner to the propulsion bus, a low probability of successful supply from either could pose a significant reduction in the overall probability of successful supply through the network. In this particular study, where $R_{GSC} = 0.167616$ any benefit resulting from increasing the number of MFs is limited by 0.167616 of the initial increase exhibited by the MF. In order to achieve the additional reliability benefits gained from the connection of further MF additional parallel GSC must also be added (as shown in case study 6.4.1) to enhance the attainable benefits to reliability.

Once all the reliability data has been gathered and tabulated for each contingency scenario, T-R diagrams can hence be created, illustratively showing how reliability and power may be traded and how the reliability changes with each set of operational constraints placed upon the network.

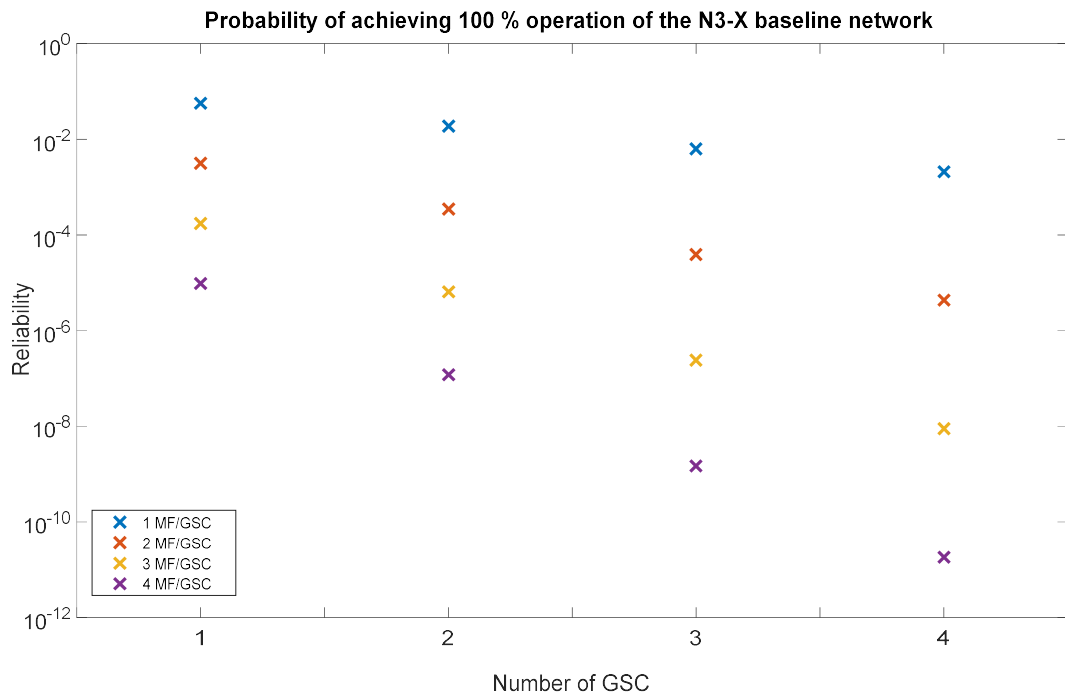


Figure 6.2 Baseline N3-X T-R graph for 100 % network operation

Figure 6.2 shows each of the MF and GSC combinations detailed within Table 6.3. While Table 6.3 showed that the reliability of the network decreased with each additional component, displaying the same results in graph form, **Error! Reference source not found.**, the results can be illustrated far more clearly. The graph of Figure 6.2 shows the large, order of magnitude difference incurred with the additional modular GSC or MF sections of network. This graph shows that the reliability is far greater at lower power availability levels (more power is available with each added GSC) decreasing dramatically for each additional MF or GSC added to the network. Higher reliability levels are obtainable with fewer connected MF per GSC as displayed in Table 6.3. it can also be seen more clearly from the T-R plot that the highest achievable reliability for the $n+1$ generator case is significantly lower than the highest achievable reliability for the n generator case.

Again this same trend can be seen in Figure 6.3 for the probability of achieving at least 50 % propulsive power.

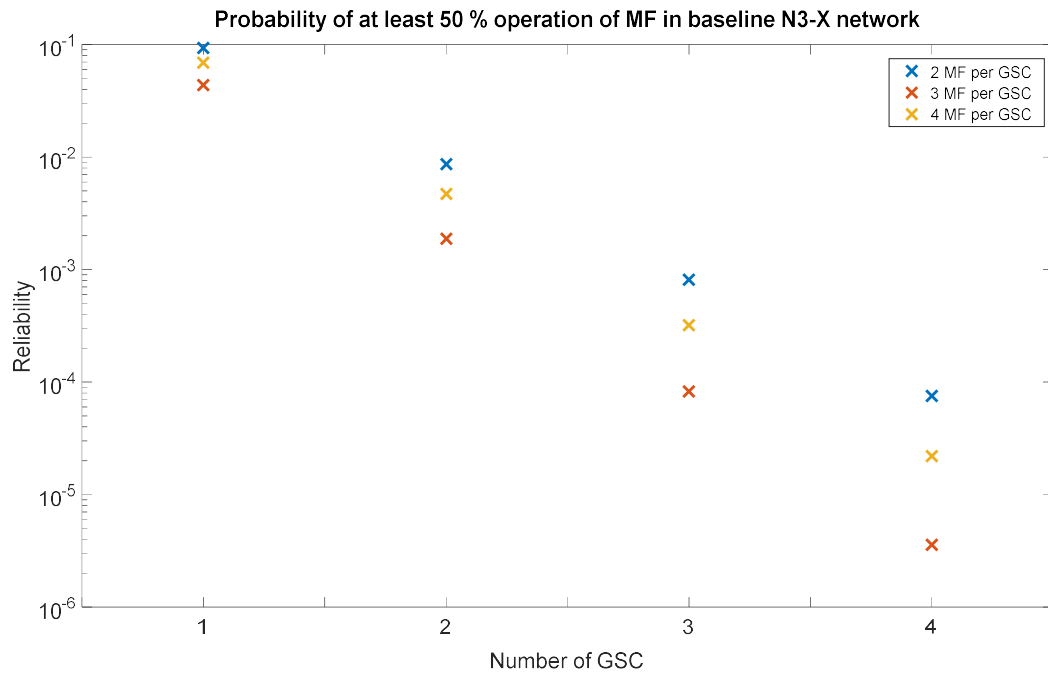


Figure 6.3 Probability of achieving at least 50% propulsive power for the N3-X network

The T-R graph of Figure 6.3 shows the data provided within Table 6.4. In the case for supplying only 50 % of installed power, the reliability of the baseline network increases due to the lesser number of individual components and which are required to be operational for the network to operate successfully. Also of note is that there exists a discernibly different reliability level between each individual analysis point, with the difference becoming larger with each additional GSC or MF.

To conclude the analysis on the N3-X Base Case, Figure 6.4 shows the T-R graph of the case where only one MF per GSC or SS need be operational for the network to operate as desired.

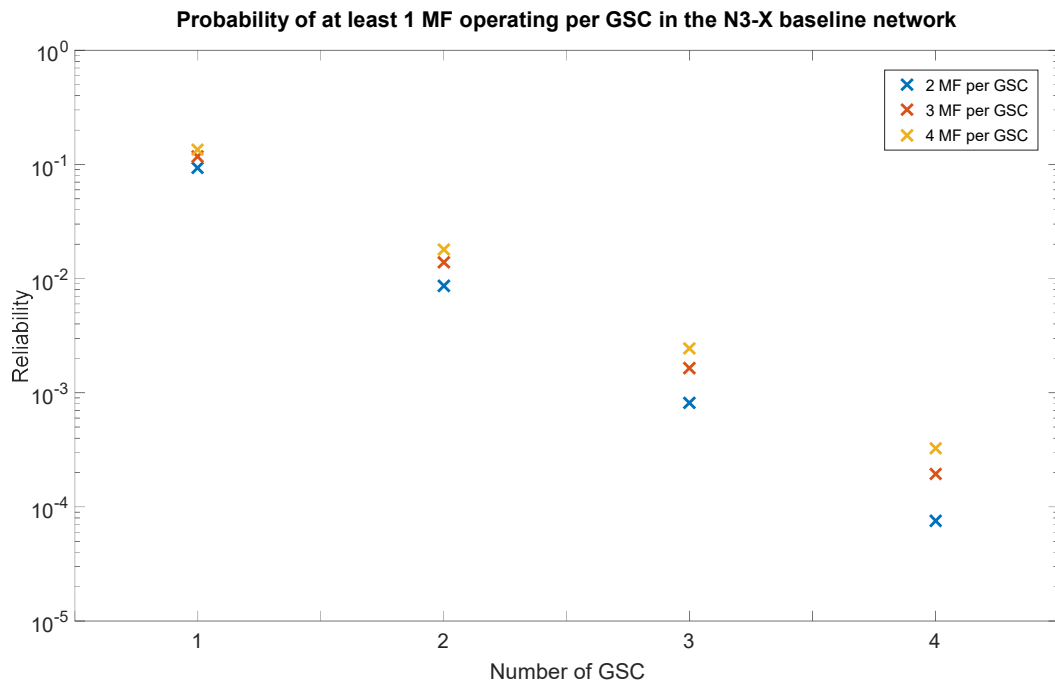


Figure 6.4 T-R Graph for the N3-X Single operational MF case

Figure 6.4 shows the T-R graph of Table 6.5 and indicates how the network reliability has significantly increased as the criteria for the required number of operational components has decreased. Again the reliability value achievable by each T-R profile is increasingly spread and each profile becomes more distinct except for the case when there are 4 SS to the network as the reliability of these profiles is still much smaller in comparison to the single SS profile.

This analysis has provided a number of useful baseline figures to which subsequent studies may be compared. Significantly the cases with 4 SS each including 1 GSC and 4 MF and their associated network reliability value will be used to compare against the further N3-X studies in sections 6.3 and 6.4, using additional redundancy and enhanced individual reliability values to observe the effects on reliability within this chapter.

6.1.2 Case Study Determining the Reliability of the Baseline NASA Hybrid AC-DC Network

The analysis of this case study is used to provide the baseline reliability for the NASA Hybrid network under three separate operating conditions. The three

conditions examined are the same 100 % operation, 50 % operation and the operation of a single MF per SS as examined in Case Study 6.1.1 and the results of this study will be used to compare the results of the redundancy scenarios and sensitivity studies presented in sections 6.3, 6.4 and 6.7 and be used to determine the relative benefits gained. T-R graphs are plotted to help visualise the results of each contingency scenario.

The analysis for this study is again that of Chapter 4, using the k-out-of-n method illustrated within the example case study of section 4.9. This Study of the NASA Hybrid baseline is carried out in the same manner as in the Case Study of 6.1.1 through constructing separate equations for the GSC, MF and SS sections of the network. These equations are then combined with equations (4.1) to (4.3) according to the network architecture described in Figure 5.5. This network schematic is shown again in Figure 6.5 for clarity.

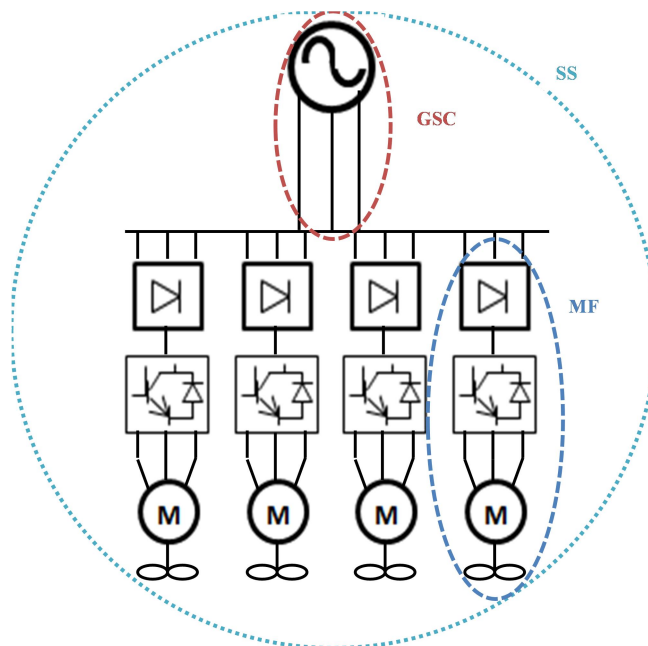


Figure 6.5 NASA Hybrid AC/DC network schematic

From inspection of the network schematic shown in Figure 6.5, it can be seen that the reliability of the GSC section can be expressed as a series reliability calculation:

$$R_{GSC} = R_G R_F R_{CAC} R_B. \quad (6.4)$$

Additionally, as in the N3-X case, the engine controller component is assumed as part of the generator symbol. Similarly, the reliability of the MF section of network can be expressed as:

$$R_{MF} = R_{CAC} R_{CON} R_{ACD} R_M R_P. \quad (6.5)$$

Finally, through observation it can be determined that as with the N3-X design that the reliability of each of the 4 network subsections can be described as:

$$R_{SS} = R_{GSC} R_{MF}^4 \quad (6.6)$$

Using the component values from Table 6.2, the specific SS, MF and GSC reliability values (assuming all components are operating as desired) can be shown to be:

$$R_{GSC} = 0.527436 \quad R_{MF} = 0.490552 \quad R_{SS} = 0.030543$$

The values of R_{GSC} and R_{MF} can then be used in conjunction with equation (4.3)

$$R_S = \sum_{x=k}^n P(x) \quad (4.3)$$

where $P(x)$ is the probability of successful operation of the whole network operating with the indicated connected components, to determine the network reliability, R_S .

By repeating the calculation process for a single GSC connected to an increasing number of parallel connected MF, it is possible to evaluate the reliability of power provision for the network SS and hence the overall network. The output of this exercise is detailed in Table 6.6 for the case where 100 % successful operation is required and in Table 6.7 for the case where at least 50 % propulsive power is required. A further case is presented and detailed in Table 6.8 to show how the reliability changes when only a single MF per network SS is required to operate.

This first section of the analysis shows how the reliability of the network (where 100 % operation is desired) changes as the network is built up. The network is built up from a single GSC and single associated MF to four GSCs all with four associated and parallel connected MFs as in the baseline design. In this example, where successful operation is obtained when 100 % of the network components are

operational, $k = n$. in the case of the GSC n is fixed at one while for the MF, n is increased incrementally from one to four as indicated in Table 6.6.

Table 6.6 Probability of 100 % operation for baseline NASA Hybrid network

Number of MF per GSC	Number of GSC			
	1	2	3	4
1	0.258735	0.066944	0.017321	0.004481
2	0.126923	0.016109	0.002045	0.000260
3	0.062262	0.003877	0.000241	1.503×10^{-5}
4	0.030543	0.000933	2.85×10^{-5}	8.702×10^{-7}

The results in Table 6.6 agree with the N3-X baseline configuration that the probability of the combination of each working correctly decreases as the number of MFs and GSCs in the network increases. It is also apparent when comparing Table 6.6 with Table 6.3 that for every corresponding network configuration that the Hybrid Network can operate at a greater reliability than the baseline N3-X configuration. This is due to the fact that, through a fewer number of components used to create the network, the reliability of both the GSC, MF and hence SS are significantly higher. The probability of successful supply from one MF and one GSC is 2.97×10^5 times greater than the case where the network is operating with four GSC in four individual SS and a combined total of 16 MF, four in each SS. Should the network consist of only two GSC and a total of eight MFs, the reliability in this case would be 0.000933 a total of 1.07×10^3 times more reliable than the four GSCs and 16 MFs case. This two GSCs, 8 MFs configuration would be able to supply the minimal power for safe rolling take-off and would therefore be preferable in reliability terms. This configuration however would have no contingency plan in the case of any propulsion network failure. Additionally it is clear that with each additional MF per GSC the reliability of the system drops significantly: around one or two orders of

magnitude for the addition of the second MF and around six orders of magnitude smaller for the addition of the 4th parallel MF.

The second evaluation within this case study examines the probability of the network being able to supply at least 50 % of the installed power successfully, the level of power required for safe rolling take-off. The first set of results is shown in Table 6.7 and assumes that all GSC must be operational and studies the effect of failed MF in the successful supply of power. In the case where there are three MFs connected to a single GSC, at least two of the three must be operational to supply at least 50 % of the installed power and so $k = 2\text{-out-of-}n$. This analysis assumes that each GSC is directly connected to a maximum of four MFs and that there are up to four parallel SS as in the considered baseline network.

Table 6.7 Probability of 50 % operation for baseline NASA Hybrid network

Number of MF per GSC	Number of GSC			
	1	2	3	4
2	0.390547	0.152527	0.059569	0.023264
3	0.256244	0.065661	0.016825	0.004361
4	0.355068	0.126073	0.044764	0.015894

Table 6.7 shows the probability of successful supply of power from at least 50 % of the connected network MFs. Table 6.7 also shows, as expected, that in all cases the network can supply a minimum of 50 % of the available power with a higher reliability than it can supply 100 % power and again at a greater reliability than the N3-X due to the significantly reduced number of components within the network. It is instructive to compare the extremes of these probability ratios for 50% to 100 % power using the calculated results in Table 6.6 and Table 6.7. In the case of one GSC and 2 associated MF the power can be supplied 1.51 times more reliably, however more importantly in the case of four GSC each with four associated MFs the network can provide the minimum level of power with a reliability which is greater by 18.2648×10^3 (or four orders of magnitude).

In addition to considering the effect of only failed MF on the ability of the network to supply at least 50 % power, the network can be analysed in a different manner to incorporate the potential failure of GSC. In this study, at least $k=2$ out-of-4 SS (at least two out of the total 4 SS) have to be successfully operational in order for the network to successfully supply the required power. In this specific study the probability that the network can successfully supply at least the 50 % required power is 0.005372 (based on the value of R_{SS} above) and 208.12 times greater than the equivalent operating criteria for the same study in the N3-X network. The probability of successfully supplying at least 50 % propulsive power in this case is 0.338 times that of only considering MF failures, showing that in this case the most reliable way of providing 50 % power is with all GSCs supplying power and only half of the network MFs available.

For the final case of this study, the reliability of the system is determined when only a single MF is required to be successfully supplying power. In addition to showing the ability of the network to successfully transmit power, Table 6.6 and Table 6.7 further show that the probability of at least 50 % and 100 % of the MF operating at any one time decreases as an increasing number are connected to the bus. This reduction in system reliability suggests that rather than for reliability gains, as in the N3-X case, the key driver behind utilising larger numbers of connected MFs is to provide aerodynamic benefits through the incorporation of smaller physical motors spread over a large area to maximise BLI benefits [16].

To highlight the benefits of using a greater number of total connected propulsors, the final item of consideration in the study of the Hybrid network, investigates the reliability of the network when $k \geq 1$ out-of- n (k is greater than or equal to 1). For fixed values of R_{GSC} and R_{MF} , increasing the number of MFs connected to the bus should (at least) increase the overall reliability of supply. As this is not clearly demonstrated in either Table 6.6 or Table 6.7, the k -out-of- n method was utilised as before to show how the probability of supply for the scenario where $1 \leq k \leq n$ for the MF section can be affected by the increase to the overall total number of MF connected. The results are tabulated within Table 6.8 where the probability of achieving at least $k = 1$ out-of- n for the MF section is shown.

Table 6.8 Probability of at least one MF per GSC operating for the baseline Hybrid network

Number of MF per GSC	Number of GSC			
	1	2	3	4
2	0.390547	0.152527	0.059569	0.023264
3	0.457698	0.209487	0.095882	0.043885
4	0.491908	0.241974	0.119029	0.058551

Table 6.8 shows that the probability of at least one MF operating increases with each additional MF added to each of the buses within the network. As with the N3-X case of Table 6.5 however the incremental benefits diminish with each addition. Additional MF added to the network in this manner will continue to improve the reliability of a supply of power for the system; however the overall reliability increase will be limited by the reliability of supply from the GSC. This could be remedied through adding parallel GSCs in the same manner as the MF with the requirement that for successful operation $k \geq 1$. As the GSCs and MFs are connected in a series manner to the propulsion bus, a low probability of successful supply from either could pose a significant reduction in the overall probability of successful supply through the network. In this particular part of the study, where $R_{GSC} = 0.527436$ any benefit resulting from increasing the number of MF is scaled by this value.

After all the reliability data has been gathered and tabulated for each of the Hybrid network contingency scenarios, T-R diagrams are generated. These illustratively show (as before) how reliability and power may be traded and how the reliability changes as a consequence of each set of operational constraints placed upon the network.

The T-R graph of Figure 6.6 corresponds to the results shown in Table 6.6. This graph shows that the reliability is greater when fewer GSC and hence SS are present within the network and decreases dramatically for each additional MF or GSC added. Higher reliability levels are obtainable with fewer connected MFs per GSC as displayed in Table 6.6.

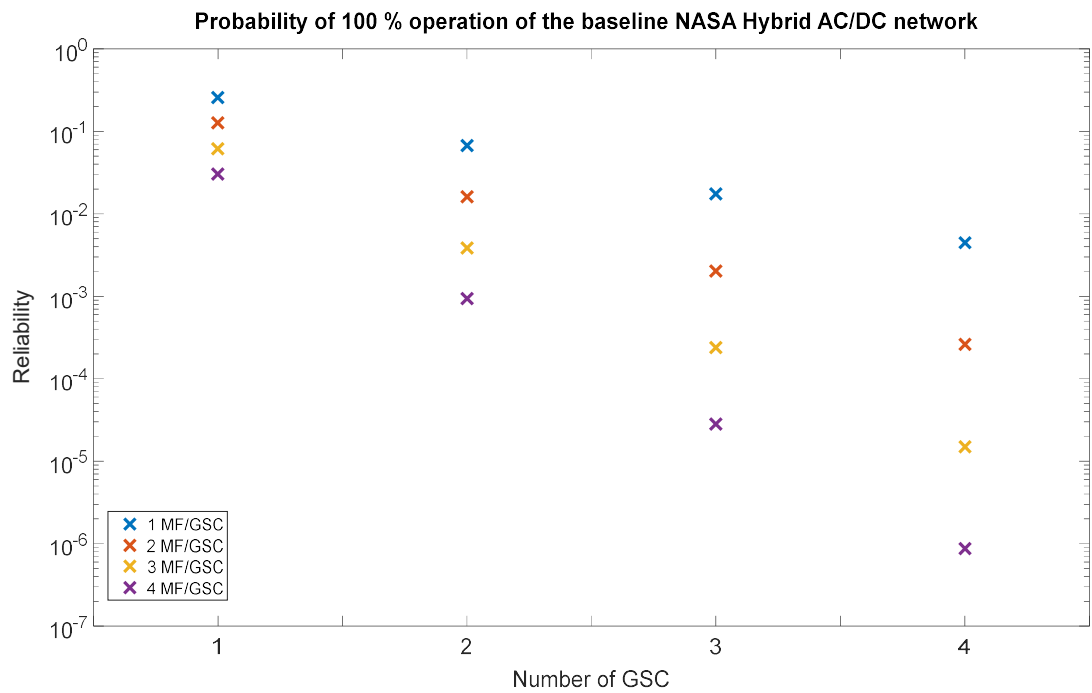


Figure 6.6 T-R Graph for probability of 100 % operation of baseline NASA Hybrid TeDP network

Figure 6.6 also shows how the reliability values for this case have a far greater variation in reliability than the 100 % operation case of the N3-X. The graph also shows that the NASA Hybrid network has greater reliability values at all equivalent evaluated points with a smaller distribution between each point. Again this same trend can be seen in Figure 6.7 for the probability of the network being able to supply at least 50 % propulsive power.

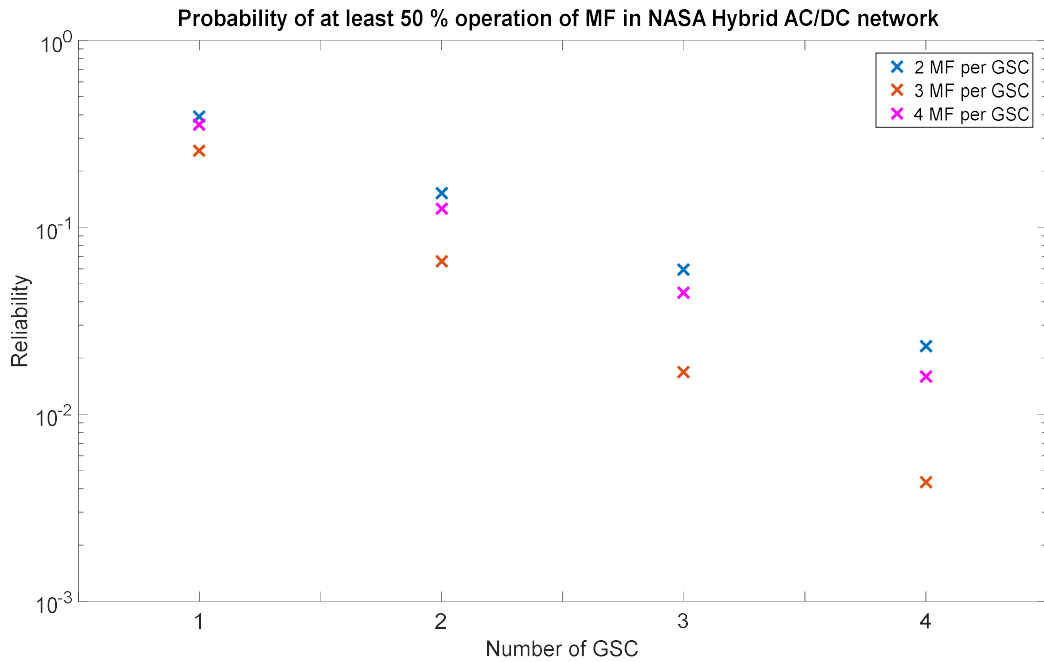


Figure 6.7 T-R graph for at least 50 % operation of the baseline NASA Hybrid TeDP network

The T-R graph of Figure 6.7 shows the data provided within Table 6.7. In the case for supplying only 50 % of installed power, the reliability of the baseline NASA AC/DC network increases at each evaluated point due to the lesser number of individual components and hence fewer number which are required to be operational for the network to operate successfully. The family of points for every GSC section shows a significant reduction in reliability for every parallel MF section added to the GSC's bus where each individual point exhibits a greater change in reliability than in either the equivalent N3-X case or the 100 % NASA hybrid operation case. The highest achievable reliability value for any of the network configurations in the 50 % case is an additional 0.3 more than in the equivalent N3-X baseline case.

Finally Figure 6.8 shows the T-R graph of the final NASA Hybrid AC/DC network base case (presented in Table 6.8 where only one MF per GSC or SS need be operational for the network to operate as desired.

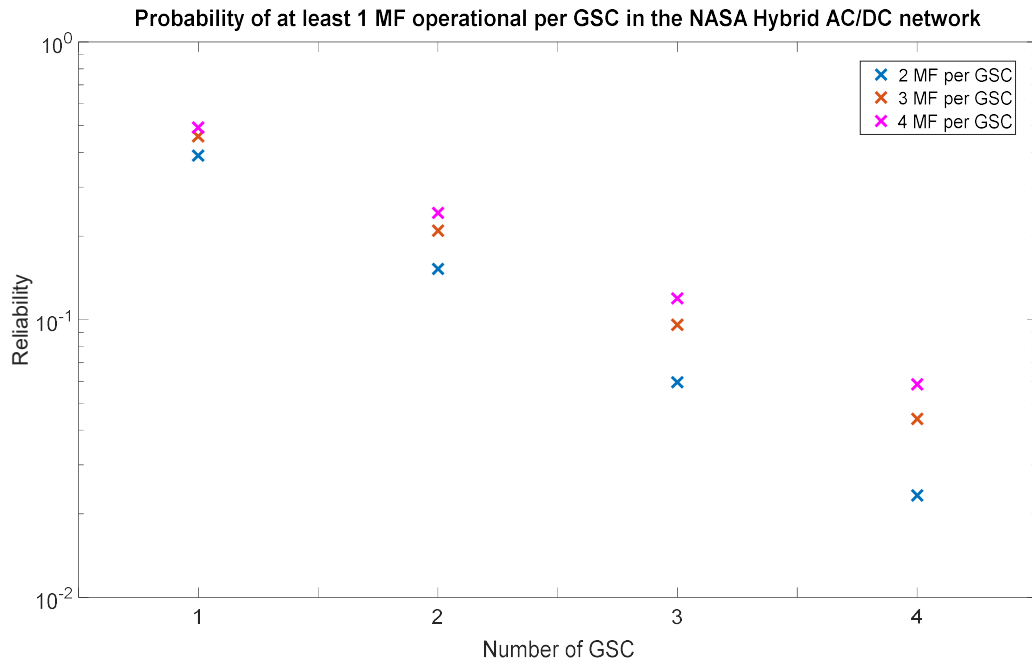


Figure 6.8 T-R Graph for single operational MF case of the baseline NASA Hybrid TeDP network

Figure 6.8 shows the T-R graph of the results shown in Table 6.8. It shows how the network reliability has significantly increased as the criteria for the required number of operational components has decreased. Again the distinction between adjacent T-R profiles is significantly increased with greater differences in reliability for each additional MF added to a SS.

This analysis has again provided a number of useful baseline reliability figures to which subsequent studies may be compared. Significantly the reliability results from the network cases with four SS each including one GSC and four MFs will be used to compare against the further NASA Hybrid network studies within this chapter.

6.1.3 Case Study to Determine the Reliability of the Rolls-Royce and Airbus Baseline Network

This case study is based upon the Rolls-Royce and Airbus network of Figure 5.7 and repeated for clarity in Figure 6.9.

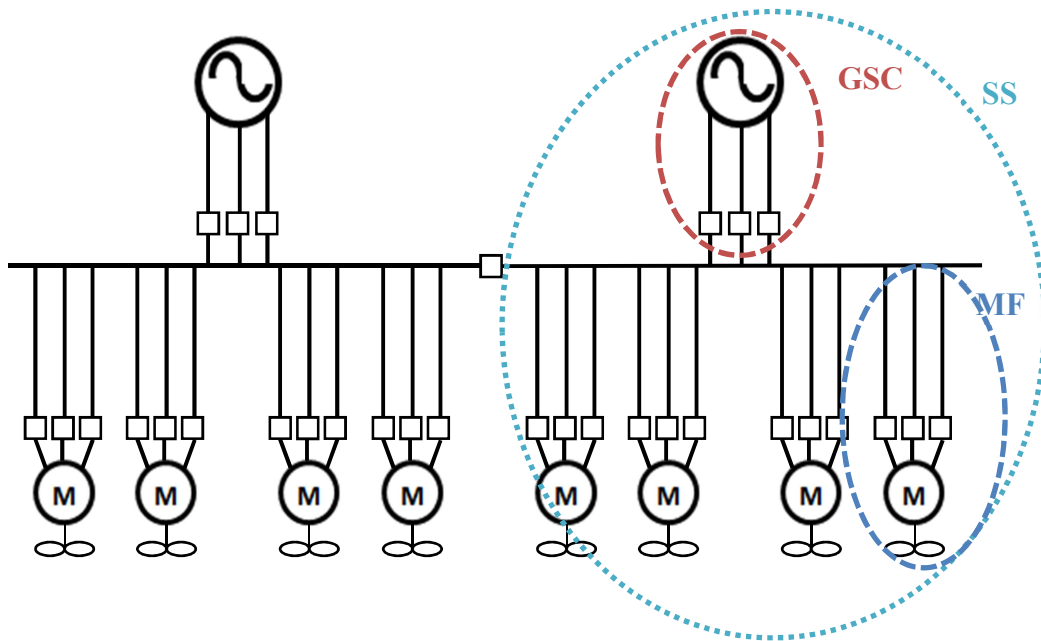


Figure 6.9 Rolls-Royce and Airbus TeDP network architecture [23]

This analysis assumes that the bus tie linking the two halves of the baseline network shown in Figure 6.9 remains normally open. As this network has been extended to include four parallel SS to provide fair comparison with the four parallel SS of the other networks, the analysis for this network with address both the original network configuration and the extrapolated four SS network.

The analysis of Chapter 4 is carried out in the same manner as in Case Studies 6.1.1 and 6.1.2 through constructing separate equations for the GSC, MF and SS sections and then, as before, combining these with equations

$$P(x) = \binom{n}{x} R^x (1 - R)^{n-x} \quad (4.1)$$

$$\binom{n}{x} = \frac{n!}{x!(n-x)!} \quad (4.2)$$

$$R_S = \sum_{x=k}^n P(x) \quad (4.3)$$

according to the network architecture described in Figure 6.9. The results of this study can then be used to determine the relative benefits gained through adding redundancy methods as presented in case studies 2 and 3 within sections 6.3 and 6.4. As in previous studies, a T-R graph may be plotted to help visualise the results of each contingency scenario.

From inspection of the network schematic shown in Figure 6.9, it can be seen that the reliability of the GSC section can be expressed as a series reliability calculation:

$$R_{GSC} = R_G R_F R_{3PH} R_{CAC} R_B. \quad (6.7)$$

Similarly, to the NASA Hybrid network, the inclusion of the AC cable term is dependent on the location of the generator with regards to the bus. All studies within this thesis however will include this term. Additionally, the reliability of the MF section of network can be expressed as:

$$R_{MF} = R_{CAC} R_{3PHB} R_M R_P. \quad (6.8)$$

Finally through observation it can be determined that as with the other two designs that the reliability of each of the 4 network subsections can be described as:

$$R_{SS} = R_{GSC} R_{MF}^4 \quad (6.9)$$

Using the component values from Table 6.2, the specific SS, MF and GSC reliability values (assuming all components are operating as desired) can be shown to be:

$$R_{GSC} = 0.421949 \quad R_{MF} = 0.569664 \quad R_{SS} = 0.044436$$

Through repeating the calculation process for a single GSC connected to an increasing number of n parallel connected MFs, it is possible to evaluate the reliability of power provision for a single SS and hence the full network operating at both full and partial power. The output of this exercise is detailed in Table 6.9 for the case where 100 % successful operation is desired and in Table 6.10 for the case where at least 50 % propulsive power is desirable. The results of a further study are presented within Table 6.11 to show how the reliability of the network changes as more components are added.

In this first study to evaluate the reliability for 100 % operation, the network is built up from a single GSC and single associated MF to 4 GSC all with four associated and parallel connected MF as in the baseline design of Figure 6.9. The number, k , MFs, required to operate in each case is given by $k=n$ and n is increased incrementally from one to four. In the case of the GSC n is fixed at 1 for each SS. The results of this analysis are shown in Table 6.9.

Table 6.9 Probability of 100 % operation of the Rolls Royce and Airbus concept aircraft

Number of MF per GSC	Number of GSC			
	1	2	3	4
1	0.240369	0.057777	0.013888	0.003338
2	0.13693	0.01875	0.002567	0.000352
3	0.078004	0.006085	0.000475	3.7022×10^{-5}
4	0.044436	0.001975	8.77×10^{-5}	3.8989×10^{-6}

Table 6.9 shows that, as in the previous baseline configurations, as the number of MF and GSC in the network increases the probability of all operating correctly decreases. Comparing Table 6.9 to both Table 6.3 and Table 6.6 also shows that this is the most reliable network of the three, operating 4.48 times more reliably than the next most reliable network, the NASA Hybrid network, when operating with 4 SS and 4 connected MF in each. The Rolls-Royce and Airbus network reliability is not as high as the Hybrid network for the case where there is only a single MF connected in each of the network SS. The probability of successful supply from one MF and one GSC is only 92.9 % that of the corresponding case in the NASA Hybrid network, decreasing to only 74.4 % of the reliability for the case of four SS each with one MF. In every other configuration, where there is two or more MF per SS, this network is the most reliable of the three. Additionally it is clear from the data that as with the other two configurations that with each additional MF per SS the reliability of the system drops significantly. This decrease is between 0.5 - 1 order of magnitude for the addition of the 2nd feeder and up to around 3 orders of magnitude for the addition of the fourth feeder (in the case of four parallel SS).

The next data to be calculated from this part of this case study example is the probability of the network being able to supply at least 50 % of the installed power successfully, the level of power required for safe rolling take-off. The first part of the analysis is shown in Table 6.10, and assumes that all GSCs must be operational and studies only the effect of failed MFs in the successful supply of power. In the case where there are 3 MF connected to a single GSC this study rounds the required number of operational MF up, that is *k=2-out-of-n*. This analysis assumes that each

GSC is directly connected to a maximum of four MFs and that the network has again been extrapolated to four parallel SS to allow the results to be directly compared.

Table 6.10 Probability of Operation of at least 50 % of the Airbus and Rolls-Royce network

Number of MF per GSC	Number of GSC			
	1	2	3	4
2	0.206879	0.042799	0.008854	0.001832
3	0.254781	0.064913	0.016539	0.004214
4	0.330855	0.109465	0.036217	0.011983

Table 6.10 shows, as expected, that in all cases the network can supply a minimum of 50 % of the available power with a significantly higher reliability than it can supply 100 % power and also significantly, in all cases at a lesser reliability than the Hybrid network. In the 50 % power case and a network configuration of one GSC and two associated MFs the power can be supplied 1.43 times more reliably than the 100 % operation case. More importantly however, in the configuration of four GSC each with four associated MF the network can provide at least the minimum level of power for a safe rolling take off with a reliability which is greater than the 100 % power case by over 3000 times.

The second part of the supply of at least 50 % power study considers the effect of not only failed MF but of the potential failure of GSC on the ability of the network to supply at least 50 % power. In this study, at least $k = 2$ -out-of-4 SS have to be successfully operational in order for the network to supply the required power. The probability of the network operating to these criteria is 0.011157 (based on the R_{SS} value above), 432.24 times greater than the value for the equivalent operating criteria for the N3-X and 2.08 times greater than the NASA Hybrid network. The probability of successfully supplying at least 50 % propulsive power in this case is 0.93 times that of only considering MF failures from Table 6.10, showing that in this case the most reliable way of providing 50 % power is with all GSC supplying power and only half of the network MF available.

For the final case of this study, the reliability of the system when at least one MF per GSC or SS is required to operate is examined. In addition to showing the ability of the network to successfully transmit power, Table 6.9 and Table 6.10 further show that the probability of at least 50 % and 100 % of the MF operating at any one time decreases with an increasing number connected to each SS as in the previous two cases.

Again to highlight the benefits of using a greater number of total connected propulsors, the final Rolls-Royce and Airbus baseline network study investigates the reliability of the network when, for the MF section, $k \geq 1$ (the number of MFs required to operate must be at least one). For fixed values of R_{GSC} and R_{MF} , increasing the number of MF connected to the bus should increase the overall reliability of supply. As this is not clearly demonstrated in either Table 6.9 or Table 6.10, the k-out-of-n method is utilised to show how the probability of supply for the scenario where $1 \leq k \leq n$ for the MF section can be affected by the increase in the total number of connected MFs. The results of this study are presented in Table 6.11 where the probability of achieving at least $k = 1$ -out-of- n for the MF section is shown, again, with the results for the extrapolated network.

Table 6.11 Probability of at least one MF per GSC operating for the Airbus and Rolls-Royce network

Number of MF per GSC	Number of GSC			
	1	2	3	4
2	0.343808	0.118204	0.04064	0.013972
3	0.388322	0.150794	0.058557	0.022739
4	0.407478	0.166038	0.067657	0.027569

As with the corresponding study undertaken for both the N3-X and the Hybrid network Table 6.11 shows that the probability of at least one MF operating increases with every additional MF added to each bus. Further, in line with the results of the previous two architectures the incremental benefits diminish with each addition and will continue to improve the reliability of power supply for the system but will be limited by the reliability of the GSC unless additional parallel GSC are added in the same manner as the MF. As the GSC and bank of MF are connected in a series

manner, a low reliability value from either could pose a significant reduction in the overall probability of successful supply through the network. In this particular study, where $R_{GSC} = 0.421949$ any benefit resulting from increasing the number of MF, in keeping with the results of the two previous architectures, is scaled by this value.

Once the reliability data has been tabulated for each of the network operation scenarios, T-R diagrams can hence be created, illustratively showing the reliability and power trades and how these change with each set of operational constraints placed upon the network. The T-R graph of Figure 6.10 corresponds to the results shown in Table 6.9. This graph shows that the reliability is greatest when fewer SS are present within the network and decreases dramatically for each additional MF or GSC added. Higher reliability levels are obtainable with fewer connected MF per GSC as shown by the data in Table 6.9.

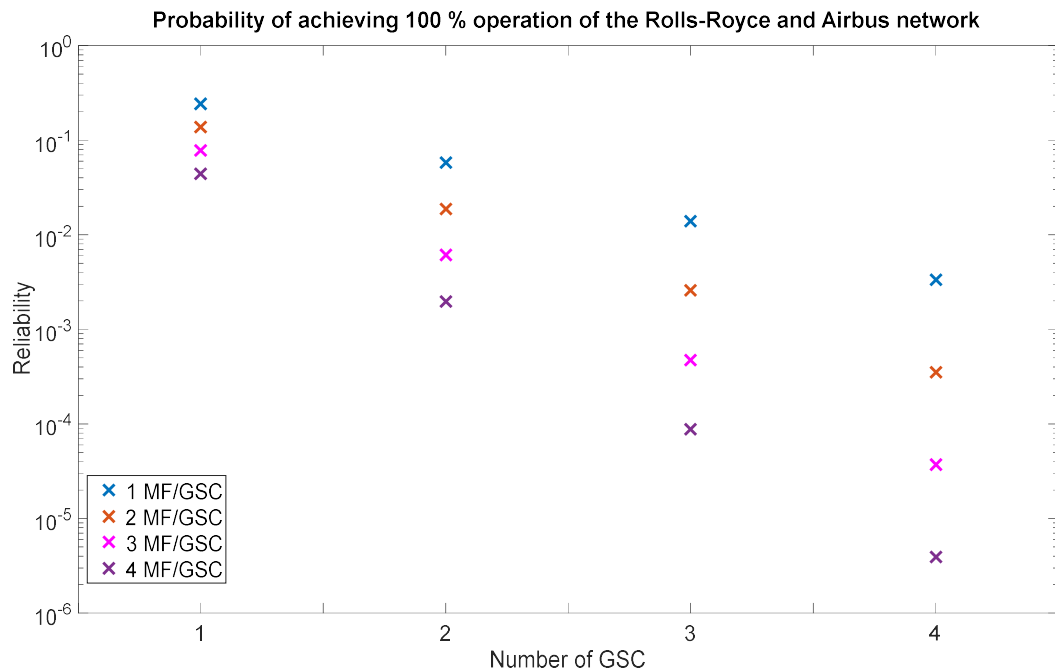


Figure 6.10 T-R Graph showing the probability of 100 % operation of Rolls-Royce and Airbus TeDP network

Figure 6.10 shows how the reliability values for this case have a far greater magnitude at all points and hence comparable network configurations than in the N3-X case. However in terms of the NASA Hybrid case while the worst case reliability for each connected GSC is a greater value, the best case for each GSC is approximately the same. Similarly to the NASA Hybrid case, the reduction in

reliability with each additional MF per GSC increases with the number of GSC and hence SS within the network. This trend can also be seen in Figure 6.11 for the probability of the network being able to supply at least 50 % of installed propulsive power.

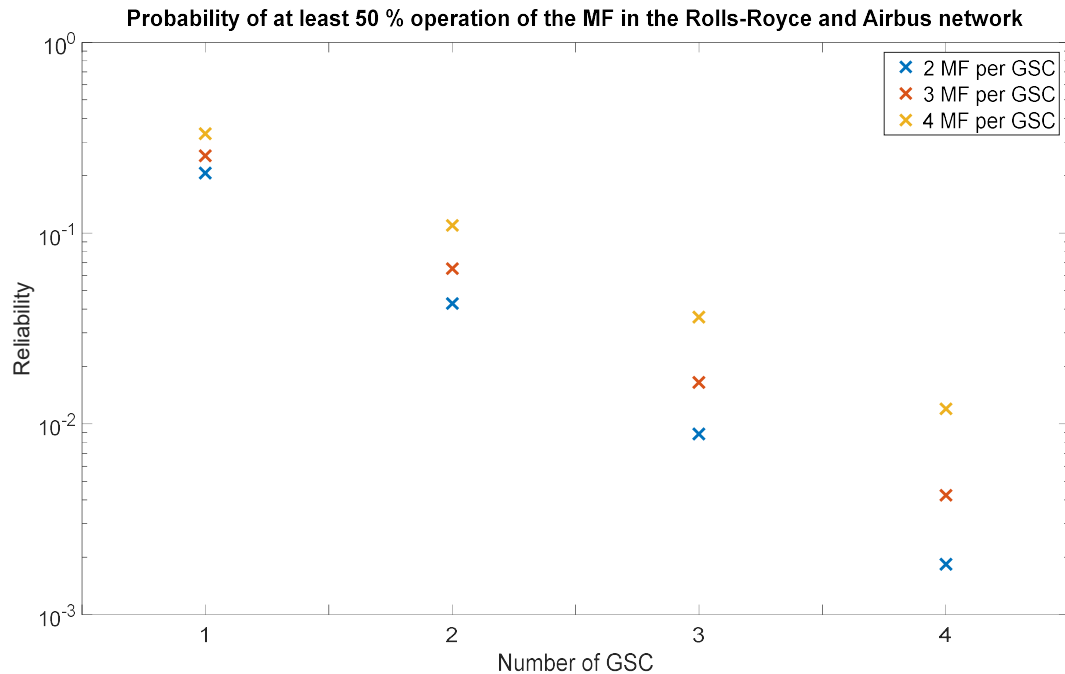


Figure 6.11 T-R Graph Showing the Probability of at least 50 % Operation of Rolls-Royce and Airbus TeDP Network

The T-R graph of Figure 6.11 illustrates the data provided within Table 6.10. In the case for supplying only 50 % of installed power, the reliability of the baseline network increases due to the lesser number of individual components which are required to be operational for the operating criteria to be fulfilled. Similar to the other networks, the decrease in reliability with each additional MF increases and in this network this decrease in reliability is not as severe as in the NASA Hybrid or the N3-X equivalent network. In comparison with the T-R profile for 100 % operation of this network, the worst case reliability for this 50 % case is visibly greater than the 100 % operation.

Figure 6.12 shows the T-R graph of the final part of the core Rolls-Royce and Airbus architecture analysis, presented in Table 6.11 where only one MF per GSC or SS need be operational for the network operating criteria to be fulfilled.

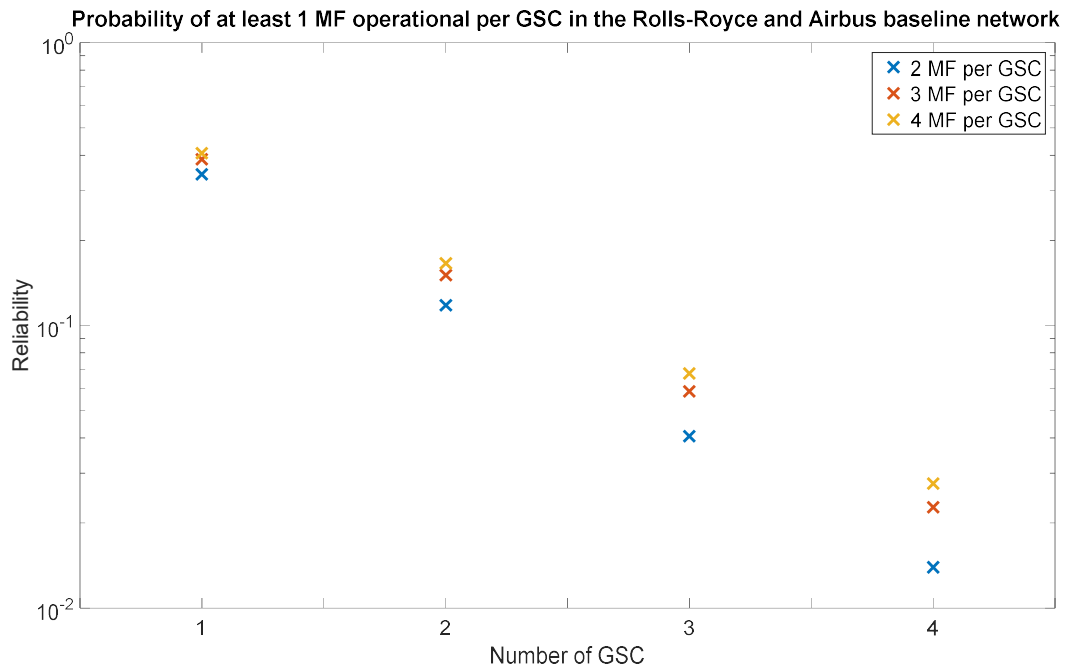


Figure 6.12 T-R graph showing the probability of at least one operational MF on the Rolls-Royce and Airbus TeDP network

Figure 6.12 shows the network reliability increases as the criteria for the required number of operational components decreases. As with the other networks the reliability value achievable by each T-R profile is increased through each additional MF with a worst case achievable reliability in the four GSC four MF case similar to results possible with only tree GSC in the 50 % operation case. This is significant as it shows a net improvement effect in the network reliability when increasing the number of network components required to construct the baseline network providing enough power for take-off.

This analysis has provided the baseline figures which will be used for the subsequent studies for comparison. As with the other networks the configuration with 4 SS each exhibiting one GSC and four MF and their associated network reliability value will be used to compare against the further network studies in sections 6.3, 6.4 and 6.7, where additional redundancy and enhanced individual reliability values will be examined.

6.2 Summary of the Baseline Studies

Through observation of the data gathered within the tables presented in section 6.1, conclusions can be drawn over which of the network architectures yield the greatest baseline reliability. The network configuration of the most interest is that where the network consists of 4 SS, 4 GSC and 16 MF as in the reviewed N3-X and NASA Hybrid baseline configurations and the extrapolated Rolls-Royce and Airbus baseline configuration. In terms of network reliability when operating with all installed components functioning as desired, the Rolls- Royce and Airbus network performs best with the greatest level of observed reliability 4.47 times greater than the Hybrid network and 2.1×10^5 times greater than the N3-X. When considering the network's ability to provide at least 50 % of the installed power, the Hybrid network performs the best exhibiting a reliability 1.34 times greater than the Rolls – Royce and Airbus network and 727.21 times greater than the N3-X architecture. It should be noted that due to the considerably fewer components present on the Rolls-Royce and Airbus original network design this network compares the most favourably of all the considered networks. This has a reliability which is greater by 506.55 times over the extrapolated Rolls – Royce and Airbus network in the 100 % operation case, 6.89 times greater than the NASA Hybrid network in the 50 % case and when only one MF is required to operate, performs over 500 times greater in reliability terms than the N3-X network.

The results show that more reliable, partial operation can be achieved with larger numbers of GSCs and MFs, however with a significant weight penalty attached. Each additional generator or other component, especially power electronic devices [23] added to the network results in a significant amount of undesired weight to the system. Whereas it may be desirable to increase the number of additional GSC's or MF's until there is no observable change to reliability, the weight penalties of each additional section must be carefully considered, in a separate, additional study. Through the use of a small number of electrical machines, overrated to provide excess power to the network, a better power density could be attainable than through using a larger number of lower rated generators [128].

The results of the three baseline studies are compared in the T-R graph of Figure 6.13. This graph displays results for the three networks for the case where each network consists of a total 4 SS and 16 MF. Each separate level of power provision has an individual marker as outlined within the legend.

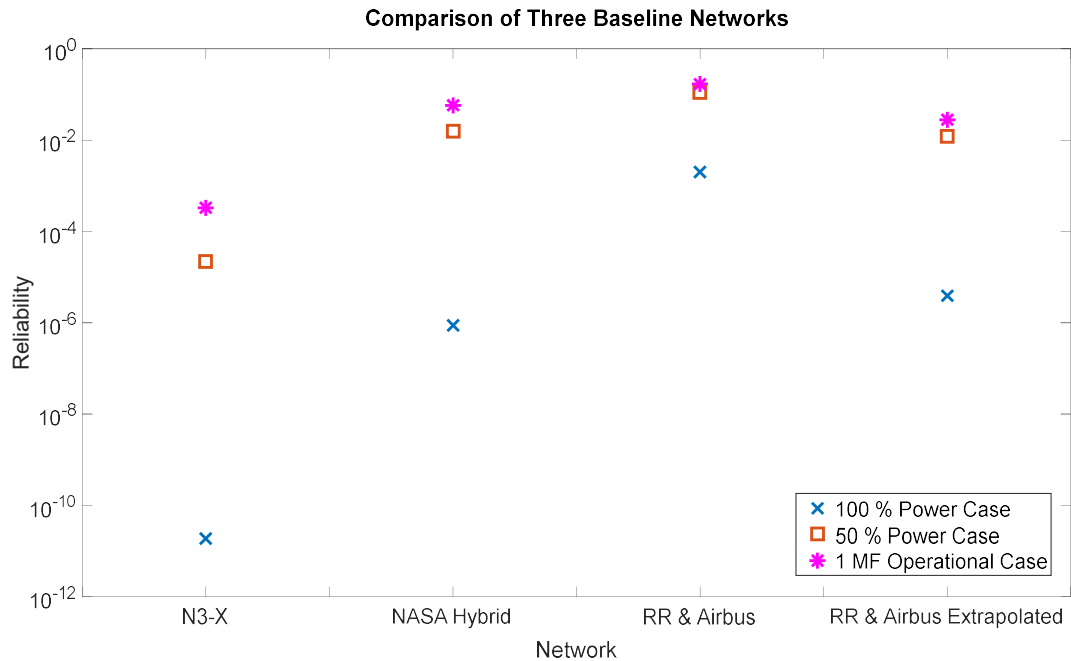


Figure 6.13 Comparison of Three Baseline TeDP Networks

Figure 6.13 confirms the results of the case studies and would show that the Rolls – Royce and Airbus network can supply 100 % of installed power at the greatest reliability, however the Hybrid Network exhibits the greatest reliability for provision of 50 % of installed power. The graph illustrates with consummate clarity, that after all analysis has been undertaken, that of the three considered networks that the N3-X configuration clearly provides all considered power levels at the lowest reliability of all the networks.

The subsequent studies within this chapter will investigate the effect to the baseline values derived within this section through using a number of redundancy features and through altering individual reliability values of select components. Additional, parallel connected additional feeders will be added in the GSC as well as the MF sections of network and bus ties will be considered to allow power to be routed from one GSC to the MF of another SS. The new reliability values will be recorded and

comparisons made to determine which redundancy method offers the greatest increase in network reliability for all three networks.

6.3 Case Study 2: Examining the Effect of Adding Bus Ties to a TeDP Network to enhance Reliability

Bus ties may be used within a TeDP network to enhance reliability through linking adjacent SS through their bus and allowing power generated in the generator of one SS to be routed to the MF of another SS. Each bus tie consists of either an AC or DC breaker (as described by Table 6.2) depending on the network architecture and links the bus of adjacent network SS. Through linking network SS in such a manner, the effects of generator failures may be mitigated as described within the Contingency Scenarios section 4.7.2 in Chapter 4.

This study will look at the effects to network reliability through adding bus ties between each bus and the bus directly adjacent. In the case where there are two busses at opposite ends of the network an additional tie will be added to link these busses creating a ring type network. The study will consider the use of four ties for each network except for the original, non-extrapolated Rolls – Royce and Airbus network where only a single tie is considered, tabulating the results in Table 6.12. This case study is completed with a round-up of the results determining which network performs the best in terms of reliability using this redundancy method. A T-R graph showing a performance comparison between all three networks will be provided for visual analysis. These results are then compared with the respective baseline equivalents to determine the benefit to reliability of this reliability enhancement method.

This study will examine the ability of each of the networks to provide at least 50 % of total installed electrical power. In this case that requires $k \geq 2$ -out-of-4 GSC to be operational as well as at least 8-out-of-16 installed MF. Additionally to this at least 3-out-of-4 of the 4 installed bus ties must be operational combined with 4-out-of-4 electrical busses. When operating under these explicit outlined conditions, the bus

and bus tie section becomes a single modular section resulting in a singular network SS. The parallel connected GSC sections may be considered a singular modular section connected in series to the Bus and tie section which is in turn connected in series to a singular modular MF section.

In order to conduct the study, the equations for the GSC are altered slightly from the baseline equations presented in section 6.1. In each case the bus component is removed from the GSC equation as regardless of the operating status of the rest of the GSC, if there is a fault or a failure within the bus then the power cannot be routed through the tie. For each of the three considered networks in this section a new R_{GSC} term will be derived based on the removal of the bus term. A separate term for the bus tie R_{BT} , inclusive of the bus will also be derived.

In the case of the N3-X network, the bus ties may be added in the manner as shown in Figure 6.14.

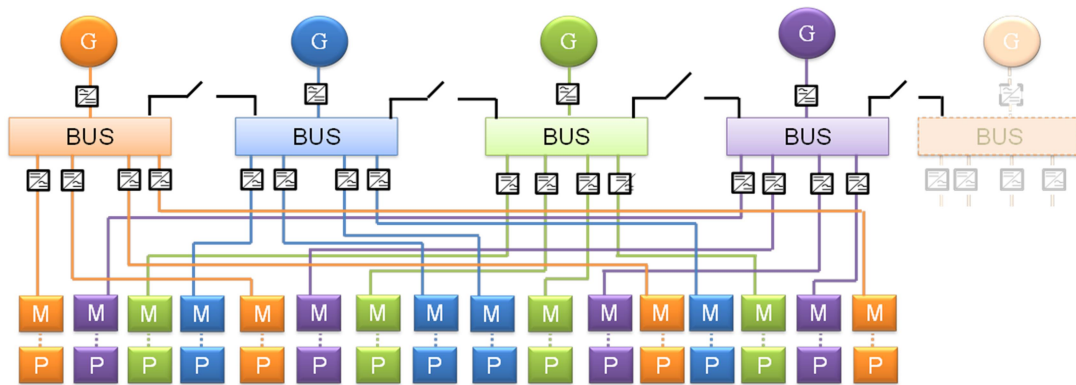


Figure 6.14 N3-X architecture with added bus ties

Figure 6.14 shows that the bus ties are added into the DC distribution section of the network and therefore the bus tie will be comprised of a DC breaker. The GSC equation as presented in equation 6.1 becomes:

$$R_{GSC} = R_G R_F R_{3PHB}^2 R_{CAC} R_{SFCL}^2 R_{CON} R_{DCB}^2 R_{CDC} \quad (6.10)$$

This equation remains otherwise unaltered compared with 6.1 after the removal of the bus term. The bus tie equation becomes:

$$R_{BT} = R_B R_{DCB} \quad (6.11)$$

The DC breaker of each tie exhibits a reliability value as shown in Table 6.2 for component R_{DCB} . The second of the considered networks, the NASA Hybrid network with the added bus ties is shown in Figure 6.15.

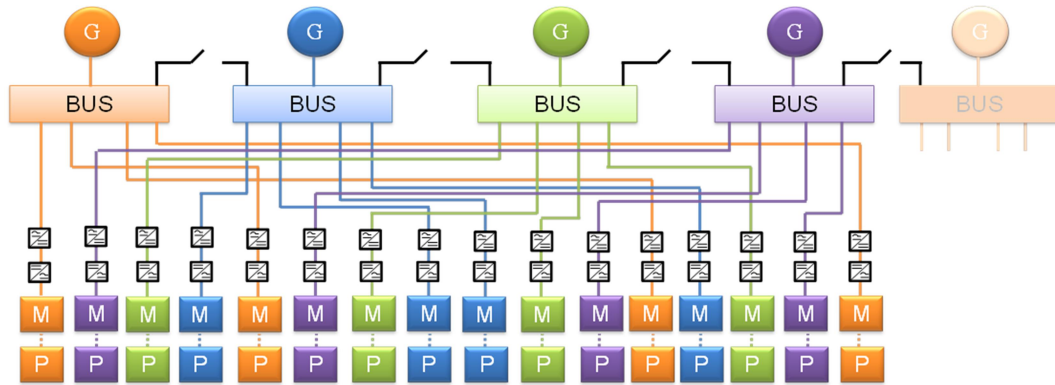


Figure 6.15 NASA Hybrid network with bus tie redundancy

For this network it can be seen that the bus ties exist in the AC side of the network and as such the ties will consist of an AC breaker. Removing the bus term from equation 6.4 provides a new equation for the GSC:

$$R_{GSC} = R_G R_F R_{CAC} \quad (6.12)$$

Equation 6.12 now contains only the first four terms of equation 6.4 and is otherwise unchanged apart from the removal of the bus term.

$$R_{BT} = R_B R_{3PH} \quad (6.13)$$

As mentioned, the bus ties exist in the AC section of the network and as such the AC breaker will take the reliability value defined in Table 6.2. As in the baseline studies, the Rolls-Royce and Airbus network is analysed twice – once as the network was intended and again with the additional analysis to provide a comparison with the other two networks. The bus tie in conjunction with the baseline two SS network is shown in Figure 6.16.

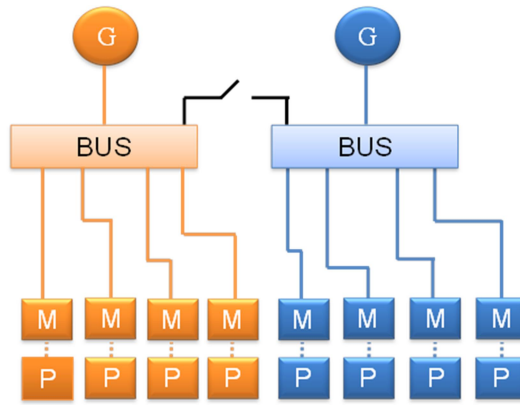


Figure 6.16 Rolls-Royce and Airbus two SS TeDP network

Figure 6.16 shows how the two halves of the network may be joined through the use of a bus tie. This is the concept which was presented in [23], however for the purposes of fair comparison is analysed next to the other two networks when considering added bus tie redundancy. When extrapolated as in the baseline considerations, the network is shown in Figure 6.17.

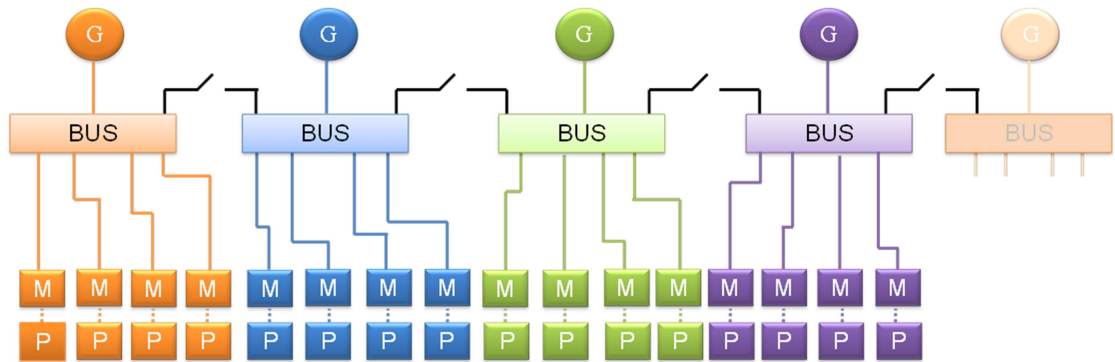


Figure 6.17 Rolls-Royce and Airbus TeDP network extended to 4 SS

As can be seen in Figure 6.17, when the network is extrapolated to include four buses it can also accommodate up to four bus ties. Removing the bus term from equation 6.7 to incorporate the use of bus ties yields:

$$R_{GSC} = R_G R_F R_{3PHB} R_{CAC} \quad (6.14)$$

The bus ties, similar to the NASA Hybris Network, connect on the AC side and therefore the reliability for the bus tie in this network is considered as the reliability of the AC breaker or R_{3PHB} component:

$$R_{BT} = R_B R_{3PHB} \quad (6.15)$$

Once equations 6.10 to 6.15 have been derived, analysis of each of the three networks using the component reliability values presented in Table 6.2 yields the values presented within Table 6.12.

Table 6.12 Network reliability when using bus tie redundancy

Network	Reliability	Baseline Reliability	Improvement Factor
N3-X	0.01419036	2.18562×10^{-5}	649.260
NASA Hybrid	0.318810	0.015894	20.059
Rolls-Royce Airbus 2 SS	0.411041	0.109465	3.755
Rolls-Royce Airbus 4 SS	0.345753	0.011983	28.854

Table 6.12 shows the probability of successful supply of power from at least 50 % of the connected network MFs. Table 6.12 shows that through using four bus ties within the network to link the SS, the exhibited reliability can be grossly enhanced from the baseline values. The network which sees the greatest improvement over the baseline network is the N3-X where the reliability has improved by 649.26 times. Conversely, the network that sees the smallest increase in reliability is the 2 SS Airbus and Rolls-Royce network however of the 4 SS networks the smallest increase in reliability is attributed to the NASA hybrid network with only a 20.06 times improvement. Unlike the results presented within the baseline studies, the network which can provide at least 50 % of the installed power with the greatest reliability is now the Rolls-Royce and Airbus network which exhibits a reliability of 0.345753 and is 1.08 times greater than the next most reliable network, the NASA hybrid network. While the 2 SS Rolls-Royce and Airbus network is on face the most reliable of the networks, this is only supplying half the power of the other three. As the initial reliability of the bus tie was large the overall increase in network reliability was high; selecting a lower initial reliability value for the bus tie would reduce the benefits of this redundancy method proportional to the decrease in initial reliability.

6.3.1 Conclusions From Bus Tie Study

From this study it can be seen that the reliability of all networks significantly increases through the use of bus ties. This redundancy method provides the greatest increase of reliability to the N3-X network where the new reliability is 649026 times larger than that of the baseline. Conversely, the network where this redundancy method has the least impact is in the original Rolls-Royce and Airbus network where reliability is only increased by a still welcome 3.755 times. Although the reliability of the N3-X network is increased the most, the overall reliability is still 0.041042 times that of the Rolls-Royce and Airbus network and only 0.04451 times that of the Hybrid network. This information was then synthesised to create the T-R graph shown in Figure 6.18.

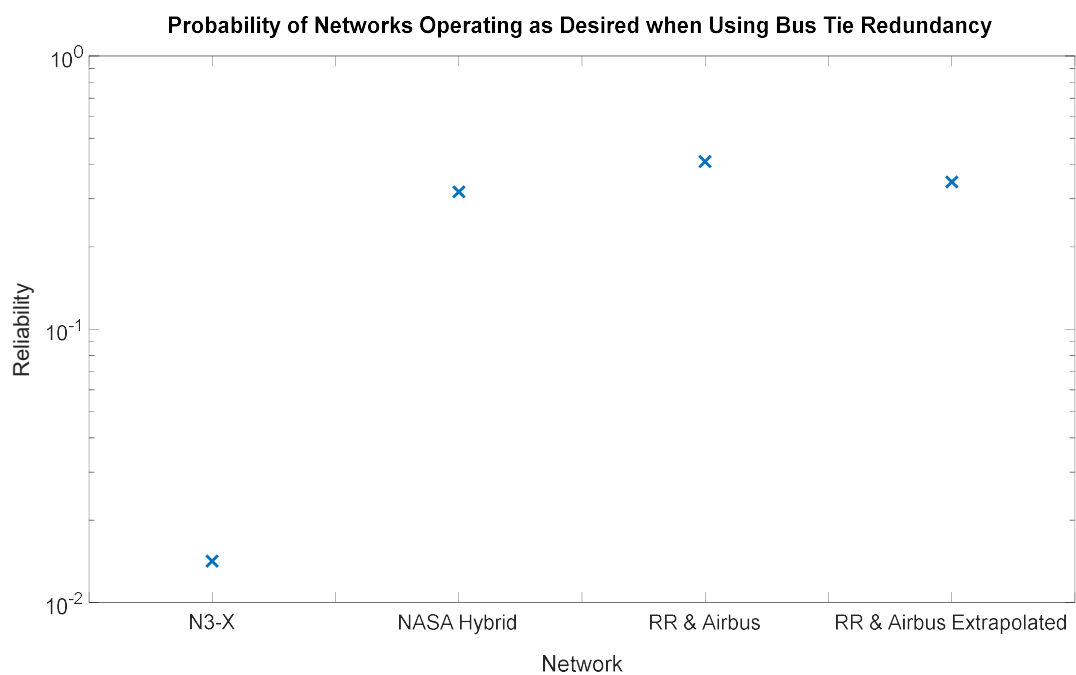


Figure 6.18 T-R graph of three Analysed networks using additional Bus Ties

The graph of Figure 6.18 shows like as before, the reliability of the N3-X architecture is significantly lower than in the other cases. Out of the three 4 parallel SS networks, the Rolls-Royce and airbus network can now achieve a greater reliability than the Hybrid network when supplying at least 50 % of the installed

power and that all of the networks can now supply this level of power at a much improved reliability.

6.4 Case Study 3: Using Parallel Redundant Feeders to Enhance Network Reliability

In addition to using bus ties to increase network reliability, redundant parallel feeders may also be used. The additional feeders make use of the existing generation capabilities within the network, enabling faulted areas to be isolated and power to be rerouted around these areas and delivered to un-faulted areas without the need for additional heavy generators or motors. This network redundancy method does not introduce additional power electronic devices and as such keeps additional weight penalties to a minimum; isolators and breakers introduce the biggest weight penalties. Superconducting tapes are likely to be thin and lightweight and hence are not expected to make a significant increase to the overall weight of the aircraft.

The case studies in this section build upon the baseline networks as before and take three separate parts: the first will examine the effect to network reliability of adding in parallel feeders in the MF section (MFP). The second case will determine what effect the addition of parallel GSCs (GSCP) has to the network and the final study will determine the effect to reliability of adding both sets of parallel feeders at once. In this study, each propulsion bus is directly connected to each of the motors and propulsors, resulting in a total of 64 parallel feeders in the MF section alone. The network of Figure 6.19 for example only shows two connections from each of the bus ports, mainly for schematic clarity; however there will be four connections from each port in the case study analysis, totalling 64 connections for the 4 busses. While these additional interconnections help to increase the reliability of the individual networks, they also increase the network complexity, potentially resulting in undesirable effects, especially for network fault detection and isolation.

In order to conduct the study, the equations for the GSC and MF are altered from those presented in Case Study 1 for the baseline networks. An additional bus term is

added to the MF equation section to allow for de-multiplexed connections from multiple parallel connected feeders, MFP. This is done in the same manner as in [49]. The original MF term is replaced with two new terms, MF1 and MFP. The MF1 term contains those components which do not form a parallel feeder (such as the motor) and the MFP term which represents the de-multiplexed connections from all the other busses, consisting of a number of cables and breakers.

Similarly for the GSC section of the networks, the GSC equation is split into two parts: GSC1, the section which is not multiplexed into redundant feeders and the GSCP section, constituting the redundant parallel feeders. As with the MF and MFP the GSCP is connected to the GSC1 through a connection bus which is included within the GSC1 equation.

This study will examine the ability of each of the networks to provide at least 50 % of total installed electrical power with the relevant parallel feeders in place. In this case that requires all GSC1 to be operational as well as at least 8-out-of-16 installed MF1. Additionally to this at least 1-out-of-4 of the GSCP and MFP must be operational for the network to satisfactorily supply the 50 % of installed thrust. This study could alternatively be conducted in the same manner however considering the case for only 2-out-of-4 operational GSC1 supplying the minimum required 50 % power to a subset of connected MF1.

This section will conclude with a roundup of results including a T-R graph where the reliability of the architectures after the addition of the parallel feeders will be compared between networks.

6.4.1 Using MFP to Increase the Baseline Network Reliability

The first of the considered cases analyses network reliability when a combination of MFP and MF1 are connected within the original MF section. In the case of the N3-X the parallel feeders are added between the bus and the DC to AC motor drive; the network diagram of Figure 6.19 shows how these connections may be made.

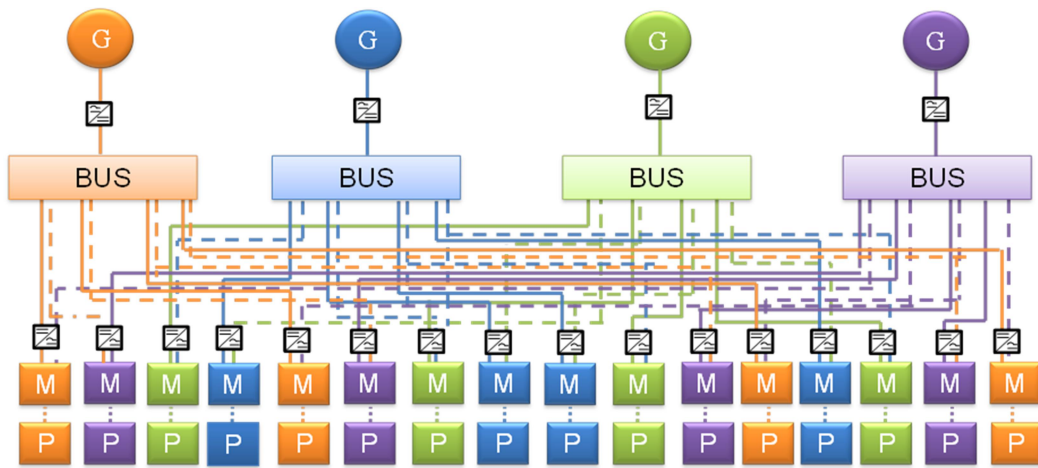


Figure 6.19 N3-X Using redundant parallel feeders in MF section to increase reliability

Figure 6.19 is a simplified network diagram showing the principle of how the MFP may be connected to the network to improve reliability. The diagram shows the original connection as in the baseline study (solid line) and additional connections to a second set of motors through the system of parallel feeders (dotted lines), the diagram also shows how the network complexity quickly builds up as the number of parallel feeders increases. The summarised diagram only shows 2 connections per bus port connecting to the MF1 however each port can have a maximum of four such connections. Using the data provided in Table 6.2 the equation for the N3-X parallel feeder section can be defined as:

$$\bar{R}_{MFP}^n = R_{DCB}^2 \cdot R_{CDC} \quad (6.16)$$

Where n is indicative of the number of parallel feeders from the available SS and in this case $n=4$. Each of the parallel feeders is then connected to the motor through a second bus [49] and a number of components (MF1) which do not form part of the parallel connection. This section of the network can be described by:

$$R_{MF} = R_B \cdot R_{ACD} \cdot R_{3PHB} \cdot R_M \cdot R_P \quad (6.17)$$

These two equations can then be resolved (multiplied) together in the same manner as was used within section 6.1.1 for the baseline N3-X study to determine the reliability of a 4 SS network providing 50 % of installed power.

Similarly for the NASA Hybrid Network the equations are based on the principles of the connections used in the summarised network diagram of Figure 6.20.

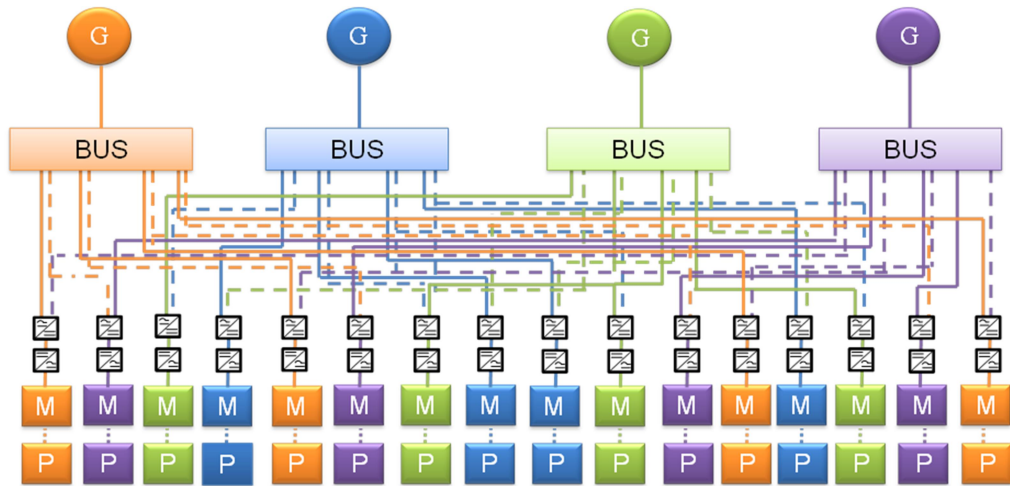


Figure 6.20 NASA Hybrid network using only parallel MF feeders to increase reliability

It can be seen from Figure 6.20 that the MFP sections begin at the bus and are then joined to the MF1 section at the DC/AC convertor. The new equation for the MFP section therefore becomes:

$$\bar{R}_{MFP}^n = R_{CAC} \quad (6.18)$$

Where again $n=4$. The new equation for the network MF1 section includes a bus to allow the de-multiplexed connection of the parallel feeders and becomes:

$$R_{MF1} = R_B \cdot R_{CON} \cdot R_{ACD} \cdot R_M \cdot R_P \quad (6.19)$$

Finally, the network diagram for the extrapolated four SS Rolls-Royce and Airbus Network is presented in Figure 6.21:

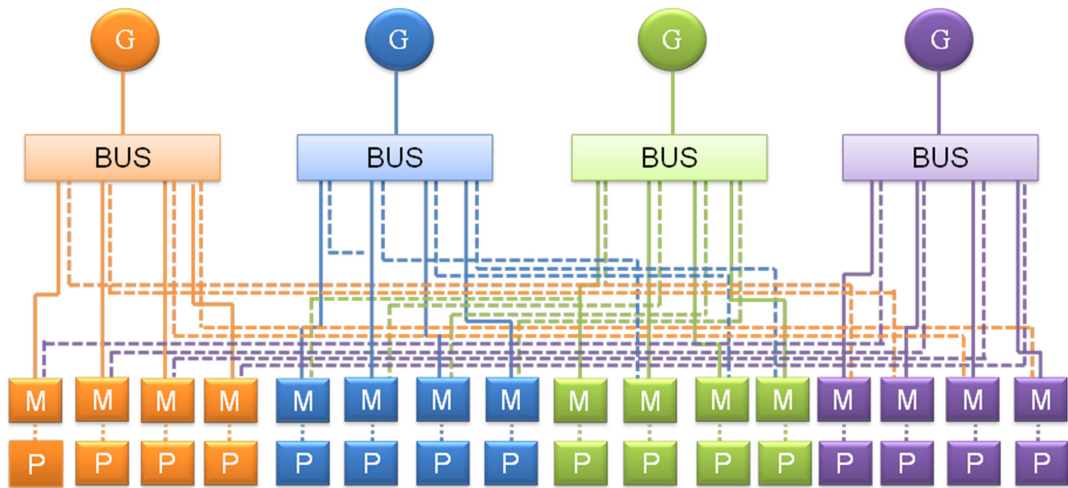


Figure 6.21 Rolls - Royce and Airbus network using additional parallel MF to increase reliability

Again the diagram only shows two out of the total four parallel feeders which are considered in this study. As this network has no power electronics sections, the parallel aspect of the feeder only consists of an AC cable and breaker. The new equation for the parallel MFP becomes:

$$\bar{R}_{MFP}^n = R_{CAC} \cdot R_{3PHB} \quad (6.20)$$

And the MF1 equation becomes:

$$R_{MF} = R_B \cdot R_M \cdot R_P \quad (6.21)$$

Through substitution of $n=4$ and the values presented in Table 6.2 into equations 6.16 to 6.21 and resolving each of the equations using a four SS network with 16 MF1 (where $k \geq 8$) and each MF1 has 4 associated MFP Table 6.13 is produced for the provision of at least 50 % installed power. In the case of the original two SS Rolls-Royce and Airbus network, there are only eight MF1 sections and each has only two MFP of which $k \geq 1$ to supply at least 50 % installed power. Table 6.13 is shown below.

Table 6.13 Network reliability when using four parallel MFP per MF1 and supplying at least 50 % power

Network	Reliability for 4 MFP per SS	Baseline Reliability (50 % Power)	Improvement Factor
N3-X	0.000170	2.18562×10^{-5}	7.778
NASA Hybrid	0.020855	0.015894	1.312
Rolls-Royce and Airbus 2 SS	0.150861	0.109465	1.378
Rolls Royce and Airbus 4 SS	0.026025	0.011983	2.172

Table 6.13 shows that the biggest increase to reliability is exhibited within the N3-X network is 7.778 times greater than in the baseline study. It is also apparent that as before the NASA Hybrid Network is least affected in terms of reliability by the inclusion of parallel feeders. The increase in reliability over the baseline for this network is 1.312 times. Finally, the table also shows that the most reliable of the three four SS networks is once again the Rolls-Royce and Airbus network where the reliability is 2.172 times greater than the baseline and 1.248 times greater than the next most reliable network, the NASA Hybrid network.

Not only may parallel feeders be added in the MF side of the network, they may also be added within the GSC side of the network as well. This analysis is shown in section 6.4.2.

6.4.2 Redundant Feeders in the GSC side of the Network

Again the same analysis can be undertaken within the generator side of the network. In the case of the N3-X network the parallel feeders are added in after the AC/DC convertor and extend to the bus as shown in Figure 6.22.

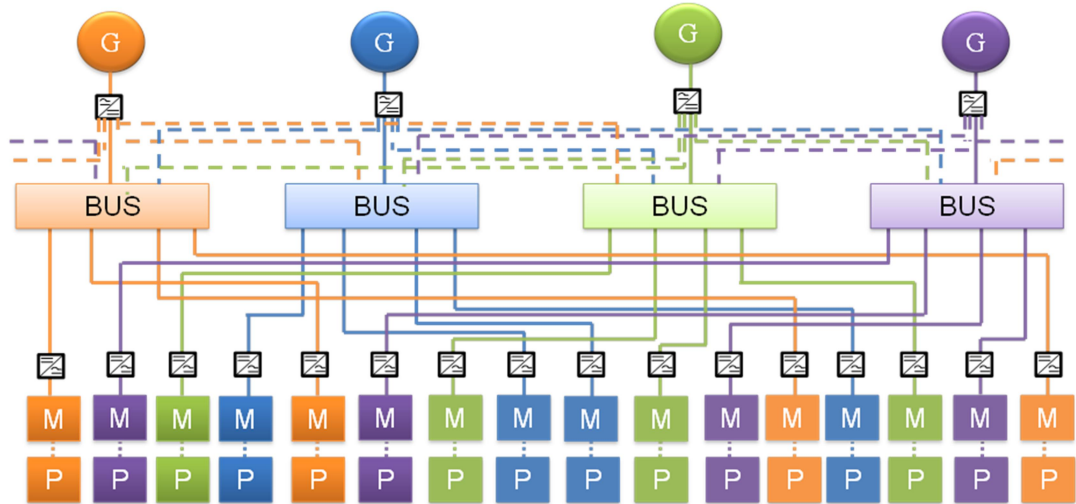


Figure 6.22 N3-X network utilising additional parallel GSCP to enhance reliability

Figure 6.22 shows how the GSCP sections are added in to the network and how each bus is linked to each generator and GSC1 section. It can also be seen that when the maximum number of these connections are made there are only $\frac{1}{4}$ of the number of additional MFP connections which could be made resulting in a lesser penalty in terms of network complexity. The GSCP equation can be expressed as:

$$\bar{R}_{GSCP}^n = R_{SFCL} R_{DCB}^2 R_{CDC} \quad (6.22)$$

And the new GSC1 can be expressed as:

$$R_{GSC1} = R_G R_F R_{3PHB}^2 R_{CAC} R_{SFCL} R_{CON} R_B^2 \quad (6.23)$$

The same analysis can be undertaken on the NASA Hybrid network where the parallel feeders are added at the connection to the generator and EEC unit as shown in Figure 6.23.

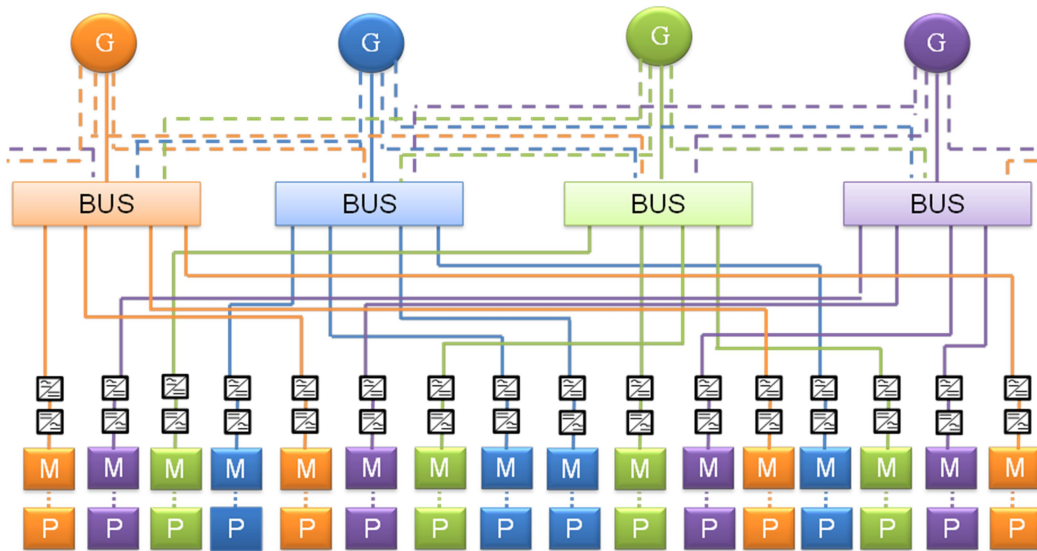


Figure 6.23 NASA Hybrid network using GSCP for enhanced reliability

Figure 6.23 shows how a three phase connection is made from the generator to the three phase network bus. This results in a GSCP term which is inclusive of only a three phase cable. The GSCP equation can therefore be stated as:

$$\bar{R}_{GSCP}^n = R_{CAC} \quad (6.24)$$

As in the MFP study, n is equal to the number of parallel feeders in each SS and in this case $n=4$. The new GSC1 can be expressed as:

$$R_{GSC1} = R_G R_F R_B^2 \quad (6.25)$$

Finally the Rolls – Royce and Airbus network may be redrawn as shown in Figure 6.24:

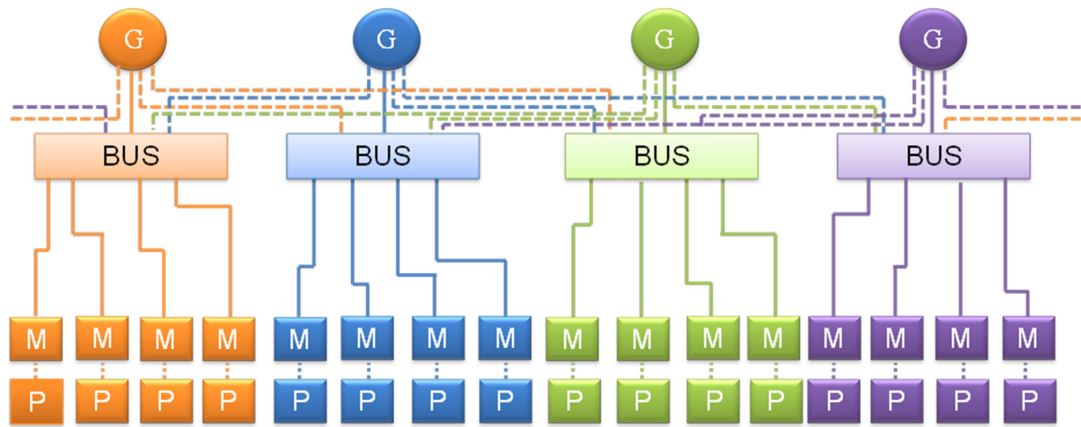


Figure 6.24 Rolls - Royce and Airbus network utilising redundant parallel GSCP

In this case the GSCP are added like in the NASA Hybrid network only with the addition of a three phase breaker. The GSCP equation can be shown to be:

$$\bar{R}_{GSC}^n = R_{DCB}R_{CAC} \quad (6.26)$$

As this network will be analysed twice – once for the original network of [23] and again for the extrapolated network, n will take on two values: for the two SS network $n=2$ and for the four SS network $n=4$. The equation for GSC1 can be expressed as:

$$R_{GSC1} = R_G R_F R_B^2 \quad (6.27)$$

Undertaking analysis for a four SS network utilising four GSCP per SS and where for the GSCP section $k \geq 1$ must be operational and using the original MF equations from the baseline networks yields Table 6.14. Through substitution of $n=4$ and the values presented in Table 6.2 into equations 6.22 to 6.27 and resolving each of the equations using a 4 SS network with 16 MF (where $k \geq 8$) and each GSC1 has 4 associated GSCP Table 6.14 is produced for the provision of at least 50 % installed power. In the case of the original two SS Rolls-Royce and Airbus network, there are only eight GSC1 sections and each has only two GSCP of which $k \geq 1$ to supply at least 50 % installed power. Table 6.14 is shown below.

Table 6.14 Network reliability using 4 parallel GSCP sections

Network	Reliability Using 4 Redundant GSCP	Baseline Reliability (50 % Power)	Improvement Ratio
N3-X	0.000123	2.18562×10^{-5}	5.628
NASA Hybrid	0.020461	0.015894	1.287
Rolls-Royce and Airbus 2 SS	0.167966	0.109465	1.534
Rolls-Royce and Airbus 4 SS	0.036939	0.011983	3.083

The results of Table 6.14 show both the reliability achievable for each network through using parallel GSCP sections as well as the associated baseline value for that network in order to meet 50 % power requirements. For clarity an additional column is added to the table showing the improvement to reliability over the baseline value. From the resultant values it can be seen that the biggest increase in reliability still occurs in the N3-X network where the reliability with the GSCP sections is now 5.627 times greater than the baseline. Similarly the network which is least effected by the addition of GSCP is again the NASA Hybrid network where the reliability is only 1.287 times greater than the baseline value. The table also shows that the most reliable of the three 4 SS networks is once again the Rolls-Royce and Airbus network where the reliability is 1.81 times greater than the next most reliable, the NASA Hybrid network.

As a result of the way each of the networks are constructed, both the N3-X and the NASA Hybrid network have a greater increase in reliability when using only MFP sections compared to the reliability using the GSCP sections 0.7247 and 0.9811 times that of the MFP analysis respectively. The Rolls-Royce and Airbus configuration however experiences a greater increase to reliability when only using

GSCP sections with an increase of 1.11 times for the 4 SS network. In order to determine the advantages of using both parallel MFP and GSCP sections within the network, the analysis of sections 6.4.1 and 6.4.2 is repeated within a single network and is shown in 6.4.3.

6.4.3 Parallel Feeders Case Study Using both GSCP and MFP

This part of the study uses the equations as derived within the first two sections of this case study (6.4.1 and 6.4.2) however considers the use of both of the additional redundant pathways within the same network.

The network diagram for the N3-X network using both sets of parallel feeders is shown in Figure 6.25.

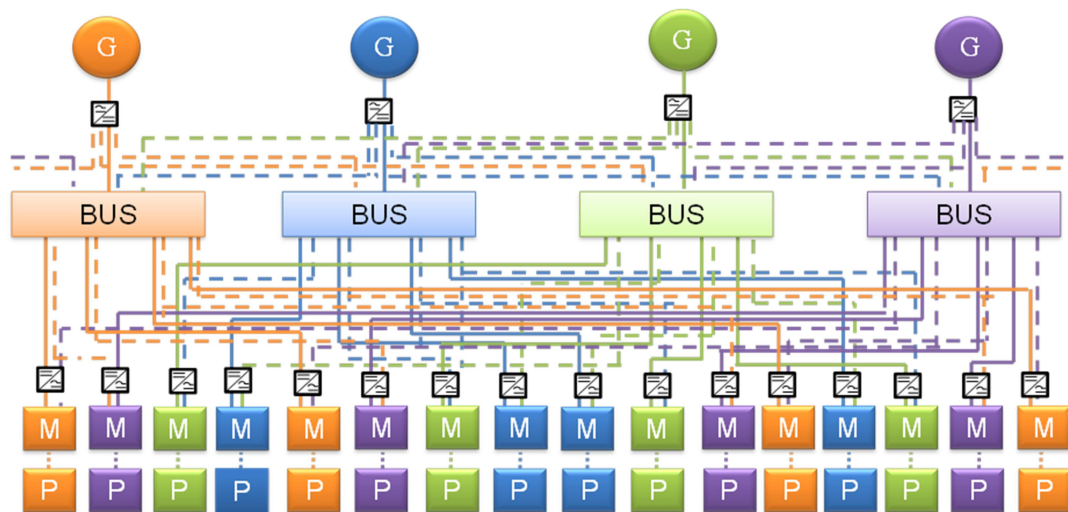


Figure 6.25 N3-X network utilising both parallel GSCP and MFP

Figure 6.25 is used in conjunction with equations 6.16 and 6.17 for the MF1 and MFP as well as equations 6.22 and 6.23 for the GSCP and GSC1. Again for this analysis: n in both cases is set to equal four. The network diagram for the NASA Hybrid network using the same parallel feeders is shown in Figure 6.26:

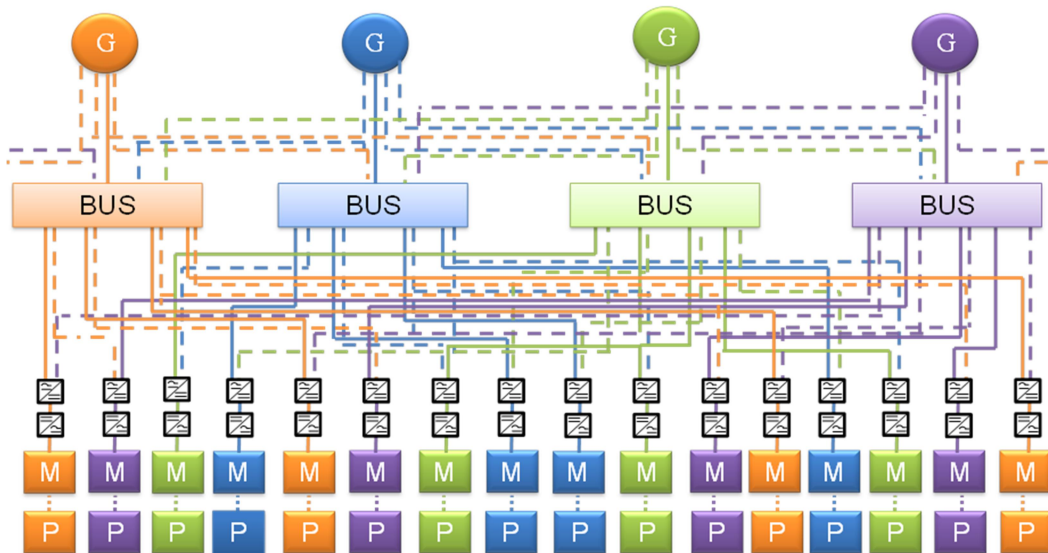


Figure 6.26 NASA Hybrid network using both MFP and GSCP redundant sections

Equations 6.18 and 6.19 for the MFP and MF1 as well as 6.24 and 6.25 for the GSCP and GSC1 are used in conjunction with Figure 6.26 with a value for n of 4. The Rolls-Royce and Airbus network is shown in Figure 6.27.

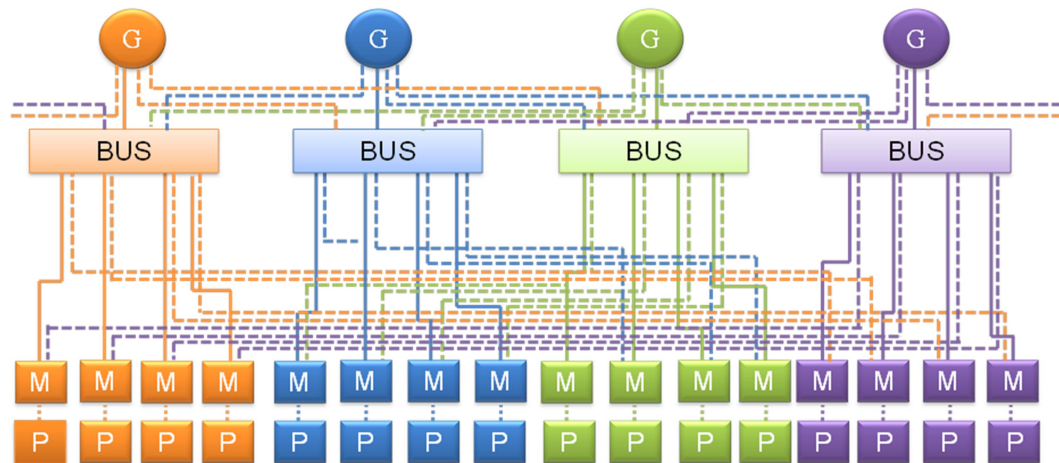


Figure 6.27 Rolls-Royce and Airbus Network Using both MFP and GSCP

Finally Figure 6.27 was used in conjunction with equations 6.20 and 6.21 for the MFP and MF1 as well as 6.26 and 6.27 for the GSCP and GSC1. Again for this analysis $n=4$. This study is undertaken for the networks as in the two previous sections: for the four SS networks each exhibiting four MFP and four GSC per corresponding MF1 and GSC1 within each SS. The results of this study are shown in Table 6.15.

Table 6.15 Network reliability when using both 4 GSCP and 4 MFP

Network	Reliability Using GSCP and MFP	Baseline Reliability (50 % Power)	Improvement Ratio
N3-X	0.00096	2.18562×10^{-5}	43.923
NASA Hybrid	0.026847	0.015894	1.689
Rolls-Royce and Airbus 2 SS	0.227903	0.109465	2.082
Rolls-Royce and Airbus 4 SS	0.080229	0.011983	6.695

The results of Table 6.15 show both the reliability achievable for each network through using parallel GSCP and MFP sections as well as the associated baseline value for that network. The table also provides the ratio of the associated increase. From the resultant values it can be seen that the biggest increase in reliability still occurs in the N3-X network where the reliability with both parallel feeder types is now 43.92 times greater than the baseline, approximately the product of the individual gains in reliability. Similarly the network reliability which is least effected by the addition of both sets of parallel feeders is again the NASA Hybrid network where the reliability is only 1.689 times greater than the baseline value. The table also shows that the most reliable of the three four SS networks is once again the Rolls-Royce and Airbus network where the reliability is 2.988 times greater than the next most reliable, the NASA Hybrid network for this study.

6.4.4 Summary of the Parallel Redundant Feeders Case Study

From this study it can be seen that the reliability of all networks is increased through using parallel feeders with gains enhanced through using both feeder types to achieve an even greater reliability value for each network. These studies have shown that the parallel feeder type that affects the reliability of the network most is different between the networks: for the N3-X and the NASA Hybrid network, the MFP implementation is the most successful at enhancing reliability and for the Rolls-Royce networks the GSCP approach is the most effective.

This redundancy method again provides the greatest increase of reliability to the N3-X network where the new reliability is 43.92 times larger than that of the baseline. Conversely, the network where this redundancy method has the least impact is in the NASA Hybrid network where reliability has only increased by 1.689 times. Although the reliability of the N3-X network is increased the most, the overall reliability when using both sets of feeders is still only 0.03576 times that of the Rolls-Royce and Airbus network and only 0.011966 times that of the Hybrid network. This information is used to create the T-R graph shown in Figure 6.28.

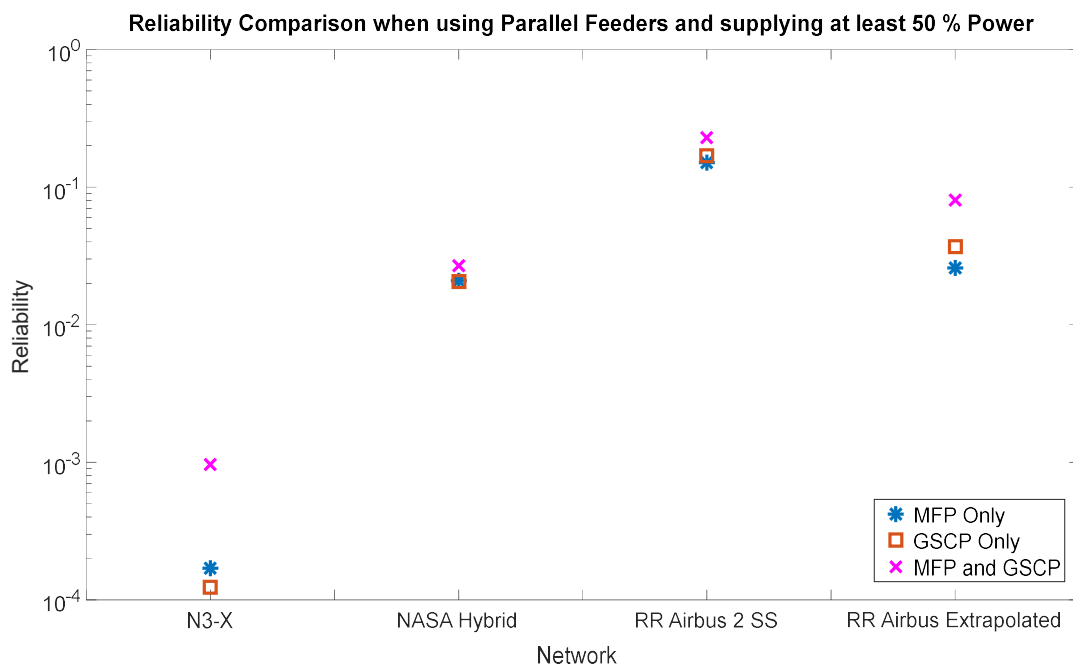


Figure 6.28 T-R graph for parallel feeders studies

The graph of Figure 6.28 shows like as before, the reliability of the N3-X architecture is significantly lower than in the other cases. Out of the three 4 parallel SS networks, the Rolls-Royce and airbus network can now achieve a significantly greater reliability than the Hybrid network when supplying at least 50 % of the installed power and that all of the networks can now supply this level of power at a much improved reliability. The T-R graph also verifies that significant reliability enhancements can be made through using a combination of both types of parallel feeder within the same network.

6.5 Summary of Added Redundancy Case Study Findings

Through undertaking a number of Case Studies the following observations can be made about the three considered networks, the N3-X, NASA AC/DC Hybrid and the Rolls-Royce and Airbus Network as well as the redundancy methods employed to enhance network reliability. Of the three considered networks, the N3-X has the lowest observed reliability score at both the baseline and in every additional redundancy configuration due to the greatest number of components which combine to create the network. In terms of baseline network reliability when operating with all installed components functioning as desired, the extrapolated 4 SS Rolls- Royce and Airbus network performs with the greatest level of observed reliability, 4.47 times greater than the NASA Hybrid network and 2.1×10^5 times greater than the N3-X. Conversely, when considering the networks ability to provide at least 50 % of the installed power, the NASA Hybrid network performs the best exhibiting a reliability 1.34 times greater than the Rolls-Royce and Airbus network and 727.21 times greater than the N3-X architecture.

When considering the added redundancy methods, the method which affords the greatest level of reliability when the operating constraint is to provide at least 50 % of installed power is the bus tie method. This is shown in the T-R graph of **Error! Reference source not found.** which shows all the redundancy methods considered within Case Studies 1, 2 and 3. Additionally, the network with the largest percentage increase from baseline 50 % provision of power case is the N3-X. This observation

holds true for all considered redundancy methods. When considering the parallel feeder redundancy, the N3-X and NASA Hybrid networks both have a greater increase to reliability when operating using the MFP sections; the Rolls-Royce and Airbus variant performs better using the GSCP and is the most reliable of all the networks considered in these parallel feeder case studies.

A comparison of all the results from case studies examining the ability of all considered networks to provide at least 50 % installed thrust is presented in the T-R graph of Figure 6.29 below. This graph compares network operation of the Baseline configuration as well as when operating with bus ties, MFP, GSCP and finally when using both MFP and GSCP.

Comparison of network baseline reliability and reliability when using the different presented redundancy measures

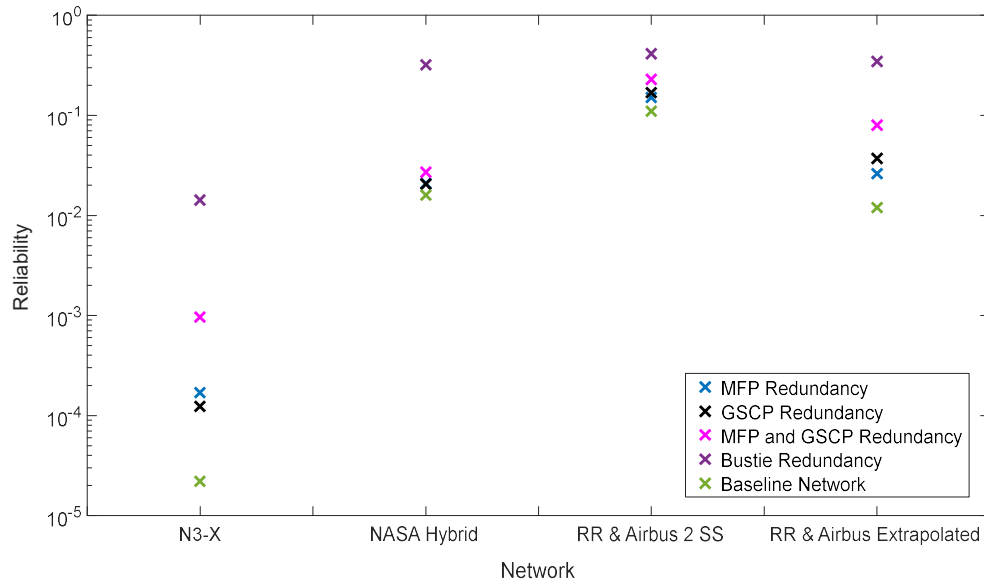


Figure 6.29 Comparison of redundancy methods when supplying at least 50 % of installed power

Figure 6.29 shows the reliability performance for all the four SS networks as well as the 2 SS Rolls – Royce and Airbus network. The T-R graph shows that in all cases the bus tie redundancy method clearly increases reliability more than any parallel feeder method. It also shows that in the case of the NASA Hybrid network all parallel feeder methods afford a similar level of increase to reliability from the baseline which in turn does not provide a significant increase over the baseline network. It should be seriously considered if increases to network reliability when using this redundancy method outweigh the significant weight penalties incurred.

6.6 Case Study 4: Investigating the Effects to Reliability of a Common Protection System

The reliability analysis conducted within sections 6.1 to 6.5 showed that the N3-X network results were systematically the least reliable of the three networks, due in part to the large number of additional components over the other two architectures. Using the baseline results and comparing to the far more reliable performance of the joint Rolls-Royce and Airbus network and the NASA Hybrid network, one of the key differences between these network architectures lies in the approach each group has taken towards protecting against the effects of large electrical fault currents within their architecture. While the Rolls-Royce and Airbus network uses isolators, the N3-X uses both isolators and SCFCL's yet in the hybrid network there is no dedicated protection system. All networks however use self-quenching properties, i.e. the cable resistance dramatically increases if the cable current surpasses a critical level and thereby is a self-current limit of the superconducting cables to provide a level of power system protection. The significance in the differing protection methodologies lies in the number of additional components and hence reduction in overall network reliability which the more complex system used by the N3-X affords. Should the single isolation method used in conjunction with the cable quenching properties prove sufficient for the N3-X network, the reliability of the architecture will be significantly increased. Repeating the analysis of the baseline studies using a common approach to the protection system of all networks provides a valuable study to both industry and to further enhance the knowledge of the performance of each network under a more controlled set of operating criteria.

This case study investigates the reliability of the three TeDP networks when using a single, common approach to electrical fault current protection. This study proposes the use of the isolator and breaker method proposed by the Rolls-Royce and Airbus network architecture as well as making use of the superconducting cable quenching properties of all networks as before. This protection network method removes the SCFCL components introduced within the N3-X network as well as a number of

cables and breakers linking the fault current limiters and adds additional components to the NASA Hybrid Network where no dedicated protection system previously existed. New network diagrams are constructed for the three networks, shown in Figure 6.30 illustrating one interpretation of how the N3-X and NASA Hybrid networks may be redrawn when considering a single common protection system using a network of breakers and isolators.

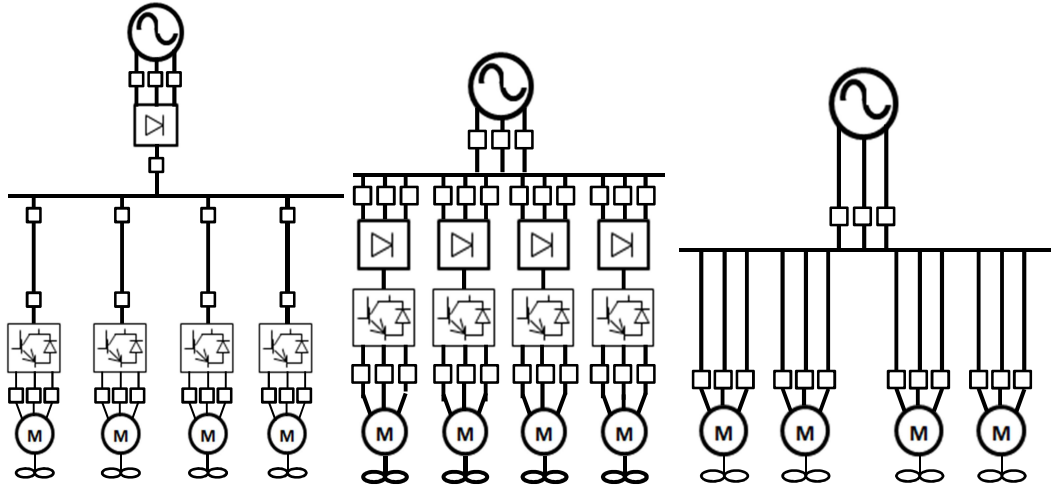


Figure 6.30 N3-X (left), NASA Hybrid network (centre) and Rolls-Royce and Airbus network (right) architectures using a common protection scheme

To enable consistency between the networks, the second of two DC breakers is removed from the GSC in the N3-X network as is the second set of AC breakers and the DC cable in the same section of this network as these components become surplus to requirement in the new architecture configuration. The NASA Hybrid Network is also altered from the original baseline configuration. A set of AC breakers are placed within each GSC as well as two sets of AC breakers within each of the MF sections. The Rolls-Royce and Airbus network remains unaltered from the baseline configuration.

Based upon the architecture defined within Figure 6.30 for the N3-X, the new GSC equation becomes:

$$R_{GSC} = R_G R_F R_{3PHB} R_{CON} R_{DCB} R_{CDC} R_B \quad (6.28)$$

While the new equation for the MF becomes

$$R_{MF} = R_{DCB}^2 R_{CDC} R_{ACD} R_{3PHB} R_M R_P \quad (6.29)$$

Meanwhile the GSC for the NASA Hybrid is

$$R_{GSC} = R_G R_F R_{CAC} R_{3PHB}^2 R_B \quad (6.30)$$

and its corresponding MF becomes

$$R_{MF} = R_{CAC} R_{CON} R_{ACD} R_{3PHB}^2 R_M R_P . \quad (6.31)$$

The corresponding equations for the joint Rolls-Royce and Airbus network however remain unchanged.

Undertaking analysis on a 4 SS network with a total of 4 GSC and 16 MF per network while providing at least 50 % installed power yields the results of Table 6.16.

Table 6.16 Network reliability when using a common protection system configuration

Network	Reliability Using Common Protection Network	Baseline Reliability (50 % Power)	Improvement Ratio
N3-X	0.000207	2.18562×10^{-5}	9.4886
NASA Hybrid	0.000191	0.015894	0.012022
Rolls-Royce and Airbus 2 SS	0.109465	0.109465	-
Rolls-Royce and Airbus 4 SS	0.011983	0.011983	-

Table 6.16 shows that through the removal of a number of additional components to rearrange the baseline architecture into the format stipulated by this case study, the N3-X network now exhibits a reliability score far greater than previously achievable. The improvement factor shown in Table 6.16 shows that the new score of 0.000207

is 9.4886 times greater than that of the baseline configuration. The reliability score is now not the lowest of the 4 SS networks and is now more reliable than the NASA hybrid network (when considering the corresponding alterations made to the NASA Hybrid network). This decrease in reliability of the NASA Hybrid Network is directly due to the number of additional components required to be added to ensure the correct protection network is employed. The most reliable of the three networks is still the Rolls-Royce and Airbus configuration, however this increase over the other two considered networks is now only due to the lack of power electronic components featured by the other networks to enable decoupled motor and generator shaft speeds. These components form a vital part of the network and as such cannot reasonably be considered in a separate sensitivity study. In undertaking alterations to the network architectures, the reliability score of the NASA Hybrid architecture has decreased and is now only 0.0120 that of the baseline score and only 92.14 % that of the NASA N3-X network. This suggests that when considering a common approach to fault current protection, the N3-X no longer performs as poorly in contrast to the other two networks as when operating with an additional protection network. The N3-X however still exhibits a reliability 548.3 times smaller than the Rolls-Royce and Airbus network architecture directly resulting from the additional power electronics of the N3-X network so additional engineering effort to increase the reliability of these components is required.

6.7 Case Study 5: Network Reliability Sensitivity to changes in Component Reliability

In addition to showing the benefits to network reliability from additional parallel feeders (Case Study 6.4) and bus ties (Case Study 6.3) the k -out-of- n T-R profiling method can also facilitate a sensitivity analysis around the individual components to be conducted. Thus, by varying the reliability of individual components and modular sections within the network a better understanding of the interdependences between network elements can be gained. Furthermore, those network components that will require research and engineering investment to improve their reliability to acceptable

improvements within a realistic development budget can be revealed and explored. Additionally the merits of a sensitivity analysis can be extended to rule out expensive development costs on component reliability where no significant improvement in network reliability materialises; this shows itself as limiting effort in a law of diminishing returns or, conversely, setting design targets on component reliability so as to meet network reliability targets.

The case studies to be described in this section identify how known data may be handled to find the reliability of the network R_S , and then subsequently used to assess the effect of variations in the individual component values, R on network reliability. This case study will use the equations derived for each of the baseline networks in section 5.2 and will consider the ability of the network to supply at least 50 % of the installed power within the network.

This process can be realised by utilising a fixed number of MF and GSC, n_{MF} and n_{GSC} within the baseline networks, while varying the reliability of select components and hence R_{SS} . As in previous studies, the reliability of all three architectures will be analysed however only the extrapolated Rolls-Royce and Airbus network will be adopted for the sensitivity analysis. There is not a specific target value for R_S which must be attained by the architectures as it is the effect that changing individual component reliability values which is the focus of this study. For each of the architectures considered, the effect of increasing the reliability values of individual components which occur either frequently, seldom and/or in both modular sections are investigated through first implementing a 10 % then 20 % increase in each case. All the considered components for each of the three architectures are then combined in the same network in a final comparison. The sensitivity of each case is then compared within a scatter graph to show how each network responds to each change and how different starting reliability values, the modular section the component occurs in and frequency of occurrence of individual components impacts network reliability R_S . This illustrates a practical implementation of the sensitivity analysis.

6.7.1 Sensitivity Study of the N3-X Architecture

The baseline network described within Section 5.1.1 is used as the network within the N3-X study and is shown in Figure 6.31.

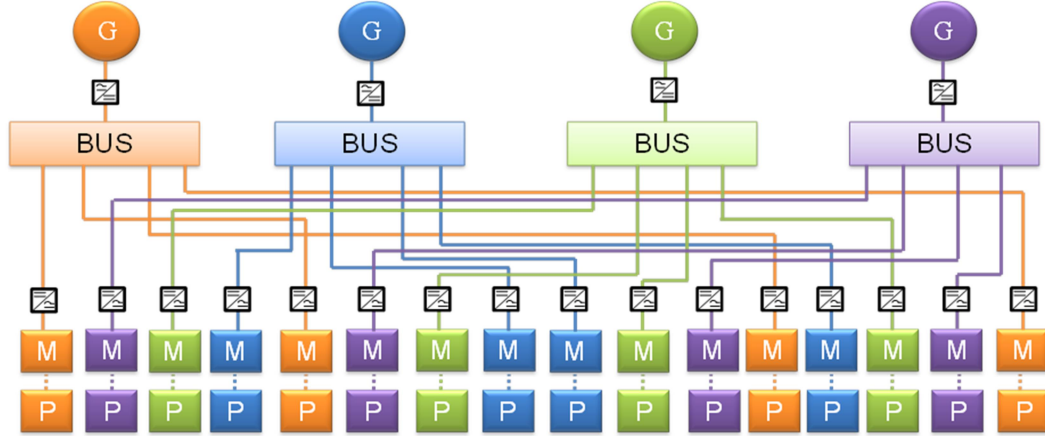


Figure 6.31 Baseline N3-X TeDP propulsion network

The study uses the baseline equations (6.1), (6.2) and (6.3) as defined in Case Study 6.1.1 (and repeated below) for the reliability of the GSC (R_{GSC}), MF (R_{MF}) and SS (R_{SS}) these equations are subsequently combined in the same manner as before to obtain R_S .

$$R_{GSC} = R_G R_F R_{3PHB}^2 R_{CAC} R_{SFCL}^2 R_{CON} R_{DCB}^2 R_{CDC} R_B. \quad (6.1)$$

$$R_{MF} = R_{DCB}^2 R_{CDC} R_{ACD} R_{3PHB} R_M R_P. \quad (6.2)$$

$$R_{SS} = R_{GSC} R_{MF}^4 \quad (6.3)$$

Based upon equations (6.1) and (6.2), three components which have varying effects on the network reliability are the Three Phase Breaker R_{3PHB} , DC Breaker R_{DCB} and the converter R_{CON} with reliability scores of 0.8, 0.84 and 0.83 respectively. This study is based on the ability of the network to supply at least 50 % of the installed propulsive power from the MF.

Through observation it can be seen that the three phase breaker and the DC breaker appear in both modular sections of the network, however the reliability score associated with the three phase breaker is significantly lower than (95 % of) that of the DC breaker. The convertor by comparison only appears in the GSC and has an

initial reliability score which is more similar to the DC breaker. All three of these component values are increased as described within section 6.6 above with the results of the increase to network reliability R_S from these changes tabulated in Table 6.17.

Table 6.17 N3-X sensitivity analysis system reliability

Component	R_S (R_{3PHB})	R_S (R_{CON})	R_S (R_{DCB})	R_S All Components
R_S Baseline	2.19×10^{-5}	2.19×10^{-5}	2.19×10^{-5}	2.19×10^{-5}
R +10 %	8.05×10^{-5}	3.2×10^{-5}	0.000135	0.000685
R +20 %	0.000259	4.532×10^{-5}	0.0005534	0.010575

The data of Table 6.17 should be read top to bottom and shows how the reliability of the network R_S is affected by the indicated increase in the individual reliability, R , of the indicated component within the network. The final column show how the reliability is affected when all noted component have been increased by first 10 % and then 20 %. The tabulated data can be displayed in the graph of Figure 6.32 to highlight the highly non-linear reaction of the network to the implemented changes.

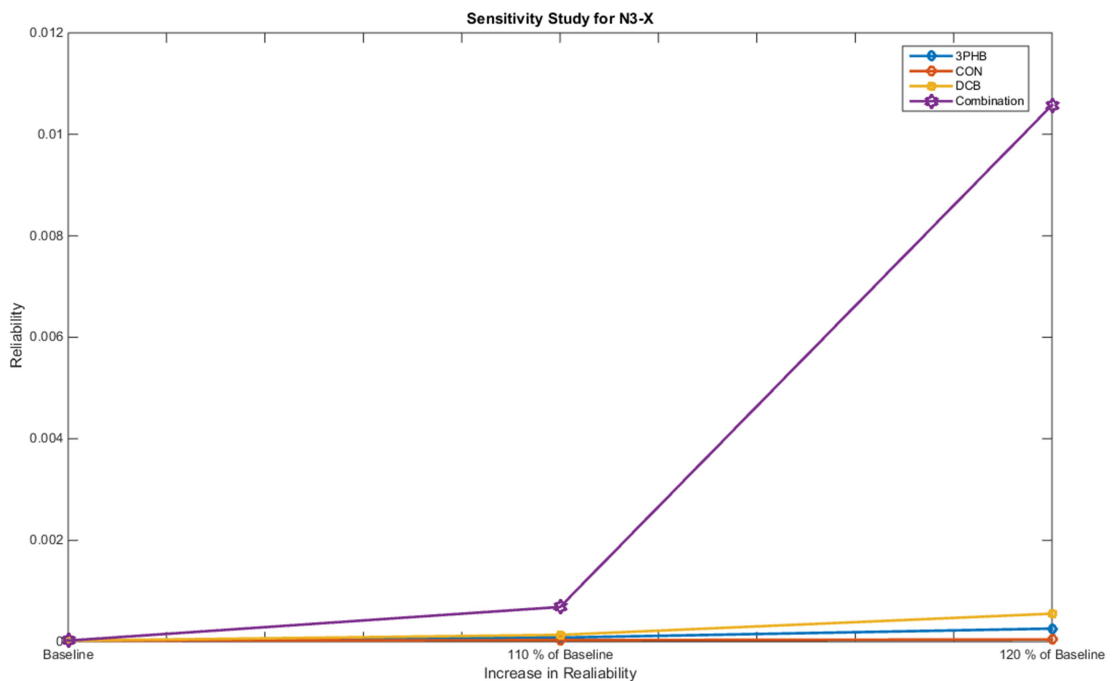


Figure 6.32 N3-X Baseline Network Sensitivity Analysis

It can be seen from Figure 6.32 that the component which provides the single biggest individual effect to the network reliability is the DC breaker – the component with the greatest individual reliability score as well as the component which occurs most frequently within the network. Conversely the converter has the lowest individual impact on the network and only occurs within the GSC however has a reliability score similar to that of the DC breaker illustrating how the location within the network has just as much significance as the individual reliability score for a component. For both the 10 % increase and 20 % increase case, when all components are combined, the compounded impact on reliability is far more significant than any individual increase in reliability for this network. As the two types of breaker appear multiple times in both the GSC and the MF the combined increase for these two components has a significant bearing in the overall increase in reliability that when combined with the new convertor value which ≈ 1 provides the marked improvement to the overall reliability score R_S .

6.7.2 Sensitivity Analysis of the Hybrid Network Architecture

Again for the Hybrid architecture the network considered is the baseline network as in section 5.1.2 and shown in Figure 5.4, the network is shown again in Figure 6.33 for clarity.

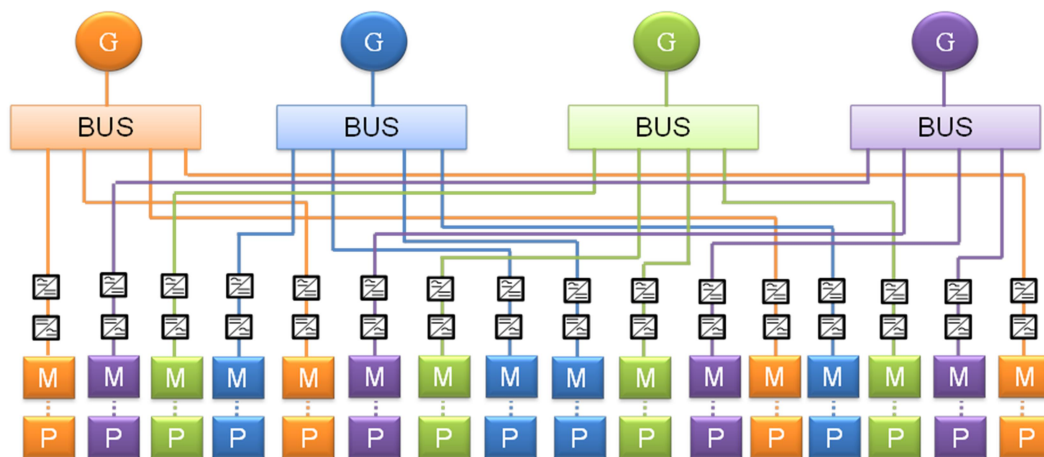


Figure 6.33 NASA Hybrid network baseline propulsion network configuration

The study uses the baseline equations (6.4), (6.5) and (6.6) as defined in Case Study 6.1.2 for the hybrid network for the R_{GSC} , R_{MF} and R_{SS} terms; these equations are subsequently combined in the same manner as in previous studies to obtain R_S (4.2).

The equations for the network are repeated for reference and clarity:

$$R_{GSC} = R_G R_F R_{CAC} R_B. \quad (6.4)$$

$$R_{MF} = R_{CAC} R_{CON} R_{ACD} R_M R_P. \quad (6.5)$$

$$R_{SS} = R_{GSC} R_{MF}^4 \quad (6.6)$$

Examination of equations (6.4), (6.5) and (6.6) shows that the three phase cable and convertor play differing roles within the network: the three phase cable occurs in both modular sections with a reliability score of 0.92 and the convertor, only occurs in the MF, exhibiting a reliability score of 0.83. As in the N3-X case the two component values are first increased by 10 % then 20 % and substituted into the relevant equations to determine R_S . In this study only two separate components are considered due to the fact a far fewer number of component types are used to construct the network. The results of this exercise are shown in Table 6.18.

Table 6.18 Hybrid network sensitivity analysis system reliability

Component	R_S (R_{CAC})	R_S (R_{CON})	R_S (All Components)
R Baseline	0.015894	0.015894	0.015894
R +10 %	0.031628	0.023768	0.045349
R+20 %	0.031628	0.032903	0.060091

Table 6.18 is read in the same manner as Table 6.17 and shows that when a component is initially assigned a higher reliability score, the gains experienced by the network when increasing the component reliability towards 1 are minimal. As a reliability score cannot increase beyond 1, the percentage increase is bounded by maximum reliability instead of the true percentage value, in this case resulting in $R_S = 0.031628$ being the maximum upper limit in the AC cable case. The results of

Table 6.18 are illustrated in Figure 6.34 showing the full extent of the sensitivity study results graphically.

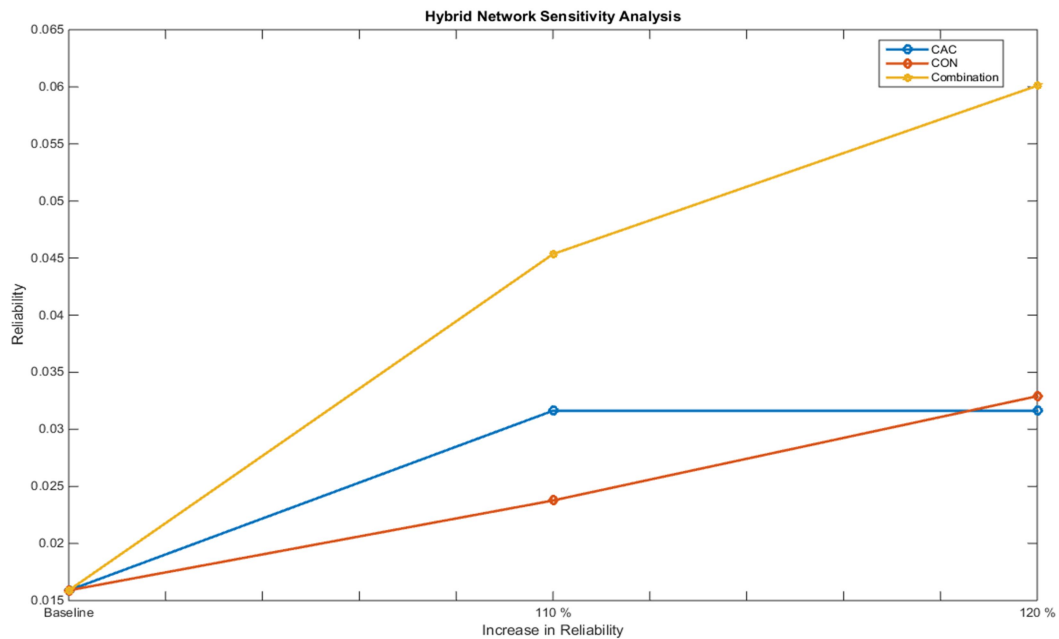


Figure 6.34 Hybrid Network Sensitivity Study

Figure 6.34 shows how the increase to the convertor reliability score in this study has the greater impact of the two components to system reliability as although it only appears in a single modular network section (the MF), this component has a lower start score and can hence be increased to the full 120 % of the baseline value. It can also be seen the network reliability increases with that of the converter reliability and as such the graph would become useful to find the point where overall network reliability gradient reduces – indicating further improvements in converter reliability are pointless on their own in improving network reliability further. The impact is also significant as the component occurs in each of the MF sections and the benefits are compounded through the significantly greater number of MF over the GSC sections.

6.7.3 Sensitivity of the Airbus and Rolls-Royce Architecture

For the final sensitivity study, the extrapolated 4 SS Rolls –Royce and Airbus network is considered. The baseline network was described within section 5.1.3 is repeated for clarity in Figure 6.35.

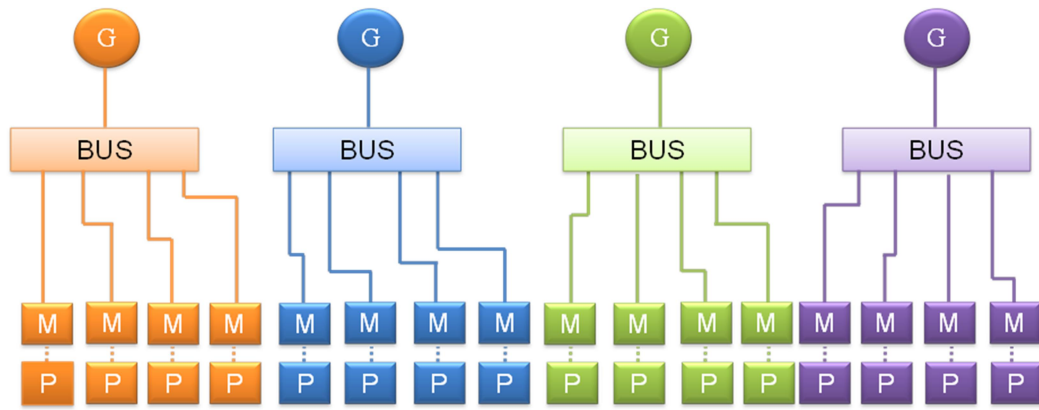


Figure 6.35 Rolls-Royce and Airbus concept baseline architecture

The baseline equations that were generated for this network in equations (6.7), (6.8) and (6.9) are repeated below for reference.

$$R_{GSC} = R_G R_F R_{3PHB} R_{CAC} R_B. \quad (6.7)$$

$$R_{MF} = R_{CAC} R_{3PHB} R_M R_P. \quad (6.8)$$

$$R_{SS} = R_{GSC} R_{MF}^4 \quad (6.9)$$

Observation of the baseline components for this architecture reveals that the three phase cable is a component with a high reliability score and occurs frequently throughout the network - in both the MF and GSC modular sections. As noted within Case Study 6.7.2, the baseline reliability for this component is initially high and so the increases to this component are limited by the maximum obtainable reliability limit. The three phase breaker occurs with the same regularity as the three phase cable within the network however the baseline reliability of this component is much lower at only 0.8. Together with the cable and three phase breaker the final component considered for this study is the EEC. This component only occurs once in the GSC and has the lowest considered baseline reliability of 0.78. The analysis will be carried out as described within section 6.6 with the results displayed in Table 6.19.

Table 6.19 Rolls-Royce and Airbus sensitivity analysis system reliability

Component	R_S (R_{CAC})	R_S (R_{3PHB})	R_S (R_{EEC})	R_S (All Components)
R Baseline	0.011983	0.011983	0.011983	0.011983
R +10 %	0.022262	0.024238	0.017544	0.062595
R+20 %	0.022262	0.043774	0.024847	0.151864

Table 6.19 shows how, similarly to the Hybrid network the reliability of the network in the Three Phase Cable case is capped (in this case at 0.022262) due to the initial high R_{CAC} value reaching the limit of 1 before the full increase of 20 %. It can also be seen that the component alteration which yields the highest resulting system reliability R_S is the three phase breaker. The results can be more clearly observed within the graph of Figure 6.36.

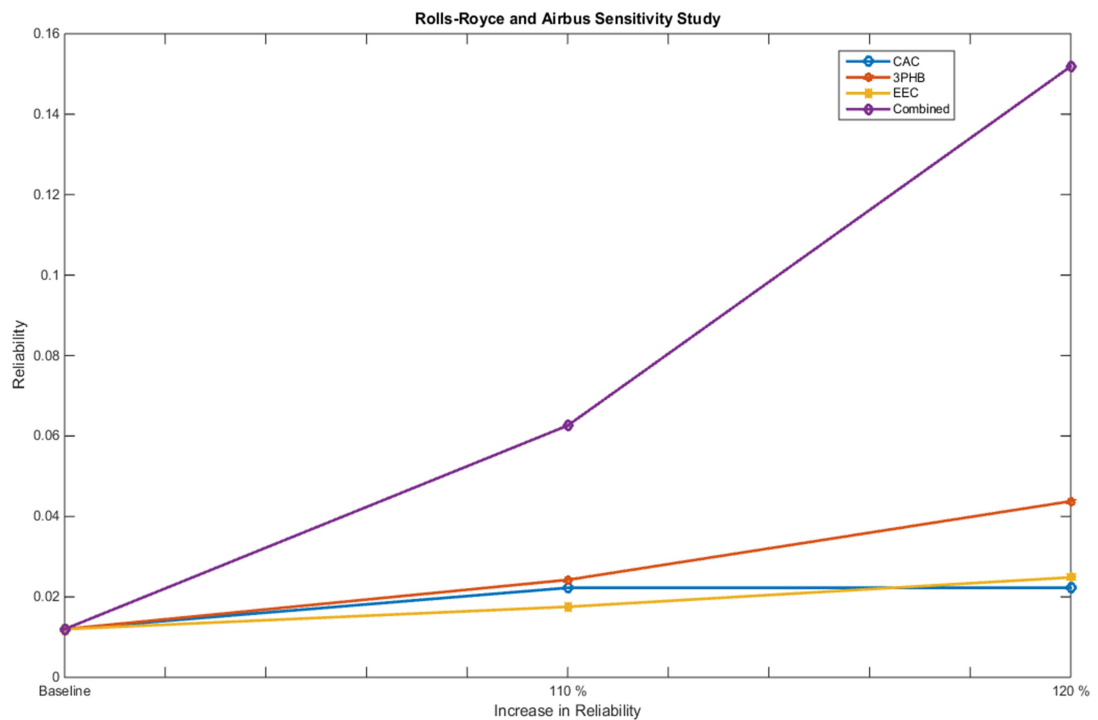


Figure 6.36 Sensitivity analysis of the Rolls-Royce and Airbus TeDP network

Figure 6.36 shows how that due to the already high level of the reliability of the three phase cable, the increases to R_S are minimal and the alteration has the least effect on network reliability R_S . Additionally Figure 6.36 shows how a 20 % increase to the

baseline value of the EEC brings network reliability to approximately the same level as with a 10 % increase in both of the other components. When compared with the sensitivity studies shown in the graphs of Figure 6.32 and Figure 6.34 where a component only occurs within the MF side of the network it can be seen that the location of the single occurring EEC in the GSC side makes no difference to the degree of increase of network reliability which remains constant at 2.07.

6.7.4 Sensitivity Study Summary

Should the network architectures be standardised and redesigned to incorporate only a single fault current and voltage protection method, it is apparent that the design of the NASA Hybrid network performs less favourably than either of the two other considered concepts. Altering the network equations for this architecture to incorporate the common protection network results in an MF section with a far reduced reliability score from the baseline network and hence results in significantly reduced network reliability. Additionally, it can be seen that the poor reliability performance of the N3-X can be mitigated through the removal of the additional protection provided by the fault current limiters to a score more in line with the other two concepts.

If the network architecture were to be altered to provide a greater reliability through the reliability improvements of components, it is apparent that the components which appear multiple times within each area of the network are those which would provide the largest improvement to reliability and are those which should be initially concentrated on. Additional observations reveal that upgrading components with an initially high reliability score provides little benefit to overall network reliability as their score tends towards 1. In order to extract the highest gains from increasing component reliability, those components which occur frequently and with the lowest reliability such as the three phase breaker should be focussed on. It can be seen that the greatest overall increase in reliability and hence the most sensitive to component alterations was exhibited by the N3-X network which, when all increased components are included in the same network is 483.86 times greater than the baseline: the network with the smallest increase to reliability was the hybrid network with an increase of only 3.78 times however a fewer number of components were

altered in this variation. As ever to keep the network reliability high the design should be kept simple with as few components as possible.

6.8 FTA of two Variations of the N3-X Network

Not only may the reliability of a TeDP network be analysed through using the *k-out-of-n* method, the FTA method as described within Chapter 3 may also be used to determine the corresponding failure rate. The first part of the study will utilise FTA as described within Chapter 3 on the N3-X baseline network of Figure 5.1 to determine the network failure rate. FTA will then be undertaken in the second part of the Study on the network utilising both GSCP and MFP using the same component configuration as in the final part of the Parallel Feeders study (6.4).

This Case Study will specifically evaluate the rate at which the loss of thrust from one single propulsor would occur as well as the rate at which the network fails to supply the specified 30,000 hp required for a safe rolling take-off. To determine how effective the combination of redundant feeders is in reducing the failure rate and minimising the effect of common cause failures, the analysis is then repeated on the networks based on that of Figure 6.25 for both the failure of MF_{2,2} and for the provision of 30,000 hp.

6.8.1 FTA on Baseline N3-X Network

As stated within Section 6.8 the object of the first part of the case study is to determine the failure rate of MF_{2,2} as shown in Figure 6.37.

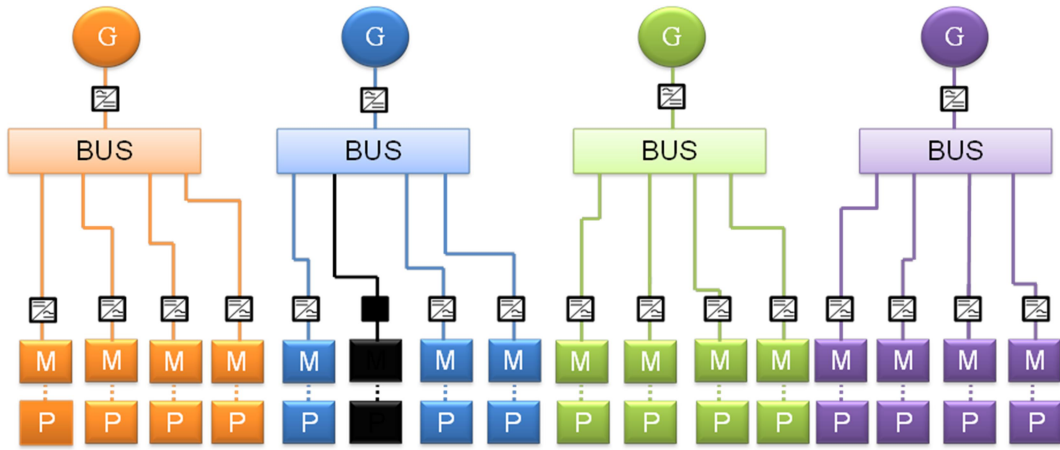


Figure 6.37 TeDP Network schematic showing motor connections and failed MF highlighted in black

The network diagram of Figure 6.37 shows the physical connections of the network. As noted in Section 5.1.1 presenting the network in this way provides a means to quickly establish all connections within the network as well as to further reference individual aspects of the network as described above.

In this case, the loss of thrust from propulsor $P_{2,2}$ (using the positional referencing derived in Chapter 3) as indicated in Figure 6.37 with the black fill, is the top event. The case study determines the rate at which this event will occur. This study evaluates only the primary power component failures of the TeDP network contributing to this top event. Hence, while a control system failure may occur causing a failure of the propulsion system, this failure type is not considered in this study. The rate of failure for both the GSC and MF of the network can be defined using a representative equation for each as shown in equations (6.25) and (6.26) respectively. Each equation is based upon the individual failure rate of each component within each section of network.

Each GSC is connected in a series manner and therefore a failure of any of these components will cause a GSC failure, as such all of these components would fall under a single OR gate within the FTA methodology and the rate at which the GSC fails to transmit power may be summed as shown by equation (6.32).

$$\lambda_{GSC} = 2\lambda_{3PHB} + \lambda_{CAC} + 2\lambda_{SFCL} + \lambda_{CON} + 2\lambda_{DCB} + \lambda_{CDC} + \lambda_B \quad (6.32)$$

Similarly as each MF is connected in a series manner, the rate with which a single MF will fail to transmit power is given by equation (6.33).

$$\lambda_{MF} = 2\lambda_{DCB} + \lambda_{CDC} + \lambda_{ACD} + \lambda_{3PHB} \quad (6.33)$$

Resolving equations (6.32) and (6.33) yields:

$$\lambda_{GSC} = 9.9784 \times 10^{-5} \text{ failures per hour and } \lambda_{MF} = 7.461 \times 10^{-5} \text{ failures per hour.}$$

The values obtained for the rate of failure of both the GSC and MF (λ_{GSC} and λ_{MF}) can now be used within this case study. The fault tree for this event and network is shown in Figure 6.38

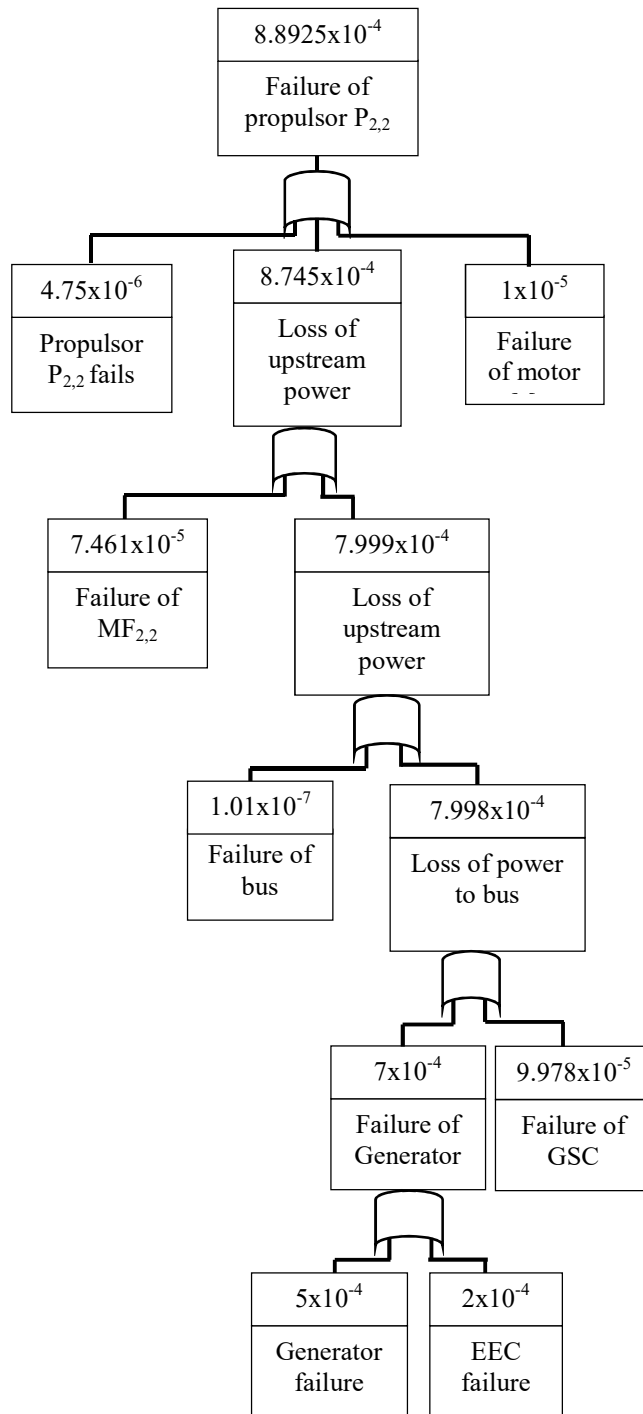


Figure 6.38 FTA of N3-X baseline propulsion network

The FTA presented in Figure 6.38 shows that the rate of failure of propulsor $P_{2,2}$ in producing thrust is 8.8925×10^{-4} failures per hour. More importantly than the loss of only a single bus or propulsor however, is the consideration of one of the main design points of this particular concept aircraft which is to provide at least 30,000 hp of thrust at take-off [19]. This design requirement determines the acceptable rate at

which any failure or combination of failures leaving the aircraft with less than 30,000 hp of thrust can occur. [49]. In [19] it is assumed that two generators are required to provide 30,000 hp and as such a loss of three generators would result in failure to supply the required 30,000 hp. The rate of failure for such an event is 5.118×10^{-10} $((7.999 \times 10^{-4})^3)$ per flight hour. This is based upon two propulsion busses failing to supply upstream power and then a third experiencing a failure event. This indicates that the architecture in its baseline form does indeed meet the modern requirement for a catastrophic loss of thrust. This ability to meet the required target determines that the baseline network architecture would be appropriate for operations. Additional redundancy within the network, or a decrease of individual failure rates of components could ensure that the ability to meet the targets are enhanced or enable reductions in the oversizing of motors within the MF.

As well as indicating any shortfall of a network in terms of failure rate, the FTA can also be used to identify areas of the network where component or common cause failures (CCF) may dominate the rate of failure. The conducted FTA shows that the loss of supply to the bus (specifically due to a failure of the generator) and the failure of the propulsor itself are the most likely failure events which will contribute to the loss of thrust from propulsor P_{2,2}. In order to reduce the failure rate of such a network, based upon these observations, either a more reliable composite generator design with associated controller should be utilised or the tolerance of the network to such failure events should be increased.

It is desirable to utilise methods of reducing the existing failure rate which also result in a minimal weight penalty. As the generators are the largest, heaviest network components [42] installing further generators to the wingtip to increase reliability of thrust is undesirable in terms of weight and volume and so increasing reliability through lighter means if possible is preferred. This aspect is explored in further detail in the subsequent case study.

6.8.2 FTA on N3-X Network Utilising Redundant Parallel Feeders

In order to achieve a lesser failure rate for minimum take-off thrust than is possible in the baseline network, yet utilise the existing generation capabilities, a number of redundant feeders can be added to provide interconnections within the network to reduce the effect of the identified dominant failure mechanisms. This is described in detail in Case Study 2, Section 6.4. These additional parallel feeders are illustrated in Figure 6.39.

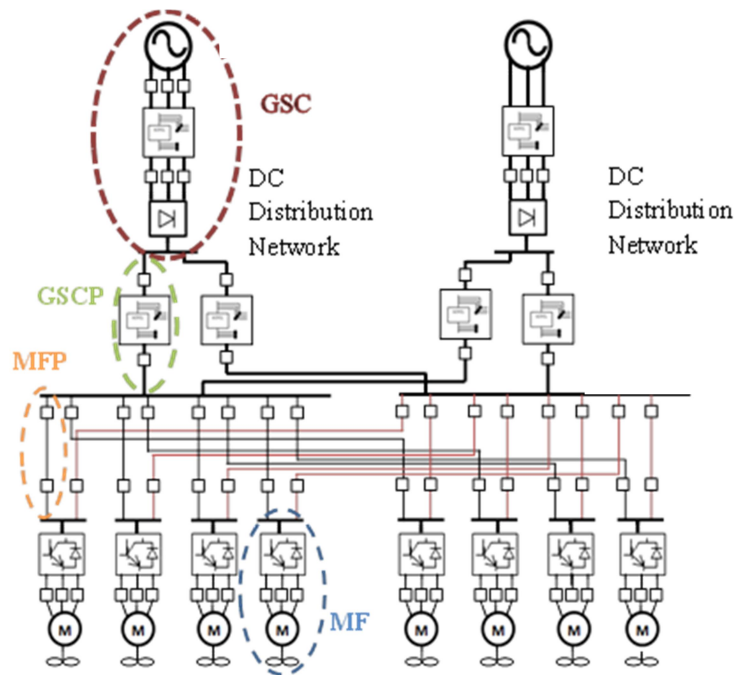


Figure 6.39 N3-X network with parallel GSC and MF

Figure 6.39 shows how additional redundant feeders can be added to both the GSC and the MF side of the network, increasing the tolerance of the network to failures in these areas and specifically reducing the likelihood that the supply of power to the bus will be lost. Each bus can potentially have a connection to each motor through a number of parallel feeders, where each additional parallel feeder MFP is joined to the network at the propulsion bus. With the introduction of the additional redundant paths, new system equations must be derived based on the system's composition and can be described (using the components in Table 6.1) by:

$$\lambda_{\text{MFP}} = 2\lambda_{\text{DCB}} + \lambda_{\text{CDC}} \quad (6.27)$$

Additionally the GSC, through the addition of parallel feeders has the potential to connect to every other propulsion bus through a parallel feeder (GSCP) after the AC/DC converter and via a connection bus [49] to another of the propulsion busses. Again, the bus remains as a separate entity for ease of analysis and the series connection of the network architecture stipulates an OR logical function. The failure rate equation for the parallel feeder section, GSCP, becomes:

$$\lambda_{\text{GSCP}} = \lambda_{\text{SFCL}} + 2\lambda_{\text{DCB}} + \lambda_{\text{CDC}} \quad (6.28)$$

where the original equations for GSC and MF failure rates (equations (6.1) and (6.2)) become equation (6.29) and (6.30) respectively:

$$\lambda_{\text{GSC}} = 2\lambda_{3\text{PHB}} + \lambda_{\text{CAC}} + \lambda_{\text{SFCL}} + \lambda_{\text{CON}} \quad (6.29)$$

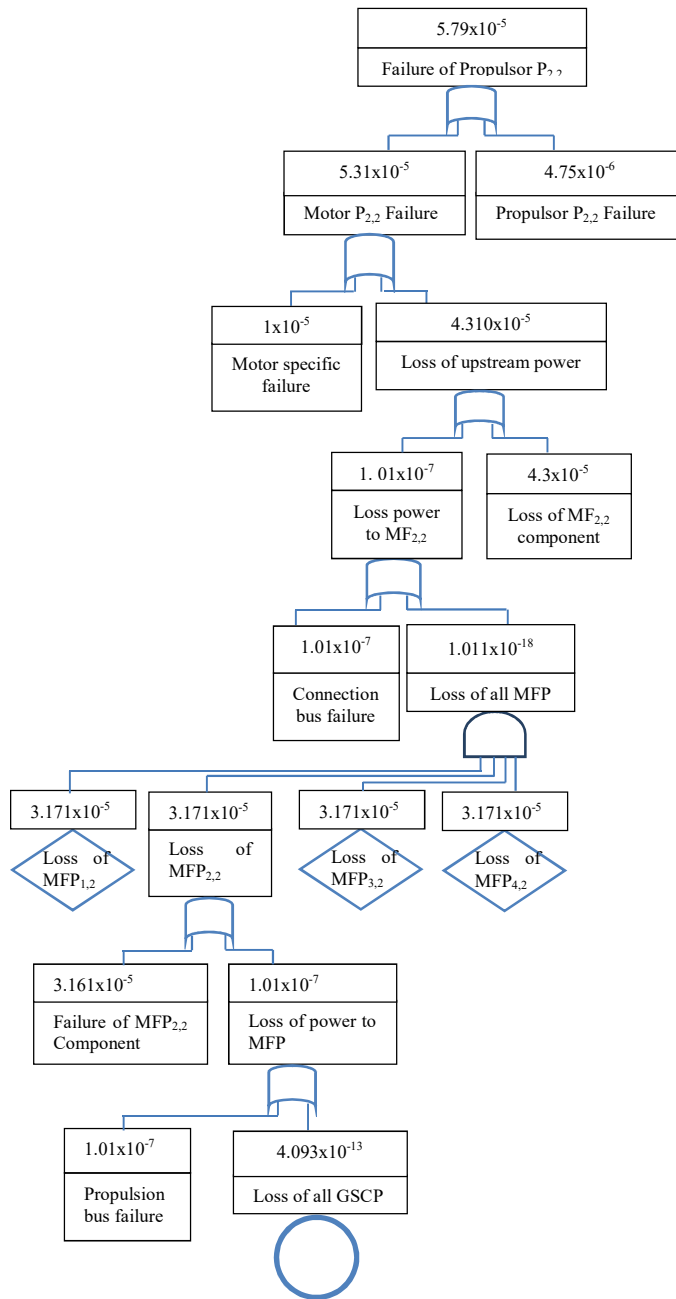
$$\lambda_{\text{MF}} = \lambda_{\text{ACD}} + \lambda_{3\text{PHB}} \quad (6.30)$$

Using the failure rate figures as provided in Table 6.1, these new equations can be resolved as:

$$\lambda_{\text{GSC}} = 6.7592 \times 10^{-5} \text{ failures per hour} \quad \lambda_{\text{MF}} = 4.3 \times 10^{-5} \text{ failures per hour}$$

$$\lambda_{\text{GSCP}} = 7.999 \times 10^{-4} \text{ failures per hour} \quad \lambda_{\text{MFP}} = 3.161 \times 10^{-5} \text{ failures per hour}$$

It can be seen from Figure 6.39 that the supply of power to the MF sections will only be lost if both GSCP and both MFP sections fail. Similarly for a system with x number GSCP or MFP feeders, all x feeders must fail to cause a failure of that GSC or MF section. To determine how effective the redundant feeders are in reducing the failure rate, an FTA (which is illustrated in Figure 6.40) is undertaken. The analysis uses the failure rate values and components as presented in Table 6.1.



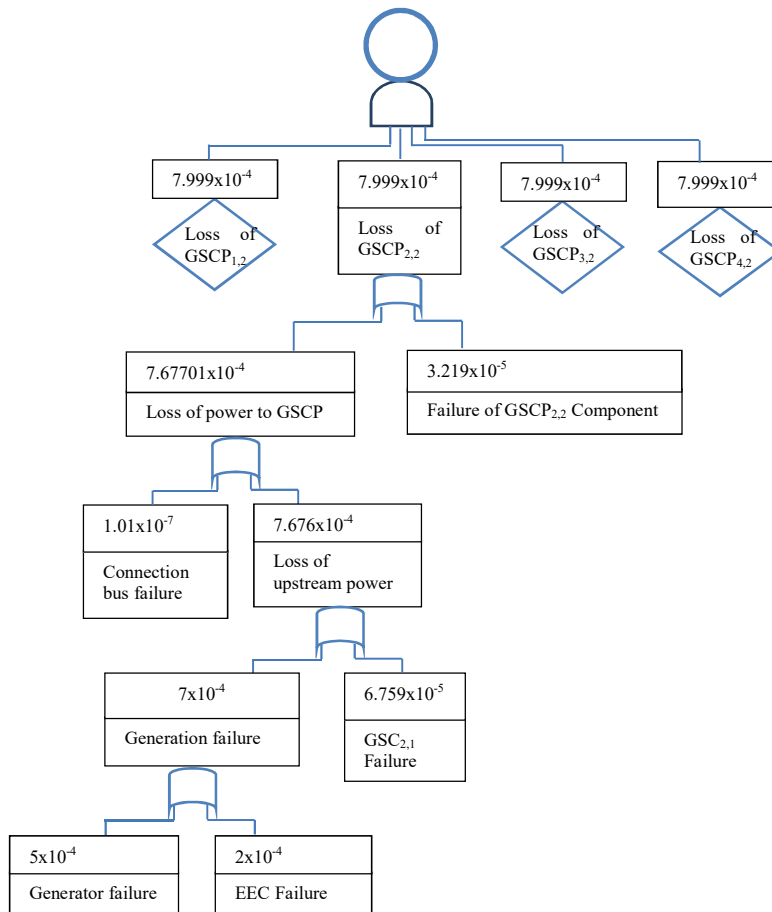


Figure 6.40 FTA of N3-X network utilising both GSCP and MFP

From the FTA presented in Figure 6.40 it can be seen that the rate at which there is a loss of thrust from the propulsor $P_{2,2}$ is 5.79×10^{-5} per flight hour, which is notably less than that of the baseline network (8.8925×10^{-4}). It can also be seen that the rate of failure of all propulsors associated with a single network SS in this case would occur if each individual propulsor or motor were to fail and is in the region of 1.124×10^{-18} per hour. Through increasing the number of available flow paths for power to reach the motor from the bus, the failure rate has decreased from 8.745×10^{-4} per flight hour to 4.310×10^{-5} per flight hour. Similarly the rate of failure attributed to the supply of power to the propulsion bus (from the GSC) in the base case was previously 7.998×10^{-4} per flight hour, dramatically decreasing to 4.093×10^{-13} per flight hour through the utilisation of additional GSCP. This also shows that dominance of the generator failure rate in shaping the top event failure rate has been successfully negated.

Additionally, it can be determined that the rate at which propulsive power is lost to all propulsors is approximately equal to the rate at which all generation is expected to fail. This occurs at a rate greater than any other combination of failures that would produce the same result. By evaluating the failure of all generation it can be seen that this failure occurs 2.401×10^{-13} times per flight hour. This is only 58.6 % of the equivalent failure rate of calculated for the base case.

Finally, the ability of the aircraft network to supply the 30,000 hp required for take-off is determined by the failure of three generators and their EEC units. This occurs 3.43×10^{-10} times per flight hour (7×10^{-4} cubed). Not only is this rate of failure significantly less than that of the base case (5.118×10^{-10} failures per flight hour), it also satisfies the critical failure rate for modern civil aircraft. This significant reduction in failure rate for the propulsion network indicates that an effective means of redundancy is provided to the network by adding redundant parallel feeders.

6.8.3 FTA Summary

This Case Study has undertaken a thorough FTA based failure rate analysis for both the baseline N3-X TeDP network and the same network utilizing additional parallel feeders. This has shown that the significant factors contributing to the rate of thrust loss in a propulsor are the GSC successfully supplying power to the propulsion bus and the failure rate of the propulsor itself. To enhance reliability it is advantageous to include a number of GSCP to increase the system tolerance to any faults or failures in this section of network. Adding a number of parallel paths in this manner also significantly reduces the failure rate for the minimum required thrust for take-off on the N3-X aircraft network studied from 5.118×10^{-10} failures per flight hour to 3.43×10^{-10} failures per flight hour.

Chapter 7

Conclusions and Further Work

In recent years there has been a shift in aircraft research resulting in an increased focus on electrical concepts and features to be adopted within aircraft architectures. The evolution of this research and continued utilisation of increasingly electrical architectures is likely to see the adoption of architectures far removed from today's conventional tube and wing designs. One such design which has resulted from an increased electrification ideology is TeDP. This work has analysed three pre-proposed TeDP architectures for their ability to provide at least the minimum required thrust for a safe rolling take off, in the case of this work that level is half the installed thrust. The work has additionally analysed the networks for comparable performance when operating with additional bus ties to enhance network reliability as well as when utilising additional parallel feeders in both the generation and propulsion halves of each network. Each of the networks has been analysed in terms of how sensitive it is to a change in reliability of a number of constituent components before an FTA was completed on one network (the N3-X) to highlight how analysis may alternatively be undertaken.

Drawing upon the knowledge gained through research of the area and of the TeDP aircraft concept as well as from the analysis of each network, a number of conclusions can be made and are presented within this Chapter. Following the conclusions a recommendation for future work is provided in addition to some closing remarks.

7.1 Summary of Key Findings from *k-out-of-n* Analysis

Through undertaking a *k-out-of-n* analysis on the N3-X, NASA AC/DC Hybrid and the Rolls-Royce and Airbus Network, the following observations can be made about

the three considered networks baseline reliability as well as the reliability when using a number of redundancy methods. The N3-X network consistently exhibited the lowest reliability score at all the considered baseline configurations and in every additional redundancy configuration due to the greatest number of components which combine to create the network. In terms of baseline network reliability when successfully providing 100 % of installed power, the extrapolated 4 SS Rolls- Royce and Airbus network exhibits the greatest level of observed reliability, 4.47 times greater than the NASA Hybrid network and 2.1×10^5 times greater than the N3-X. Conversely, the NASA Hybrid network exhibits the highest reliability score when the requirement is to provide at least 50 % of installed power or greater. This is provided at a reliability of 1.34 times greater than the Rolls-Royce and Airbus network and 727.21 times greater than the N3-X architecture.

When considering the added redundancy methods, the bus tie method was shown to allow the greatest increase to reliability in each of the three networks. The network with the largest percentage increase resulting from the introduction of bus ties between all network SS was the N3-X. This observation holds true for all considered redundancy methods: the N3-X has the largest percentage increase in reliability. When considering the parallel feeder redundancy, the N3-X and NASA Hybrid networks both have a greater increase to reliability when operating using the MFP sections; the Rolls-Royce and Airbus variant performs better using the GSCP sections and is the most reliable of all the networks considered in these parallel feeder case studies.

The studies conducted in chapter 6 showed that in the case of the NASA Hybrid network all parallel feeder methods afford a similar level of increase to reliability from the baseline which in turn does not provide a significant increase over the baseline network. It should be seriously considered if increases to network reliability when using this redundancy method outweigh the significant weight penalties and increased complexity incurred through using a large number of additional components.

The sensitivity studies for the networks revealed that should the network architectures be standardised and redesigned to incorporate a standardised fault

current and voltage protection method, the design of the NASA Hybrid network performs the least favourably of all three considered concepts. Additionally, it can be seen that the poor reliability performance of the N3-X can be mitigated through the removal of the additional protection provided by the fault current limiters to a score more in line with the other two concepts.

If the network architecture were to be altered to provide a greater reliability through the reliability improvements of components, it is apparent that the components which appear multiple times within each area of the network are those which would provide the largest improvement to reliability and are those which should be initially concentrated on. Additional observations reveal that upgrading components with an initially high reliability score provides little benefit to overall network reliability as their score tends towards 1.

Based upon the observations of the case studies presented in chapter 6, a number of suggestions can be made regarding optimal TeDP network design. The case studies consider using parallel feeders in both the GSC and MF side of all networks however do not consider the benefits to reliability in using parallel connections from the motor or generator windings to the power electronics components. Using parallel connections in this area would eliminate the dominating failure rate and hence increase overall network reliability for a minimal added weight penalty. Keeping the use of heavy power electronic components minimised should also be a key design consideration unless significant reductions in their mass and volume can be made. Any TeDP network should have bus ties utilised between all major busses in the SS, however could also be considered between the busses at the point where the GSCP and MFP join reducing the risk of failure in these areas too. Finally based upon the findings of the studies, an alternative 5 bus design using only 4 generators and additional GSC to supply the additional, central bus could be developed. The network MF could then be redistributed to allow power to be evenly distributed to the motors however introducing an additional point which would have to fail before a significant loss of power was observed.

7.2 Review of Chapter Summaries

This work provides a comprehensive reliability evaluation tool which is of great use to a number of interested parties during the design and development stage of new TeDP network architectures. In the first instance it is of importance to system engineers developing new TeDP network architectures allowing decisions to be made on optimal inclusion of network components and redundancy methods, not only for propulsion but potentially in load sharing network branches. Other interested parties would include safety engineers who require a means to provide assurances to both a customer and to industrial partners that a network can achieve a set reliability while providing a guaranteed level of thrust. The presented k-out-of-n method allows rapid profiling of a number of network scenarios to be undertaken allowing clear representation of the profiles in a T-R graph. The graph is used to not only provide information on network performance relative to a set of metrics, however is also used to display design criteria and requirements that a network must adhere to, for example minimum thrust provision. This is a feature usually carried out through the completion of a FTA, through adopting the k-out-of-n analysis, a simpler yet equally valid analysis may be provided to clients assuring them of the aircraft's safety and reliability. Due to the modular nature of this analysis, it may also help reduce costs over an FTA as sections of the analysis may be reused between networks mitigating the need to redraw a new fault tree for small network changes. This method is not limited to the TeDP concept however and may be adopted in a number of network settings where identical, parallel network sections exist such as in a low voltage distribution network or on shipboard networks.

Research into TeDP has identified that a gap within the existing research existed in the area of network reliability and that there was significant scope for identifying an appropriate method for analysis of these new network configurations. The work of this thesis has presented a method which improves upon existing analysis to provide a thorough capability to not only determine the reliability of any TeDP architecture but to graphically represent this data in a meaningful fashion. The method allows analysis of the network in a modular fashion, reducing the large complex network into sections which are easier to analyse and then undertakes a k-out-of-n

methodology to determine the reliability of the modular sections before recombining into the original network. A positional referencing structure is identified for referring to each modular section within the network and can be used both when the network is presented in schematic form or in a plan view. Once a *k-out-of-n* analysis has been undertaken, the results can be displayed on a T-R graph highlighting how each level of power achievable by the network maps to a specific reliability score.

While a number of TeDP architectures have been proposed and networks described in some level of detail, there has previously been no comparison of how the networks are likely to perform with respect to their expected reliability scores. Through undertaking the research for this thesis, three TeDP architectures of interest have been considered and through utilisation of the above method analysed in terms of the level of reliability that each can provide at least 50 % of their installed thrust (the stipulated requirement for safe rolling take off).

Through thorough analysis conducted via the *k-out-of-n* analysis, it was determined that the network jointly proposed by Rolls-Royce and Airbus consistently provided the greatest reliability score in all but the base case. This was the only network of the three not to feature generation and thrust electrically decoupled through a series of power electronic devices however exhibits a series of gearboxes to reduce shaft speeds. The architecture also features a dedicated protection network. The network which proved consistently least reliable was the N3-X which featured both a dedicated protection network as well as a DC distribution system, decoupling the shaft speeds of the electrical machines. Whereas the N3-X network continually exhibited the lowest rate of reliability in all scenarios, it also exhibited the greatest percentage increase when analysed with all redundancy measures.

Using redundancy methods throughout the network resulted in significant gains to reliability in all cases. Notably however was the case of the parallel feeders, where the Rolls-Royce and Airbus network performed slightly better when utilising parallel GSC sections while the N3-X and NASA Hybrid network performed better while using MFP sections. While this result is in part due to the network architecture and part due to the individual component reliability scores, in all cases the gains experienced through using both sets of parallel feeders in the same network provide

far greater network reliability. In the case of the N3-X where this is most apparent, the benefit from using MFP is an increase of network reliability of 7.778 times that of the baseline, through using both sets of parallel feeders, the gains are in the order of 43.9 times greater. The gains experienced by parallel feeders though are almost insignificant when compared to those of the bus tie. In all cases the gains afforded through using a much lighter redundancy method are at least three orders of magnitude greater than the baseline network making this redundancy method the preferred option to increase network reliability.

A complementary failure rate analysis has also been carried out to show how analysis may be alternatively undertaken using a FTA. This method verifies that should the future N3-X network be constructed using components equivalent to today's state of the art, that it would indeed meet the current critical failure rate target of no failures in 10^9 hours. Using this method however results in a far lengthier analysis process than the k-out-of-n method suggested within this work. The work indicates areas of the network where specific component failure rates dominate the rate for the network and where these identified points can be reduced through the inclusion of additional redundancy. The most critical area where failure rates could be improved is the rate of failure of the supply of power to the bus which links the GSC and MF modular sections, through adding additional parallel feeders into the network this failure rate can be reduced by 9 orders of magnitude.

Finally, it should be noted that both analysis methods undertaken within Chapter 6 are complimentary and combine to create a detailed picture of TeDP network thrust reliability performance. The k-out-of-n analysis provides a thorough understanding of network reliability and an understanding of the sensitivity of TeDP networks to sensitivities and statistical tolerances in individual component reliability as well as providing the means to create the T-R graph. Additionally the FTA method allows less succinct analysis however clearly illustrates both reliability weak spots as well as areas of CCF of the reviewed network architectures. These individual merits combined with the FTA status of being a current certified analysis method ensures that the application of one technique compliments the other to provide a powerful and informative analysis tool.

7.3 Key Areas of Future Work

A critical area of future work which will see this concept aircraft advance is intense study into providing highly reliable superconducting machines, capable of producing power densities far in excess of those available today. In order to produce greater power densities than are currently achievable, it is likely that both super conducting rotors and stators will be developed for machines allowing large currents to be created. The complete cooling of the propulsion network must also be considered to allow a fully superconducting network to exist. To complement the development of power dense machines and network, a large number of hours must be dedicated to proving the reliability of such a system. As the technology is far from mature, assurances must be made as to the reliability of this new network proposal if it is to replace a well understood propulsion network. This study however was far out with the scope of this project.

One area of further work which is critical to advancing the TeDP concept however out with the direct scope of this thesis is in addressing the reliability, functionality, location and dynamics of future technologies such as cryocoolers and energy storage. The superconducting nature of the TeDP network requires a light, reliable cooling system of which further effort should be made to enhance the currently available technology while maintaining a non-prohibitive cost for the concept. Similarly a lightweight and reliable energy storage system could complement the existing propulsion network through providing a backup to the generators or in replace of a percentage of the thrust output of the network. Additional extensive research into the reliable performance of battery technology for extended durations as part of a wider network would allow this to represent a meaningful alternative to a turbofan.

Another interesting further study which could have been completed had time permitted takes the results of the FTA and addresses the larger failure rates within the network which were not addressed through the addition of parallel feeders. These specific areas have been identified as the connection point of the GSC1 to the GSCP and the MFP to the MF1 sections within all networks. These specific failures could

be reduced through connecting a number of MF1 and GSC1 sections in parallel to increase the tolerance of the network to failure and specifically reducing the likelihood that the supply of power to the bus (in the GSC side) and from the bus (in the MF side) will be lost. Introducing parallel connections from the inverter to the motor could allow a lesser failure rate to be achieved – the magnitude of which determined by the further study. In addition the AC Motor Drive or the AC/DC convertor would then form the new point at which the failure rate of the network was at a maximum and as such engineering effort should be made on this network component to enable greater gains to be made from the additional parallel network connections.

One area which could also benefit from further study is the reliability of the networks under varying voltage and current magnitudes. The studies presented within this thesis assume that the networks have a reliability score which remains constant with differing power requirements however in practice this may not be the case. The N3-X and Hybrid networks are designed to operate at a much higher power level than the Rolls-Royce and Airbus network and in order that the theoretical results be validated an assessment how the reliability of comparable network elements perform at the differing voltage and current inputs (and power levels) must be made. Of additional interest, however outwith the scope of this work, an evaluation whereby reliability scores are weighted to take into account the effect of atmospheric conditions such as altitude on a TeDP network should be conducted. Due to the reduced dielectric strength of air at high altitudes, and the potentially higher voltage levels used within TeDP aircraft careful design practices must be used to prevent electrical arcing of voltages between network components. Additionally, a means of determining appropriate reliability scores attributed to network components to account for the increased stressed which extremes of temperature and altitude may present would form a valuable additional design and analysis capability.

A further adaption for the T-R graph would see it being used in a quality control setting to both quantify and qualify engineering improvements made to a network. In this application, additional system specifications such as weight can be mapped against the T-R profiles in each of the configurations analysed before adding

redundancy or reliability boosting over-ratings. A different coloured set of points could show the outcome of a fix where a single configuration point is bolstered and maybe causes another configuration to fail simulations. Finally a last set of points superimposed on the chart in a more dominant colour would show the results from all those configurations which pass all corners of the propulsion system spec. At the end of an architecture's design stage this chart would be the stamp of system quality tracking showing, if required, the areas investigated, the sensitivity effects of a reliability fix somewhere being a liability elsewhere within the system and the final document proving architecture worthiness for service. The benefits of a T-R graph should not be limited to only an aircraft setting.

The scope could easily be extended beyond the scope of the TeDP analysis to consider applications such as smart-grids where storage in future networks is an important consideration. The T-R graph in this setting could display both the lifetime and reliability of different components and use types such as smart cities and in turn future critical infrastructure. Design of such infrastructure requires an in-depth and informed planning stage and through mapping parameters such as expected reliability and storage capacity which can be provided by the k-out-of-n and hence T-R style graph. The graph can also display important usage metrics and lifespan information and can therefore help in planning retrofits of networks and successor programs to replace systems as they become obsolete.

Finally, looking beyond the next stage of analysis, undertaking Reliability Growth Trials (RGT's) on individual components to obtain crucial reliability data for more accurate and less generalised results is required. These trials seek to grow the achievable reliability exhibited by individual components or Line Replaceable Units (LRU's) (such as the motor drive) through subjecting them to continuous cycles of rigorous climactic stresses. These RGT's would provide more specific and reliable data which is more fine tuned to the future concept and not based upon current day alternative components. This work should be used in conjunction with a Duane reliability parametric model for predicting reliability growth to allow an accelerated programme to be undertaken. RGT's should, in the first instance be undertaken on prototypes and concept architectures and would be most effective in determining a

realistic reliability figure for each network and verifying the theoretical results presented within this thesis.

7.4 Concluding Remarks

The work of this thesis has presented a thorough reliability analysis of three potential future aircraft architectures and has indicated that if the N3-X architecture were to be implemented using modern day components that it could certainly meet present day failure rate targets for civil aircraft. Through analysing the anticipated network architectures as well as highlighting how reliability may be altered through the addition of redundancy features, this research will prove a valuable tool in the eventual implementation of TeDP networks. Implementing the noted additional studies to determine how the concept may benefit from additional research effort into power electronic sections and a standardised power level and protection approach will further solidify the feasibility of the concept and push TeDP concepts closer to civil aviation. It should be noted however that the TeDP concept remains at the early concept stage and is subject to a number of design iterations before full scale prototypes are investigated. Next steps should consider the suggestions made within this thesis – specifically the standardised approaches to protection as mentioned in Chapter 6 to ensure fault currents are handled appropriately and for a minimised penalty to overall network reliability. Furthermore, adopting the bus tie redundancy method allows the preferable low-weight, high reliability benefit characteristics to be achieved by all TeDP network architectures going forward.

Bibliography

- [1] Boeing 787. c2016. Wikipedia. [accessed 12/02/16].
http://pl.wikipedia.org/wiki/Boeing_787#mediaviewer/Plik:B787-2155a.jpg.
- [2] A380. c2016. Airbus. [accessed 14/01/16]. <http://www.airbus.com/galleries/photo-gallery/dg/idp/417-a380-5/?share=1>
- [3] Bigger is Better. 2015. NASA. [accessed 07/15]. <http://www.nasa.gov/content/down-to-earth-future-aircraft-0?id=341932>
- [4] Down to Earth Future Aircraft. 2015. NASA. [accessed 08/15].
http://www.nasa.gov/topics/aeronautics/features/future_airplanes_index.html#lowerAccordion-set2-slide19
- [5] Technology Readiness Level. 2012. NASA. [accessed 04/03/15]
<http://www.nasa.gov/content/technology-readiness-level/#.VM-LdC72TYC>.
- [6] Envisioning Tomorrow's Aircraft. c2010. Boeing. [accessed 05/05/15].
http://www.boeing.com/Features/2010/06/corp_envision_06_14_10.html
- [7] Banke, J. Beauty of Future Airplanes is More than Skin Deep. 2010. NASA [accessed 12/16/15]
http://www.nasa.gov/topics/aeronautics/features/future_airplanes.html#.VRlzTuFcDYA.
- [8] Gatto, K. Future planes to get a 'magic safety skin'. 2011. phys.org. [accessed 14/07/15].
<http://phys.org/news/2011-04-future-planes-magic-safety-skin.html>.
- [9] Warwick, G. eConcept - EADS's Hybrid-Electric Airliner. Things With Wings 2013. 2013. [accessed 14/16/15]. <http://aviationweek.com/blog/econcept-eadss-hybrid-electric-airliner>.
- [10] Faleiro, D.L., '*Summary of the European Power Optimised Aircraft (POA) Project*', in 25th international congress of the aeronautical sciences 2006: Hamburg.
- [11] Felder, J., Kim, H., Chu, J., and Brown, G., '*Turboelectric Distributed Propulsion in a Hybrid Wing Body Aircraft*', in 20th International Society for Airbreathing Engines (ISABE), Gothenburg, 2011.
- [12] Kelch, K. Mavris and ASDL Team Collaborate on Efficient Wing Design. 2014. aerospace systems design laboratory. [accessed 12/05/15].
http://www.asdl.gatech.edu/News.html#Mavris_and_ASDL_Team_Collaborate_on_Efficient_Wing_Design.
- [13] Cumpsty, N., '*The Gas Turbine Cycle*', in *Jet Propulsion: A simple guide to the aerodynamic and thermodynamic design and performance of jet engines*, Cambridge University Press: p. 30-46, 2003.
- [14] McLoughlin, A., '*Engine Powerplant Electrical Systems*', in *More Electric Aircraft Forum*, MOET, Madrid Spain, 2009.
- [15] Sinnett, M., '*787 No - Bleed Systems: Saving Fuel and Enhancing Operational Efficiencies*', in *Boeing Aero Magazine*, p. 6, 2007.
- [16] Kim, HD., Brown, GV. and Felder, J., '*Distributed Turboelectric Propulsion for Hybrid Wing Body Aircraft*', in *International Powered Lift Conference*, London, 2008.
- [17] Moir, I., Seabridge, A., '*Electrical Systems*', in *Aircraft Systems-Mechanical, Electrical and Avionics Subsystems Integration*, Wiley: Chichester. p. 221, 182, 230, 232, 2010.
- [18] Collier, F., '*Environmentally Responsible Aviation Project: Real Solutions for Environmental Challenges Facing Aviation*', 50th AIAA Aerospace Sciences Meeting, Nashville, 2012.

- [19] Armstrong, M., Ross, C., Phillips, D., Blackwelder, M., '*Stability, Transient Response, Control and Safety of a High-Power Electric Grid for Turboelectric Propulsion of Aircraft*', Rolls - Royce Liberty Works North American Technologies, NASA, 2013
- [20] Luongo, C., Masson, P., Nam, T., Mavris, D., Kim, H., Brown, G., Waters, M., Hall, D., '*Next Generation More-Electric Aircraft: A Potential Application for HTS Superconductors*', in IEEE Transactions on Applied Superconductivity, vol. 19, no. 3, pp. 1055-1068, June 2009.
- [21] Faleiro, L., '*Power Optimised Aircraft (POA) - a keystone in European Research in More Electric Aircraft Equipment Systems*', Aerodays, Vienna, 2006..
- [22] Hirst, M., McLoughlin, A., Norman, P., Galloway, S., '*Demonstrating the more electric engine: a step towards the power optimised aircraft*', in IET Electric Power Applications, vol. 5, no. 1, pp. 3-13, January 2011.
- [23] Berg, F., Palmer, J., Miller, P., Husband, M., Dodds, G., '*HTS Electrical System for a Distributed Propulsion Aircraft*', in IEEE Transactions on Applied Superconductivity, vol. 25, no. 3, pp. 1-5, June 2015.
- [24] Rogers, M.M., '*Technical Challenges to Reducing Subsonic Transport Drag*', in AIAA Aerospace Sciences Meeting, Nashville, 2012.
- [25] Taminger, K., '*Technical Challenges to Reducing Subsonic Transport Weight*', in AIAA Aerospace Sciences Meeting, Nashville, 2012.
- [26] Roboam, X. 'New trends and challenges of electrical networks embedded in "more electrical aircraft"', 2011 IEEE International Symposium on Industrial Electronics, Gdansk, 2011, pp. 26-31.
- [27] US Department of Defense, '*Reliability Prediction of Electronic Equipment*', in MIL-HDBK-217F section 15.11991.
- [28] Fletcher, S., Norman, P., Galloway, S., Burt, G., '*Impact of Engine Certification Standards on the Design Requirements of More-Electric Engine Electrical System Architectures*', in Aircraft Systems and Technology Conference, SAE: Cincinnati, 2014.
- [29] Schmidt, V. Is Limiter. 2005. ABB.com. [accessed 14/06/15] [http://www02.abb.com/global/sgabb/sgabb005.nsf/bf177942f19f4a98c1257148003b7a0a/4550d4a6117088e9482574d70038223c/\\$FILE/C1_H3_H6_High%20short%20circuit%20current%20in%20medium%20voltage%20application.pdf](http://www02.abb.com/global/sgabb/sgabb005.nsf/bf177942f19f4a98c1257148003b7a0a/4550d4a6117088e9482574d70038223c/$FILE/C1_H3_H6_High%20short%20circuit%20current%20in%20medium%20voltage%20application.pdf).
- [30] Reliability, M., Reliability of a electric motor.
- [31] Bailey, A. '*Protection and switching of large loads for the more electric aircraft*'. in 13th European Conference on Power Electronics and Applications, Barcelona, 2009.
- [32] IEEE Standard Computer Dictionary '*A Compilation of IEEE Standard Computer Glossaries*', IEEE Std 610, p. 1-217, 1991.
- [33] Banke, J., 'NASA Helps Create a More Silent Night.', News & Features 2010:NASA. [accessed 14/09/15]. http://www.nasa.gov/topics/aeronautics/features/bridges_chevron_events.html#.VAhGK2Pb7Qg.
- [34] Felder, J., Kim, H.. '*Materials Aspects of Turboelectric Aircraft Propulsion*'. 2009, Fundamental Aeronautics programme:2009 annual meeting. [accessed 12/10/15]. http://ntrs.nasa.gov/archive/nasa/casi.ntrs.nasa.gov/20090042355_2009042905.pdf
- [35] Norman, PJ, Galloway, SJ, Burt, GM, Trainer, DR., Hirst, M., '*Transient analysis of the more-electric engine electrical power distribution network*', in 4th IET Conference on Power Electronics, Machines and Drives (PEMD), York, pp. 681 - 685, 2008.

- [36] Moir, I., Seabridge, A., '*Advanced Systems*', in Aircraft Systems: Mechanical, Electrical, and avionics subsystems integration, John Wiley and Sons Ltd: Chichester, p. 375,381,382, 388., 2010,
- [37] Gohardani, A., Doulgeris, G., and Singh, R., '*Challenges of future aircraft propulsion: A review of distributed propulsion technology and its potential application for the all electric commercial aircraft*', Progress in Aerospace Sciences, 47(5), p. 369-391, July 2011.
- [38] Moir, I., Seabridge, A., '*Flight Control Systems*', in Aircraft Systems: Mechanical, Electrical, and avionics subsystems integration, John Wiley and Sons Ltd: Chichester, p. 1-50 (31&33), January 2010.
- [39] Garcia, A., Cusido, I., Rosero, J., Ortega, J., Romeral, L., '*Reliable electro-mechanical actuators in aircraft*', Aerospace and Electronic Systems Magazine, IEEE, 23(8): p. 19-25, 2008.
- [40] Nelson, T.. '787 Systems and performance'. 2005. The Boeing Company, [accessed 24/05/15]. <http://myhres.com/Boeing-787-Systems-and-Performance.pdf>
- [41] Karimi, K.J., '*Future Aircraft Power Systems-Integration Challenges*'. 2008. EMU:The Boeing Company. [accessed 04/05/15]. <https://www.ece.cmu.edu/~electriconf/2008/PDFs/Karimi.pdf>
- [42] Brown, G.V., '*Weights and Efficiencies of Electric Components of a Turboelectric Aircraft Propulsion System*', in 49th AIAA Aerospace Sciences Meeting Orlando Florida, 2011.
- [43] Armstrong, M.J., Ross, C., Blackwelder, M., Rajashekara, K., '*Propulsion System Component Considerations for NASA N3-X Turboelectric Distributed Propulsion System*', SAE International Journal of Aerospace, vol 5(2), pp 344-353, 2012.
- [44] Masson, P.J., Luongo, C.A., 'High power density superconducting motor for all-electric aircraft propulsion', IEEE Transactions on Applied Superconductivity, Vol 15(2), pp. 2226-2229, 2005.
- [45] Palmer, J., Shehab, S., Husband, M., '*Cryogenic Systems Study for Turbo-Electric Distributed Propulsion Aircraft Solution*', More Electric Aircraft Conference, Bordeaux, 2012.
- [46] Palmer, J., Shehab, S., Fan, IS, Husband, M., '*Quality Function Deployment and Sensitivity Analysis of Requirements for Future Aircraft Propulsion Cryogenic Cooling Systems*', in 11th International Conference on Manufacturing Research, Cranfield University, 2013.
- [47] Felder, J., Kim, H., Brown, G., '*Turboelectric Distributed Propulsion Engine Cycle Analysis for Hybrid-Wing-Body Aircraft*', in 47th AIAA Aerospace Sciences Meeting Including The New Horizons Forum and Aerospace Exposition, American Institute of Aeronautics and Astronautics, Orlando, 2009.
- [48] Armstrong, M., Blackwelder, M., Ross, C., '*Sensitivity of TeDP Microgrid Systems Weight and Efficiency to Operating Voltage*', 50th AIAA/ASME/SAE/ASEE Joint Propulsion Conference, Cleveland Ohio,2014.
- [49] Armstrong, M., Ross, C., Blackwelder, M., Rajashekara, K., '*Trade Studies for NASA N3-X Turboelectric Distributed Propulsion System Electrical Power System Architecture*', SAE International Journal of Aerospace, vol.5(2), 2012.
- [50] Jones, C.E., Norman, P., Galloway, S., Bollman, A., Armstrong, M., '*A pre-design sensitivity analysis tool for consideration of full-electric aircraft propulsion electrical power system architectures*', ESARS 2015, Aachen Germany.
- [51] Bollman, A., Armstrong, M., Jones, C., Norman, P., Galloway, S., '*Development of Voltage Standards for Turbo-electric Distributed Propulsion Aircraft Power Systems*', in ESARS 2015, Aachen Germany.
- [52] Davies, K.M., Norman, PJ., Jones, CE., Galloway, SJ., Burt, GM., '*Fault Behaviour of a Superconducting Turboelectric Distributed Propulsion Aircraft Network: A Comprehensive Sensitivity Study*', ESARS 2015, Aachen, Germany.

- [53] Kostakis, T., Norman, P., Fletcher, S., Galloway, S., Burt, B., 'Evaluation of Paralleled Generation Architectures for Civil Aircraft Applications', Aerotech Congress and Exhibition, SAE International: Seattle, 2015.
- [54] Mraz, S. 100 Years of Aircraft Engines. Technologies 2003. Machine Design. [accessed 01/06/15]. <http://machinedesign.com/technologies/100-years-aircraft-engines>.
- [55] Rolls-Royce. Trent XWB poster. 2014. Rolls-Royce. [accessed 01/08/15]. <http://www.rolls-royce.com/Images/trent-xwb-infographic.html>
- [56] Moir, I., 'More-electric aircraft-system considerations', in IEE Colloquium on Electrical Machines and Systems for the More Electric Aircraft (Ref. No. 1999/180), pp 10/1-10/9, 1999.
- [57] Airbus Group. Simpler electrical architecture. Optimised systems. 2015. Airbus Group. [accessed 13/05/15]. <http://www.a350xwb.com/advanced/systems/#simpler-electrical-architecture>.
- [58] Ahmed, A. Why we use 400Hz Power Supply in Aircraft? c2016. [accessed 03/03/16]. http://www.academia.edu/4768401/Why_we_use_400Hz_Power_Supply_in_Aircraft.
- [59] Hook-Barnard, I., Norris, S., Alper, J., 'Technology Readiness Levels in the Department of Defense', in Technologies to Enable Autonomous Detection for BioWatch, The National Academies Press, 2014.
- [60] Rolls-Royce. Trent 700 poster. 2014. Rolls-Royce. [accessed 01/08/2015] <http://www.rolls-royce.com/Images/trent-700-poster.html>
- [61] Marburger, J., National Aeronautics Research and Development Policy, NASA, Washington DC, 2006.
- [62] Felder, J., Kim, H., Brown, G., 'Turboelectric Distributed Propulsion Engine Cycle Analysis for Hybrid-Wing-Body Aircraft', AIAA 2009, NASA Glenn Research Center: Cleveland. p. 1-25.
- [63] Del Rosario, R., Wahls, R., Follen, G., Madavan, N., 'Overview of Technical Challenges for Energy Efficient, Environmentally Compatible Subsonic Transport Aircraft', in AIAA Aero Sciences Meeting. Nashville Tennessee, 2012.
- [64] Airports Commission. Discussion Paper 03: Aviation and Climate Change. 2013. Gov.uk: [accessed 13/09/15]. www.gov.uk/government/organisations/airports-commission
- [65] Cumpsty, N., 'The Creation of Thrust in an Engine', in Jet Propulsion: A Simple Guide to the Aerodynamic and Thermodynamic design and Performance of Jet Engines, Cambridge University Press: New York, 2013.
- [66] Moir, I., Seabridge, A., 'Flight control Systems', in Aircraft Systems: Mechanical, electrical, and avionics subsystems integration, John Wiley and Sons, Chichester, p. 1:50, 2010
- [67] Moir, I., Seabridge, A., 'Hydraulic Systems', in Aircraft Systems: Mechanical, electrical, and avionics subsystem integration, John Wiley and Sons, Chichester, p. 137:180, 2010.
- [68] Moir, I., Seabridge, A., 'Engine Control Systems', in Aircraft Systems: Mechanical, Electrical and avionics subsystems integration, John Wiley and Sons, Chichester, 2010.
- [69] Hall, N. Turbofan Engine. 2015. NASA. [accessed 15/03/15]. <https://www.grc.nasa.gov/WWW/k-12/airplane/aturbf.html>.
- [70] Wickerson, J., 'Hollistic Gas Turbines', Rolls-Royce, pp. 172, 2013.
- [71] Kumar, B.V.R., 'A review on blisk technology', International Journal of Innovative Research in Science, Engineering and Technology, Vol 2(5), 2013.
- [72] Benson, T.. How does a jet engine work?. 2014. Engines:NASA. [accessed 13/02/15]. <https://www.grc.nasa.gov/www/k-12/UEET/StudentSite/engines.html>.
- [73] NASA Environmentally Responsible Aviation Project N+2 Advanced Vehicle Concepts NASA Research Announcement (NRA) Draft Solicitation, NASA: Washington, DC. 2010.

- [74] Airbus. A380. Passenger Aircraft 2014. Airbus Group. [accessed 12/01/15]. <http://www.airbus.com/aircraftfamilies/passengeraircraft/a380family/>.
- [75] Boeing 787 Dreamliner Provides New Solutions for Airlines, Passengers. 2015. Boeing. [accessed 12/01/15]. <http://www.boeing.com/boeing/commercial/787family/background.page?>
- [76] Airbus. A380 Dimensions and Key Data. 2015. Airbug Group. [accessed 14/03/15]. <http://www.airbus.com/aircraftfamilies/passengeraircraft/a380family/specifications/>.
- [77] Jie, C. and Anhua, W., '*New VF-power system architecture and evaluation for future aircraft*', IEEE Transactions on Aerospace and Electronic Systems, 42(2): p. 527-539, 2006.
- [78] Izquierdo, D., Barrado, A., Raga, C., Sanz, M., Zumel, P., Lazaro, A., '*Protection devices for aircraft electrical power distribution systems: a survey*', 34th Annual Conference of IEEE, Orlando, FL, pp. 903-908, 2008.
- [79] Trainer, D.R., Whitley, C.R., '*Electric actuation-power quality management of aerospace flight control systems*', in Power Electronics, Machines and Drives, 2002. International Conference on (Conf. Publ. No. 487), pp. 229-234, 2002.
- [80] Wheeler, P., Clare, J., Bozhko, S., and Kulshreshtha, A., 'Regeneration in Aircraft Electrical Power Systems?', in SAE Power Systems Conference, SAE International: Seattle USA, 2008.
- [81] Lyshevski, S.E., Skormin, V.A., and Colgren, R.D., '*High-torque density integrated electro-mechanical flight actuators*', IEEE Transactions on Aerospace and Electronic Systems, 38(1): p. 174-182, 2002.
- [82] Gerada, C., Bradley, K., Whitley, C., Towers, G., '*Integrated Machine design for Electro Mechanical Actuation*', Industrial Electronics, 2007 IEEE International Symposium on Industrial Electronics, Vigo, 2007, pp. 1305-1310.
- [83] Bennett, J.W., Mecrow, B.C., Atkinson D.J., Atkinson, G.J., '*Safety-critical design of electromechanical actuation systems in commercial aircraft*', IET Electric Power Applications, vol. 5, no. 1, pp. 37-47, 2011.
- [84] Lambert, C.. 3: Open Rotor Engines. 2015. SBAC Aviation and Environment Briefing Papers: www.sustainableaviation.co.uk.
- [85] Patel, P. Super-thin Superconducting Cables New compact cables show promise for power transmission and high-field magnets. 2011. MIT Technology Review. [accessed 03/05/15]. <http://www.technologyreview.com/news/423089/super-thin-superconducting-cables/>.
- [86] Baran, M.E., Mahajan, N.R., '*DC distribution for industrial systems: opportunities and challenges*', in IEEE Transactions on Industry Applications, vol. 39, no. 6, pp. 1596-1601, Nov.-Dec. 2003.
- [87] Airbus Group. E-Thrust: electrical distributed propulsion concept for lower fuel consumption, fewer emissions and less noise. Electric and hybrid Aircraft Projects 2014. E-thrust Brochure:Airbus Group [accessed 12/15/15]. http://www.airbusgroup.com/int/en/news-media/media~item=2efe334d-1141-403c-8449-1b7180c8e7fa~ref=6234b3fe-0207-4c59-84ff-2c6183a3c163~press_kit=6234b3fe-0207-4c59-84ff-2c6183a3c163~.html.
- [88] Ross, C., Armstrong, M., Blackwelder, M., Jones, C., Norman, P., Fletcher, S., '*Turboelectric Distributed Propulsion Protection System Design Trades*', in SAE 2014 Aerospace Systems and Technology Conference2014: Cincinnati, 2014
- [89] NASA, '*Advanced Concept Studies for Subsonic and Supersonic Commercial Transports Entering Service in the 2030-35 Period*', in NASA Research Announcement, Pre-Proposal Conference, NASA: L'Enfant Plaza Hotel, Washington, 2007

- [90] Boeing SUGAR volt Hybrid Plane. 2015. Transportation Electrification Community:ieec.org. [accessed 13/09/15]. <http://tec.ieee.org/aeronautical/boeing-sugar-volt-hybrid-airplane/>.
- [91] Dunbar, B., Down to Earth Future Aircraft, 2015. NASA. [accessed 15/08/15]. http://www.nasa.gov/topics/aeronautics/features/future_airplanes_index.html#lowerAccordion-set2-slide19
- [92] NASA awards \$16.5 million towards development of the future airliner.... c2016. aircraft-completion.com [accessed 12/08/15]. <http://aircraft-completion.com/aircraft-news/development-of-the-future-airliner-magic-skin/>.
- [93] Blanco, E., and Greitzer, E.M. Subsonic civil transport aircraft for 2035. 2010. AeroAstro Magazine: MIT. [accessed 14/06/15]. <http://web.mit.edu/aeroastro/news/magazine/aeroastro7/n-3.html>.
- [94] Bettex, M. Fly the eco-friendly skies. 2010. [accessed 06/09/15] <http://phys.org/news193301378.html#nRlv>.
- [95] Ross, C., Armstrong, M., Blackwelder, M., Jones, C., Norman, P., Fletcher, S., '*Turboelectric Distributed Propulsion Protection System Design Trades*', in SAE 2014 Aerospace Systems and Technology Conference, Cincinnati, 2014.
- [96] Federal Aviation Regulations, FAR part 25, in Airworthiness Standards: Transport Category Airplanes.
- [97] SAE International, '*Certification Considerations for Highly-Integrated or Complex Aircraft Systems*', ARP4754, 1996.
- [98] Smith, D.J. and Simpson, K.G.L., '*Reliability Modelling Techniques*' in Safety Critical Systems Handbook: a Straightforward Guide to Functional Safety, IEC 61508 (2010 Edition) and Related Standards, Including Process IEC61511 and Machinery IEC 62061 and ISO 138492010, Butterworth Heinemann. p. 89-106, 2010.
- [99] Wetherholt, J. Common Cause Failure Modes. 2011. [accessed 13/09/15]. <http://ntrs.nasa.gov/archive/nasa/casi.ntrs.nasa.gov/20110015733.pdf>.
- [100] SAE International, '*Guidelines and Methods for Conducting the Safety Assessment Process on Civil Airborne Systems and Equipment*', in Aircraft and Systems Development and Safety Assessment ARP4761, 2004.
- [101] Davies, K.M., Norman, P., Jones, C., Galloway, S.J, Husband, M., '*Modelling the Fault Behaviour of a Superconducting Turboelectric Distributed Propulsion Network*', in SAE 2014 Aerospace Systems and Technology Conference, Cincinnati, 2014.
- [102] Davies, K.M., Norman, P., Jones, C., Galloway, S.J, Husband, M., '*A review of Turboelectric Distributed Propulsion technologies for N+3 aircraft electrical systems*', in 48th International Universities' Power Engineering Conference (UPEC), Dublin, 2013.
- [103] Davies, K.M., Norman, P., Jones, C., Galloway, S.J, Husband, M., '*Examining the Fault Behaviour of a Superconducting DC Network*', in The 12th International Conference on Developments in Power System Protection, Copenhagen, Denmark, 2014.
- [104] Vesely, W., Stamatelatos, M., Dugan, J., Fragola, J., Minarick, J., Railsback, J., '*Fault Tree Handbook with Aerospace Applications*', 2002, NASA. <http://www.hq.nasa.gov/office/codeq/doctree/fthb.pdf>.
- [105] Moir, I., and Seabridge, A., '*System Design and Development*', in Aircraft Systems: Mechanical, Electrical and Avionics Subsystems integration, John Wiley and Sons, Chichester, 2010.
- [106] Ebeling, C.E., '*Reliability of Systems*', in An Introduction to Reliability and Maintainability Engineering, McGraw-Hill, 1997.

- [107] Weisstein, E.W., Bayesian Analysis. Wolfram Research. [accessed 14/03/16]. <http://mathworld.wolfram.com/BayesianAnalysis.html>.
- [108] Brown, C. An Introduction to Bayes Theorem. Trinity University. [accessed 14/12/15]. <http://www.trinity.edu/cbrown/bayesweb/>.
- [109] Ebeling, C.E., 'Introduction', in An Introduction to Reliability and Maintainability Engineering, McGraw-Hill, 1997,
- [110] Norman. Bayes Rule. 2015. Queen Mary University London. [accessed 14/03/16]. Available from: https://www.eecs.qmul.ac.uk/~norman/BBNs/Bayes_rule.htm.
- [111] Susova, G.M., Petrov, A.N., 'Markov model-based reliability and safety evaluation for aircraft maintenance-system optimization', in Reliability and Maintainability Symposium, Philadelphia, p. 29-36, 1997.
- [112] Ebeling, C.E., 'State-Dependant Systems', in An Introduction to Reliability and Maintainability Engineering, McGraw Hill Education (India), New Delhi. p. 108 - 123, 2013.
- [113] Vesely, W.E., Goldberg, F.F., Roberts, N. H., Haasl., 'Fault Tree Handbook', in US Nuclear Regulatory Commission, Washington DC 1981. <http://www.nrc.gov/docs/ML1007/ML100780465.pdf>
- [114] Marshall, J. 2012. An Introduction to Fault Tree Analysis. Warwick University. [accessed 11/12/15]. http://www2.warwick.ac.uk/fac/sci/wmg/ftmsc/modules/modulelist/peuss/slides/section_11b_fta_lecture_slides_compatibility_mode.pdf
- [115] European Aviation Safety Agency, 'Certification Specifications and Acceptable Means of Compliance for Large Aeroplanes CS 25', in CS-25 Large Aeroplanes Amendment 162015, 2015
- [116] Vesely, B. Fault Tree Analysis (FTA): Concepts and Applications. Mission Success Starts with Safety. 2002. [accessed 10/12/15]. <http://www.hq.nasa.gov/office/codeq/risk/docs/ftcourse.pdf>.
- [117] Ebeling, C.E., 'Design for Reliability', in An Introduction to Reliability and Maintainability Engineering, McGraw-Hill. p. 178, 1997
- [118] Ciobotaru, M. Fault Tree Analysis of an Aircraft Combustion Engine. The Fault Tree Tutorial. [accessed 12/12/15]. http://mateic.home.ro/fault_tree_site/example1.html.
- [119] Beginner's Guide to Aviation Efficiency. 2010. Air Transport Action Group [accessed 01/04/16]. www.atag.org
- [120] Mishra, V.J., Khardensis, M.D., 'Contingency analysis of power system', in, 2012 IEEE Students' Conference on Electrical, Electronics and Computer Science (SCEECS). Bhopal, 2012.
- [121] Grainger, J., Stevenson, W., 'ZBus Methods in Contingency Analysis', in Power Systems Analysis, McGraw - Hill. p. 591-640, 1994
- [122] New ETOPS Regulations. 2007. FAA. [accessed 13/09/15]. http://www.faa.gov/other_visit/aviation_industry/airline_operators/airline_safety/info/all_infos/media/2007/info07004.pdf.
- [123] Bachtel, B. 2003. ETOPS, Extended Operations, and En Route Alternate Airports. [accessed 13/09/15]. <http://www.boeing.com/assets/pdf/commercial/airports/faqs/etopseropenroutealt.pdf>
- [124] SAE International, 'Guidelines for Time-Limited-Dispatch (TLD) Analysis for Electronic Engine Control Systems', in ARP5107B, 2006.
- [125] SAE International, 'Guidelines for Engine Component Tests', ARP5757, 2008
- [126] Binomial Distribution. c2000-2016. Stats Direct:Statistical Help, [accessed 13/03/16]. <http://www.statsdirect.com/help/default.htm#distributions/binomial.htm>.

- [127] Ebeling, C., '*Time-Dependent Failure Models*', in '*An Introduction to Reliability and Maintainability Engineering*', 1997, McGraw-Hill.
- [128] Brown, G., Kascak, A., Ebihara, B., Johnson, D., Choi, B., Siebert, M., Buccieri, C., '*NASA Glenn Research Center Program in High Power Density Motors for Aeropropulsion*', NASA, 2005.
- [129] Miller, P., '*Potential Propulsion Solutions for Hybrid-Electric Aircraft*', Disruptive Green Propulsion Technologies Conference, Institute of Mechanical Engineers, 2014, London, United Kingdom.
- [130] Shaw, J. C., Fletcher, S., Norman, P., Galloway, S., Burt, G. "*Failure Analysis of a Turboelectric Distributed Propulsion Aircraft Electrical Network: A Case Study*", SAE Technical Paper 2015-01-0299, 2015
- [131] yoon, J., 400 Hz Electrical Systems, <http://www.aerospaceweb.org/question/electronics/q0219.shtml>, accessed 23/07/16